Bartosz Grzyb

Doctoral Thesis

PREPARATION AND CHARACTERIZATION OF MESOPHASIC CARBON MATERIALS ENRICHED IN NITROGEN

The work was completed as „thèse en cotutelle" in the
Institute of Chemistry and Technology of Petroleum and Coal
at Wrocław University of Technology
and
Laboratoire de Chimie et Applications
at University of Metz

Supervisors
Professor Jacek Machnikowski
Professor Jean-Victor Weber

Wrocław. Metz 2003

The thesis has been submitted to the Scientific Council
of the Institute of Chemistry and Technology of Petroleum ~~and Coal~~
at Wrocław University of Technology
and Graduate Committee including:

Professor François Béguin, (Referee)
CNRS-University of Orleans

Professor Stanisław Błażewicz, (Referee)
Academy of Mining and Metallurgy, Kraków

Doctor Maria Antonia Diez,
Instituto Nacional del Carbon, CSIC, Oviedo

Professor Grażyna Gryglewicz,
Wrocław University of Technology

Professor Jacek Machnikowski, (Supervisor)
Wrocław University of Technology

Professor Eric Millon,
University of Metz

Professor Jean–Victor Weber, (Supervisor)
University of Metz

in partial fulfillment of the requirements for the degree of
Doctor of Philosophy
of Wrocław University of Technology
and
University of Metz

To My Parents

In memory of Tadeusz Grzyb

Preface

Present work is a result of four years of work directed by Professor Jacek Machnikowski. I would like to express my gratitude for his guidance and invaluable contribution increased the quality of my research.

I am also deeply indebted to my advisor Professor Jean-Victor Weber, without his help this thesis would not have been possible. I thank him for guidance, help and friendship.

I want to give the special thanks to Dr. Alain Koch and Dr. Andrzej Krztoń for sharing with me some of their profound knowledge concerning IR spectroscopy and creative scienticic discussions.

I also want to take the opportunity to thank Dr. Olivier Heintz for the help in the XPS analyses.

All the colleagues from my parent Institute and LCA laboratory deserve special recognition for the friendly atmosphere, supportive environment and scientific assistance they provided.

I am grateful for the support from the CNRS (GDRE « Materiaux carbones » and « Jumelage ») and French embassy to enable me to study at University of Metz, Laboratoire de Chimie et Applications in Saint-Avold.

Finally, with all my love I wish to thank my wife, Ewa for her unwavering support ane encouragement during last years.

Contents

I Introduction 1

II Literature 2

2.1. Carbon materials produced by condensed-phase pyrolysis of organic precursors 2
2.1.1. Carbonization of aromatic precursors – carbonaceous mesophase 2
2.1.2. Carbonization of polymeric precursors 5
2.1.3. Heteroatoms in carbonaceous materials 8
2.2. Synthesis of nitrogen enriched carbons 11
2.2.1. Pyrolysis of N-polymers 11
2.2.2. Catalytic carbonization of heteroaromatic compounds 19
2.2.3. Ammonization and ammoxidation 20
2.2.4. Other methods of preparation of nitrogen enriched carbons 23
2.3. Nitrogen functionalities in carbonaceous materials 24
2.3.1. The role of x-ray photoelectron spectroscopy in the identification of nitrogen functionalities 24
2.3.2. Nitrogen introduced by ammonization and ammoxidation 27
2.3.3. Nitrogen in carbonaceous materials produced by pyrolysis of organic precursors 28
2.3.4. Effect of oxidative atmosphere on nitrogen evolution 31
2.4. Surface and bulk properties of nitrogen doped carbons 32
2.5. Perspective application of nitrogen doped carbons 35

III Objective 40

IV Experimental 41

4.1. Scope of research 41
4.2. Raw materials 43
4.3. Procedures 44
4.4. Analyses 47

V Results and discussion 53

5.1. Characteristics of parent materials 53
5.2. Co-pyrolysis of pitch with polyacrylonitrile 56
5.2.1. Weight loss behavior 56
5.2.2. Structure and properties of co-pyrolysis products 62
5.2.2.1. Optical texture of semi-cokes from pitch-PAN and pitch-PANox blends 62
5.2.2.2. Elemental composition of semi-cokes 66
5.2.2.3. Chemical structure evolution on pyrolysis 67
5.2.2.4. The evaluation of the interactions between pitch and polymers on pyrolysis 80
5.3. Co-pyrolysis of pitch with polyvinylpyridine 81
5.3.1. Weight loss behavior 81
5.3.2. Structure and properties of co-pyrolysis products 91

5.3.2.1. Optical texture of semi-cokes from pitch-PVP25 and pitch-PVP25ox blends 91
5.3.2.2. Elemental composition of semi-cokes 94
5.3.2.3. Chemical structure evolution on pyrolysis 95
5.4. Ammoxidation of pitch-derived carbonaceous materials 104
5.4.1. Preparation of starting carbonaceous materials for ammoxidation 104
5.4.2. Synthesis of ammoxidized materials 109
5.4.3. Evaluation of surface chemistry of ammoxidized materials 113
5.5. The behavior of nitrogen enriched semi-cokes on thermal treatment in inert and oxidative atmosphere 121
5.5.1. Structural evolution of nitrogen enriched carbonaceous materials produced by co-pyrolysis 121
5.5.1.1. Weight loss behavior 121
5.5.1.2. Microtexture characteristics of the carbonization and activation products derived from pitch-PAN blends 131
5.5.1.3. Elemental composition of the carbonization and activation products produced from pitch-polymer blends 133
5.5.1.4. Evolution of nitrogen and oxygen functionalities on the carbonization and activation of PAN and PVP25ox derived semi-cokes 135
5.5.2. Structural evolution of nitrogen enriched carbonaceous materials produced by ammoxidation of pitch-derived materials 144
5.5.2.1. Weight loss behavior 144
5.6. Determination of surface properties of N-doped carbons 162
5.6.1. Porosity development of activation products 169
5.6.2. Polarity of nitrogen doped carbons 172
5.7. Evaluation of nitrogen doped carbons as a potential anode material in lithium-ion cell 172
5.7.1. Composition of calcined carbons from pitch-polyacrylonitrile blends 172
5.7.2. Multiscale structural and textural characteristics of the CTP-PAN derived cokes 178
5.7.3. Electrochemical properties of the CTP-PAN derived carbons 184

VI Summarizing discussion 188

VII Conclusions 203

References 205

I. Introduction

Carbonaceous materials of greatest importance for the industrial practice, including metallurgical coke, carbon or graphite artefacts and activated carbons, are produced by the pyrolysis of various organic precursors occurring in the condensed phase. The major way of arranging of carbon atoms in all the resultant materials is two-dimensional array in a form of the graphene plane. The essential differences in the mutual orientation and the extent of cross-linking of carbon layer planes as well as the proportion of disorganised carbon are a basis of classification into two broad categories of graphitizing or non-graphitizing carbons (Franklin, 1951a;b).

The aromatic precursors such as coal-tar and petroleum pitches and bituminous coals lead, via liquid state pyrolysis, to graphitizing or soft carbons of larger range orientation of structural units, which are readily distinguishable by optically anisotropic texture. Polymeric type precursors, including low rank coals, cellulosic materials and synthetic resins are typical parent materials which give on thermal treatment non-graphitizing or hard carbons. Characteristic of these carbonaceous residues is a random orientation of graphene layer stacks corresponding to optically isotropic appearance.

The selection of suitable organic precursor, modification of pyrolysis conditions and the various post-treatments have been widely used for the tailoring of structure and texture of carbonaceous materials to meet specific requirements for advanced applications. The efficient way of further modification of the properties can be introducing of foreign atoms in the form of both the substituent for carbon and/or attached functional group. This type of modification seems to be of particular importance in the case of advanced porous carbons for application as a specific adsorbent, catalyst or catalyst support and electrode in electric double layer capacitors.

Coal-tar pitch is an aromatic feedstock of great practical importance in the manufacturing of carbon and graphite artefacts. As distinct from the common use the present thesis is focused on the synthesis of pitch based carbons of specific properties due to the presence of nitrogen in the network together with controlled structural ordering. Blending of coal-tar pitch with selected nitrogen containing polymers and the reaction of pitch derived carbonaceous materials with ammonia-air mixture are the explored methods of modification.

II. Literature

2.1. Carbon materials produced by condensed-phase pyrolysis of organic precursors

2.1.1. Carbonization of aromatic precursors – carbonaceous mesophase

The principal reactions involved in the conversion of aromatic precursors to optically anisotropic and graphitizing carbonaceous solids occur in the liquid phase, as it is maintained within the temperature range of 400-500°C. The fluid phase offers a sufficient mobility to the reacting molecules which is the primary requirement for the development of long-range order in the carbonizing system.

The discovery of the fundamental importance for the current understanding of the fluid phase pyrolysis was done by Brooks and Taylor (1965, 1968). Using polarized light optical microscopy they observed in a coal-tar pitch heat treated at about 450°C the nucleation of small anisotropic spherules. As the process continued the spherules grew in the result of the assimilation of suitable molecules from the surrounding melt and then coalesced to form large regions of fusible anisotropic phase. On further heat-treatment the entire pitch was converted into the anisotropic phase which next was transformed into the infusible semi-coke. The fusible phase, intermediate in the transformation of pitch to coke, was called mesophase and regarded as a special, discotic case of nematic liquid crystals.

Fitzer et al. (1971) considered that the conversion of suitable hydrocarbon precursor into mesophase has to include following steps:

- first step: formation of planar molecules by the way of building reactions within the fluid phase
- second step: parallel arrangement of these planar molecules due to the dispersion effect
- third step: preferential growth of planar molecules of diameters exceeding 2.5 nm, these molecules acting as nuclei
- fourth step: agglomeration of such molecular structures leading to molecular weights of the order of 500 D; the resulting structures can be detected as liquid spherulites using light microscopy

- fifth step: agglomeration (coalescence) of these mesophase spherulites leading to an uniform mesophase, the microscopic structure of which can be found in the solid pyrolysis residue, i.e. in the coke.

The general requirement for the mesophase nucleation is a sufficiently high concentration of large planar molecules of polycyclic aromatic hydrocarbons (molecular masses above 400-500 D) in the carbonizing system. These molecules (mesogens) are able to associate together through physical interactions to form the liquid crystal system. The chemistry of mesogens formation on heat treatment of various hydrocarbons is extremely complex. Based on the study of model compounds pyrolysis, Lewis (1982) considers following reaction types to have a relevant contribution to the process:

- C-H, C-C bond cleavage to form reactive free radicals
- molecular rearrangement
- thermal polymerization
- aromatic condensation
- elimination of side chains and hydrogen

The bond cleavage, which is the initial thermal reaction in the carbonization of an aromatic hydrocarbon results in the formation of two types of free radical intermediates. The first one is a very unstable σ-radical with the localized free electron, produced by the abstraction of aromatic hydrogen. Π-radicals produced by the breaking of the methyl carbon-hydrogen bonds are considerably more stable. In this case the unpaired electron is resonance stabilized. The initial reactions in the carbonization of aromatics often involve the hydrogen transfer. As shown in Fig.1, the polymerization of anthracene proceeds by the reaction with the π-radical generated from the unstable anthryl σ-radical. Due to the thermal rearrangement occurring in the early stage of carbonization the conformation of the resultant intermediate molecule is often difficult to be related to the structure of starting compound.

It has been generally accepted that the principal chemical reaction associated with the mesophase formation is the dehydrogenative polymerization of aromatic hydrocarbons. The process occurs in two stages described as the thermal polymerization and aromatic condensation (Lewis, 1982). In the first stage the dimer units linked by single C-C bonds are formed (Fig. 2-2).

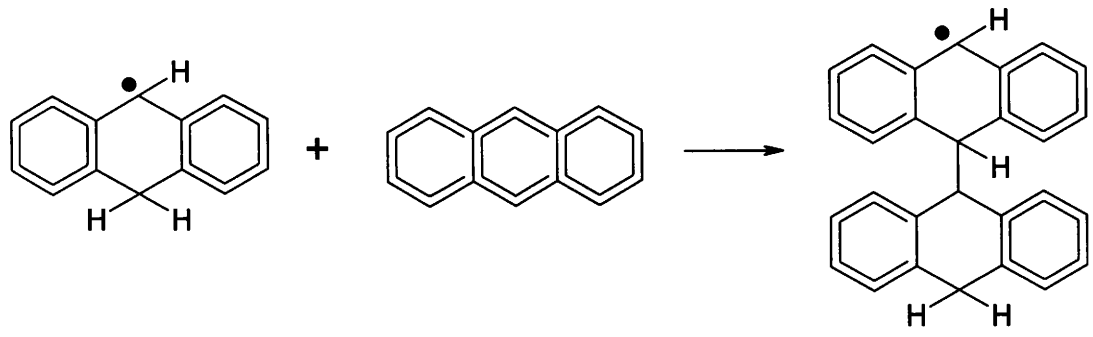

Fig. 1. Initial reactions in the pyrolysis of anthracene (Lewis, 1982).

The preferential polymerization sites on the aromatic ring can be predicted according to the reactivity parameters calculated using various quantum mechanics theories (Zander and Collin, 1993, Yokono et al., 1979, Mochida et al., 1988). The aromatic condensation leading to the ring closure can occur only in those dimers which attained the favorable conformation (Fig. 2-3). Based on the anthracene polymerization study, it was shown that reactions leading to the non-fully condensable dimers occur to a considerable extent.

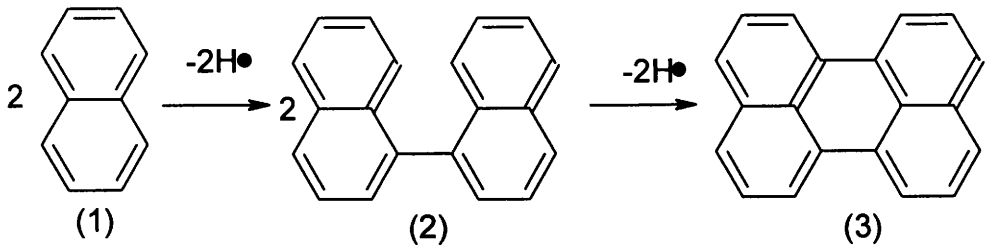

Fig. 2. Mechanism of the polymerization and condensation of aromatic hydrocarbons (Lewis, 1980).

In the case of practical raw materials as pitches, the general description of the carbonization process must consider the volatilization on the heat-treatment of lower molecular weight compounds and the polymerization of more reactive species. Both the distillation and polymerization increase the average molecular weight of the isotropic phase and result in the initial development of long-range molecular order.

The detailed study of petroleum pitch carbonization using the gel permeation chromatography (Greinke, 1986, 1994) revealed that molecules with MW less than 400 D were distilled before polymerization. The major reaction during mesophase formation was polymerization of molecules of MW about 580 D to form dimers with MW about 1200 D. The chemical bonds in the dimerized molecules were predominantly the aryl-aryl bridges with smaller amount of the methylene bridges. The dealkylation reactions, which increase the aromaticity and molecular planarity of pitch molecules, had only a minor influence on the mesophase formation. The next stage of the thermal carbonization involved polymerization reactions of the mesophase constituents to built up the molecules with MW greater than 2000 D. The process led to a significant increase in the viscosity and melting point in the advanced mesophase stage and finally to the formation of semi-coke.

As the temperature increases above 500°C, a further conversion of solid semi-coke into the coke occurs. This process is initiated by the splitting off peripherical hydrogen, methyl and oxygen groups which forces the aromatic lamellae to condensate and compact into stacks of graphene layers.

2.1.2. Carbonization of polymeric precursors

Organic materials which are either polymeric in nature or develop a cross-linked macromolecular system in the very initial stage of the heat-treatment give on carbonization the isotropic non-graphitizable carbons. Various natural materials including biomass (wood, sawdust, coconut shells, nut shells, fruit stones, agriculture wastes) and fossil fuels (peat, lignite, coals) as well as synthetic polymers such as phenolic resin, polyfurfuryl alcohol and polyvinylidene chloride are suitable for the preparation of non-graphitizing carbons. Due to the thermosetting character of the parent materials the primary pyrolysis reactions are completed within the solid phase and some features of the original macromolecular system can be preserved in the resultant char.

Though detailed mechanism of the pyrolysis is rather specific of any polymeric precursor, some general trends concerning the degradation of the initial macromolecular network can be established (Marsh and Menendez, 1989, Byrne and Marsh, 1995). The early stages of carbonization beginning at temperatures as low as 300-350°C involve the cleavage of bonds within the macromolecular system to give free radicals. This process is accompanied by the loss of volatile matter in the form of small molecules like water,

carbon dioxide, methanol and methane, together with the re-arrangement of carbon atoms to form more stable six-membered rings of carbon lamellae. As small molecules are removed from the macromolecular network, the resultant chemically reactive lattice immediately combines around the created vacancies. In that way the porosity is developed within the rigid macromolecular system. With the heat treatment temperature increasing above 500^0C, the macromolecular network becomes more carbonaceous and more aromatic due to the preferential loss of hydrogen and oxygen. At temperatures exceeding 700^0C, there is created a macromolecular network made up of small clusters of six-membered ring systems. The defective non-lamellar configuration of the clusters hardly approximates to the graphene layer of graphitic carbon and their random bonding together ensures spaces in between them, which constitute the microporosity.

The pyrolysis of polymeric in nature materials is a process of considerable practical importance. In the case of natural parent materials as wood, coconut shells, peat, lignite and coals, the carbonization followed by the gasification has been widely used for many years for the manufacturing of general purpose activated carbons. The growing recently interest in the pyrolysis of synthetic polymers is concerned with two fields, the disposal of waste plastics and the manufacturing of carbonaceous materials with tailored structure and properties. As to the latter field, especially great research activity is focused on carbon fibers (Bacon et al. 1973) and porous carbons (Byrne and Marsh, 1995).

The suitability of a given polymer for any carbon technology is closely related to its propensity for producing the solid residue on the heat treatment. This is closely related to the mechanism of the thermal decomposition which can occur either by the chain depolymerization (depropagation), i.e. the successive release of monomer units from a chain end or at a weak link, or by the random degradation consisting in the chain rupture at random points along the chain. The depolymerization, which is often the dominant degradation process in vinyl polymers usually yields a small solid residue, whereas the random scission of the polymer backbone is often followed by the cross-linking and condensation resulting in the considerably bigger residue yield. Van Krevelen (1990) attempted to relate the residue yield to the structural peculiarities of polymers and introduced the parameter called the char forming tendency (CFT), which is defined as the amount of the char per structural unit divided by 12 (the atomic weight of carbon), i.e. the amount of carbon equivalents in the char per structural unit of polymer. Since each structural group contributes to the char residue in its own

characteristic way, the char residue (CR) on pyrolysis can be estimated according to the equation:

$$CR = \frac{\sum (CFT)i}{M} X1200$$

where M is the molecular weight per polymer unit and char yield is expressed as a weight percentage.

The pyrolysis of polystyrenes is a good demonstration of the effect of polymer conformation on the residue yield (Neely, 1981). Due to complete depolymerization and chain scission the linear polymer produces no carbonization residue on heat treatment. Conversely, cross-linked polystyrenes readily convert to a solid carbon by the condensation mechanism. Introducing functionality following sulfonation, oxidation and chlorination can further enhance the carbonization yield.

The high residue yield is a critical requirement especially in the case of selecting precursors for making carbon fibers with attractive mechanical properties. Among natural and synthetic polymeric fibrous materials polyacrylonitrile (PAN) and viscose rayon (regenerated cellulose) have received major attention.

The superior performance of PAN derived carbon fibers is related to a great extent to the larger residue yield as related to the pyrolysis mechanism (Bahl et al., 1998). The pyrolysis of PAN proceeds via cyclization, aromatization and condensation reactions leading to the solid residue with a relatively little contribution of depolymerization to light volatile products. The formation of large aromatic lamellae of near perfect graphene layer structure occurs with the final carbon yield in the range of 50 –55 %.

The chemistry of pyrolysis of synthetic cellulose fibers includes the splitting up of the structural water, thermal cleavage of ring to ring linkages and breaking down of each cellulose unit into a residue containing four carbon atoms which then repolymerize into clusters of aromatic rings. Finally, the defective graphene layers of carbon fibers are formed with carbon yield in the range of 10-30% in dependence on the precursor nature and the processing parameters.

2.1.3. Heteroatoms in carbonaceous materials

Oxygen, nitrogen and sulphur are intrinsically associated with the organic matter in naturally occurring materials of practical value as precursors of carbons. When the primary pyrolysis reactions are practically completed i.e. at the temperature of 500-550°C, a part of the heteroatoms, which is dependent on the composition of precursor and the individual thermal degradation pathway, remains in the solid residues. Heteroatoms left in the carbonaceous residue at this stage of heat-treatment are rather strongly bonded within the ring system of the aromatic lamellae and their evolution occurs within the temperature range which is characteristic of a given element. It is well established that the bonding of oxygen is relatively weak and its evolution is completed below 1000°C. Most of nitrogen and sulphur are released within the temperature range of 1200-1400°C and 1400-1800°C, respectively.

In terms of mesophase development and graphitizability, the heteroatom bearing compounds are regarded as harmful components of carbonization feedstock. As a rule, heteroaromatic and heterosubstituted compounds contribute to the enhanced thermal reactivity and give on pyrolysis non-planar intermediates (Fitzer et al., 1971). The oxygen, nitrogen and sulphur level is therefore strongly restricted as the feedstock is to be used for the manufacturing of mesophase pitch carbon fibers and needle cokes. Singer and Lewis (1981) observed that quinones, which were formed by the air oxidation of polynuclear aromatics, pyrolyzed to give nonplanar radicals and resulted in the decrease of graphitizability. As an exception, a good graphitizability was reported for the variety of nitrogen containing heterocyclic compounds occurring in coal tar pitches. The behavior was explained by the formation of reactive aromatic intermediates during elimination of the heteroatom at the early stage of pyrolysis (Edstrom and Lewis, 1969).

On the other hand, the introducing of heteroatom into carbonaceous material or doping is an attractive way of synthesis of carbons with improved properties. The elements considered as suitable for the doping include nitrogen, oxygen, boron, sulphur, phosphorus, silicone, halogens and others. The foreign atoms can be either substituted for carbon in the aromatic ring system, chemically bound to the aromatic clusters or located in the interstitial sites.

The doping with foreign atoms is expected to affect the following properties of carbon material (Marchand, 1971):

- the distribution of electrons between energy levels

- the graphitization process (positive or negative "catalysis")
- the chemical state of the surface of carbon particles.

From the point of view of the electronic properties the important effect of the doping is a lowering (if the foreign atoms are acceptors) or an increasing (if the foreign atoms are donors) of the Fermi level.

Several metals, including iron, nickel, vanadium, titanium, copper, chromium and boron have a catalytic effect upon the graphitization process. The negative effect is reported for sulphur and chlorine.

The doping with heteroatoms influences the chemical state of the surface in the resultant carbonaceous material. The modification can be of great importance when the porous material is to be used as a catalyst, catalyst support or specific adsorbent.

Such surface-bound elements as oxygen, nitrogen, sulfur and halogens, owing to the electronegativity different from that of carbon, influence the sorption properties of carbons. The doping with various heteroatoms affects diversely the amphoteric character of carbon surface (Boehm, 1994). Further, the polarities of the surface functional groups are strongly affected by the neighboring chemical structures. Therefore the properties of corresponding functional groups on the carbon surface and in organic molecule are different, moreover, there are no two groups of exactly the same behaviour on a carbon surface. This is one of the main aspects of carbon surface heterogeneity (Leon y Leon and Radovic, 1994).

The ways of heteroatom introducing into carbonaceous material

Chemical vapor deposition

The chemical vapour deposition (CVD) can be used for the synthesis of thin films of doped carbons. Since the chemical reactions occur at a state which is far from the equilibrium, it is possible to prepare in that way the films of very high concentration of the introduced element. Using CVD, the carbons containing up to 25 at% of boron were synthesized by the co-deposition of benzene and boron trichloride (Kouvetakis et al., 1986) and layered carbons of nitrogen concentration corresponding to the formula $C_{14}N$ and $C_{16}N$ were prepared from acetonitrile and pyridine with nickel or cobalt catalysts at 850^0-1000^0C (Nakajima and Koh, 1997).

Pyrolysis of organic molecules containing foreign atoms

The pyrolysis of heteroatom-containing precursors in the condensed phase enables the preparation of carbons having the element uniformly distributed in the bulk of the matrix. This method has been reported as particularly suitable for the synthesis of nitrogen-containing carbons because the radius of nitrogen atom is close to that of carbon and N-polymeric precursors are readily available (Mikhalovsky, 1996). The same method was reported as applicable for the synthesis of sulphur and phosphorus containing carbons. The appropriate precursor for S-carbons can be prepared by the co-polymerization of tiophene with phenol and formaldehyde. P-containing polymers can be produced by the treatment of phenol-formaldehyde resin with phosphorus oxychloride or phosphoric acid. Konno et al. (1999) studied the doping of carbons with boron and nitrogen based on the Kapton-type polyimide precursors.

Chemical treatment of carbonaceous material

The variety of the functional groups can be generated on the carbon surface by the chemical treatment. The process is regarded as a suitable way for the control of acidic/basic properties of the surface. The introducing of different oxygen functionalities using air, nitric acid or hydrogen peroxide as oxidation agents is known to develop the surface acidity. Basic properties are commonly associated with the presence of nitrogen. Jansen and Bekkum (1994) developed basic properties in commercial activated carbons by the treatment with ammonia (ammonization) or ammonia-air mixture (ammoxidation). Very rich in nitrogen carbonaceous materials can be rather readily produced by ammoxidation of lignites and pitches (Jurewicz et al., 2002, Wachowska et al., 2000). The reaction of lignites and coals with ammonia, hydrazine, hydroxylamine or urea in the liquid phase was the initial stage in the preparation of nitrogen-functionalized porous materials of high efficiency for H_2S and SO_2 removal (Bimer et al. 1998). The chemical modification of carbon surface by direct treatment with SO_2 and sulphur vapour resulted in the enhanced affinity for the heavy metal ions (Mikhalovsky et al, 1994).

2.2. Synthesis of nitrogen enriched carbons

2.2.1. Pyrolysis of N-polymers

Pyrolysis of nitrogen-containing polymers (N-polymers) is a method of preparation of synthetic carbons in which the element is uniformly distributed in the bulk of the material. The carbonization yield and nitrogen content in resultant chars is strictly dependent on polymer macromolecule constitution. Rich in nitrogen chars are frequently produced from polymers having nitrogen already present as a component of the rings. Stańczyk et al. (1995) observed that nitrogen content in solid residues obtained by the carbonization at 800^0C in an autoclave of acridine, aminoacridine or polyvinylpyrrolidone, having nitrogen in heterocyclic rings, is twice higher than in chars produced from aminoanthracene and cyanoanthracene, where nitrogen occurs in groups attached to rings (about 6 and 3 wt%, respectively). The low carbonization yield is one of the essential limitations in polymers use as precursors of enriched with nitrogen carbons. Such N-polymeric compounds as polyvinylcarbazol, polyvinylpyridine or polyvinylpyrrolidone are thermally unstable. The degradation of the polymers on heat-treatment occurs via the depolymerization giving very low residue yield (Schmiers et al., 1999). The solid residue yield can be enhanced by the cross-linking of polymers, either with the addition of copolymer (e.g. divinylbenzene) or by means of the thermooxidative stabilization.

Carbonization of polyacrylonitrile

The N-polymer, which carbonization chemistry has been studied most extensively over the years was polyacrylonitrile (PAN). The interest in thermal behavior of PAN is related with its common use as a precursor for developing high performance carbon fibers. Seventy to eighty percent of commercially available carbon fibers are basically derived from PAN polymer. PAN has following significant advantages over pitch and viscose rayon (Bahl et al., 1988):

1) PAN structure permits faster rate of pyrolysis without much disturbance to its basic structure and to the preferred orientation of the molecular chains along the fiber axis present in the original fiber.
2) It decomposes before melting.

3) Higher degree of preferred orientation of the molecular chains is possible during spinning wherein PAN can be stretched to as high as 800%. Further improvement in the orientation is also possible during thermal stabilization when it becomes plastic at around 180^{0}C and through various post spinning modifications

4) It results in high carbon yield (50-55%) when pyrolyzed to 1000^{0}C and above.

Fig. 3 presents main steps involved in the production of various grades of carbon fibers using polyacrylonitrile as starting material. First step is a spinning to obtain a preferred orientation of polymer molecule. Next step is a stabilization in an oxidizing atmosphere at constant length or even with additional stretching of PAN fibers. This stabilized fiber is then treated in inert atmosphere to 1500^{0}C or even higher to get the carbon fibers.

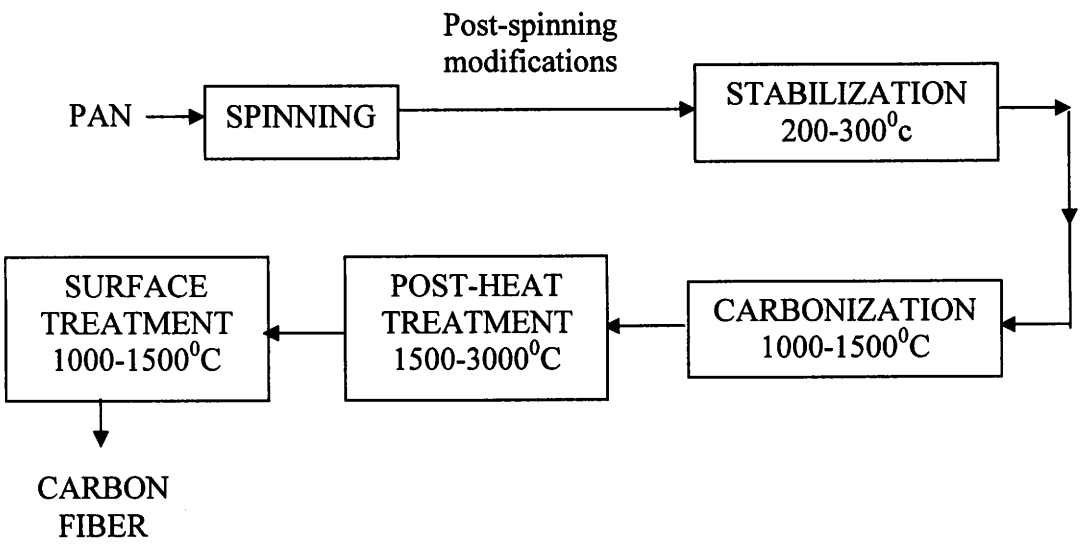

Fig. 3. Process steps of carbon fiber production from PAN (Bahl et al., 1988).

The oxidative treatment (stabilization) is regarded as the most decisive step in terms of final fiber performance. The stabilization is carried out by a controlled heating, usually in air, in the temperature range of 180°C to 300°C for extended period of time, varying from 1 to 24 hours (Gupta and Harrison, 1997). PAN shows the unique behavior during the treatment. The thermoplastic backbone of PAN undergoes a complex transformation resulting in the formation of highly cross-linked heteroaromatic structure. Such modification enhances the fiber yield on subsequent high-temperature carbonization.

The sequence of reactions which occur during the thermooxidative stabilization of PAN is shown in Fig. 4. The process includes cyclization, dehydrogenation, and oxidation. The dehydrogenation precedes cyclization, but continue during and after cyclization. Oxygen functionalities are formed only within cyclized part of polymer (Fitzer et al., 1986; Martin et al., 2001).

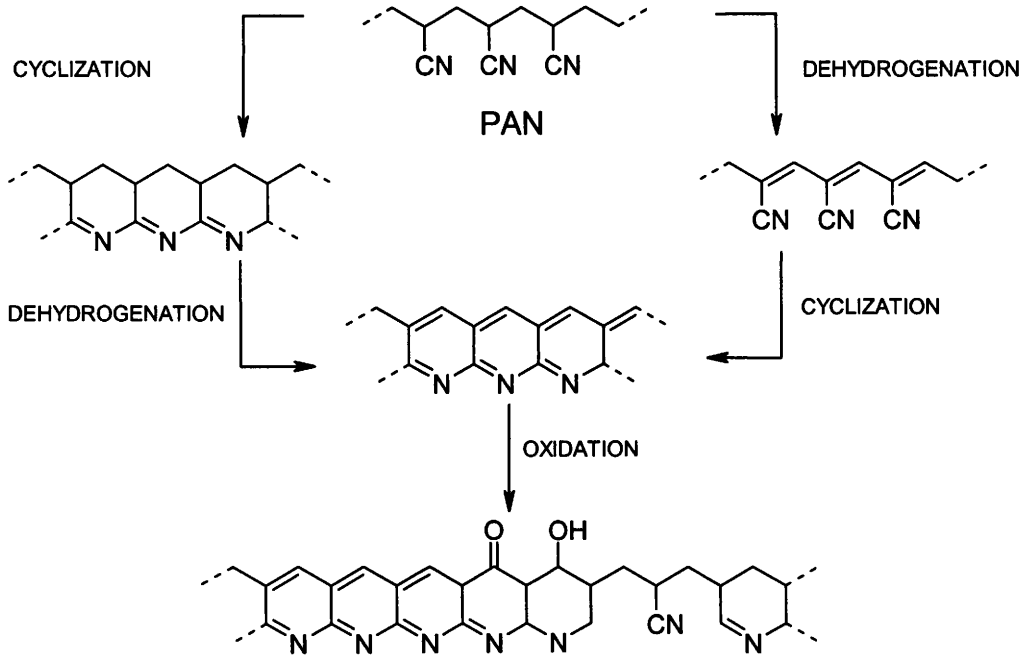

Fig. 4. Scheme of reactions during the thermooxidative stabilization of PAN precursor (Fitzer and Müller, 1975).

Various spectroscopic methods employed to follow these initial reactions comprise FTIR spectroscopy (Gupta et Harrison, 1997, Xue et al., 1997, Dalton et al., 1999), pyrolysis gas chromatography / mass spectrometry (Py-GC-MS) (Surianarayanan et al., 1992), solid state ^{13}C NMR (Surianarayanan et al., 1992, Martin et al., 2001), in situ ^{1}H NMR (Martin et al., 2001). Spectroscopic studies of PAN cyclization indicate that the onset of this process is at about 175^{0}C (Gupta et Harrison, 1997).

It is generally accepted, that the initial step in the PAN degradation is an exothermic intramolecular oligomerization of adjacent nitrile groups (Coleman et al., 1981, Xue et al.,1997). This phenomenon is believed to be initiated by the nucleophilic attack of an anion X^{-}, most likely derived from an impurity or a polymer degradation

product. Xue et al. (1997) studied the thermal degradation of PAN in the inert atmosphere. The authors attributed the initiation of the cyclization to the presence of the nucleophilic alkoxy group incorporated into the PAN backbone during the hydrogen peroxide catalyzed polymer synthesis. On the basis of the spectroscopic studies, Xue with coworkers proposed the mechanism of the cyclization giving rise to the formation of polyimine structure (Fig. 5). The polyimine readily undergoes the tautomerization to the more stable polyenamine, which isomerises to linear backbone conjugated intermediates. From this point aromatization occurs as a stepwise process with the initial loss of ammonia. Finally, a heteroaromatic ladder polymer backbone is formed. As shows elemental analysis, PAN gives nitrogen-rich char. Concentration of nitrogen diminishes rather moderately during pyrolysis from about 26 wt% in the parent polymer to 21 wt% in char prepared at temperature 750^0C. It should be pointed out that the cyclization mechanism proposed for the process is very similar to the postulated one for the oxidative stabilization. Also in this case the intramolecular cyclization of the nitrile groups gives the similar imine–enamine tautomeric structure. Moreover, a characteristic exothermal behavior in the temperature range of 200^0-350^0C, being ascribed to the cyclization of PAN, has been observed by Fitzer and Mueller (1975) in the case of thermal treatment performed in oxidative as well as in inert atmosphere. The onset of cyclization performed in inert conditions was shifted to a higher temperature compared to the oxidative stabilization. Based on this observation the authors concluded that oxygen does not catalyze the cyclization itself, though the oxygenative atmosphere promotes the initiation of the cyclization.

The cyclization is not continuous throughout the chain. Some uncyclized units left at random in the molecular chain can act as sites for a chain scission (Bahl et al., 1998). It has been suggested that the cyclization can be interrupted by tautomerization. As shown in Fig. 6, this can leave an uncyclized nitrile group in a β position relative to the condensed aromatic system. The hydrogen abstraction at the α or benzylic position would produce a stable free radical from which cyanide can be eliminated producing HCN and unsaturation along the main polymer chain. Thus a radical process can account for the HCN evolution. Another volatile product being released is ammonia produced from the terminal imine structure.

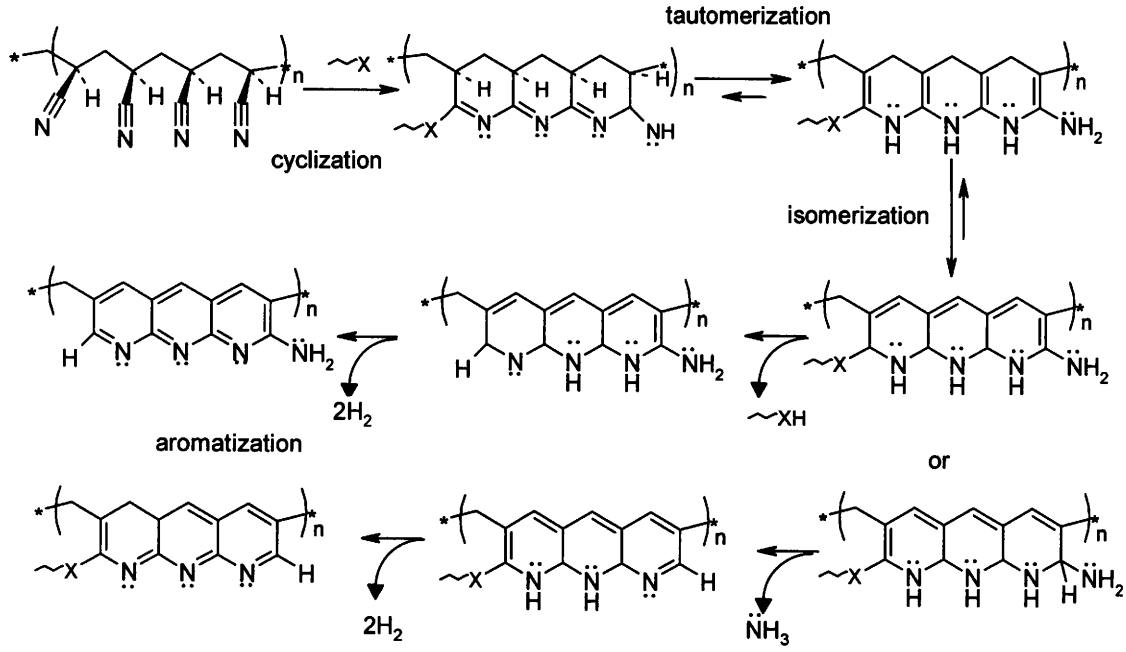

Fig. 5. Degradation scheme leading to the formation of ammonia and aromatization (Xue et al., 1997).

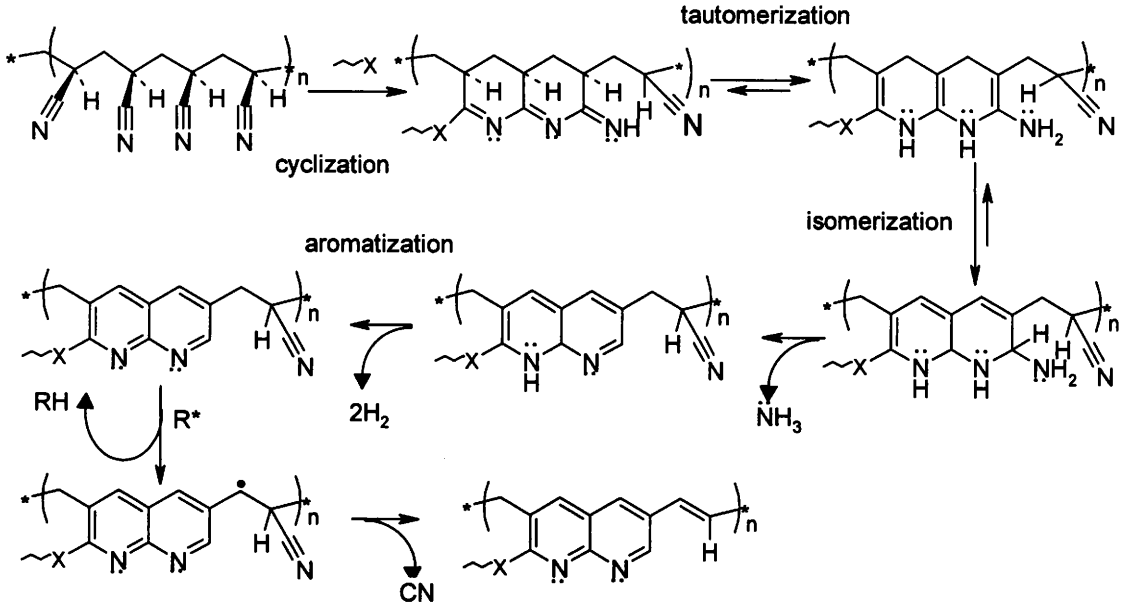

Fig. 6. Degradation scheme showing the formation of HCN and NH_3 from an uncyclized part of PAN chain (Xue et al., 1997).

The course of PAN thermal degradation depends on heat treatment conditions. High heating rate leads to the damaging of PAN fibers due to the random chain scission.

Surianarayanan et al. (1992) showed that during PAN pyrolysis performed at a heating rate of 20^0C/min ammonia and hydrogen cyanide constituted only a minor part of volatile products, while the production of oligomers via homolytic thermal cleavage of the polymer backbone chain accounted for the weight loss.

The heat treatment in an inert atmosphere to about 1500^0C is commonly used for the conversion of stabilized PAN fibers into carbon fibers. This process is accompanied by the evolution of hydrogen cyanide as a main volatile by-product, with a minor contribution of hydrogen, water, ammonia, carbon oxides and nitrogen (Fitzer et al., 1986). Hydrogen cyanide and nitrogen are evolved due to the intermolecular cross-linking of the adjacent polymer backbones (Fig. 7). Hydrogen evolves as a result of dehydrogenation. During cross-linking, the carbon atoms of one cyclized sequence fit in to the spaces left by the nitrogen of the adjacent sequence. This helps in the growth of a graphite like structure in the lateral direction. The final structure still contains a few percent of nitrogen.

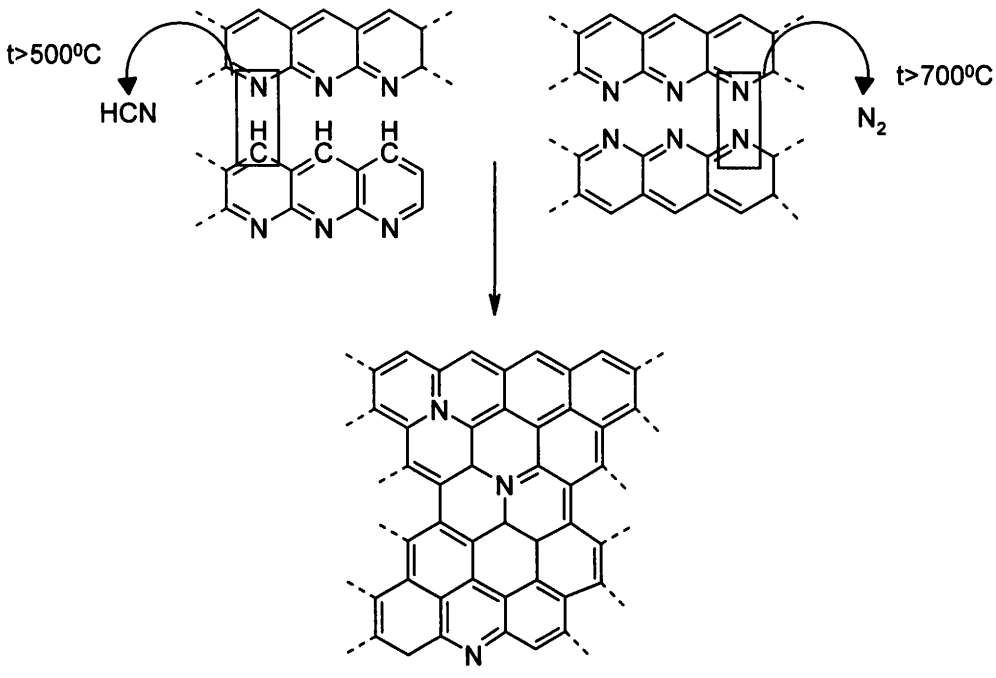

Fig. 7. Intermolecular cross-linking of PAN backbones during carbonization (Fitzer et al., 1986).

Carbonization of polyvinylpyridines

Polyvinylpyridines (PVPs) are an important class of polymers which exhibits interesting properties due to the presence of nitrogen atom in the pyridine ring. Co-polymers of polyvinylpyridines can be classified according to the position of nitrogen in the ring (poly4(-vinylpyridines) and poly2(-vinylpyridines)) and the content of divinylbenzene (DVB) added as a crosslinking agent. The weakly basic nitrogen atom accounts for a variety of reactions of vinylpyridine: neutralization of acids, quaternization and complexation of metals (Dias et al., 1997). In relation to these unique properties both the homopolymers and the cross-linked forms of PVP have a great potential for the application as polyelectrolites and polymeric reagents (Zhou et al., 1998) and ion-exchange and macroporous resins (Wu et al., 2003; Lebrun et al., 1998). Recently reported application of copolymers PVP-DVB is the preparation of spherical nitrogen containing carbons (i.e. SCN-type carbons) (Lahaye et al., 1999a). The main criterion in the selection of polymeric precursor for the preparation of nitrogen containing carbonaceous materials is a considerably high residue yield on the pyrolysis. The homopolymer PVP is thermally unstable and exhibits 98-100 % weight loss on the pyrolysis under inert conditions (Li, 1999). This behavior is due to the mechanism of the degradation, consisting mainly in the depolymerization to 4-vinylpyridine monomer and traces of pyridine and 4-methylpyridine (Azhari and Diab, 1998). The thermal depolymerization in an inert atmosphere occurs via three steps, with the major stage of the largest weight loss of 35~90 wt% in the temperature range of 300-450^{0}C (Li, 1999).

The thermal stability and the pyrolysis residue of polyvinylpyridines can be enhanced by the thermooxidative stabilization prior to the carbonization process. As has been shown few years ago (Kartel and Puziy, 1996, Lahaye et al., 1999a), the pre-treated in air vinylpyridine cross-linked with 10 wt% of divinylbenzene produces the solid residue with a higher yield and nitrogen-to-carbon atomic ratio than non-modified polymer treated in the same conditions. The oxidation affects primarily the divinylbenzene part of the polymer, resulting in the dehydrogenation of styrene chains. During the carbonization and activation the additional cross-linking of polymer followed by condensation of pyridinic rings occurs (Fig. 8). Finally, the condensed heteroaromatic structure, containing 1.5-3.5 wt% nitrogen is obtained.

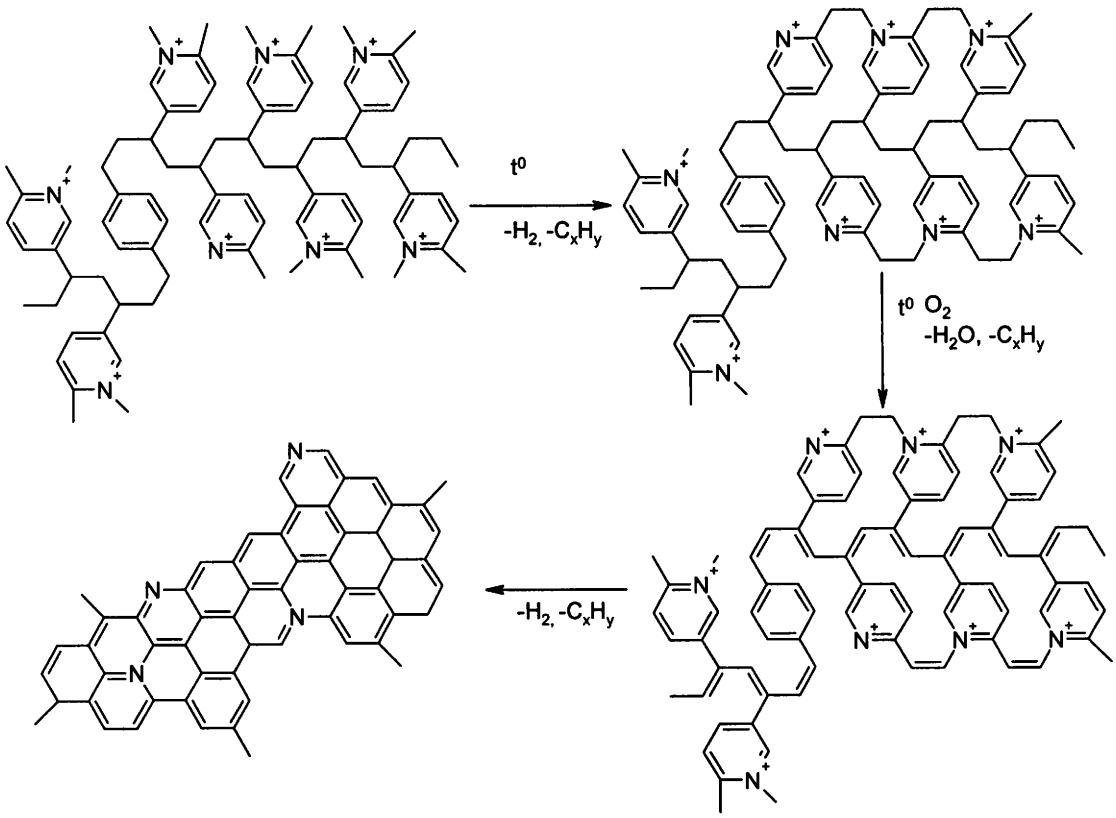

Fig. 8. Scheme of thermal transformation of vinylpyridine-divinylbenzene co-polymer (Kartel and Puziy, 1996).

Co-pyrolysis of pitches with polymers

The interest in the co-pyrolysis of pitch-polymer mixtures arose recently from the concept of disposing waste plastics by the treatment with coal-tar pitch at ~350^{0}C. A coal-tar pitch is a specific high boiling mixed solvent capable of dissolution under these conditions of most polymers. The resultant "reactive pitches" are considered as useful additives to coal blends for manufacturing of metallurgical coke (Collin et al., 1997).

The effect of variuos polymeric additives on the carbonization behavior and the optical texture of resultant carbonaceous residues was evaluated recently by Brzozowska et al., (1998) and Machnikowski et al. (2002a). Typically, the addition of polymers resulted in an acceleration of mesophase unit growth in the early stage of its developing, and, at the advanced stage, in an increase in proportion of disordered matter in the optical texture. Thus, the enhanced heterogeneity of the optical texture of composition cokes is observed. The effects of co-pyrolysis of polymers with coal-tar pitch do not follow the additivity rule in terms of the carbonization yield. Different

physical and chemical interactions between degradation products of polymers and pitch molecules are proposed as an explanation of the behavior occurring during co-pyrolysis.

The large scale application of polymeric precursors as a source of nitrogen containing carbons is limited by their high cost. A possible solution seems to be the pyrolysis of N-compounds in the pitch matrix. The co-pyrolysis of pitch with melamine resin was recently evaluated as a way of the preparation of nitrogen enriched activated carbon fibers (Raymundo-Piñero et al., 2002). The method consists in blending of the pitch with the polymer at 350^{0}C followed by the spinning and the oxidative stabilization of the resultant fibers. Finally, the carbonization at 1000^{0}C and the activation with CO_2 at 850^{0}C led to the carbon fibers having similar nitrogen content to the commercial PAN fibers and the same surface area. The increase in the softening point of the pitch after mixing with melamine proves that interactions between both materials occur, though it is not related with any significant change in the distribution of nitrogen functionalities as compared to the single treated polymer.

2.2.2. Catalytic carbonization of heteroaromatic compounds

Mochida with coworkers have developed the method of the preparation of nitrogen enriched carbons from pure heteroaromatic hydrocarbons using $AlCl_3$ as a Friedel-Craft type catalyst. The precursors used for the synthesis of nitrogen containing pitches were quinoline and isoquinoline (Mochida et al., 1995a, Mochida et al., 1995b, Mochida et al., 1999); diazanaphtalenes: quinoxaline, quinozaline and phtalazine (Mochida et al., 1996). The process comprised of two stages. First, the synthetic N-pitches were prepared by the catalytic polymerization at 240-300^{0}C. Next, the N-pitches were carbonized at temperatures in the range of 700-1200^{0}C. The authors observed a distinct effect of nitrogen position in the aromatic ring of precursor molecules on the condensation reactions as well as nitrogen content, optical texture and basicity of carbonization products. The condensation reactivity during the preparation of pitch was promoted by the presence of nitrogen atoms at the α position in the aromatic ring. Isoquinoline with nitrogen located at the β position gave much smaller pitch yield (11 wt%) than quinoline containing α nitrogen (75 wt%) (Mochida et al., 1995a).

It was also found that nitrogen occurring at the α position is preserved at a higher extent during the heat-treatment than β nitrogen. The carbonization of the quinoline pitch was accompanied by a rather gradual nitrogen evolution below 1000^{0}C, but by a rapid loss of this element above the temperature. The calcination at 1200^{0}C of

synthetic N-pitches gave the solid residue with nitrogen content of about 3 wt%. (Mochida et al., 1999).

The cokes prepared by carbonization of pitches derived from β-nitrogen containing precursors show distinctly higher basicity than those from precursors having α nitrogen (Mochida et al., 1996). The explanation of so different properties supplies the chemistry of catalytic condensation. The reaction occurs only at α position, capturing most of the α-nitrogen atoms in the condensed rings as the quaternary nitrogen. Consequently, in carbons from the isoquinoline, quinazoline or phtalazine derived pitch most of nitrogen should be located at the periphery of condensed units (pyridinic nitrogen) due to β-position in the precursor molecule.

The position of nitrogen in the precursor molecule has a great influence on the optical texture. It is interesting that pitches prepared from a α-nitrogen containing precursor exhibit a large proportion of coalesced anisotropic spheres in the isotropic matrix, while others, having nitrogen at the β position are basically isotropic (Mochida et al., 1995a). Further carbonization of α-N and β-N containing pitches gives cokes exhibiting the large flow domain and very fine mosaic textures, respectively. Obviously, the former cokes show high graphitizability, while the latter do not, reflecting their anisotropy.

The synthesis method of N-carbons based on heteroaromatic precursors has been developed by using nitro co-catalysts (Mochida et al., 1995b). Addition of such solvents as nitroethane or nitrobenzene distinctly enhances the pitch yield and improves the nitrogen retention during carbonization. The resultant cokes exhibit much higher basicity than those obtained from the pitch synthesized without the co-catalyst.

Synthetic pitch derived N-carbons were tested in terms of their application as the anode material in lithium-ion batteries. The anisotropic char prepared from the quinoline pitch at 700^0C showed much lower discharge capacity than that derived from naphthalene pitch, whereas the inverse situation was observed in the case of the carbons prepared at 1000^0C and above (Mochida et al., 1999).

2.2.3. Ammonization and ammoxidation

The ammonization and ammoxidation are the methods of nitrogen doping consisting in the treatment of carbonaceous materials with ammonia and ammonia-air mixture, respectively. Nitrogen can be incorporated effectively at relatively mild temperatures, typically 200^0-450^0C. Both methods have been recognized as an efficient

way of enrichment in nitrogen in the case of such precursors as activated carbons (Jansen and Bekkum, 1994, 1995, Xie et al., 2000), lignites (Andrzejak and Wachowska, 1970; Jurewicz et al., 2002), pitches and mesophase (Wachowska et al., 2000).

The intrinsic feature of the ammonization and ammoxidation of activated carbons is the nitrogen incorporation taking place at the available surface of particles only, leading to the non-uniform distribution of nitrogen throughout the bulk of sample. The concentration of nitrogen at the surface calculated according to XPS data is about three times higher than this determined for the bulk of samples by elemental analysis (Jansen and Bekkum, 1994). This aspect of ammoxidation was not discussed in the case of lignite and mesophase.

It has been shown by Jansen and Bekkum (1994) that the oxidation of carbons with diluted nitric acid prior to the reaction with ammonia has a beneficial effect on the amount of introduced nitrogen. It is believed that nitrogen can be fixed by the reactive carboxylic groups which are formed by the oxidation of side groups as well as of the ring system. As reported by Xie et al. (2000), the activated carbon treated with 5N nitric acid adsorbs more ammonia and more strongly than the untreated sample. TPD and Boehm titration studies show that the preoxidized sample has a high concentration of at least three types of acidic surface groups: strong carboxylic groups, phenolic groups and lactones. During the ammoxidation the reaction is expected to occur only at aliphatic substituents on the aromatic ring system.

Fig. 9 presents a variety of nitrogen groups chemically bound to the carbon surface mostly by the aliphatic side groups.

The reaction pathways leading to the creation of pyrrolic and pyridonic surface groups by the ammonization of oxidized activated carbon is given in Fig. 10. In the first stage, the reaction of ammonia with one or more carboxylic groups may lead to amides, lactams and imides. The following heat-treatment results in the dehydration, decarboxylation or decarbonylation of the intermediates to give pyrroles and pyridines, possibly through nitriles.

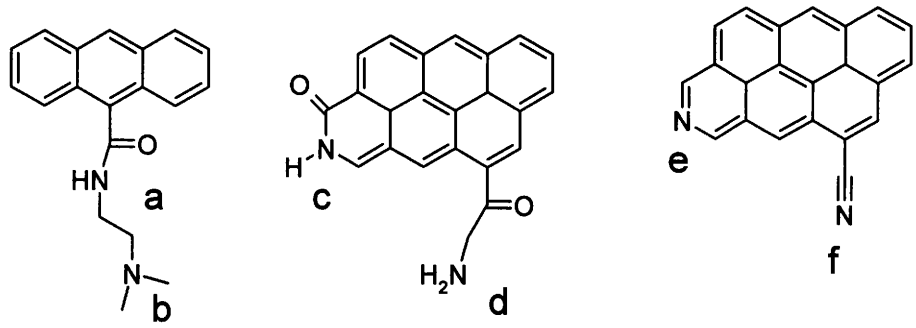

Fig. 9. Types of nitrogen functionalities created on activated carbons during ammonization and / or ammoxidation : (a) N-alkylamide, (b) tertiary amine, (c) lactam, (d) amide, (e) pyridine and (f) nitrile (Jansen and Bekkum, 1994).

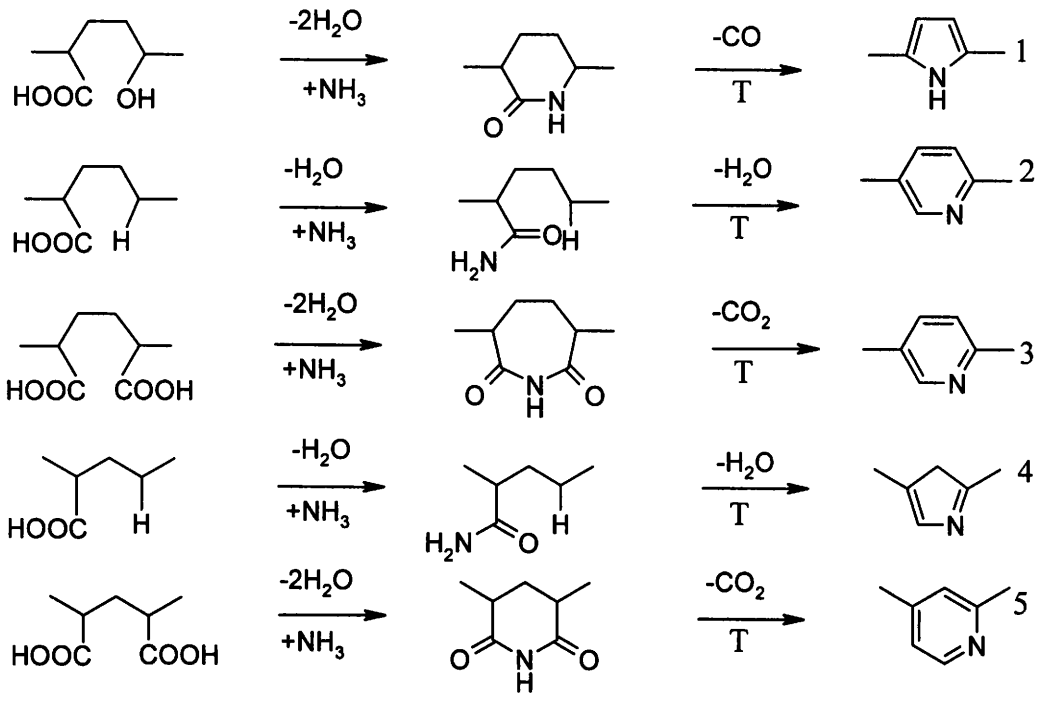

Fig. 10. The ammonization reaction pathway of carboxylic groups most frequently occurring on the edge of a basal plane:

(i) reaction with ammonia gas, resulting in amide- (2 and 4), imide- (3 and 5), and lactam- (1) groups, (ii) heat treatment resulting in pyrroles (1 and 4) and pyridines (2,3 and 5) (Jansen and Bekkum, 1994).

A measure of the efficiency of ammonization and ammoxidation treatment is the nitrogen content in the final product. For a given precursor the extent of nitrogen

incorporation depends significantly on the process variables, in particular ammonia/air ratio, temperature and time of treatment, preoxidation used. Among different carbonaceous precursors studied the lignites were most readily ammoxidized. The product containing up to 25 wt% of nitrogen could be obtained using relatively mild conditions: ammonia / air ratio 1:3, temperature 250^0C (Andrzejak and Wachowska, 1970).

Moreover, Jurewicz et al. (2002) have reported that the calcination and activation of ammoxidixed brown coals performed at 700^0C gives the carbons of still considerably high nitrogen concentration (13.2 and 9.6 wt% respectively).

In the case of activated carbons, the study of Jansen and Bekkum (1994) show that ammonization yields a somewhat bigger content of nitrogen than ammoxidation (4.4 wt% and 3.2 wt%, respectively). The ammoxidation temperature is the parameter which most strongly affects the nitrogen concentration. Optimal conditions for the nitrogen incorporation into the carbon surface were: T = 420 ± 20^0C, NH_3/O_2=2/5.

Wachowska et al. (2000) studied the ammoxidation of pitches and pitch derived mesophase. The optimum conditions established for the materials comprised heat-treatment at 250^0C in the ammonia-air mixture of 1:4 ratio. It has been shown that the nitrogen incorporation was increased in the case of preoxidized with HNO_3 samples. Moreover, the origin of pitch had an essential influence on the susceptibility to oxidation and ammoxidation. The highest level of incorporated nitrogen was noted in the case of pitch from coal hydrogenation and spherical mesophase (about 9 wt%). The least reactive was petroleum pitch (nitrogen content of 2.5 wt%). Carbonization (900^0C) products derived from the ammoxidized pitches contained up to 4 wt% of nitrogen.

2.2.4. Other methods of preparation of nitrogen enriched carbons

Another possible way of preparation of nitrogen enriched carbons is the treatment of carbonaceous precursor with a nitrogen-containing reagent in a condensed phase. Bimer et al. (1998) studied the reaction of lignites with ammonium carbonate, hydrazine, hydroxylamine and urea in an autoclave at elevated temperature (300^0C) in terms of preparation of active carbons for sulfur removal. The reaction with urea led to the highest level of nitrogen (13 wt%) in association with a good thermal stability of the created functionalities during the following carbonization and activation. The treatment with other N-reagents appeared less efficient due to the formation of thermally unstable nitrogen functionalities like lactams, amides and nitriles.

A high reactivity of urea was confirmed by the study of Cagniant et al. (1998) and Burg et al. (2002).

Chemical vapor deposition (CVD) using hydrocarbon and nitrogen containing gas mixtures has been studied extensively over the years as a method of preparation of nitride films. The process is of interest for three different areas: (1) the production of β-C_3N_4, the compound expected to have a hardness similar to or greater than that of diamond; (2) the manufacturing of such electronic components as the electron emitters in the flat panel displays; (3) the search for a better understanding of the diamond growth process.

The amount of introduced nitrogen depends primarily on the used source of this element. The nitride films containing up to 3 wt% of introduced nitrogen were obtained using molecular nitrogen in methane – hydrogen mixture (Zhang et al., 1999). In attempts to increase the incorporation of nitrogen ammonia and urea were used as a source of nitrogen (Baranauskas et al., 1999).

2.3. Nitrogen functionalities in carbonaceous materials

The understanding of nitrogen functionalities present in carbonaceous materials and their transformation during heat-treatment in an inert and oxidative atmosphere has received a considerable attention during last twenty years. There are at least two goals of the research activity. First, to establish a link between the nitrogen functionalities occurring in fossil fuels and NOx emission during combustion (Kambara et al., 1995, Wójtowicz et al., 1995). Second, to understand the possible role of nitrogen, particularly its concentration and functionality in the designing of carbonaceous materials with superior catalytic and adsorptive properties (Boehm et al., 1994, Stöhr et al., 1991).

2.3.1. The role of X-ray photoelectron spectroscopy in the identification of nitrogen functionalities

The analytical methods most useful for analysis of nitrogen functionalities in carbonaceous materials are X-ray photoelectron spectroscopy (XPS) and, to a lower extent, X-ray absorption near-edge structure (XANES). The applicability of XPS as well as the spectra fitting procedures have been greatly improved within the last years. The study of model compounds and their chars resulted in the assigning of the measured

peak binding energies to particular state of nitrogen atom (Stańczyk et al., 1995; Schmiers et al.; 1999; Pels et al., 1995).

Various forms of nitrogen functionalities identified in the carbonaceous materials and generally accepted values of their binding energy are presented in Fig. 11.

One must take care with the assignment of binding energy (BE) to a particular nitrogen bonding state. The uncertainty is caused by the spread, from 248.6 to 285.2 eV, of values which are reported in the literature for the C1s photoelectrons being commonly used for the referencing purposes (Seah, 1990). This results in a relatively broad range of BE values proposed in literature for a given functionality.

The unsolved problem is the assigning of components of BE about 400.5 and 401.4 eV. The former can be ascribed to nitrogen occurring in the 5-membered ring of pyrrole as well as to nitrogen occurring in the oxygenated derivative of pyridine, so called pyridone. Pyridone exists in two tautomers, with the more abundant carbonyl lactam form. Pyridone exhibits a BE shift relative to the pyridinic nitrogen due to a different charge distribution. In the case of pyridinic-N, the nitrogen atom contributes one p-electron to the aromatic π-system, and has a lone electron pair in the plane of the ring, while for pyridone-N, the nitrogen atom contributes two p-electrons to the π-system, and a hydrogen atom is bound in the plane of the ring. The chemical environment of the nitrogen atom in pyridone is similar to pyrrolic-N. Within the accuracy of XPS measurements, these two forms cannot be distinguished. The distinction between pyrrolic and pyridonic structures can be achieved by means of XANES (Zhu et al., 1996).

The component of N1s spectra with the BE of 401.4 eV is commonly believed to represent some forms of quaternary nitrogen (N-Q), defined as a nitrogen atom with a formal charge of +1 (Lahaye et al., 1999b). The exact nature of the quaternary nitrogen is not clearly established. This spectrum component can be attributed to more than one functionality. According to Buckley (1994), it can represent the protonated pyridinic-N. Kelemen et al. (1994) suggested that N-Q reflects a form of pyridinic-N which is protonated through formation of a H-bridge with an adjacent or nearby located hydroxyl or carboxyl group. The most common opinion is, however, that quaternary nitrogen in chars is represented by atoms substituting carbon in the aromatic graphene structure. This form is slightly more positively charged and resembles quaternary nitrogen in ammonium ions (Kelemen et al., 1998).

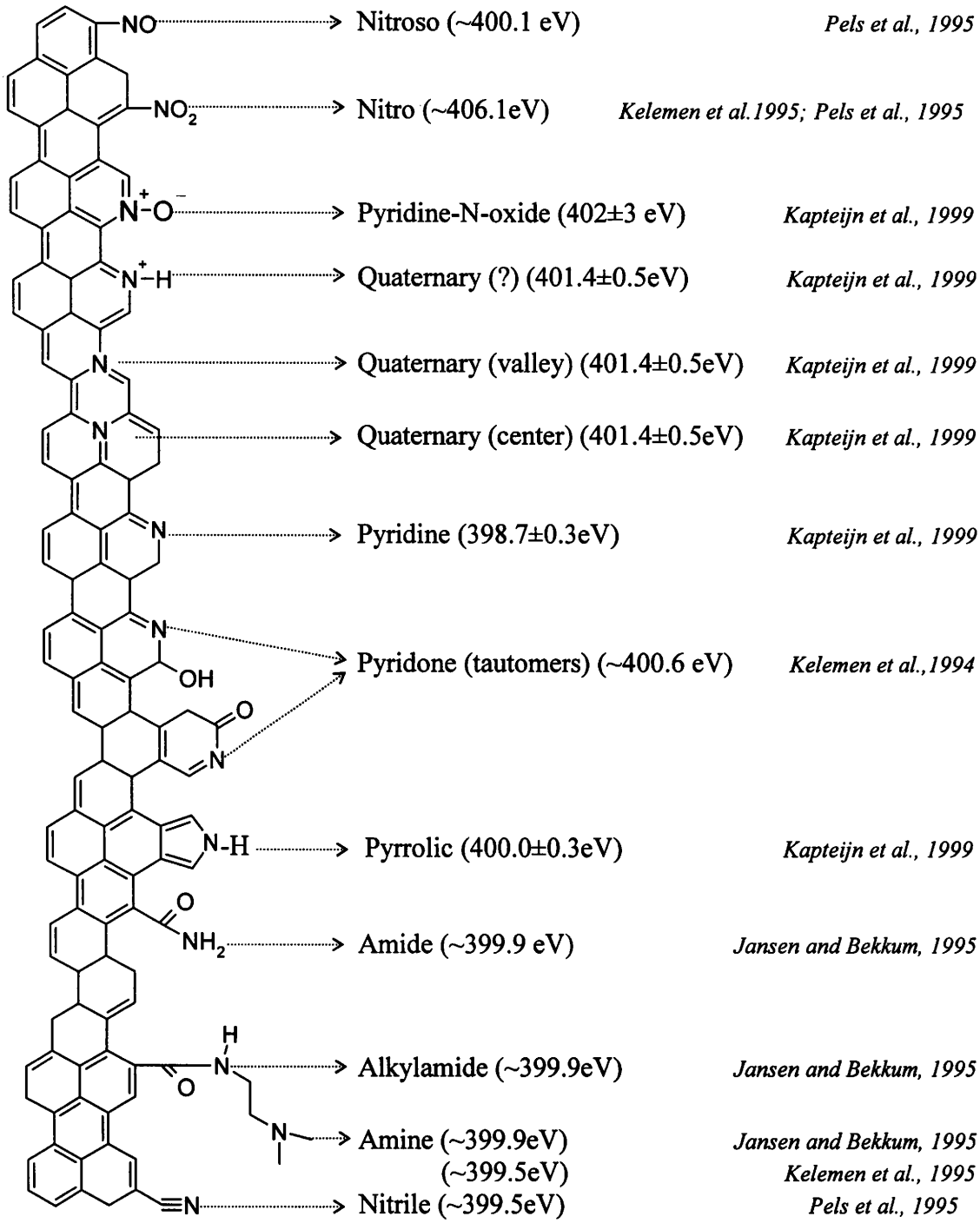

Fig. 11. Types of nitrogen functionalities occurring in carbonaceous materials with reported binding energy.

Using ab initio calculations, Pels et al.(1995) computed the effective charge of nitrogen atoms as a function of their positions in the perinaphtene-type structure. The difference between the charge on the valley N and pyridinic N reflects that observed in

BE of pyridinic and quaternary N. Though the theoretically calculated BE for centre N in perinapthene (399.2 eV) differs from the measured value, one should be cautious with the limitation of quaternary nitrogen to just the valley form. As shown by Boutique et al. (1984) a change in binding energy not necessarily has to be proportional to a change in charge. Consequently both "valley" as well as "centre" forms can account for the quaternary nitrogen in chars.

2.3.2. Nitrogen introduced by ammonization and ammoxidation

The chemistry of nitrogen functionalities introduced on the surface of carbonaceous materials using ammonization and ammoxidation was studied in details by Jansen and Bekkum (1994; 1995). The treatment of activated carbons with ammonia or ammonia-air mixture in rather mild conditions results mostly in the formation of thermally unstable nitrogen functionalities like amides, lactams and imides. The amide-lactam-imide ratio depends on the method used. The ammoxidation mainly gives rise to the amide formation, whereas during the ammonization the synthesis of imide and lactam groups is favored. Thermally more stable pyrrolic and pyridinic groups constitute about 20% of the total nitrogen introduced under conditions of both methods.

A decomposition model for the nitrogen–containing surface groups obtained by ammonization and ammoxidation is given in Fig. 12.

Upon the heat-treatment these thermally unstable groups are converted gradually into pyrrolic and pyridinic surface groups. With the increase in the temperature of carbonization, there is a shift in the BE, from a value close to that of lactam, imide and amide to one close to that of pyridine. The N1s signal of samples calcined at 1000^0C solely consists of contribution from the pyridine- and pyrrole- type heteroaromatic groups. Amides are regarded as least stable and are fully converted or decomposed about 600^0C (Jansen and Bekkum 1994; 1995; Schmiers et al., 1999). A possible decomposition route of amides is via nitriles, which are reported to remain unchanged after treatment at 460^0C (Stańczyk et al., 1995). The conversion of amides into pyrroles and pyridines can proceeds through lactam structures which are detected after the treatment at 800^0C. Lactams can be also formed by the decarbonylation of imides.

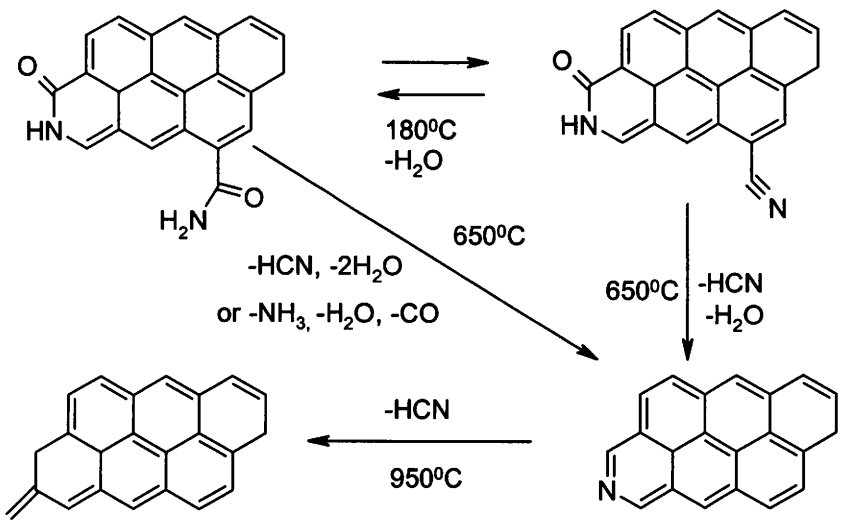

Fig. 12. Thermal decomposition model for nitrogen-containing surface groups that are formed during ammonization/ammoxidation at temperatures between 200 and 400°C (Jansen and Bekkum, 1994).

Lactams and imides constitute major population of nitrogen functionalities formed in ammonization below 400°C. At higher temperatures, pyridine- and pyrrole-type nitrogen-containing functional groups are most abundant.

The decomposition of amides, lactams and imides is accompanied by the evolution of HCN. The temperature programmed desorption (TPD) gives two maxima in HCN evolution – around 600°C and around 900°C. The maximum at lower temperature should be attributed to the decomposition of amides. The degradation of lactam and imide groups can account for HCN desorption around 950°C. Also a part of the pyridinic (and pyrrolic) surface groups decomposes upon treatment at 950°C.

2.3.3. Nitrogen in carbonaceous materials produced by pyrolysis of organic precursors

Nitrogen left in a char derived from the pyrolysis of natural or synthetic organic matters occurs mostly as a part of the condensed ring system. Four or five types of nitrogen functionalities are usually distinguished in the char using XPS method: pyridinic (N-6) (398.7±0.3eV), pyrrolic/pyridonic (N-5) (400.3±0.3eV), quaternary (N-Q) (401.4±0.5eV), and oxidized pyridinic nitrogen (N-X) (402±3eV) (Kelemen et al., 1999). Based on the study of pyrolysis of model compounds including acridine, carbazole and polyacrylonitrile, Pels et al.(1995) proposed a consistent and generally

approved scheme of the transformation of nitrogen functionalities during a severe heat-treatment. Fig. 13 presents the fate of ring-bounded nitrogen during the pyrolysis in an inert atmoshere.

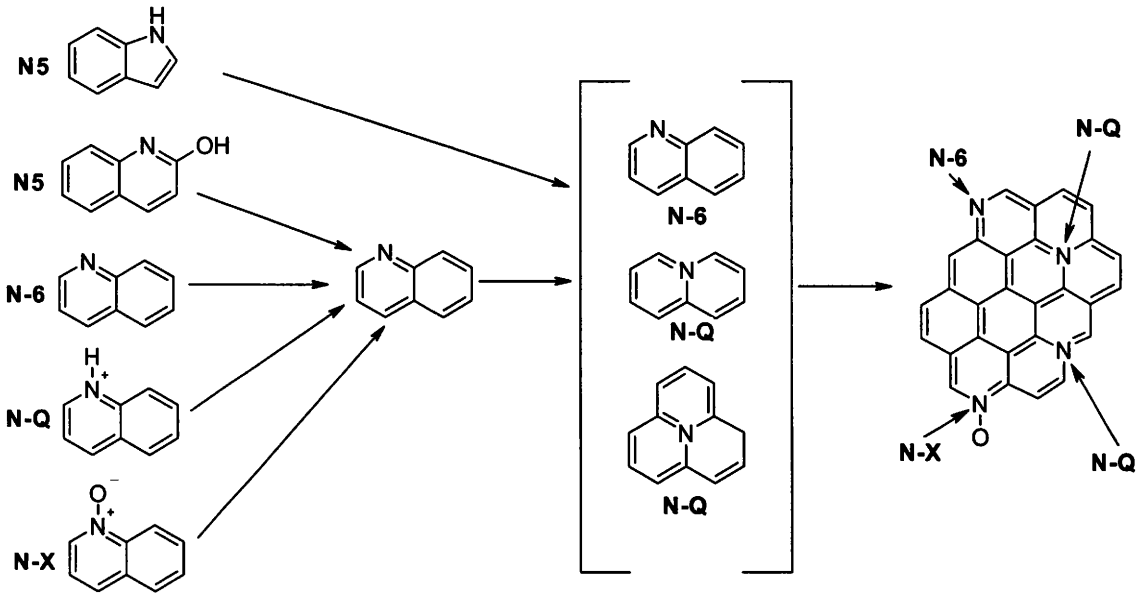

Fig. 13. Evolution of nitrogen functionalities in carbonaceous materials during heat-treatment (Pels et al., 1995).

It is assumed that pyridonic-N and protonated pyridinic-N are responsible for a considerable intensity of N-5 and N-Q peaks, respectively, in the XPS spectra of lignites (Pels et al., 1995) and coals (Kelemen et al., 1994). Under mild pyrolysis conditions (below 450^0C) a distinct decrease in N-5 and N-Q peaks in favor of N-6 one is observed.

Nitrogen present in pyrrolic rings has been reported by Pels et al. (1995) to be stable at the temperature as high as 600^0C. Above that temperature N-5 disappears gradually being converted by the ring expansion to N-6 and N-Q. The peak of quaternary nitrogen appearing at that temperature should be attributed to nitrogen atoms in the graphene layers in the position "valley" – adjacent to two carbon atoms or in the position "center" – bonded to three carbon atoms. The amount of the quaternary nitrogen increases as a result of pyrrolic groups transformation as well as condensation of pyridinic rings. The latter process commences at relatively low temperature, non-exceeding 450^0C. The difference between onsets of both kinds of condensation is

attributed to a better alignment of 6-membered pyridinic cycles compared to five-membered pyrrolic. Moreover, none C-C bonds need to be broken in N-6 condensation. The scheme of condensation reactions involving 5- and 6-membered ring structures is given in Fig. 14.

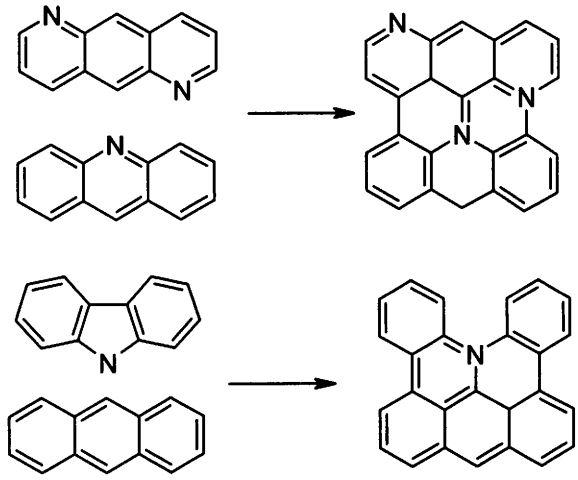

Fig. 14. Scheme of condensation reactions involving 5- and 6-membered ring structures (Pels et al., 1995).

It should be noted that the general approach proposed by Pels et al.(1985) does not conform fully with the polyacrylonitrile pyrolysis. In the case of chars of polyacrylonitrile heat-treated at about 600^{0}C, the quaternary nitrogen, if ever observed, constitutes less than 10% (László et al., 2001). Wu and coworkers (1999) deconvoluted the N1s spectra of PAN heat-treated at 600^{0}C to only two peaks at the positions of 398.5 eV and 400.2 eV. Though the latter peak was attributed to the quaternary nitrogen, the assignment of component to pyrrolic-N seems to be more appropriate.

Pels et al. (1995) stated that in chars obtained by the pyrolysis of N-precursors above a particular temperature (600^{0}C for acridine) the ratio of N-6/N-Q remains unchanged. Furthermore, in the cited study all chars prepared at severe pyrolysis conditions (1000^{0}C) from different polymeric precursors gave very similar N1s spectra. This implies that the molecular structure of a char precursor is not relevant for the final distribution of char-bound nitrogen.

2.3.4. Effect of oxidative atmosphere on nitrogen evolution

Chars derived from N-precursors are susceptible to oxidation. Upon exposure to air, oxygen reacts with the pyridinic cycles present in the char to form pyridine-N-oxides (402-405eV) or pyridone (Pels et al., 1985). The chars prepared between 350 and 650^{0}C seem to be most reactive. The chars treated at a higher temperature have a more condensed structure and thus are less sensitive to oxidation, which takes place at the edges of graphene layers.

As has been recently observed by László et al. (2001), the activation of PAN based char with a steam at 900^{0}C (burn-off ca. 50 wt%) results in a significantly modified distribution of nitrogen functionalities. During the high temperature treatment the five-membered pyrrolic rings are converted into 6-membered by the ring expansion. In the presence of water vapor, the pyridinic-N is oxidized to N-oxides and pyridones. The latter compounds contribute to the N-5 signal in the XPS spectrum. The contributions from both the reactions result in a constant proportion of N-5, the most significant effect of activation being a three-fold increase in N-Q concentration at the expense of pyridinic nitrogen.

Another effect of severe thermal treatment is a pronounced release of nitrogen. In the case of calcination and activation of PAN at 900^{0}C the nitrogen percentage decreases from 24 wt% in the parent polymer to 9.4 and 5.3 wt%, respectively. Based on these results authors suggest that carbonaceous materials contain the majority of heteroatoms in the amorphous phase, which is preferentially eliminated during activation process. In the PAN samples, the burn-off of the amorphous part goes simultaneously with an intensive nitrogen release as well as with the extension of graphitic region (László et al., 2001).

The elimination of nitrogen from 6-membered rings, being the predominant form in high-temperature chars commences at about 950^{0}C (Jansen and Bekkum, 1984; Pels et al., 1985; Li et al., 1998). Nitrogen is released mostly in the form of hydrogen cyanide (HCN) and ammonia (NH_3) (Kambara et al., 1995). The formation of HCN and NH_3 during severe heat treatment is still poorly recognized problem. Schmiers et al.(1999), based on the study of pyrolysis of model compounds presume that HCN is formed from ring fragments in a primary step, while NH_3 is synthesized after further reactions with hydrogen or water. Nevertheless, which nitrogen functionalities tend to be released as hydrogen cyanide or as ammonia is still an open question.

2.4. Surface and bulk properties of nitrogen doped carbons

The presence of nitrogen atoms affects both the surface and bulk properties of carbonaceous materials. The properties being influenced by the presence of nitrogen functionalities comprise porosity (László et al., 2000), graphitizability (László et al., 2001), polarity of the carbonaceous solids (Lahaye et al., 1999a), heterogeneity in terms of the hydrophobic/hydrophilic behavior (László et al., 2001), acid- base properties (Jansen and Bekkum, 1984, László et al., 2001, Li et al., 2002).

The distribution of nitrogen throughout the carbon sample is closely dependant on the doping method used. The preferential enrichment with nitrogen of the surface layer during the ammoxidation and ammonization leads to three fold higher nitrogen concentration in the surface as compared to the bulk of sample (Jansen and Bekkum, 1994). Conversely, Nakahashi et al. (1998) demonstrated uniform distribution of nitrogen in carbons obtained by pyrolysis of nitrogen-containing polymer films.

The ammonia and ammonia-air treatment during ammonization/ammoxidation of activated carbons when performed at moderate temperature appears to have rather little effect on pore volume and pore size distribution (Jansen and Bekkum, 1984, Li et al., 2002). The negligible changes in pore structure are attributed to the creation or removal of functional groups on or from the surface of the almost-unchanged carbon framework. Upon heat-treatment (up to 600^0C) of ammoxidation and ammonization products, the BET surface area increases. Two surface processes can account for this effect: (1) the enlargement of pores by the removal of functional groups from the inside of pore walls and, (2) the enhancement of the pores accessibility by the removal of functional groups from the blocked pore mouths.

In the case of ammonization conducted for a long time and/or at a high temperature, the increase in the BET surface area, micropore volume and average pore width is observed (Mangun et al., 2001). It is assumed that ammonia behaves at about 800^0C as an etchant, thus increasing the pore size and surface area.

Ammonization and ammoxidation enhances the basicity of carbons (Li et al., 2002; Jansen and Bekkum, 1984). The isoelectric point obtained from the acid-base titration reflects the balance between acidic and basic surface groups. In general, an oxidation with nitric acid prior to the gas phase treatment decreases the isoelectric point due to the formation of such acidic oxygen functionalities as carboxylic and phenolic

groups (Figueiredo et al., 1999, Li et al., 2002). This is in agreement with the significant amount of CO_2 desorbing during TPD experiment (Jansen and Bekkum, 1984). The ammoxidation and ammonization increases the isoelectric point due to the formation of basic nitrogen moieties of pyridine-type structure (Li et al., 2002). The isoelectric point determined for the ammoxidized carbons is between 8-9 with a slight influence of the number of carboxylic groups on the carbon. The heat treatment of the nitrogen-enriched carbons affects the acidic oxygen moieties to a greater extent than nitrogen functionalities. The evolution of carboxylic groups commences at about 200^0C, while condensed anhydride or lactone forms are lost at approximately 500^0C. Contrarily, the nitrogen-containing groups introduced by ammoxidation decompose at distinctly higher temperature as can be deduced from the maximum rate of the HCN desorption at 950^0C (Jansen and Bekkum, 1984). As a consequence of different thermal stability of nitrogen and oxygen groups the isoelectric point shifts with the increasing treatment temperature to a higher value, clearly indicating the conversion of acidic character of the carbon surface into a more basic one.

It should be taken into account that the basic character of activated carbons rises primarily from the π-electrons which are delocalized on the condensed polyaromatic sheets (Leon y Leon and Radovic, 1994). These electron-rich Lewis base sites develop as oxygen is removed from the activated carbon surface, e.g. by the heat-treatment in an inert atmosphere. Thus, the thermal treatment not only removes acidic groups, but also other oxygen-containing functionalities that decrease the basicity of activated carbons by attracting and localizing π-electrons of the condensed polyaromatic sheets.

The properties of carbons prepared from different polymeric precursors depend on the starting polymer. It was reported, that nitrogen containing synthetic carbons (SCN-type carbons) being produced from mesoporous copolymer of vinylpyridine with divinylbenzene as cross-linking agent, preserve the mesoporous texture upon carbonization and steam activation (Bagreev et al, 1996, Lahaye et al., 1999a). Hence, the development of mesoporosity in the SCN carbons can be readily controlled by the porosity of precursor. In many cases the polymer derived carbons are microporous and the activation process results in significant increase of the adsorption capacity by altering the pore size and increasing the pore volume (László et al., 2000). The striking enhancement of the adsorption capacity occurs upon steam activation of PAN derived carbons. The specific surface area of the activated PAN increases up to 540 m^2/g from about 7 m^2/g measured for the carbonized polymer. The carbonized PAN exhibits the

low pressure hysteresis characteristic of a non-rigid structure. This type of hysteresis is connected with retarded adsorption, as the adsorbing and desorbing molecules have to overcome a definite energy barrier. This barrier can arise from the presence of narrow pores, penetration in which is difficult due to the steric hindrance. In the case of PAN-derived pyrolyzed sample, the adsorption and desorption branches run parallely, i.e. there is a more or less constant extent of nitrogen hindered desorption. The activation with steam not only opens new pores but also gasifies the amorphous part of carbon blocking the pores accessibility. This results in the suppression of low pressure hysteresis. Activated PAN shows an isotherm of type I characteristic of mainly microporous material.

László et al. (2001) studied the benzene-methanol adsorption on carbonized and activated forms of PAN derived carbons. The S-shape of the resulting isotherms proves the hydrophobic/hydrophilic character of the surface in both materials with a distinct increase of the hydrophobicity on activation. Authors suggest that the change of surface character is an effect of the extension of the condensed ring systems, which is promoted by the high temperature of activation. The organization of the crystalline part of activated PAN carbon is reported to be close the graphitic structure.

The acid-base titration shows shows both acidic and basic, i.e. amphoteric character of activated nitrogen-containing carbons (László et al., 2001). With the progress of steam activation the basicity of surface increases. The activated PAN contains both Brönsted and Lewis type basic sites. The former include nitrogen functionalities developed on the edge of carbon layers, which are active in proton acceptor-donor reactions, while the latter are attributed to the presence of π-electrons in the graphitic part of the surface (Contescu et al., 1998).

As reported by Lahaye et al. (1999a) the presence of nitrogen in a carbonaceous material greatly enhances the surface polarity. The surface polarity index determined by flow calorimetric method (Groszek, 1987) is significantly higher in the case of SCN carbons than in carbons prepared from copolymer containing no nitrogen. The high polarity can be ascribed to the presence of nitrogen atoms having increased either negative charge (pyridinic nitrogen) or positive charge (quaternary nitrogen). Both the nitrogen forms play the role of polar sites on the carbon surface. A consequence of the enhanced polarity of SCN carbons is strong propensity to water sorption.

2.5. Perspective application of nitrogen doped carbons

The research activity in the field of nitrogen containing carbons is focussed mostly on the development of materials with advanced surface properties. The specific properties induced to the carbonaceous material by the presence of nitrogen, both as a substituent for carbon in the graphene layer or a functional group attached to the edge of ring system, are believed to widen the new fields of application in adsorption, catalysis and electrochemistry.

In the recent years the nitrogen enriched carbons were found as adsorbents revealing selective adsorptive properties towards such common gas by-products as SO_2, NOx and variety of volatile organic compounds (VOCs). In addition to the superior adsorption characteristics, N-carbons display the catalytic ability in various oxidation/reduction reactions playing a significant role in neutralizing of gas pollutants.

The SO_2 removal from gas is among the most extensively studied processes using porous carbons as catalyst. According to DeBarr and Lizzio (1995) the process includes the following steps: (a) SO_2 adsorption, (b) O_2 chemisorption, (c) SO_2 oxidation and (d) H_2SO_4 formation. The mechanism of SO_2 adsorption and catalytic oxidation to SO_3 has been widely discussed in the literature (Zawadzki, 1987a; 1987 b). In the presence of water vapor SO_3 reacts to give H_2SO_4, which is retained in the pores of material.

Bimer et al. (1998) assesed N-enriched carbons obtained by the reaction of coals and lignites with various nitrogen containing reagents in terms of the removal activity for traces of hydrogen sulfide and sulfur dioxide. The sulfur uptake and regeneration capabilities of activated nitrogen-enriched chars were similar or slightly superior compared to commercial activated carbons. The most efficient, in terms of sulfur removal, were activated carbons prepared by the reaction of the preoxidized subbituminous coal with urea. The SO_2 adsorption properties are influenced by the chemical nature of basic surface groups. The pyridinic and quaternary nitrogen groups, being basic in terms of Lewis definition, account for the high specific adsorption of sulfur species on nitrogen containing activated carbons.

Muñiz et al. (1998) in their study on the SO_2 retention on activated carbon fibers (ACFs) noticed an evident lack of correlation between SO_2 capacity and BET. Contrarily, the SO_2 adsorptive properties were well correlated with the surface basicity.

This is in agreement with earlier work of Carasco-Marín et al.(1992) who indicated that the increase in SO_2 adsorption capacity of carbon during activation is associated with the increase in the number of basic surface sites able to chemisorb SO_2. Based on these observations, the way to the improvement of SO_2 removal capacities leads through the introducing of basic groups instead of the developing of internal surface area. In relation with this fact Muñiz et al. (1998) have linked the relatively high SO_2 adsorption capacities of PAN-based ACFs with the enhanced concentration of pyridinic and quaternary nitrogen. The complete recovery of SO_2 adsorbed on the activated carbon can be achieved by heat-treatment at 600^0C under inert atmosphere. The high thermal stability of 6-membered nitrogen functionalities allows performing the number of sorption cycles without significant decrease in SO_2 removal capacity.

Recently, nitrogen-enriched carbons have been also tested in terms of the NO adsorption and catalytic reduction. At a commercial scale the selective catalytic reduction of NO is usually performed using TiO_2-type catalysts having vanadium oxide as the catalytic active phase. These catalysts exhibit a high conversion in the temperature range of 300-400^0C. In this temperature window, the flue gases have a high concentration of particulates and other contaminants (SO_2, As), which can cause deterioration, deactivation, and poisoning of the catalyst monoliths. Thus, there is a great interest in developing adsorbents and catalysts for selective reduction of NO at low temperatures where the gases do not carry particulates or sulfur oxides. The reduction of NO with NH_3 occurs efficiently at temperature of 300^0C. In the absence of oxygen the process can be summarized by the overall reaction (Ahmed et al., 1993):

$$6NO + 4NH_3 \rightarrow 5N_2 + 6\,H_2O$$

At temperatures lower than 250^0C a small concentration of oxygen is required for the efficient conversion of NO. The mechanism involves the oxidation of NO into NO_2 via heterogeneous route catalysed by the carbonaceous material:

$$Z^* + \tfrac{1}{2}\,O_2 \leftrightarrow Z(O)$$
$$Z(O) + NO \rightarrow Z^* + NO_2$$

Z^* is an active center which reacts with oxygen forming a reactive surface intermediate Z(O). Previous studies showed that the catalytic activity of carbons towards NO is influenced by the presence of hetereoatoms in the carbon lattice (Jüntgen et al., 1988). As suggested by Matzner and Boehm (1998), the Z^* centre could be

nitrogen substituting for carbon atoms in the carbon lattice. These nitrogen atoms have the extra electrons occupying the states of higher energy from where they can be transferred to adsorbed species forming reactive surface intermediates.

This scheme was confirmed in a more recent study indicating that at lower temperature NO_2 is adsorbed over centers with a basic character associated with nitrogen functionalities, whereas adsorption of NH_3 occurs on acidic centers related to the oxygen functionalities (Muñiz et al., 1999). The physical properties such as porosity, pore size distribution and surface area were found to have a minor effect on the catalytic activity, and only as long as they control the accessibility of the active centers to reactants.

One of the main characteristics, in terms of industrial application of carbonaceous adsorbents, is the capability of sorption of metallic cations from the aqueous solution. The removal of heavy metals from aqueous solution and the preparation of carbon supported metal catalysts are the most important examples of this field (Jankowska et al., 1983, Suh et al., 1993). The sorption capacity towards metallic cations is mainly influenced by the presence of oxygen and nitrogen functionalities (Abotsi and Scaroni, 1990). Biniak et al. (1997) demonstrated that the enhanced sorption capacity of ammonized carbons towards transition metal cations was induced by the presence of basic oxygen and nitrogen groups.

A recently reported example of N-carbon application is a catalytic dechlorination of 1,2-dichloroethane to produce vinyl chloride (Sotowa et al., 1999). A common industrial practice is the dechlorination by means of pyrolysis. The application of polyacrylonitrile derived activated carbon fibers as a catalyst was proposed as a way to overcome a number of drawbacks related with the industrial process, like the coke deposition and loses of the heat in transfer lines. The catalytic activity was attributed to the presence of basic pyridinic surface groups promoting the elimination of HCl. In contrast, quaternary nitrogen also existing on the PAN surface appeared to be non-active in the dechlorination.

One of the promising applications of carbonaceous materials is an anode in the lithium-ion secondary battery. The interactions during the lithium insertion/ deinsertion into the anode material, which are critical for the cell performance, depend on the electron donor/acceptor properties of carbon. The presence of nitrogen atoms can strongly modify these properties. Pyridinic nitrogen bound to two carbon atoms at the edge of graphene layer retains a lone pair of electrons inducing electron donor

properties to the layer. The quaternary nitrogen bound to the three carbon atoms is believed to generate a positive charge and acceptor properties (Koh and Nakajima, 2000). This may be explained by the localization of excess electrons around nitrogen resulting in an increase in the concentration of positive holes in the conduction band of the system (Inagaki et al., 1998). The study of various origin nitrogen containing materials does not present any generally approved view on the role of incorporated nitrogen on the lithium insertion/deinsertion behaviour.

Weydanz et al. (1994) reported that nitrogen containing carbons prepared by CVD from acetonitrile, pyridine and acetylene-ammonia mixture are not useful as anodes for Li-ion cells due to enhanced irreversible capacity and a shift of the cell capacity to lower voltages. The study of disordered PAN derived carbons revealed a reduction in charge capacity from 380 to 254 mAh/g but distinctly faster kinetics of the lithium insertion as the heat treatment temperature increased between 500 and 1000^{0}C (Yung et al., 1997).

Based on the comparison of polyvinylpyridine and polystyrene carbons, Wu et al. (1999) have demonstrated that those obtained from nitrogen containing polymers have higher discharge and charge capacity than carbons derived from precursors of similar structure but lacking the nitrogen moieties in the backbone. According to Wu and coworkers, nitrogen present in carbonaceous materials prepared at 600^{0}C from N-containing polymers is not involved in the reversible reaction with lithium and the reversible capacity increases with the content of nitrogen incorporated to the carbon lattice as the pyridinic groups, whereas the nitrogen occurring as the species of the binding energy of 400.2eV des not contribute to the increase in capacity.

Mochida et al. (1999) attributed the enhanced capacity of anisotropic carbon produced at 1000^{0}C from quinoline pitch compared to that from naphthalene pitch to the creation of new sites for lithium storage in vacancies left after nitrogen evolution and to the transformation of nitrogen atom state.

A very attractive recently developed field of application of carbon materials is the capacitor based on the charge storage in the electric double layer formed on the surface of electrode material. A suitable material for the electrochemical double layer capacitors (EDLC), in addition to the highly developed surface area must be characterized by a good wettability, a high electrical conductivity and resistance to the electrolyte attack (Frąckowiak and Béguin, 2001). These features result mainly from the structural and chemical composition of carbon material. Jurewicz et al. (2002) studied

the effect of ammoxidation of lignites on the performance of the resultant activated carbons as an electrode in EDLC. The beneficial effect of nitrogen was deduced from the threefold increase in capacity as nitrogen content was increased by only 50% with comparable surface area. The lack of the direct proportionality between nitrogen concentration and sample capacity suggests a meaningful role of the nature of nitrogen functionalities.

III. Objective

The general objective of the thesis is to explore the ways the synthesis of coal-tar pitch based carbons having nitrogen atoms substituted, for carbon in the lattice and to understand the structure and properties of the resultant materials.

The attention is focused in the research mostly on the understanding of following more specific aspects of the synthesis of nitrogen containing carbons:

- mechanisms of co-pyrolysis of coal-tar pitch with selected N-polymers, considered as a possible way of synthesis of carbonaceous materials of controlled structural ordering and nitrogen content
- efficiency of ammoxidation of pitch mesophase and pitch semi-coke in the manufacturing of highly anisotropic materials of enhanced nitrogen content
- behavior of the nitrogen containing low-temperature pyrolysis products during the subsequent heat treatment in an inert and oxidative atmosphere with a special attention focused on the porosity development and the evolution of nitrogen functionalities.

IV. Experimental

4.1. Scope of research

The way of producing of nitrogen enriched carbons used in this study can be, in principle, classified as a process of thermal conversion of organic precursors into solid carbon. In the monitoring such a process it is very practical to distinguish two temperature intervals. The low temperature stage (pyrolysis) lasts up to about 500°C when most of the primary thermolysis reactions are terminated and the structural and textural preorder of the solid residue (semi-coke), is basically established. The heat treatment above 500°C, usually up to 800-1100°C, i.e. the carbonization stage, implies the scission of the residual side groups from the aromatic lamellae as light volatile compounds and the consolidation of the basic structural units to form coke or char.

Similar approach has been used in this work. In the first step we studied the low temperature stage of the incorporation of nitrogen atoms into the structure of carbonaceous material. This includes the pyrolysis of N-polymers and their blends with pitch and the ammoxidation of pitch-derived materials. Further, the resultant nitrogen enriched semi-cokes, from the practical point of view the intermediate products, were treated in the inert or oxidative atmosphere, as appropriate, to produce corresponding structural or porous carbons.

Consequently, it seems reasonable to consider the research as consisting of three parts.

The first part (chapters 5.2 and 5.3) is concerned with the study on co-pyrolysis of coal-tar pitch with selected N-polymers (polyacrylonitrile and polyvinylpyridine). Oxidizing pretreatment is applied to increase the polymer residue yield. The interactions occurring during the co-pyrolysis are monitored using thermogravimetry (TG) coupled with Fourrier transform infrared spectroscopy (FTIR) of evolved gas and by Py-GC-MS. The semi-cokes produced from the pitch-polymer blends of various component ratios are evaluated in terms of optical texture and elemental composition and functionalities (elemental analysis, X-ray photoelectron spectroscopy - XPS, diffusion reflectance infrared Fourrier transform spectroscopy - DRIFT).

In the second part (chapter 5.4) nitrogen is introduced on the surface of carbonaceous mesophase and semi-coke, which are prepared by the pyrolysis of a coal-

tar pitch, using the treatment with ammonia-air mixture. The nitric acid oxidation is used in some cases to enhance the reactivity of surface toward ammonia. The ammoxidation products are characterized using the same methods as in part one.

The third part of the research (chapters 5.5, 5.6 and 5.7) comprises the thermal treatment of the nitrogen enriched semi-cokes (and mesophase) in the inert and oxidative atmospheres up to 800 or 1050°C. This part is focused on the understanding the evolution of nitrogen functionalities and the porosity development during the treatments with some preliminary evaluation of the final products as specific adsorbents and an anode material in the lithium-ion cells. The techniques used for the characterization of thermal behaviour and constitution of resultant products include thermogravimetry coupled with FTIR of evolved gas, elemental analysis, XPS and DRIFT. The porosity development is measured by the nitrogen adsorption / desorption at 77 K. A series of pitch-PAN cokes was in addition assessed in terms of the structural ordering (XRD, TEM), microporosity, including ultramicropore region (CO_2 adsorption at 298K), and electrochemical lithium insertion/deinsertion behaviour.

Scheme of the research performed in the thesis is presented in Fig. 15.

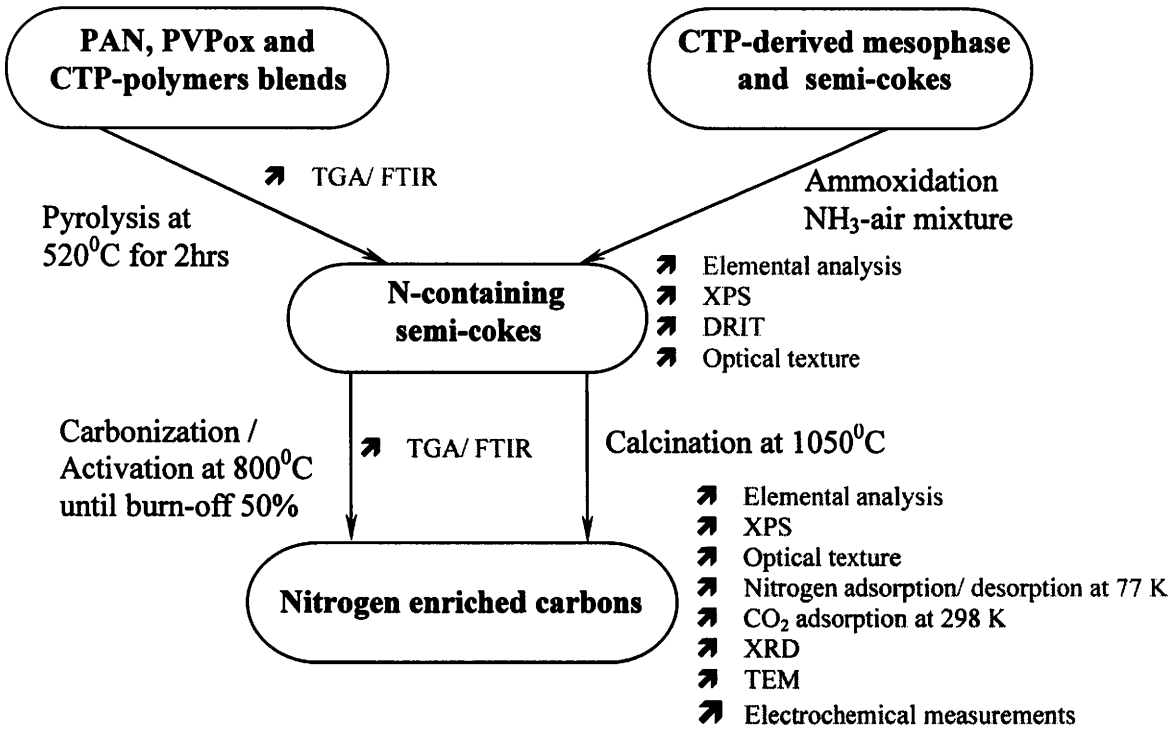

Fig. 15. Scheme of the research.

4.2. Raw materials

The raw materials for the research were coal-tar pitch (CTP), polyacrylonitrile (PAN) and poly(4-vinylpyridine) (PVP). The polymers were used in both the pristine and oxidized forms. The pitch used was quinoline insoluble free coal tar pitch. The pitch described as PMR was produced by bench scale distillation under reduced pressure of coke oven tar from Makoszowy coking plant, which was purified by centrifugation (Machnikowski et al., 2001). The basic properties of the pitch used are presented in Table 1.

Table 1. Characteristics of the parent pitch

SP, ^{0}C	CV, wt%	TI, wt%	QI, wt%	Elemental composition, wt%, daf basis					Atomic ratio	
				C	H	N	S	O[1]	C/H	O/C
99.6	47.0	15.3	0.0	92.50	4.81	0.85	0.34	1.50	1.60	0.021

[1]By difference

Polyacrylonitrile powder (PAN) was synthesized on a laboratory scale by the polymerization of acrylonitrile (Aldrich) in an aqueous solution according to the following procedure (Pielichowski and Puszyński, 1998). 80 g of acrylonitrile monomer was added to the 500 cm^3 glass flask containing 160 cm^3 of an aqueous solution of 1.6 g of ammonium persulphate and 1.12 g of sodium thiosulphate. The resultant solution was heated under reflux conditions during 6 hours. The crystalline product was washed with 3 dm^3 of 0.1N K_2CO_3 and dried.

For the preliminary study, polyvinyl(4-pyridine) cross-linked with 2 and 25 wt% of divinylbenzene (PVP2 and PVP25, respectively) was purchased from Aldrich. Poly(4-vinylpyridine) cross-linked with 25 wt% of DVB used in the larger scale preparative work was synthesized in the laboratory according to the following procedure (Pielichowski and Puszyński, 1978). 21 g of 4-vinylpyridine monomer and 4.4 g of DVB (Aldrich) were heated at 69-71^{0}C in the presence of 0.21g of benzoil peroxide as an initiator in the glass flask under reflux conditions during 6 hours. After the reaction the resultant crystalline product was washed by 2 dm^3 of 0.1N K_2CO_3 and dried.

The oxidized forms of the polymers (PANox, PVPox) were prepared by heating the parent polymers at 300^{0}C for 1h under air flow. The treatments were performed in a quartz tube placed in a tubular oven.

4.3. Procedures

Preparation of pitch-polymer blends

CTP-polymer blends of various components ratios were prepared by heating the physical mixtures of powders (30g) to 250°C at 5 K min^{-1} followed by soaking for 0.5 h in the inert atmosphere. The vigorous stirring ensured a homogeneous dispersion of polymer particles in the liquid pitch. The treatments were performed in a 45 mm diameter Pyrex retort placed in a vertical furnace which was coupled with a temperature control unit.

Pyrolysis

Two carbonization systems were used to prepare the samples of semi-cokes and mesophase.

For microscopic evaluation of carbonaceous products approximately 4 g samples of single components and blends were heat treated at 520°C for 2 hours in inert atmosphere. The treatment was performed in 19 mm diameter Pyrex test tubes in a vertical carbonization furnace, which was coupled with a temperature control unit. Heating rate was 5 K min^{-1}.

A larger scale (30g) runs were performed in the retort used for blend preparations. For semi-coke production the single components and blends ground below 0.3 mm were heated at 520^{0}C for 2h with a heating rate of 5 K min^{-1} and the stirring was maintained until the carbonized system was viscous. As the soaking was completed the retort was cooled down under argon to a room temperature and the solid residue was picked-out with a sharp chisel.

Carbonaceous mesophase was produced by heat-treatment of pitch (60g) at 430^{0}C for 8 hours. The molten pitch was stirred vigorously with an anchor-type stirrer during all the treatment.

Ammoxidation

The ammoxidation of semi-cokes and mesophase was performed in a 19 mm diameter Pyrex tube with a porous glass membrane (Fig. 16). A sample (3-4g), ground below 0.3 mm, was placed on the membrane and the tube was fixed in a vertical electric furnace. The stream of ammonia-air mixture of 1:3 volume ratio was flowing through the tube at a rate of 6 dm^3/ h. The ammoxidation runs were carried out isothermally for 5h at different temperatures in the range of 250-400^{0}C. The heating rate was 5 K min^{-1}.

The oxidation with 30% nitric acid prior to ammoxidation was used to enhance the reactivity of semi-coke and mesophase towards ammonia. The reaction was carried out at 90^{0}C for 3h at the sample to acid ratio 1:10 and followed by washing with diluted $NaHCO_3$ until neutral pH and drying.

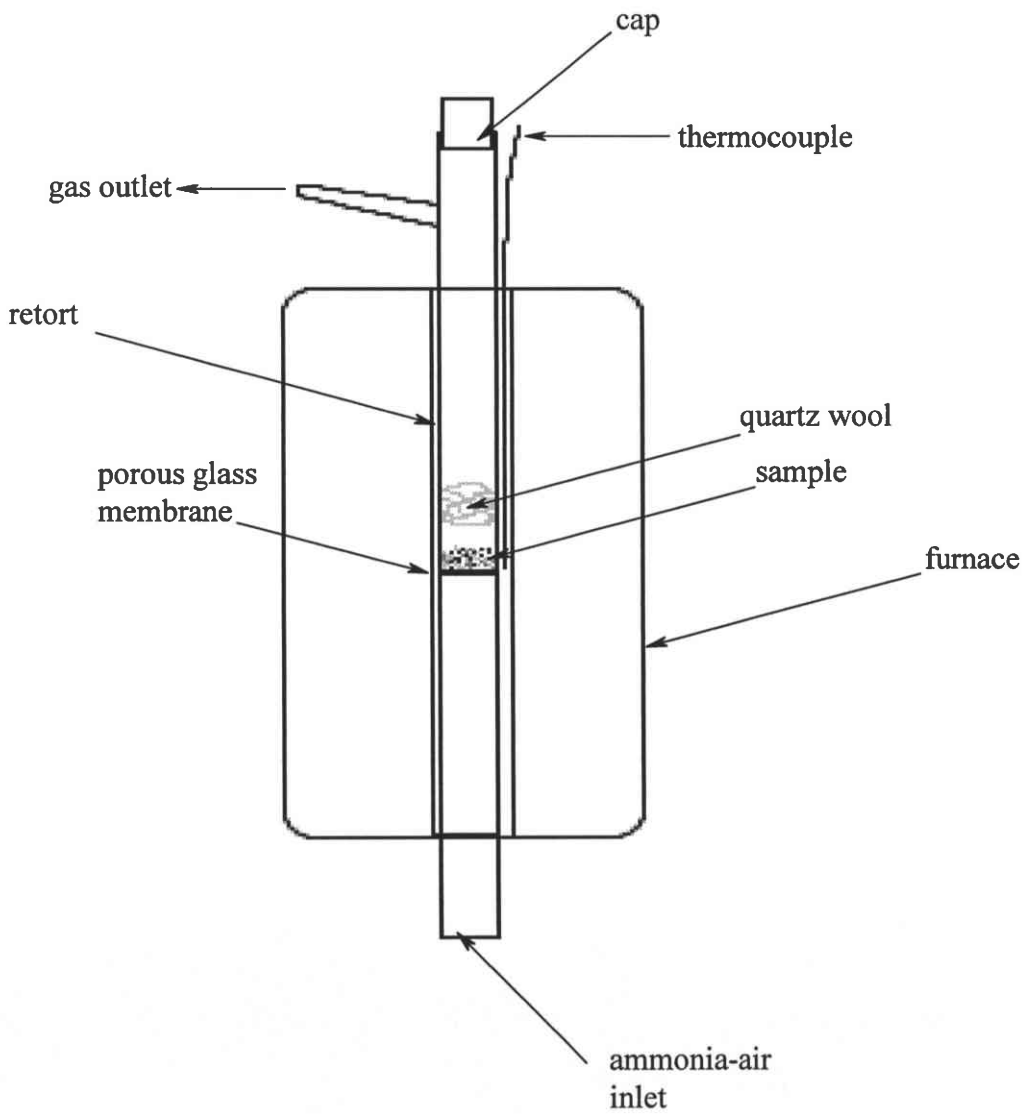

Fig. 16. Reactor used for the ammoxidation.

Carbonization and activation

The pyrolysis and ammoxidation products were steam activated in a vertical stainless steel tube reactor (Fig. 17). A sample (3-4g) of grain size 0.08-0.3 mm was placed in a container of stainless steel net, which was suspended from a recording electrobalance (RADWAG WPD 600) to control the burn-off during the process. The sample was heated up in nitrogen to 800^0C at 5 K min^{-1}. After 15 min soak a N_2 flow was switched to steam and the activation continued up to about 50 wt% burn-off. In the parallel runs the samples from ammoxidation and pyrolysis were carbonized in the same reactor in nitrogen atmosphere at 800^0C, following the soaking time applied for the activation run of the particular material.

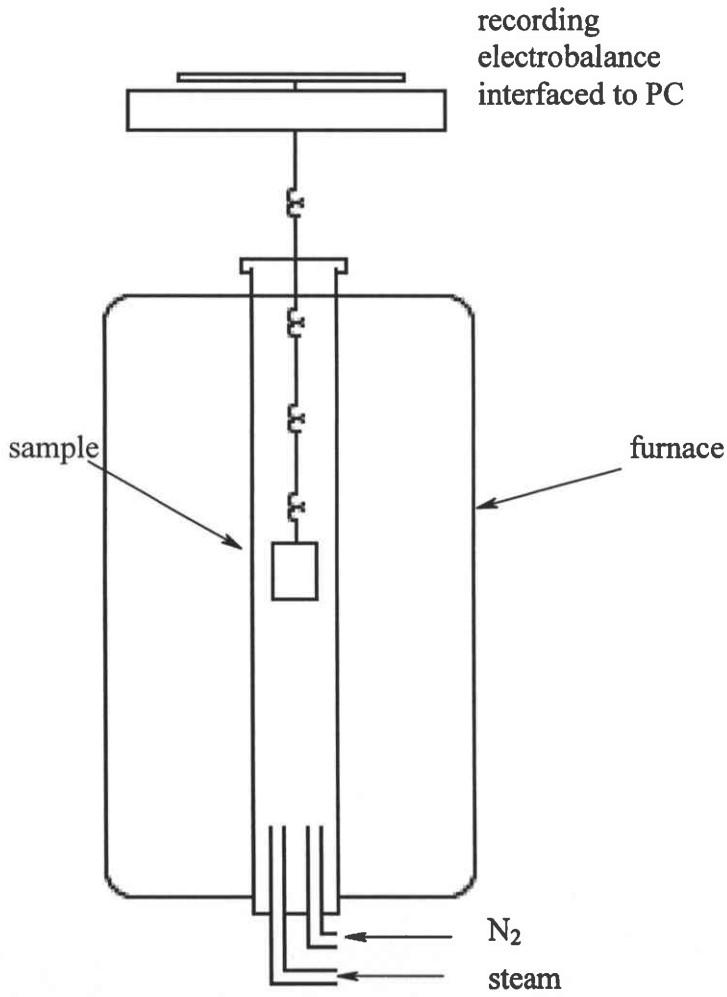

Fig. 17. Reactor used for the carbonization and activation.

Calcination

The calcined carbon materials were prepared from pitch-PAN blend semi-cokes by treatment at 1050^{0}C for 1h. The process was performed in a horizontal tube furnace in nitrogen atmosphere under atmospheric pressure.

4.4. Analyses

Softening point determination

The softening point (SP) of the parent pitch was measured using a Mettler Toledo FP 90, following the DIN 51920 standard procedure.

Coking value

Coking value (CV) was determined according to ISO 6998:1984 standard procedure consisting on heating one gram of pitch at 550°C for 2.5 hours.

Elemental analysis

Carbon, hydrogen, nitrogen and sulphur contents were determined using CHNS type VarioEl elemental analyzer. Oxygen content was calculated by difference.

Thermogravimetry, Fourier Transform Infrared Spectroscopy (TG-FTIR)

Thermogravimetry (TG) measurements were performed in a Setaram TGDTA 92 instrument. Approximately 60 mg (+/-15 mg) samples were analyzed over the temperature intervals 30-600°C and 30-900^{0}C with a linear heating rate of 5 K min^{-1}. Pyrolysis experiments were carried out under a 60 ml/min nitrogen flow.

The volatile non-condensable products evolved during the thermal treatment of reactants were identified by Fourier Transform infrared (FTIR) spectroscopy, using a BIO-RAD FTC-185 spectrometer interfaced to the TGDTA unit. The infrared cell and coupling device were heated at 250°C to avoid condensation of tarry products. The spectra were collected at 4 cm^{-1} resolution, co-adding 16 scans per spectrum. This resulted in a temporal resolution of 9.5 s. The FTIR analysis of the study was focused on the monitoring the release of light nitrogen bearing compounds (NH_3, HCN), but the carbon dioxide, carbon oxide and light aliphatic compounds were also examined. The absorbance profiles were obtained by assuming a single wavenumber interval for each

gaseous compound: 976-942 cm^{-1} for NH_3, 718-705 cm^{-1} for HCN, 2400-2270 cm^{-1} for CO_2, 2230-2140 cm^{-1} for CO, 3000-2800 cm^{-1} for aliphatics, and 3017 cm^{-1} for CH_4 (Xue et al., 1997; Marsanich et al., 2002).

Pyrolysis-gas chromatography/mass spectrometry (Py-GC/MS)

The volatile products evolved during pyrolysis of PVP25 and PVP25ox were analyzed by pyrolysis-gas chromatography/mass spectrometry (Py-GC/MS) using Pyroprobe 120 pyrolyzer (Chemical Data System) interfaced to a Hewlett-Packard 5895A gas chromatograph/mass spectrometer. Approximately 50-150 μm samples were pyrolyzed in a quartz tube using helium as a carrier gas at a 20 ml^{-1} flow rate and 20:1 split ratio. The temperature of the quartz tube was calibrated by a thermocouple. The heating rate was set to 5 K ms^{-1}. The samples were pyrolyzed at 470^{0}C for 20 s. The pyrolysis interface and the GC injector were kept at 150^{0}C. The pyrolysis products were separated on a Hewlett-Packard capillary column (25m x 0.2 mm i.d., 0.33 μm film thickness). The GC oven was programmed to hold at 50^{0}C and then increase to 300^{0}C at a rate 10 K min^{-1}. The mass spectrometer was operated at 70 eV in the EI mode. The mass range of 15-350 Da was scanned. Data acquisition and manipulation was performed on a MassLynx data system containing the NIST library of mass spectra (≈65 000 entries).

Diffuse reflectance infrared Fourier Transform (DRIFT) spectroscopy

Diffuse reflectance infrared Fourier Transform (DRIFT) spectra of starting reactants and solid pyrolysis residues were recorded on the BIO-RAD FTS-185 spectrometer equipped with a high sensitive mercury-cadmium-telluride (MCT) detector and a Graseby-Specac "Selector" accessory in an off-axis optical geometry. Spectra were recorded by co-adding 256 scans in the range 4000-700 cm^{-1} at a resolution of 2 cm^{-1}. The analysis chamber was purged continuously with dry air and infrared scanning began 10 min after sample insertion.

Potassium bromide (Spectronorm-Prolabo) ground to an average particle size of 10 μm and stored in a dessicator (110^{0}C, 24 hours) was used as sample matrix and reference material. The sample, ground separately to a particle size 40-100 μm was mixed with KBr in the proportions 5/95 (% by weight), respectively.

Multipoint baseline correction of the spectra was performed using a standard software package. For selected samples the Kubelka-Munk function was applied in an

attempt to linearize with greater precision the relationship between the concentration and spectral response (Culler, 1993).

X-ray photoelectron spectroscopy (XPS)

X-ray photoelectron spectroscopy (XPS) measurements were performed on a RIBER MAC 2 spectrometer using Al K_α radiation (12kV and 25 mA). Spectra of C1s, N1s, and O1s core levels were recorded. The energy scale was calibrated to reproduce the binding energy of Ag 3d5/2 (368.28) and kinetic energy of Ag MNN (375.84 eV). Sample charging was corrected by the C1s peak E_b(C1s) = 285.0 eV. The energy resolution of the instrument was 1.0 eV (FWHM for Ag 3d5/2 at pass energy of 10 eV).

The core-level spectra were analyzed with the CasaXPS software package by using a non-liner Shirley-type baseline correction and an iterative least-squares fitting algorithm to decompose the peaks, the curves being taken as 70% Gaussian and 30% Lorentzian. The full width at half maximum (FWHM) was varied in the range 1.8-2 eV for the C1s and N1s spectra single components and 2.5-3 eV for O1s subtrahends. The C1s, N1s and O1s envelopes were fitted using binding energies (BE) values reported in the literature (Table 2).

The bands used for C1s decomposition are: 282.7±0.3 eV (carbidic carbon); 284.8±0.2 eV ("graphitic carbon", occurring in C-C or C-H linkages); 286.7±0.4 eV (carbon linked to oxygen by a simple bond, occurring in C-N/C=N structures and/or in phenolic, alcohol, ether groups); 287.8±0.3 eV (carbon linked to oxygen by a double bond, present in carbonyl groups of ketones, quinones and amides); 289.7±0.4 eV (carbon in carboxyl or esters groups); 291.6±0.5 eV (plasmon peak and shake-up satellite peaks due to the π-π^* transitions of carbon atoms occurring in the conjugated, and especially aromatic systems).

The N1s peaks were fitted using the following binding energy values: 398.7±0.3 eV (pyridinic nitrogen, denoted N-6); 399.7±0.2 (amides, alkylamides, nitriles, imides, lactams); 400.3±0.3 eV (pyrrolic/ pyridonic nitrogen, denoted N-5); 401.4±0.5 eV (quaternary nitrogen, denoted N-Q), 402-405 eV (oxidized nitrogen functionalities).

The O1s regions were resolved into three component peaks centered respectively at 530.6±0.2 eV (oxygen in C=O groups); 532.8±0.4 eV (oxygen in C-OH and C-O-C moieties) and 535.2±0.4 eV (chemisorbed H_2O and/or O_2).

Surface atomic concentration ratios were calculated as the ratio of the corresponding peak areas, corrected with theoretical sensitivity factors based on Scofield's photoionisation cross-sections.

Table 2. The bands used in the XPS spectra deconvolution

Core level	Binding energy, eV	FWHM[1], eV	Assignment	Reference
C1s				
	282.7±0.3	1.8-2	carbidic	Biniak et al. (1997)
	284.8±0.2	1.8-2	C-H, C-C	Biniak et al. (1997)
	286.7±0.4	1.8-2	C-OH, C-N, C=N	Biniak et al. (1997)
	287.8±0.3	1.8-2	C=O	Biniak et al. (1997)
	289.7±0.4	1.8-2	COO	Biniak et al. (1997)
	291.6±0.5	1.8-2	plasmon / π- π^* transitions	Ratner and Castner (1997)
N1s				
	398.7±0.3	1.8-2	pyridinic	Kapteijn et al. (1999)
	399.7±0.2	1.8-2	amides, alkylamides, nitriles, imides, lactams	Jansen and Bekkum (1995)
	400.3±0.3	1.8-2	pyrrolic/ pyridonic	Kapteijn et al. (1999)
	401.4±0.5	1.8-2	"quaternary" nitrogen	Kapteijn et al. (1999)
	402-405	2-3	oxidized nitrogen	Kapteijn et al. (1999)
O1s				
	530.6±0.2	2.5-3	C=O	Biniak et al. (1997)
	532.8±0.4	2.5-3	C-O-C, C-OH	Biniak et al. (1997)
	535.2±0.4	2.5-3	H_2O, O_2 adsorbed	Biniak et al. (1997)

[1]Full width at half maximum

X-ray diffraction (XRD)

Powder X-ray diffraction (XRD) spectra were recorded using an URD-6 diffractometer (40kV, 20mA) with a Cu K_α radiation. The interlayer spacing d_{002} was measured from the maximum of the (002) band. The crystallite height L_c and crystallite diameter L_a were determined from the width of the (002) and (100) XRD bands, respectively according to the Scherrer formula:

$$Lc,a = \frac{k\lambda}{\beta\cos\theta}$$

The half-height line width β was corrected for the instrument broadening using the silicon as a internal standard. The shape factors k = 0.9 and k = 1.84 were used for L_c and L_a calculation, respectively.

The shape of the (002) line was characterized by a parameter R defined as the ratio of the peak count rate at the (002) peak divided by the background level at the same angle (Zheng et al., 1996).

Microscopic examinations of semi-cokes

The conventional technique was used to prepare specimens for polarised light optical microscopy. The semi-coke samples of particle size 0.3-1.2 mm were mounted in epoxy resin, ground and polished on alumina powders. A Zeiss Neophot 2 microscope equipped with a phase sensitive plate was used for qualitative observations of optical texture and taking photographs of selected areas. Anisotropic content of the semi-cokes was assessed quantitatively from the polished surfaces by point counting technique. The constituents quantified in the optical texture of carbonization product were described as flow domain, mosaic and isotropic.

Transmission electron microscopy (TEM)

Transmission electron microscopy studies were performed using a Philips CM20 microscope. The observations were done in 002 dark field mode (002 DF) to image the polyaromatic basic structural units oriented at the Bragg angle and in 002 lattice fringe mode (002 LF) to visualize directly the profile of the aromatic layers (Rouzaud et al., 1989). The examination was performed in CNRS-Université d'Orleans, Centre de Recherche sur la Matière Divisée.

Adsorption measurements

Nitrogen adsorption / desorption measurements at 77K were performed using NOVA 2200 (Quantachrom) to evaluate micropore > 0.5 nm and mesopore development. Relative pressure limit p/p_0 = 0.15 was used to determine micropore volume contribution. Specific surface areas were calculated from the isotherms by the BET equation. The mesopore size distribution was evaluated using Kelvin equation. Carbon dioxide sorption at 298 K in high vacuum gravimetric apparatus (McBain-Bakr

quartz springs) and the Dubinin-Radushkevich theory were used to characterize microporosity including ultramicropore (< 0.5 nm width) region.

Electrochemical measurements

Carbon electrodes prepared from different blends of CTP and polymers were tested for electrochemical insertion of lithium. The working electrode was pressed in the form of 11 mm disk constituted from carbon (85 wt%), polyvinylidene fluoride PVDF (10 wt %) and acetylene black AB (5 wt%). 1M $LiPF_6$ dissolved in a 1:1 mixture of ethylene carbonate and diethyle carbonate (EC:DEC, Merck) was used as an electrolytic solution. Galvanostatic charge/discharge experiments at the current load of 20 mA/g were performed in the two electrode cells where lithium played a role of working as well as counter electrode. Cycling was carried out in the potential range from 3 or 2V *vs* Li using a multichannel potentiostat/galvanostat MacPile (Biologic, France). Kinetics of lithium insertion deinsertion was investigated by the voltammetry technique at scan rates of potential from 0.2 mV/s to 5 mV/s. The measurements were performed at the Poznań University of Technology, Institute of Chemistry and Applied Electrochemistry.

V. Results and Discussion

5.1. Characteristics of parent materials

The coking value and elemental composition of pitch and polymers used in the work are given in Table 3.

Table 3. Coking value and elemental composition of parent materials

Sample	Coking value,	Elemental composition, wt%				
	wt%	C	H	N	S	O[1]
CTP	47.0	92.50	4.81	0.85	0.34	1.50
PAN	44.1	66.35	5.60	25.63	0.35	2.07
PANox	67.4	62.51	2.91	22.59	0.15	11.84
PVP2	0.2			n.d.		
PVP25[2]	9.1	83.43	6.87	9.06	0.00	0.64
PVP25ox	59.5	79.38	5.11	7.71	0.00	7.80

[1]By difference
[2]Laboratory synthesized sample

The relevant properties of polyacrylonitrile (PAN) as a precursor of nitrogen enriched carbons are relatively high coking value, which is comparable to that of coal-tar pitch, and high proportion of nitrogen in the structure. The elemental composition determined for the polymer synthesized for the study is fairly close to the theoretical one (C = 67.93 wt%, H = 5.66 wt%, N = 26.41 wt%) corresponding to the formula $[-CH_2-CH-CN-]_n$. The noticeable content of oxygen is in agreement with an earlier report and can be explained by the generation of oxygen groups on the polymer chains due to the activity of polymerization initiator (Xue et al., 1997).

The treatment of PAN in air at 300°C to produce the oxidized form of the polymer (PANox) is associated with the 26.4 wt% weight loss and brings about to an enhanced coking value and considerably increased oxygen content in the oxidized polymer. Both the findings are consistent with the established mechanism of the PANox stabilization, which includes the oxygen promoted dehydrogenation and cyclization of

chain and generation of hydroxyl and carbonyl functional groups (Fitzer and Mueller, 1975).

Vinylpyridine resins are most common representatives of N-polymers having nitrogen atom located in the six-membered aromatic ring. For the preliminary pyrolysis study we selected commercial (Aldrich) poly(4-vinylpyridines) cross-linked with 2 wt% and 25 wt% of divinylbenzene (DVB). In the larger scale experiments we used the sample cross-linked with 25 wt% of DVB which was synthesized in laboratory.

The elemental composition of the prepared polymer approaches to the calculated value (C = 84.03 wt%, H = 7.0 wt%, N = 8.91 wt%). Fig. 18 presents DRIFT spectrum of the commercial polyvinylpyridine cross-linked with 25 wt% of DVB and that of PVP25 synthesized in the laboratory. A close similarity in the absorption profiles of both the polymer samples is in agreement with the elemental analysis data and confirms a good quality of the synthesized polymer.

In terms of coking value and nitrogen content the polyvinylpyridines (PVP) are a less efficient nitrogen carrier than polyacrylonitrile. When the polymer is cross-linked with 2 wt% of DVB (PVP2), it undergoes a complete depolymerization to volatile compounds under conditions of coking value determination (550°C for 2.5 h). With the increased proportion of DVB to 25 wt%, the coking value of PVP25 increases to about 9 wt%, in agreement with an earlier report on the effect of cross-linking agent on the carbonaceous solid yield (Kartel and Puizy, 1996).

To enhance the pyrolysis residue yield, the parent polymers were oxidized under mild conditions (300°C) in air. Such a treatment was reported to be efficient in terms of the stabilization of the macromolecules of PVP cross-linked with 25 wt% of DVB (Schmiers et al., 1999). The oxidation of PVP25 in this work induced a striking increase in the coking value but was accompanied by about 24.4% weight loss of the sample and incorporation of oxygen into the organic structure. The elemental composition of PVP25ox fairly corresponds to the data reported by Schmiers et al. (1999) for the oxidized PVP (C = 80.21 wt%, H = 5.08 wt%, N = 7.95 wt%, O = 6.76 wt%).

In the case of PVP2, a lower content of DVB causes an early melting of the resin on heating, resulting in a low extent of oxidation due to limited access of oxygen to the bulk of sample.

For the above reasons the research in the study was concerned mostly with PVP25 and PVP25ox.

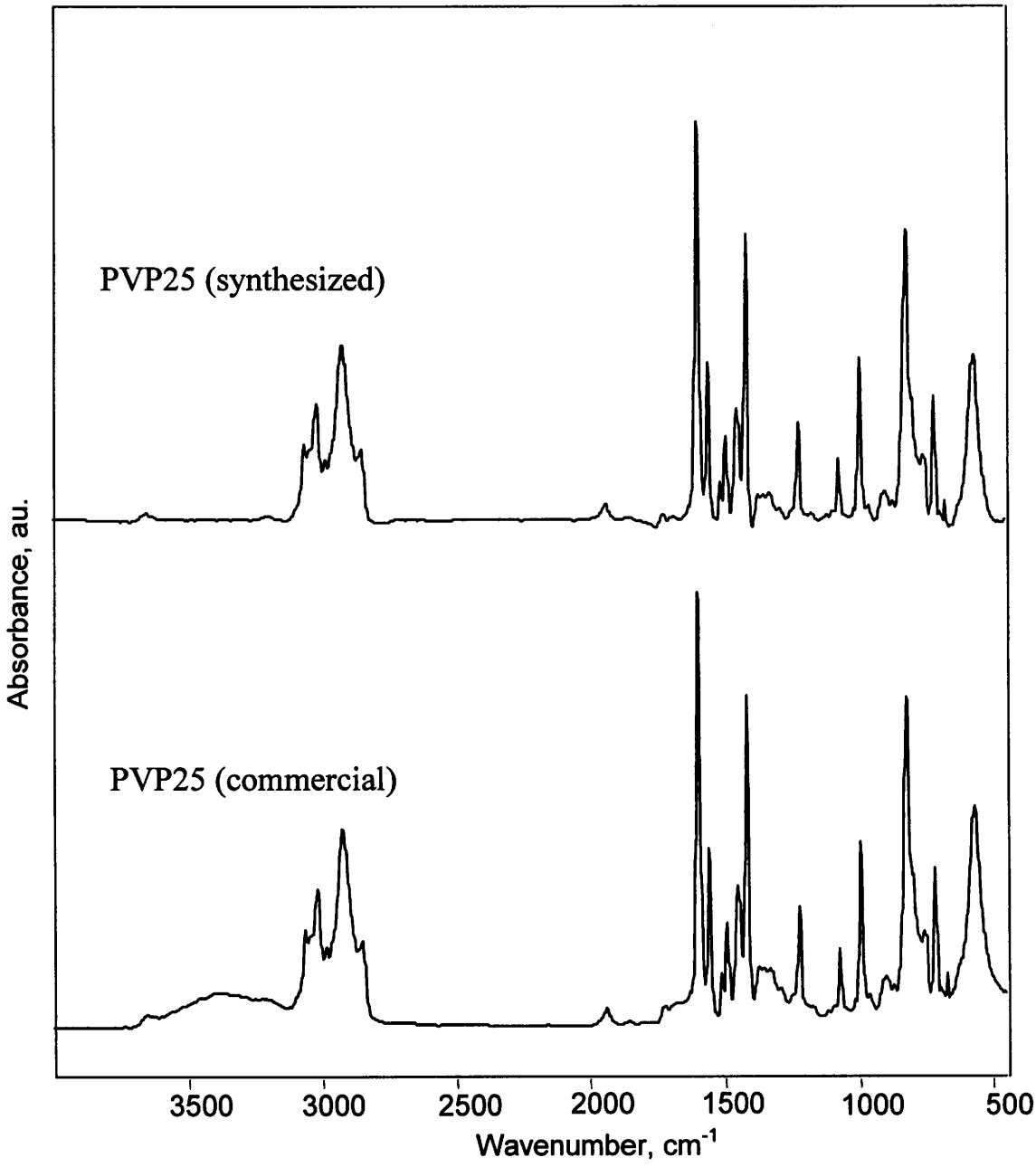

Fig. 18. DRIFT spectra of the commercial and laboratory synthesized PVP25.

5.2. Co-pyrolysis of pitch with polyacrylonitrile

5.2.1. Weight loss behavior

Thermogravimetry coupled with FTIR was used to monitor volatile evolution on the heat-treatment of individual components (CTP, PAN, PANox) and their blends of 1:1 weight ratio. TG/DTG and FTIR profiles are presented in Figs. 19-24. Thermal decomposition characteristics of single components and their blends are given in Table 4.

TG/DTG profiles of the coal-tar pitch are presented in Fig. 19. The DTG profile is typical of coal tar pitches (Martínez-Alonso et al., 1992a) and comprises a broad band within the temperature range of 250–480°C with a maximum at 360°C. The weight loss is primarily due to the distillation of lower molecular weight pitch constituents but, as the temperature increases, the contribution of by-products of pyrolytic reactions becomes meaningful in the volatiles (Martínez-Alonso et al., 1992b). The total weight loss on the treatment to 600°C is about 58 %.

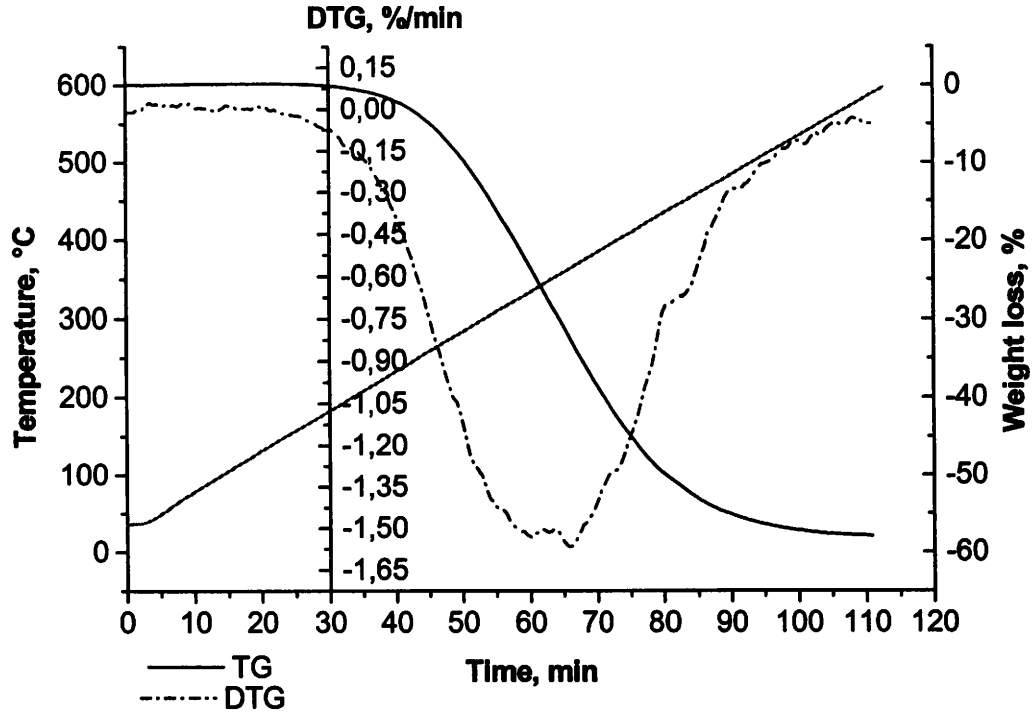

Fig. 19. TG/DTG profiles of CTP.

DTG profile of PAN (Fig. 20) includes three distinct weight loss intervals:

- very sharp peak at 270°C, accompanied by approximately 10 % weight loss;
- a band with a maximum around 300°C, corresponding to about 18 % weight loss;
- a broad band between 350-500°C, corresponding to about 25 % weight loss.

It was previously reported (Xue et al., 1997, Surianarayanan et al., 1998), that the weight loss during thermal treatment of PAN results mainly from the evolution of oligomers due to radical chain scissions followed by breaking of chemical bonds, although some quantities of low molecular weight species as hydrogen cyanide and ammonia are also formed. Consequently, the first sharp peak on Fig. 20 can be attributed mostly to the dimer and trimer evolution, the second one corresponds to heavier oligomers. Broad peak in the temperature range of 350-500°C is related mainly to the release of low molecular weight aliphatic compounds like 1,3-dicyanopropene, 1,3-dicyanobutene, acetonitrile (Surianarayanan et al., 1998).

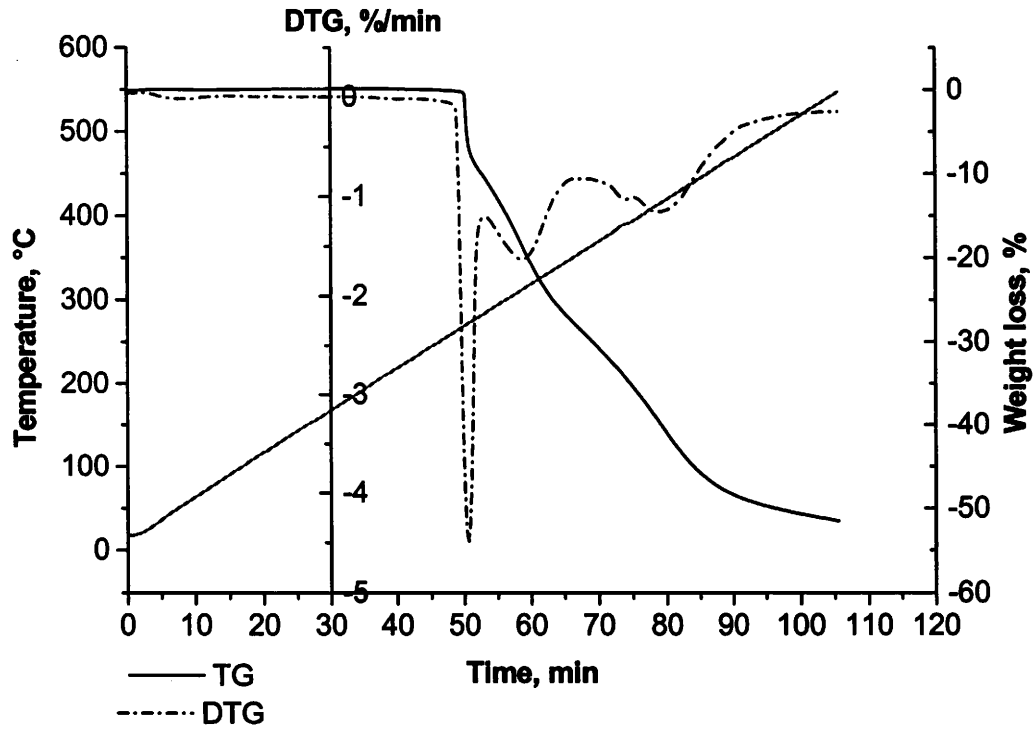

Fig. 20. TG/DTG profiles of PAN.

The analysis of light gaseous products evolved during PAN treatment using FTIR (Fig. 21) confirms that the release of nitrogen bearing compounds (ammonia and hydrogen cyanide) is closely associated with the PAN chain scission which is responsible for the first peak on the DTG curve. The second maximum in hydrogen cyanide release is observed about 380^{0}C. The evolution of methane and other light aliphatics starts above 350^{0}C and, when the temperature exceeds 480^{0}C, methane predominates in the gaseous products.

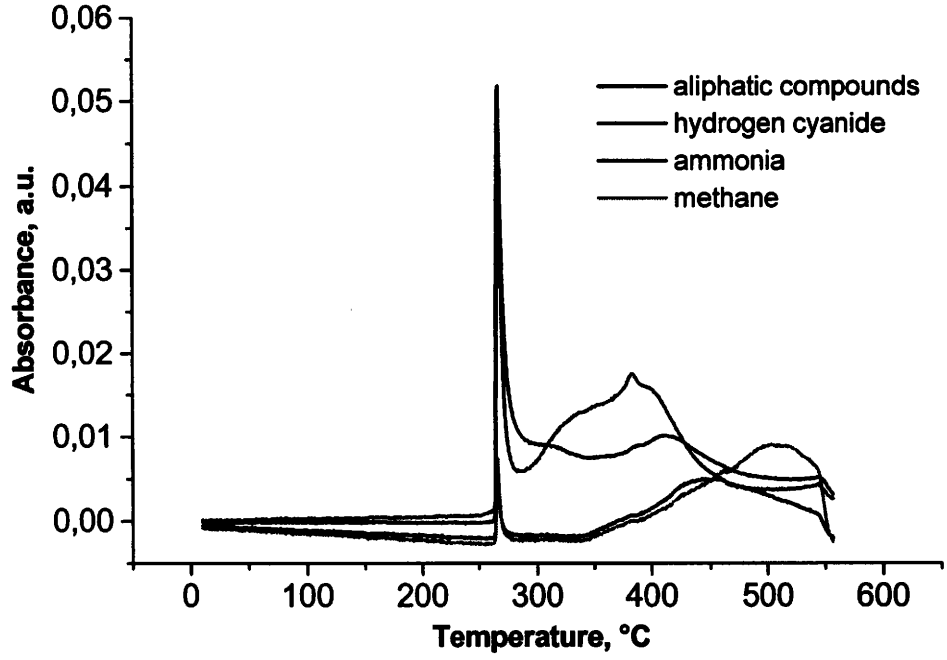

Fig. 21. Evolution of gases on pyrolysis of PAN.

Figure 22 is a thermogram of CTP-PAN 1:1 blend, which relates experimental TG and DTG curves to those computed based on single component behaviors according to the additivity rule. Most remarkable discrepancies of the experimental data from the calculated ones are an increase in the final residue yield by approximately 13 wt% and a strong reduction of the intensities of peaks at 270^{0}C and 300^{0}C, corresponding mostly to the acrylonitrile oligomers evolution. The lack of sharp peak at 270^{0}C on the blend heating is compensated by the weight loss occurring in lower temperatures. The comparison of the experimental and calculated profiles indicates that the interactions between pitch constituents and PAN degradation products which seem to be responsible

for the remarkable increase in the residue yield occur over a temperature range of 300-480^{0}C.

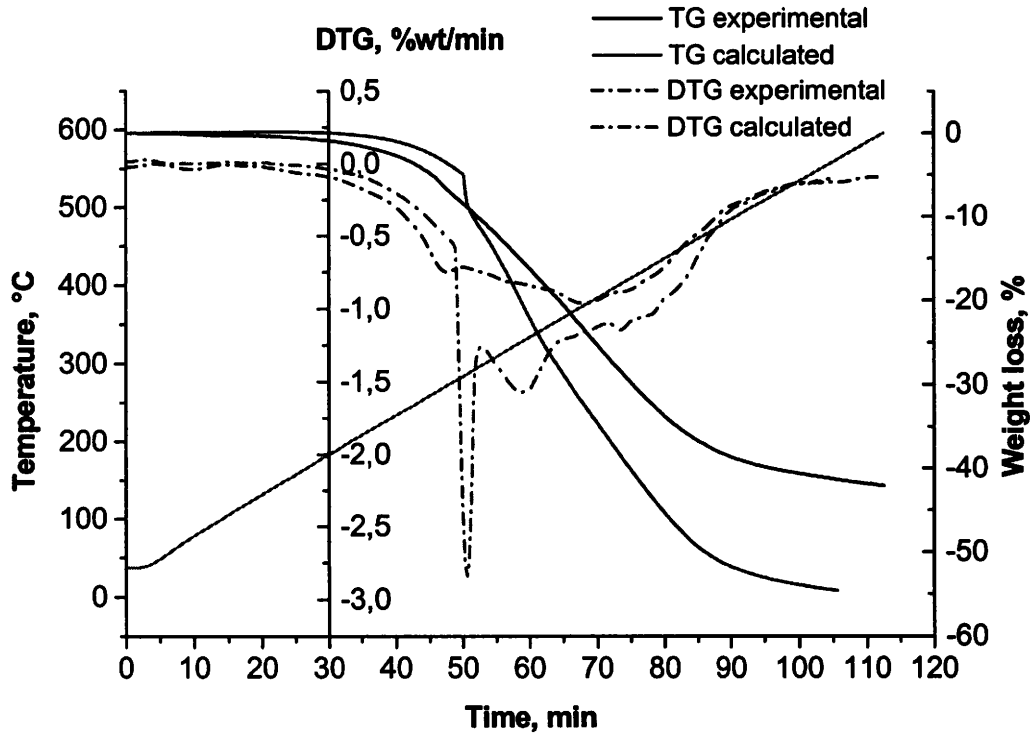

Fig. 22. TG/DTG profiles of CTP-PAN 1:1 blend.

Fig. 23 presents the thermogram of PANox. The total weight loss on the treatment to 600^{0}C is about 17.5 %. This is approximately 35 wt% less than in the case of parent polymer. Three distinct intervals; in terms of weight loss behavior, can be distinguished on DTG profile of PANox:

- peak at 100^{0}C, accompanied by approximately 3.5 % weight loss;
- near stable weight in the temperature range 175-320^{0}C;
- continuous, relatively fast weight loss over the temperature interval 320-600^{0}C.

The DTG peak centered at 100^{0}C can be attributed to the desorption of water. Nitrogen atoms in the structure of chars derived from N-polymeric precursors behave as polar sites (Lahaye et al., 1999a), hence account for the enhanced water chemisorption. The thermal stability in the temperature range 175-300^{0}C is a consequence of the preliminary treatment during oxidation. The evolution of oligomers and the formation

of HCN and NH_3 from an uncyclized part of PAN chain can acccount for the weight loss of about 12 wt% in the temperature range of 320-600^{0}C.

Two effects contribute to the reduction in the volatile evolution compared to the pristine polymer. First, the decomposition of the unstable PAN fragments during the preceding oxidation at 300^{0}C, leading to about 25 wt% weight loss during the treatment. Second, the intrinsic enhancement in the thermal stability of the polymer due to the cyclization and cross-linking induced by the oxidation.

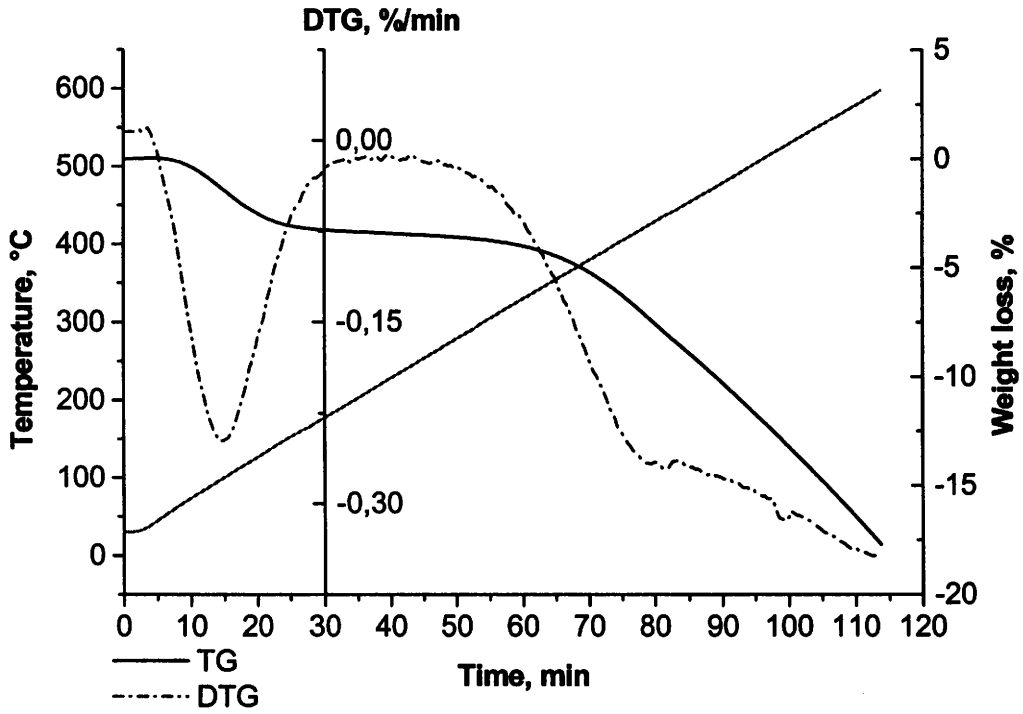

Fig. 23. TG/DTG profiles of PANox.

Fig. 24 is a thermogram of CTP-PANox 1:1 blend relating the experimental data to those computed based on single components behaviors according to the additivity rule. The discrepancy between calculated and experimental dataset is distinctly smaller than noted for CTP-PAN blend. The increase in the solid residue yield is about 7.5 wt% in the relation to the anticipated value. Similar experimental and calculated DTG profiles suggest that interactions between pitch and PANox occur to a limited extent. The dehydrogenative activity of oxygen present on PANox chains towards pitch

constituents, inducing polymerization reactions, seems to most contribute to the increase in the residue yield.

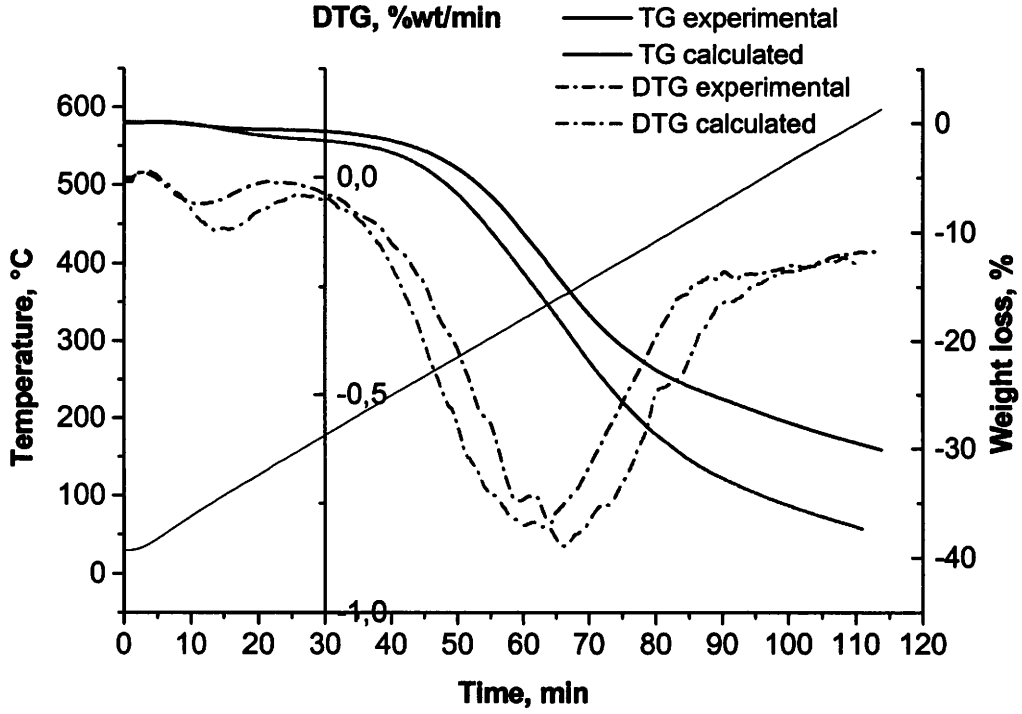

Fig. 24. TG/DTG profiles of CTP-PANox 1 :1 blend.

Table 4. Thermal decomposition characteristics of singly treated PAN, PANox and their blends with pitch

Sample	Major degradation step			Weight loss at
	Temp. range ^0C	T_{max}[1] ^0C	Weight loss %	600^0C %
CTP	250-480	360	54.0	58.0
PAN	265-485	270	48.6	51.5
CTP-PAN 1:1	225-480	267	36.0	42.0 (54.0)[2]
PANox	320-	-	14.0	17.5
CTP-PANox 1:1	250-450	350	21.2	30.0 (37.0)[2]

[1]Temperature of the maximum weight loss rate
[2] The anticipated weight loss

5.2.2 Structure and properties of co-pyrolysis products

5.2.2.1. Optical texture of semi-cokes from pitch-PAN and pitch-PANox blends

A series of semi-cokes was prepared by small-scale (4g) pyrolysis of mixtures pitch-PAN and pitch-PANox with polymer proportion varying from 0 to 40 wt% to study the effect of the additives on the optical texture

Coal-tar pitch gives on pyrolysis the carbonaceous material of flow type optical texture (Fig. 25). Solid residues produced from PAN and PANox show totally isotropic optical texture, characteristic of disordered non-graphitizing carbons.

Fig. 25. Optical texture of semi-coke from CTP.

The addition of pristine PAN to pitch strongly restricts the development of optical anisotropy on the co-pyrolysis. A gradual replacement of flow type texture, which predominates in the pitch coke, by the mosaics occurs with the increase in the PAN proportion in the blend from 0 to 10 wt% (Fig. 26). The striking effect is observed already at the content of 5 wt% of the polymer (Fig. 27). A further increase in the PAN concentration in the blend above 10 wt% results in the reduction of mosaics size (Fig. 28). The anizotropic units become undetectable, being behind the optical microscope resolution limit, when the polymer proportion is about 30 wt%. Co-pyrolysis products from blends of a given components ratio are fairly homogeneous in terms of the optical texture and the phases derived from different origin precursors

cannot be recognized under microscope. The optical microscopy observations evidence strong interactions between CTP and PAN and a dominant effect of polymer on the carbonization behavior of blend.

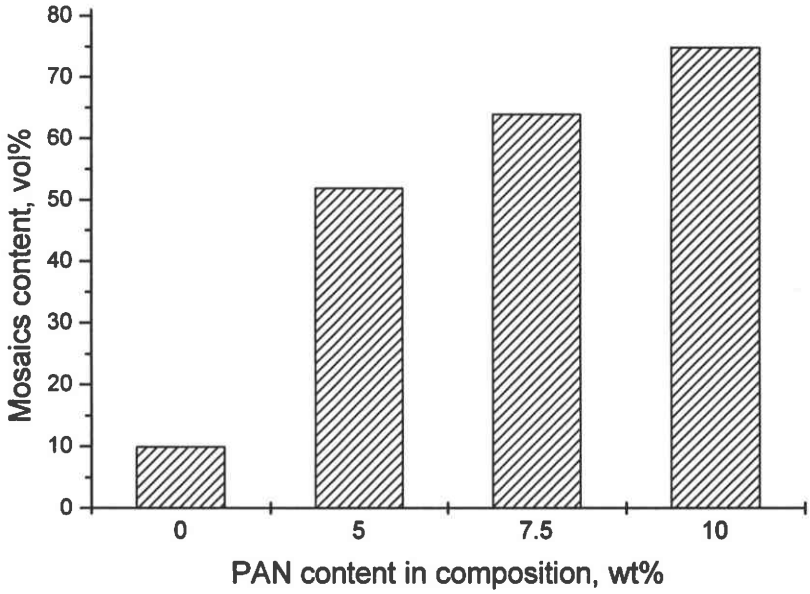

Fig. 26. Variation of mosaics proportion in the optical texture with PAN content in the blend.

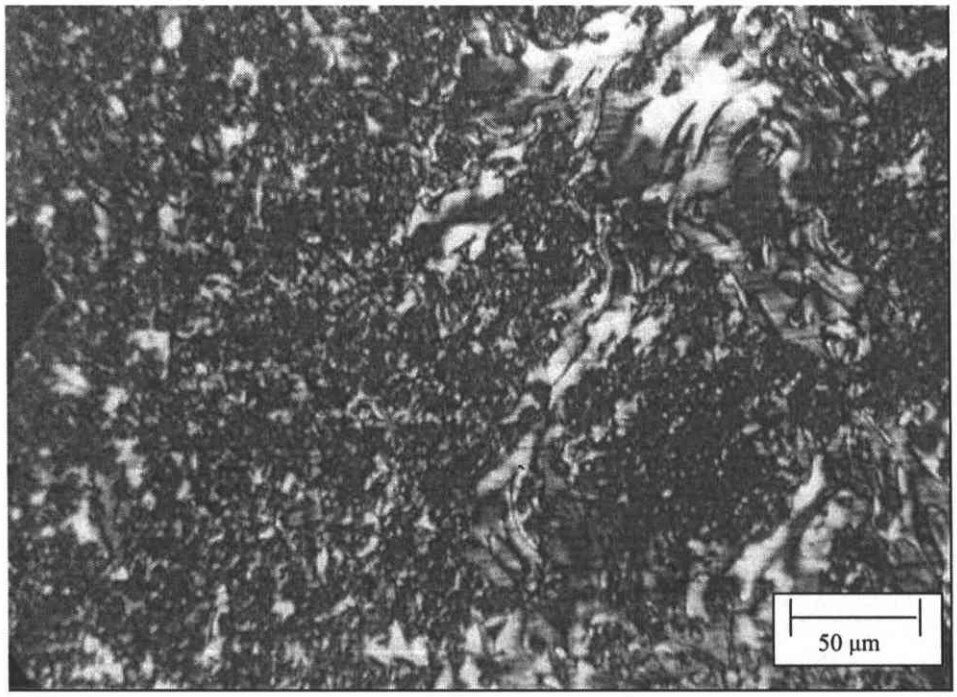

Fig. 27. Optical texture of semi-coke from blend with 5 wt% of PAN.

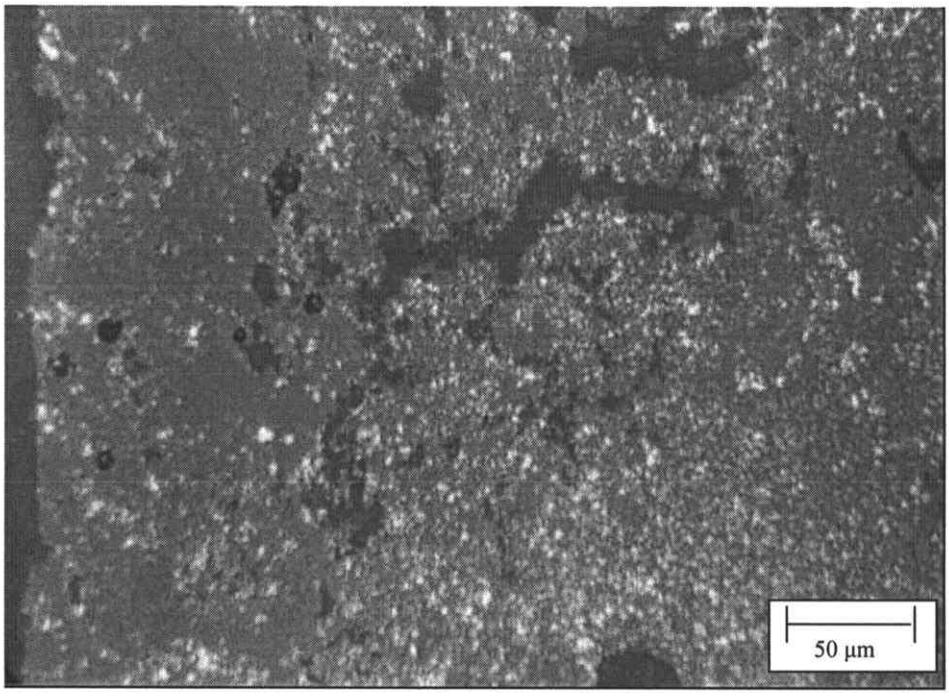

Fig. 28. Optical texture of semi-coke from blend with 15 wt% of PAN.

The carbonization of CTP-PANox blends leads to two phase products with the polymer derived residue readily distinguishable by the isotropic appearance (Fig. 29). The optical texture of pitch derived phase is practically unaffected by the additive. The content of the isotropic phase in the analyzed surface increases rather proportionally with polymer proportion in a blend (Fig. 30), being however twice higher. The heterogeneous optical texture with a sharp interface between both phases proves that the extent of interactions of components on the co-treatment is very slight. Apparently, the polymer particles behave as an inert material.

The microscopic observations indicate that the co-pyrolysis of CTP with unoxidized PAN only leads to homogeneous, at least at the optical microscopy resolution limit, carbonaceous materials. Therefore, the further study was concerned mostly with the blends of pitch with pristine polymer.

Based on the evaluation of optical texture of semi-cokes the following component ratios were selected for preparation of CTP-PAN blends in a larger scale (30 g) for further study:

CTP-PAN 9:1 (medium and coarse mosaic texture),

CTP-PAN 3:1 (fine mosaic texture),

CTP-PAN 1:1 (isotropic texture).

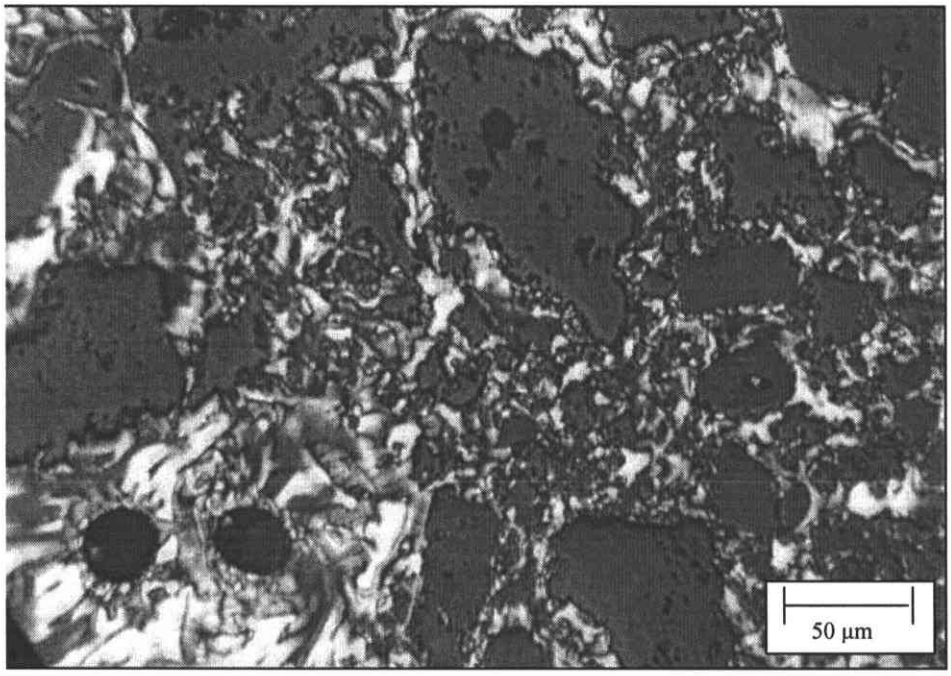

Fig. 29. Optical texture of semi-coke from blend with 5 wt% of PANox.

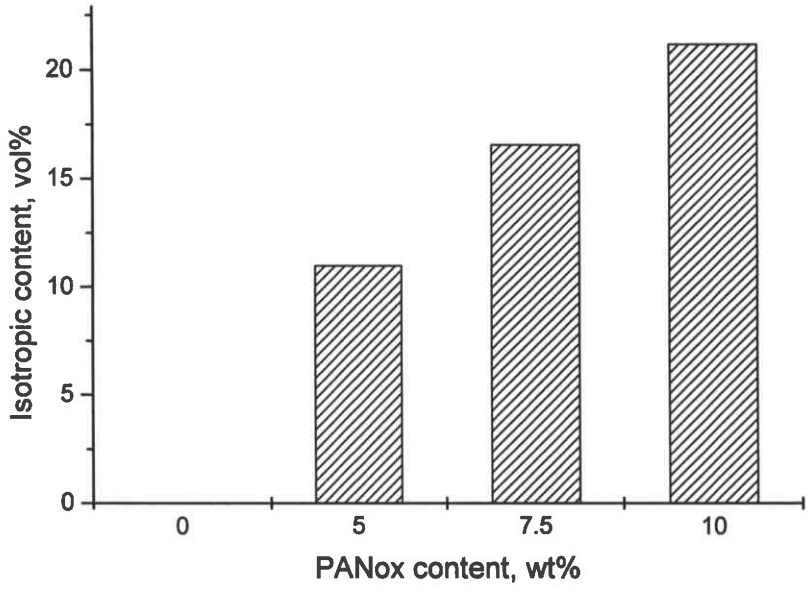

Fig. 30. Variation of isotropic matter in the optical texture with PANox content in the blend.

5.2.2.2. Elemental composition of semi-cokes

The elemental composition of semi-cokes from single components (CTP-S, PAN-S, PANox-S) and pitch-polymer blends (CTP-PAN 9:1-S, CTP-PAN 3:1-S, CTP-PAN 1:1-S) is given in Table 5.

The heat treatment of PAN at 520°C gives the solid residue with nitrogen content of about 19 wt%. The reduction of nitrogen proportion compared to the pristine PAN is due to the evolution of low molecular weight nitrogen compounds (NH_3, HCN) in addition to acrylonitrile oligomers. Keeping in mind about 35 wt% w eight loss, it means that the produced char retains about half of the constitutional polymer nitrogen. PAN and PANox semi-cokes display nearly the same concentration of nitrogen. Despite distinctly different elemental composition, both the CTP and PAN carbonization products display a similar C/H atomic ratio. The elemental composition of semi-coke from CTP-PAN blend is close to that anticipated based on the yield and composition of residues from individually treated components. The enhanced oxygen content in all semi-cokes can be attributed to the extensive oxygen chemisorption on strongly polar surface sites, which hardly can be avoided during laboratory operations. Such a behavior was also observed by Lahaye et al. (1999a) for the polyvinylpyridine char.

Table 5. The yield and elemental composition of semi-cokes

Sample	Semi-coke yield, wt%		Elemental composition,wt%					$(H/C)_{at}$	$(N/C)_{at}$
			C	H	N	S	O[1]		
CTP-S	63.2		95.30	3.05	0.78	0.09	0.78	0.384	0.007
CTP:PAN 9:1-S	65.3	(62.9)[2]	92.37	2.94	2.80 (2.64)[2]	0.12	1.77	0.381	0.026
CTP:PAN 3:1-S	63.9	(62.4)[2]	88.33	2.54	7.07 (5.44)[2]	0.10	1.96	0.345	0.069
CTP:PAN 1:1-S	68.9	(61.6)[2]	81.44	2.65	11.0 (9.85)[2]	0.12	4.73	0.390	0.116
PAN-S	59.9		69.84	2.55	19.41	0.11	8.09	0.438	0.238
PANox-S	81.5		69.10	2.53	19.24	0.19	8.94	0.439	0.239

[1]By difference
[2]Calculated according to the additivity rule

5.2.2.3. Chemical structure evolution on pyrolysis

Diffuse reflectance infrared Fourier transform spectroscopy (DRIFT) and X-ray photoelectron spectroscopy (XPS) were used to evaluate the interactions occurring on co-pyrolysis of pitch with polyacrylonitrile. This includes the monitoring the alteration of PAN structure during oxidation (300^0C in air) and CTP-PAN 1:1 blend preparation followed by the comparison of the resultant semi-cokes structure.

Diffuse reflectance infrared Fourier transform spectroscopy (DRIFT)

The characteristic features of the DRIFT spectrum of the parent pitch (Fig. 31) are bands related to the aromatic vibrations: moderate intensity band at about 1600 cm^{-1} corresponding to the aromatic ring vibrations, a strong peak at 3050 cm^{-1} attributable to the C-H aromatic stretching and strong bands between 900-700 cm^{-1} brought about by the out-of plane C-H vibrations. Presence of the hydroxylic groups is evidenced by the absorption in the region 1290-1130 cm^{-1}, attributable to υ(C-O) and δ(O-H), and the weak band at about 3420 cm^{-1} related to the OH stretching.

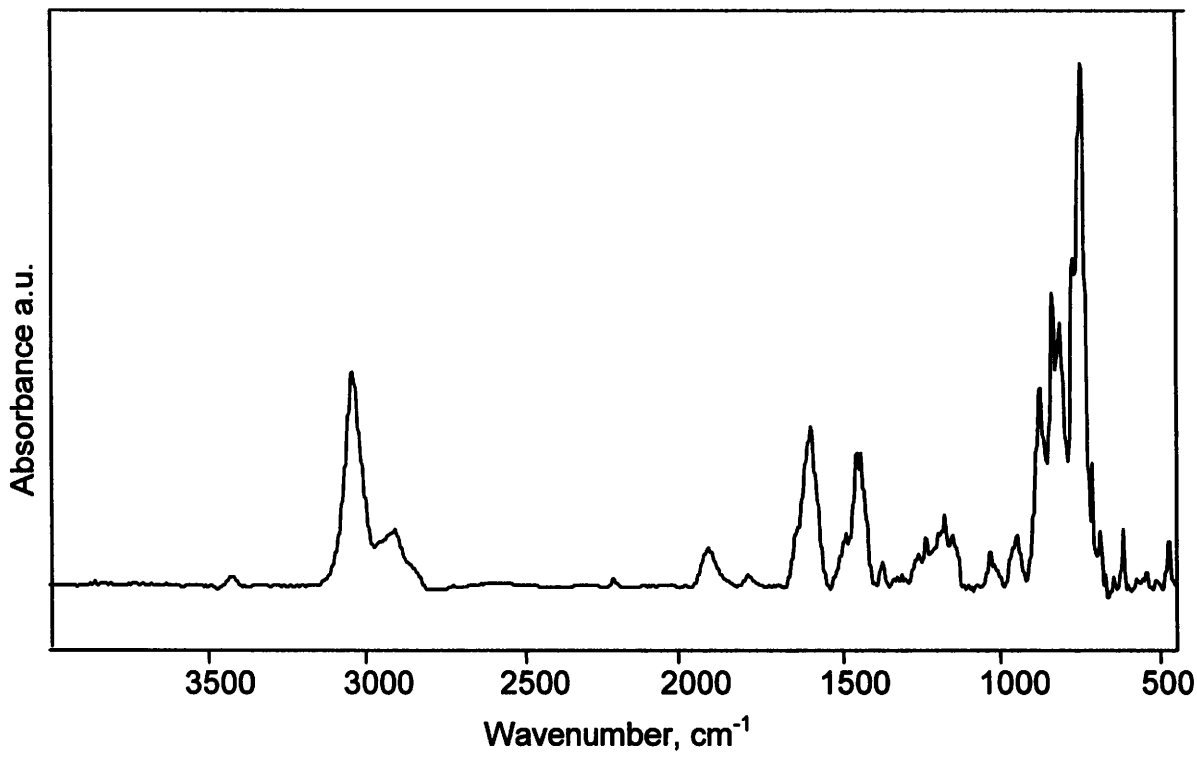

Fig. 31. DRIFT spectrum of the parent pitch.

DRIFT spectra of PAN and its derivatives produced by the treatment at blending conditions (PAN 260 and CTP-PAN 1:1) and by the oxidation (PANox) are presented in Fig. 32. The vibrations characteristic of PAN structure are those of the CN nitrile group at 2240 cm^{-1} and the aliphatic CH group at 2920 cm^{-1}, 1460 cm^{-1} and 1380 cm^{-1}. The additional bands centered at 1080 and 1250 cm^{-1} can be attributed to the CO bonds, in part related to hydroxylic OH groups as suggested by the presence of weak broad band at about 3600 cm^{-1}. The interpretation is in agreement with elemental analysis showing significant amount of oxygen in the sample. The band at 1080 cm^{-1} is also related to the ν(C-C) skeletal vibration of aliphatic polymer chain.

The rearrangement of PAN chain into cyclic polyimine/polyenamine structures, which proceeds on heat treatment at 260°C, is reflected by a decrease in the intensity of nitrile band at 2240 cm^{-1}. The corresponding transformation of nitrogen functionalities is monitored by the arising of two strong broad bands between 3500-3100 cm^{-1} and 1610-1580 cm^{-1}, which can be attributed to NH stretching (Bellamy, 1975) and both CN or CC double bonds in cyclic tautomers polyimine/polyenamine, respectively. The presence of some conjugated nitriles is reflected by the appearance of second nitrile band at 2220 cm^{-1} (Dalton et al., 1999). There are no oxygen functionalities giving signals at 1250 and 1080 cm^{-1}. Disappearance of the latter band confirms also the collapsing of the linear structure of PAN macromolecules.

DRIFT spectrum of CTP-PAN 1:1 blend contains, basically, all the characteristic bands of components. Pitch contribution includes aromatic CH vibrations at about 3050 cm^{-1} and 900-700 cm^{-1} and vibrations of aromatic ring at 1600 cm^{-1}. However, the presence of relatively strong broad bands between 3500-3100 cm^{-1} and 1400-1200 cm^{-1}, which can be in part attributed to nitrogen functionalities, seems to indicate some extent of PAN cyclization to occur during the blend preparation at 250°C.

DRIFT spectrum of PANox indicates that the transformations of nitrogen groups on the oxidative stabilization of PAN are similar to those observed for the polymer heat-treated in inert atmosphere. The cyclization to polyimine/polyenamine structures reflects in the decrease of the intensity of nitrile band at 2240 cm^{-1}. As can be concluded from the broadening and shift of the band to 2228 cm^{-1}, the remaining nitrile groups occur mainly in the conjugated form. The strong band at 1620-1580 cm^{-1} can be attributed to the CC and CN double bonds in tautomers of polyimine/polyenamine structure, but seems to be also partly associated with the onset of aromatization. The aromatization is confirmed by the appearance of band at 805 cm^{-1}. The broad band

between 3500-3100 cm^{-1} is characteristic of the NH stretching. The oxidative degradation is monitored by the appearance of broad shoulder in the region of 1750-1620 cm^{-1}. The relatively high intensity of the signal in the region of 1680 cm^{-1} indicates that conjugated ketones and quinones predominate amongst oxygen functionalities (Koch et al., 1998). The presence of the hydroxylic groups reflects in the appearing of distinguishable peak at about 1250 cm^{-1}.

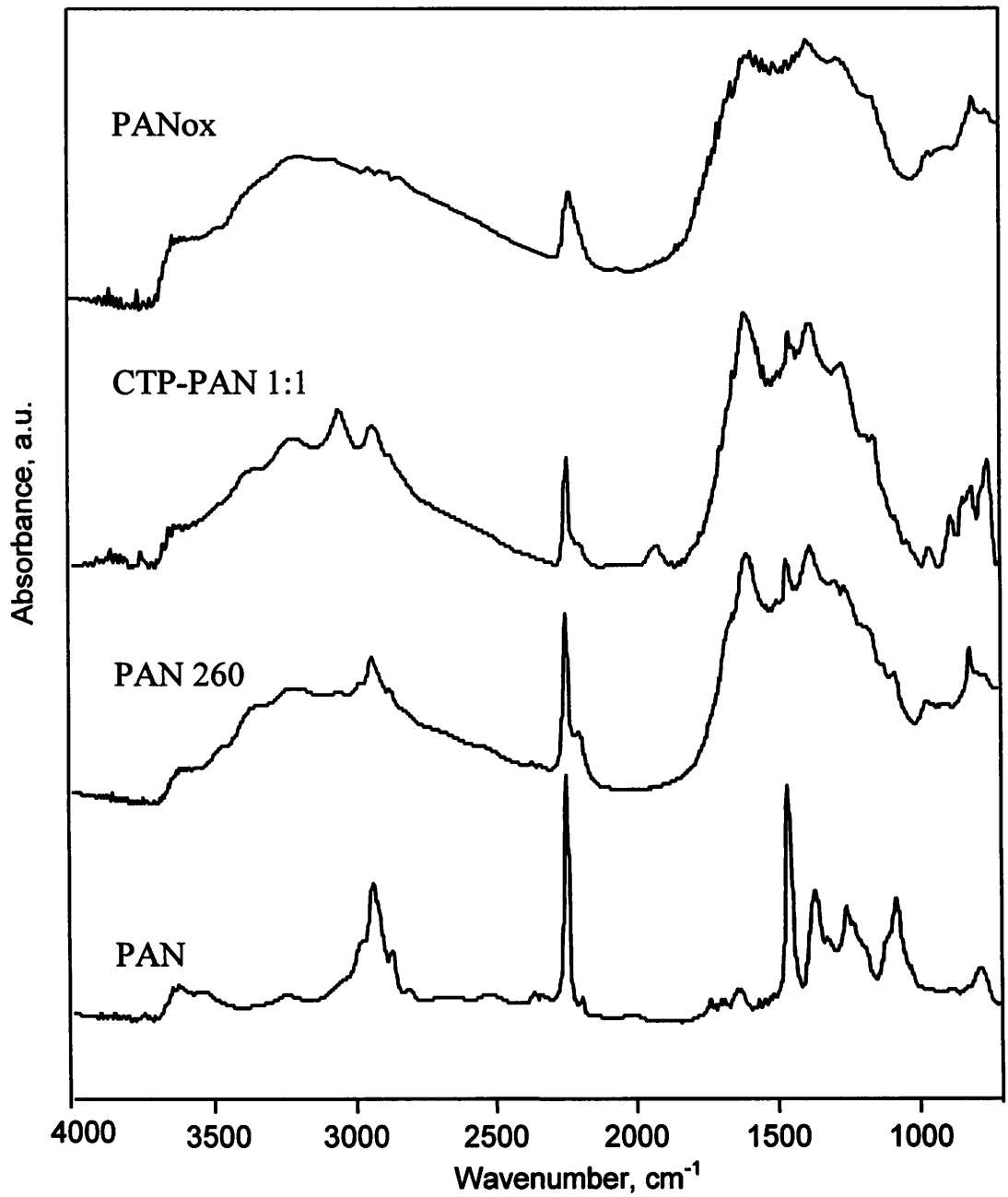

Fig. 32. DRIFT spectra of PAN and its derivatives: PAN, PAN 260, CTP-PAN 1:1, PANox.

DRIFT spectra of semi-cokes from PAN and CTP-PAN 1:1 blend (PAN-S and CTP-PAN 1:1-S) are given in Fig. 33. The characteristic features of DRIFT spectrum of PAN heat-treated at 520°C are broad bands from the aromatic ring (1600 cm^{-1}) and nitrogen functionalities (3500-3100 cm^{-1} and 1400-1200 cm^{-1}). Aromatization is also reflected by disappearance of the aliphatic C-H band at 3000-2800 cm^{-1}. An interesting point is a decrease of intensity of 3500-3100 cm^{-1} band compared to PAN 260 sample. The observation is consistent with the view of Setnescu et al. (1999) that NH group, which generates the signal, is an intermediate state in the nitrogen removal. It should be noted that some nitrile groups, mostly in the conjugated form remain even upon thermal treatment up to 520°C.

The spectrum of semi-coke from CTP-PAN 1:1 blend is similar to that of singly treated PAN. The difference in the profile of broad band between 1700 and 1100 cm^{-1} should be noted but its interpretation is doubtful. A small peak distinguishable at about 3400 cm^{-1} is commonly attributed to NH group in pyrrol ring (Granda et al., 1990).

The comparison of the DRIFT spectrum of PANox semi-coke (PANox-S) (Fig. 33) and the spectrum of the oxidized polymer (Fig. 32) allows the evaluation of the most drastic changes induced by the heat-treatment. A general increase in the spectral intensity in the region of 1700-1200 cm^{-1} indicates the formation of highly conjugated aromatic system (Celina et al., 1997). The aromatization is also reflected in the disappearance of the aliphatic C-H band at 3000-2800 cm^{-1}. The heat-treatment of PANox is accompanied by the removal of NH and oxygen groups as indicated by the decrease of intensity of 3500-3100 cm^{-1} band. A decrease in the peak at around 1250 cm^{-1} attributable to C-OH single bonds indicates that carboxylic acids are the most temperature sensitive (de La Puente et al., 1997). It is noteworthy that some conjugated nitrile groups (at about 2210 cm^{-1}) remain after the heat-treatment.

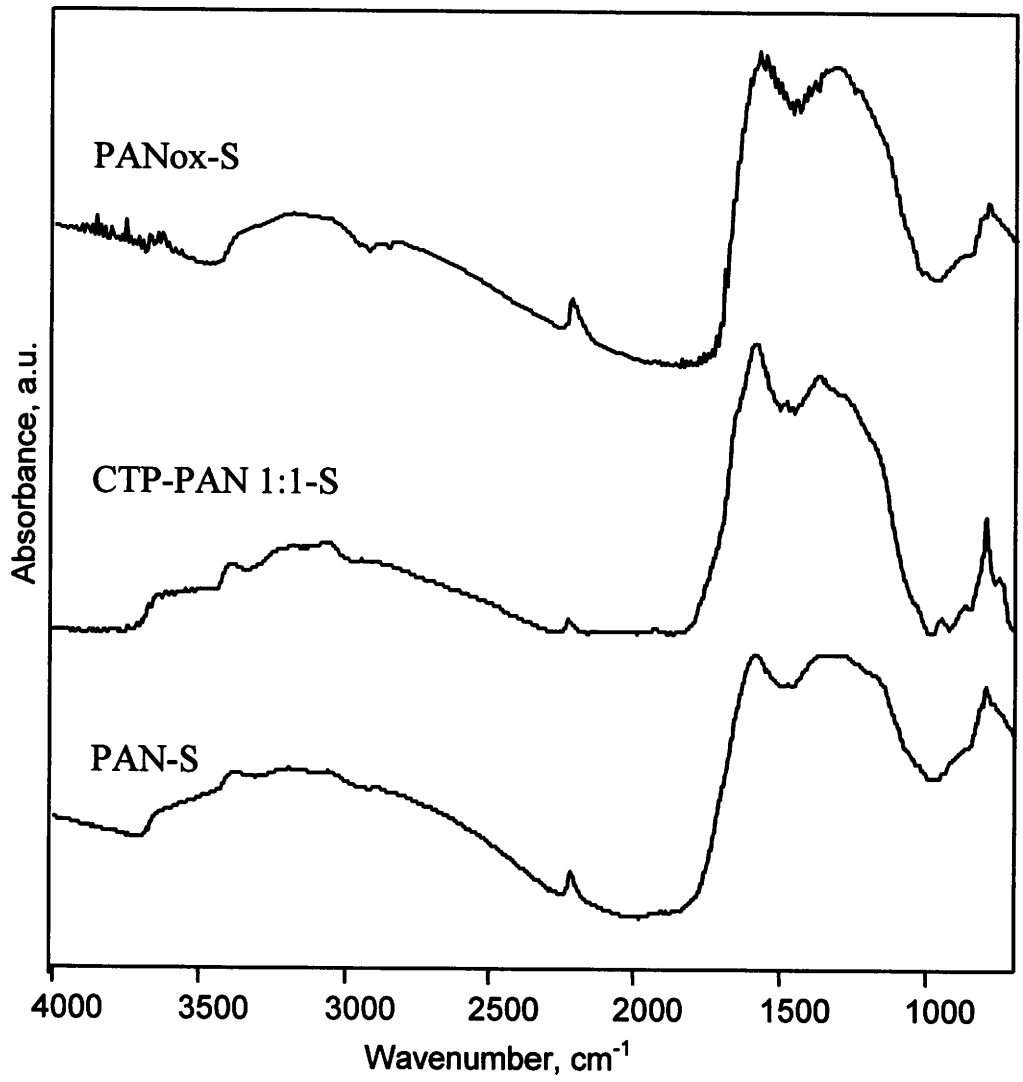

Fig. 33. DRIFT spectra of semi-cokes from PAN, CTP-PAN 1:1 and PANox.

X-ray photoelectron spectroscopy (XPS)

XPS was used to monitor the evolution of nitrogen, carbon and oxygen functionalities on the thermal treatment of PAN and CTP-PAN 1:1 blend. Fig. 34 shows the N1s spectra of pristine PAN and CTP-PAN blend at various stages of heat-treatment.

The spectrum of non-treated PAN consists of one symmetric peak of nitrile nitrogen centered at 399.5 eV. The occurrence of cyclization to imine ring on heat-treatment at 260^{0}C can be deduced from the larger FWHM of the band, which is about 3 eV compared to about 2.0 eV as typical of single component band.

The overlapping of binding energies corresponding to cyano and imine groups makes difficult a more precise evaluation of contributions from both components. N1s spectra

of semi-cokes (520^{0}C) from PAN and CTP-PAN 1:1 have very similar profiles and can be fitted by two components. The peak with a maximum at the binding energy at 398.2±0.2 eV corresponds to the pyridine type nitrogen (Pels et al., 1995, Schmiers et al., 1999, Kapteijn et al., 1999). The peak at 399.7±0.2 eV can be attributed to both nitrogen occurring in the 5-membered pyrrolic ring and to the pyridinic form in association with the oxygen functionality, so-called pyridone. These two forms cannot be distinguished within the accuracy of XPS measurements. Apparently, the presence of amine-like pyrrolic group in the semi-coke of PAN and CTP-PAN is confirmed by DRIFT spectra. However, the formation of some pyridonic groups on the surface is likely to occur due to susceptibility of N-polymer derived carbons to oxidation after exposure on air. Relevant observation is the lack of quaternary nitrogen in the semi-cokes. This is consistent with the Pels et al. (1995) view that quaternary nitrogen is mostly formed by the gradual conversion of the pyrrolic form, which starts above 600^{0}C.

It is interesting to note that the integration of area of peaks corresponding to pyridinic and pyrrolic/pyridonic components of the N 1s spectrum gives the same ratio (64:36) for semi-cokes derived from both the PAN and CTP-PAN blend. Therefore, we assume that the transformation pathway of nitrogen functionalities in pitch-polymer blend is in principle the same as in the pristine PAN.

Fig. 35 presents C1s spectra of semi-cokes produced from CTP, PAN and CTP-PAN 1:1 blend, respectively. Single symmetric peak at 285.0 ± 0.2 eV in the CTP coke spectrum corresponds to "graphitic" carbon atoms forming CC and CH bonds. The resolution of asymmetric band occurring in PAN and CTP-PAN semi-cokes spectra gives, in addition to the former peak, a component from carbon bound to nitrogen at 287.5 ± 0.2 eV (Biniak et al., 1997). The estimation shows that the peak related to CN bonds accounts for about 18% and 14% of the total C 1s peak area in the PAN and CTP-PAN semi-cokes, respectively.

FTIR and XPS analyses reveal a rather similar evolution of nitrogen functionalities on heat treatment of PAN and CTP-PAN 1:1 blend. It seems, therefore, that the direct chemical interactions between PAN fragments and pitch molecules, which could produce a new type of recombined macromolecules via radical or condensation mechanism, have rather limited influence on the nitrogen groups transformation pathway.

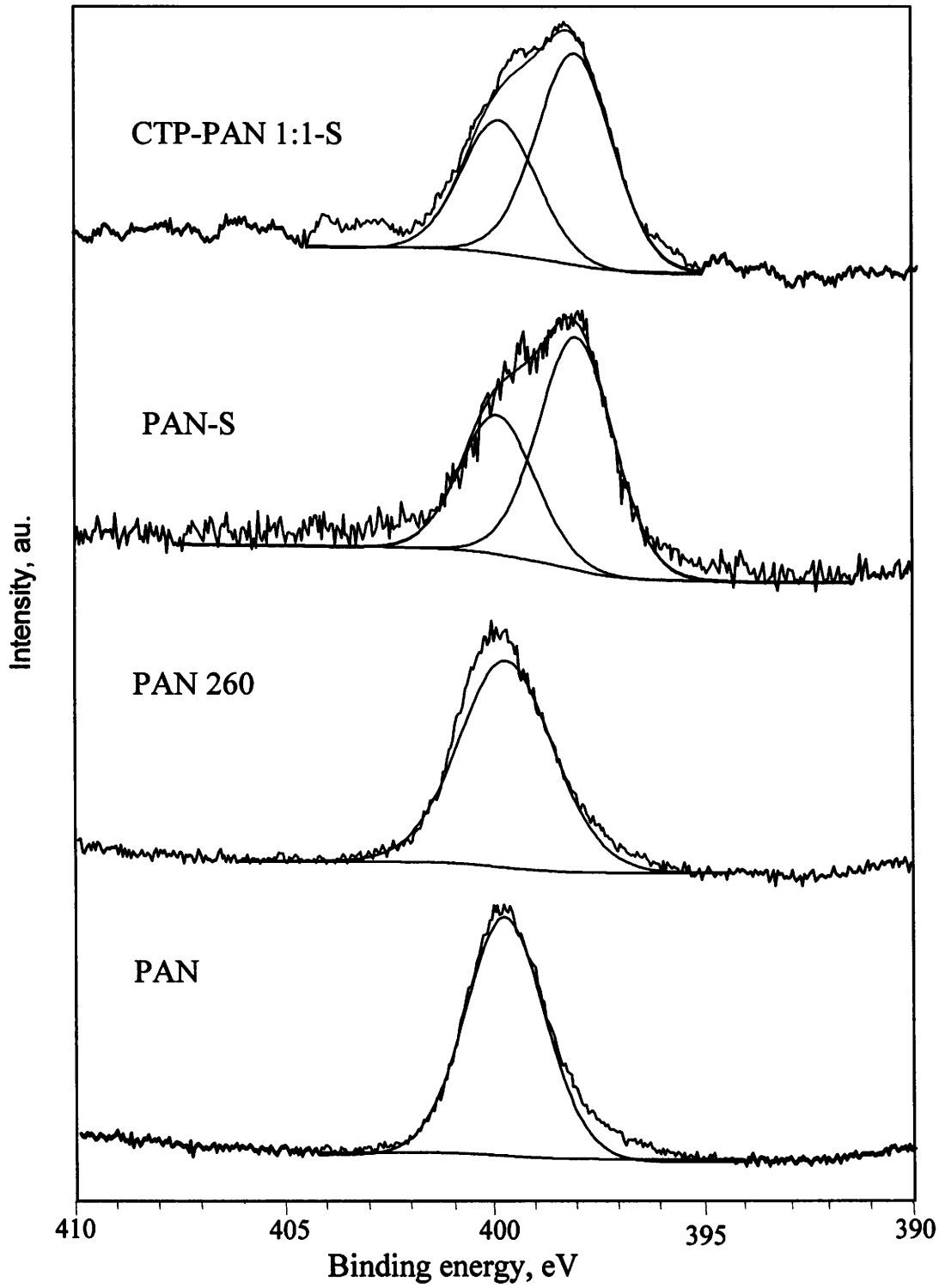

Fig. 34. N1s XPS spectra of PAN and CTP-PAN blend at various stages of heat-treatment: pristine PAN, PAN 260, PAN semi-coke, CTP-PAN 1:1 semi-coke.

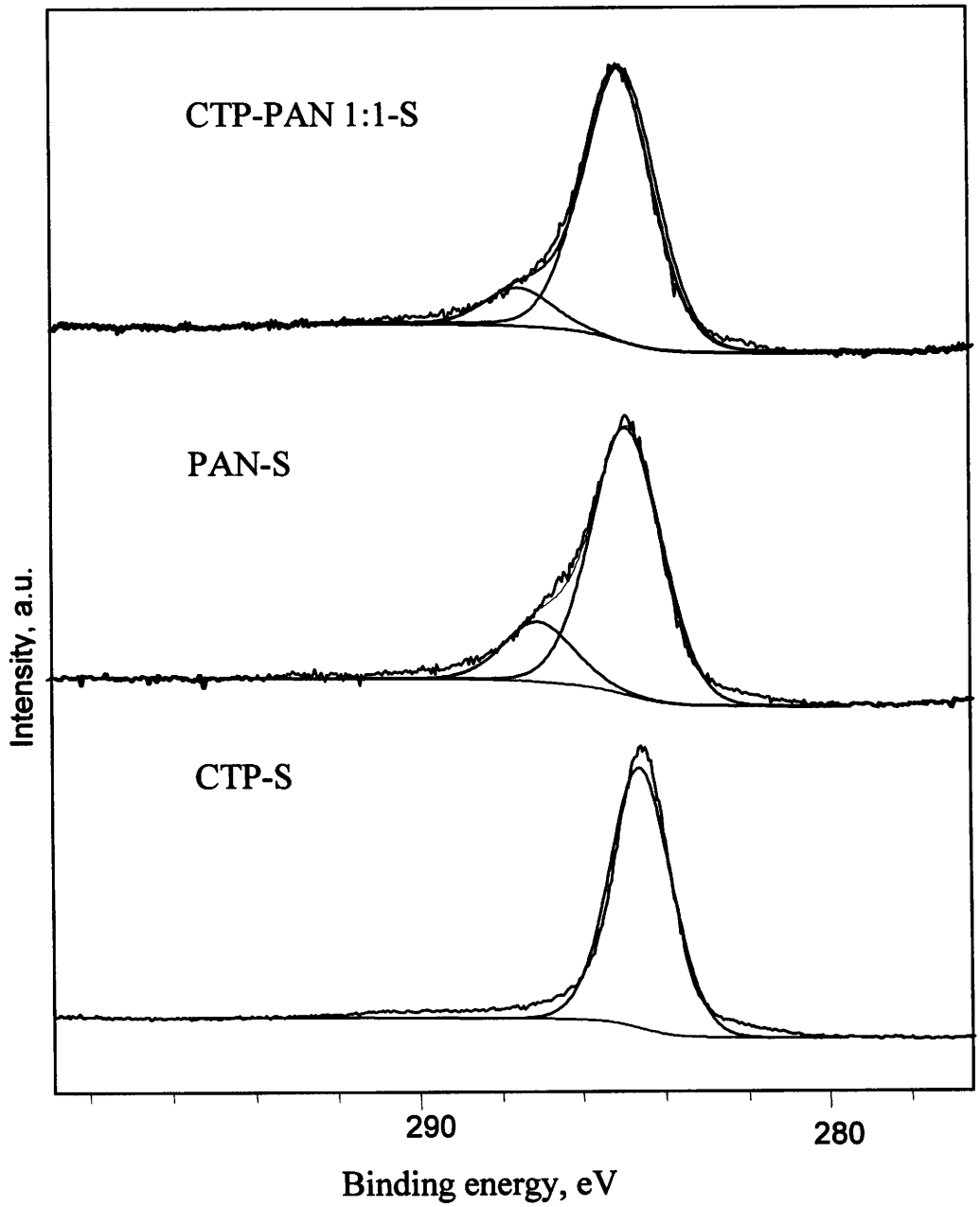

Fig. 35. C1s XPS spectra of semi-cokes from CTP, PAN and CTP-PAN 1:1.

Fig. 36 shows N1s spectra of PANox and semi-coke prepared from PANox. The component corresponding to the pyrrolic/pyridonic nitrogen (400.2±0.2 eV) constitutes the majority (52%) of N1s peak area of oxidized PAN (Table 6). Apparently, the remarkable contribution should be attributed to the pyridonic groups generated under oxidizing conditions of PANox preparation. It is interesting to note a noticeable

proportion (19.5%) of quaternary nitrogen in the PANox, despite the relatively mild conditions of oxidation. This is in contrast with the absence of quaternary nitrogen in the semi-coke prepared from the unoxidized PAN. It is noteworthy to remind that the incorporation of nitrogen into graphene layers has been reported to occur at more severe conditions of thermal treatment than used in the oxidative stabilization of PAN (Pels et al., 1995). This supports the identification of nitrogen of binding energy 401.9 eV in PANox as protonated pyridinic and/or pyridinic functionality associated with an adjacent or nearby located hydroxyl oxygen or carboxyl group, protonated through formation of a H-bridge (Kelemen et al., 1994).

The thermal treatment brings about to approximately two-fold increase in the proportion of quaternary nitrogen in the PANox-S at the expense of pyrrolic/pyridonic form. The level of pyridinic nitrogen is only slightly diminished on pyrolysis. Pyridinic N-oxides formed as a result of oxidation upon exposure on air constitute about 4 % of nitrogen in PANox-S.

C1s spectra of PANox and PANox-S (Fig. 37) are fitted by four components: "graphitic carbon"centered at 284.8±0.2 eV, peak of carbon linked to nitrogen and/or singly bonded to oxygen (286.4±0.2 eV), carbonyl or quinone carbon (288±0.2 eV), and carboxylic or esther carbon (289.6±0.2 eV). Carbon atoms linked to heteroatoms constitute more than a third part of total carbon (Table 7) in the oxidized polymer. The treatment to 600^0C decreases the proportion of carbon linked to heteroatoms in favor of "graphitic" carbon, however, the O1s spectra of PANox and PANox-S presented in Fig. 38 reveal the presence of three oxygen forms. The peak at 530.6±0.2 eV corresponds to CO double bonds, the major peak at 532.6±0.4 eV can be ascribed to C-OH and/or C-O-C, and that at 535.2±0.4 eV to the chemisorbed oxygen and/or water. Increased intensity of the peak located at 535.2±0.4 eV (Table 8) confirms the enhanced chemisorption of water on nitrogen basic sites.

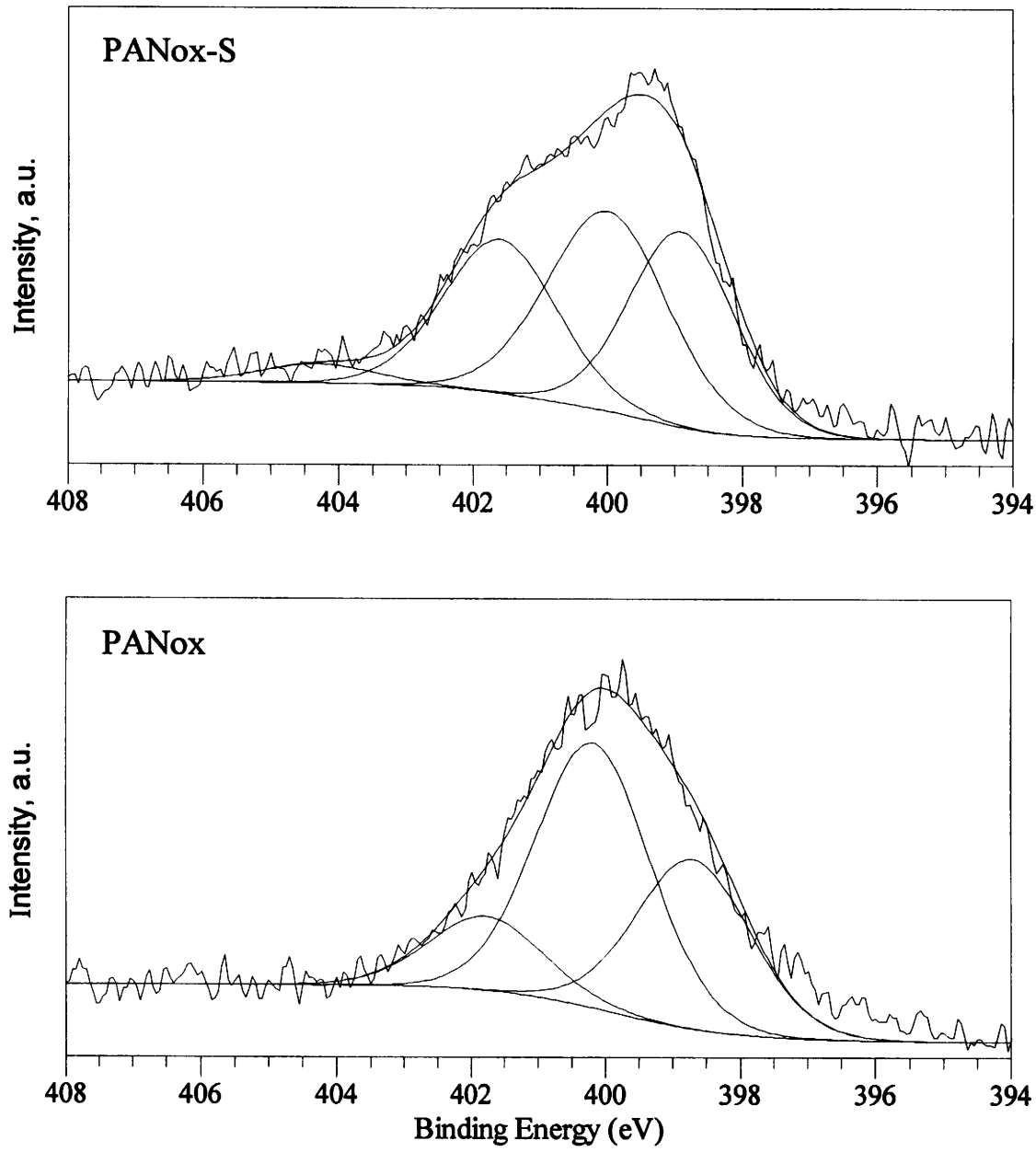

Fig. 36. N1s XPS spectra of PANox and the derived semi-coke.

Table 6. Distribution of nitrogen forms in PANox and the derived semi-coke (at%)

Sample	Pyridinic	Pyrrolic/pyridonic	Quaternary	N-oxide
PANox	33.3	52.2	14.5	0.0
PANox-S	30.2	37.4	28.1	4.3

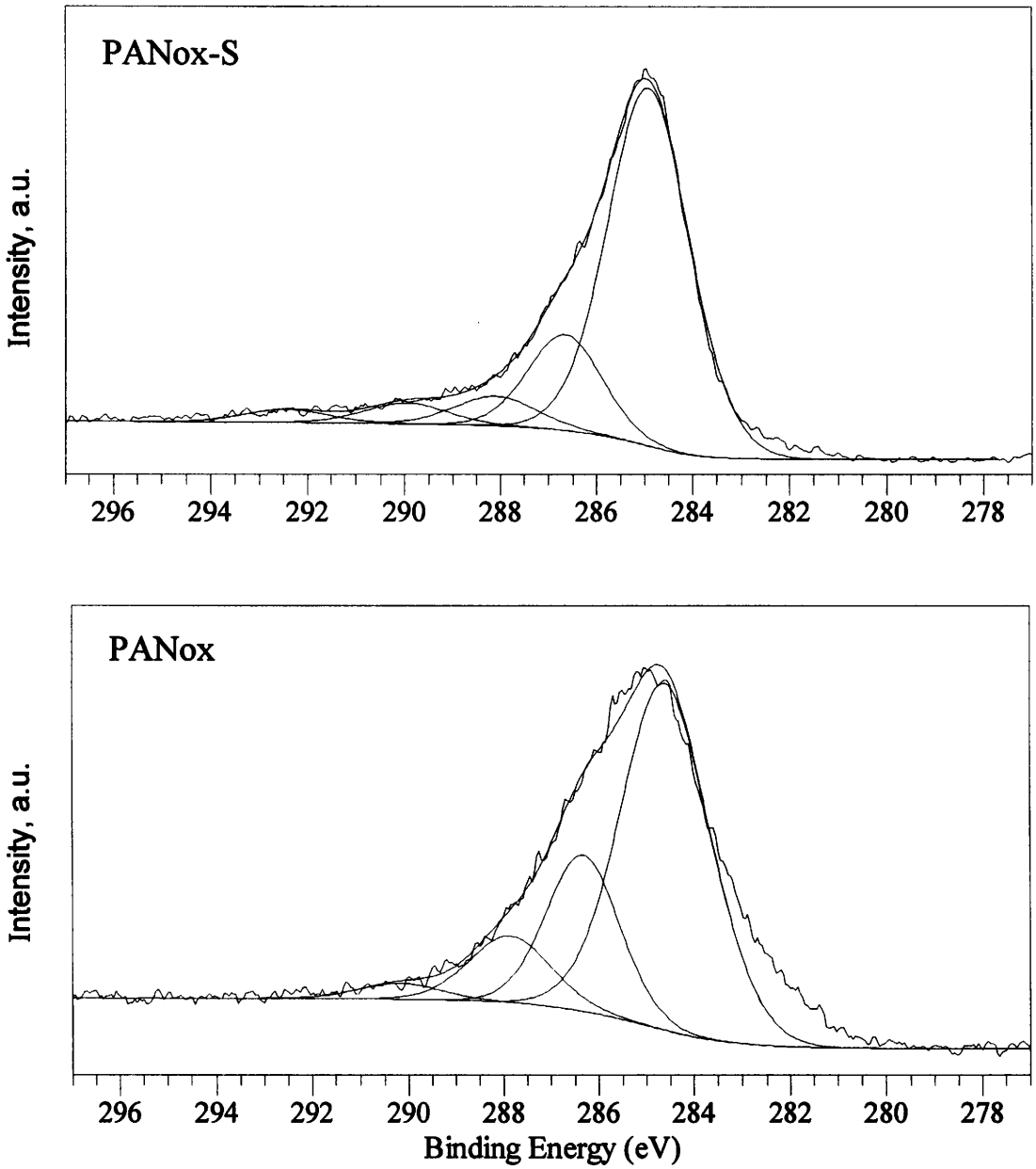

Fig. 37. C1s XPS spectra of PANox and the derived semi-coke.

Table 7. Distribution of carbon forms in PANox and the derived semi-coke (at.%)

Sample	284.8±0.2 eV	286.4±0.2 eV	288±0.2 eV	289.6±0.2 eV
PANox	63.1	23.3	11.0	2.6
PANox-S	70.6	17.0	5.8	6.6

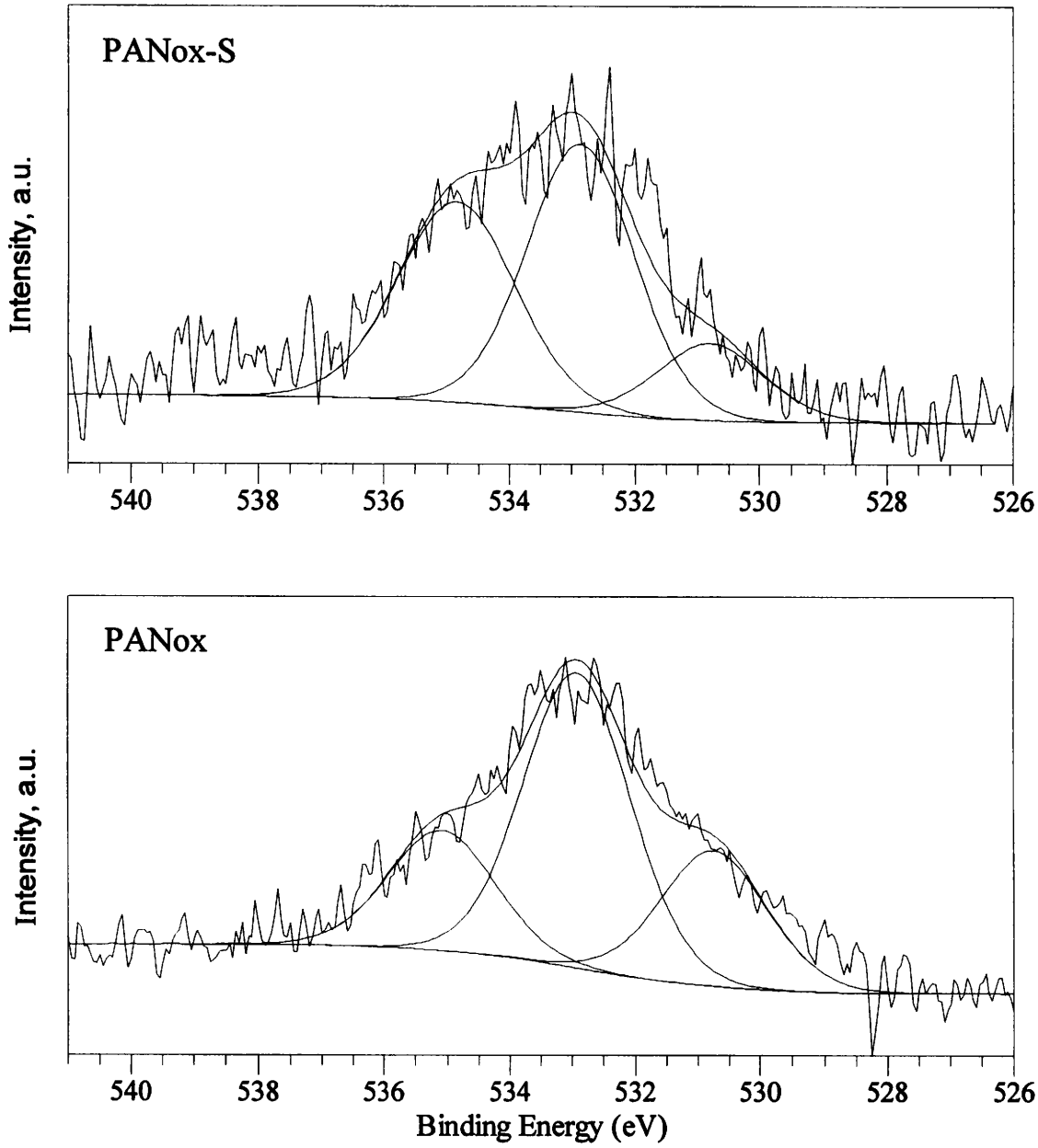

Fig. 38. O1s XPS spectra of PANox and the derived semi-coke.

Table 8. Distribution of oxygen forms in PANox and the derived semi-coke (at.%)

Sample	530.6±0.2 eV	532.6±0.4 eV	535.2±0.4 eV
PANox	24.6	53.7	21.7
PANox-S	13.6	47.4	39.0

The surface elemental composition of PAN, PANox and their semi-cokes determined by XPS is given in Tables 9 and 10. For the polymers, the elemental composition (atomic ratios) measured at the surface is fairly consistent with the elemental analysis data for a bulk of sample. In the case of semi-cokes the situation is more complex. The XPS data confirm a partial loss of nitrogen on heat-treatment at 520^{0}C of pure polymers, but also a lower proportion of nitrogen and oxygen than those measured using elemental analysis. As to oxygen, one could expect just an opposite relation due to the enhanced reactivity of the surface. We think that the deep evacuation of samples before XPS analysis results in a partial release of the occluded or weekly bound species bearing nitrogen and oxygen. This is not a case of blend semi-coke (CTP-PAN 1:1-S) where the surface analysis gives a larger proportion of oxygen. A distinctly decreased oxygen content in PANox-S compared to the initial polymer can be attributed to the decomposition of oxygen functionalities on pyrolysis.

Table 9. Elemental composition of PAN and PANox determined by XPS

Sample	Atomic concentration[1]			Atomic ratios			
	C	N	O	N/C		O/C	
				XPS	El.An.	XPS	El.An.
PAN	75.0	24.0	1.0	0.320	0.331	0.013	0.023
PANox	71.7	18.8	9.5	0.262	0.310	0.133	0.142

[1] C + N + O = 100%

Table 10. Elemental composition of semi-cokes from PAN and CTP-PAN 1:1 blend determined by XPS

Sample	Atomic concentration[1]			Atomic ratios			
	C	N	O	N/C		O/C	
				XPS	El.An.	XPS	El.An.
CTP-S	97.0	1.0	2.0	0.010	0.07	0.021	0.005
CTP-PAN 1:1-S	82.9	10.8	6.3	0.131	0.116	0.075	0.044
PAN-S	79.6	14.2	6.2	0.179	0.238	0.078	0.087
PANox-S	80.7	15.1	4.2	0.188	0.239	0.052	0.097

[1] C + N + O = 100%

5.2.2.4. The evaluation of the interactions between pitch and polymers on pyrolysis

The microscopic observations and thermogravimetry indicate that PANox behaves rather as an inert material during the pyrolysis with coal-tar pitch. Contrarily, the strong interactions of unoxidized PAN with pitch can be deduced from the enhanced residue yield and the extensive modification of the optical texture of resultant semi-coke.

A following scheme of interactions occurring on co-pyrolysis of CTP with polyacrylonitrile emerges from the results of optical microscopy and thermogravimetry. Thermal degradation of PAN occurring via radical mechanisms leads to oligomers as principal products of bond scission. The resultant radicals can be stabilized by hydrogen, which is abstracted from pitch molecules what results in the decrease of the light oligomers evolution. The coal-tar pitch seems to be therefore a stabilizer of radicals, preventing an extensive degradation of PAN. On the other hand, the abstraction of hydrogen generates radicals within pitch matrix so promoting condensation and cross-linking reactions of pitch constituents. The consequence of the enhanced thermal reactivity is the extensive deterioration of the optical texture of carbonization residue in the case of blend, which suggests a very strong dehydrogenation activity of the created polymer fragments.

Therefore the principle of the interactions can be defined as indirect chemical modifications of both pitch and PAN involving hydrogen transfer reactions. The crucial role of hydrogen donor/acceptor properties of pitch-like materials in terms of optical texture of carbonization products is well established (Yokono et al., 1981, Iyama et al., 1986).

FTIR and XPS analyses reveal similar evolution of nitrogen functionalities on heat treatment of PAN and CTP-PAN blend. It seems, therefore, that the direct chemical interactions between PAN fragments and pitch molecules, which could produce a new type of recombined macromolecules via radical or condensation mechanism are rather limited.

5.3. Co-pyrolysis of pitch with polyvinylpyridine

5.3.1. Weight loss behavior

Thermogravimetry coupled with FTIR of evolved gases was used to monitor the thermal stability of vinylpyridine resins (PVP2, PVP25 and PVP25ox) and their blends with CTP in a 1:1 weight ratio.

TG/DTG profiles of PVP2, PVP25 and PVP25ox are presented in Figs. 39-41, respectively. Figs. 42-44 are, correspondingly, the thermograms of blends of the polymers with pitch, relating the experimental TG and DTG profiles to those computed from the single components behaviours according to the additivity rule. The characteristics of thermal degradation of the polyvinylpyridines and their blends with CTP are given in Table 11.

DTG profiles of both the pristine poly(4-vinylpyridines) (Figs. 39 and 40) clearly demonstrate that the thermal degradation occurs within a relatively narrow temperature range with a rapid release of majority of volatiles. Previous studies showed that the principal chemical reaction during such a thermal treatment is the depolymerization. It was reported that poly(4-vinylpyridines) form 4-vinylpyridine monomer as a main product and traces of pyridine and 4-methylpyridine (Azhari and Diab, 1998). 4-vinylpyridine monomers have been also identified as a main product of the thermal degradation of poly(4-vinylpyridne-N-oxide (Uchiyama et al., 1998).

In the case of PVP2 and PVP25 practically the total weight loss occurs within the depolymerization temperature range (300-450^{0}C) with a maximum centered at about 400^{0}C (Table 11). Apparently, the DVB added to poly(4-vinylpyridines) as a cross-linking agent can moderately enhances the thermal stability of co-polymer.

Specific of PVP25ox thermal behaviour is a strongly reduced extent of depolymerization, as evidenced by the weight loss at this stage of 14 % only, however the volatile evolution is continued up to the final temperature giving a total weight loss of about 26 wt% (Fig. 41). When compared to 87 % weight loss in PVP25, the contribution of oxidation to the improvement of the thermal stability of vinylpyridine resin is indeed enormous.

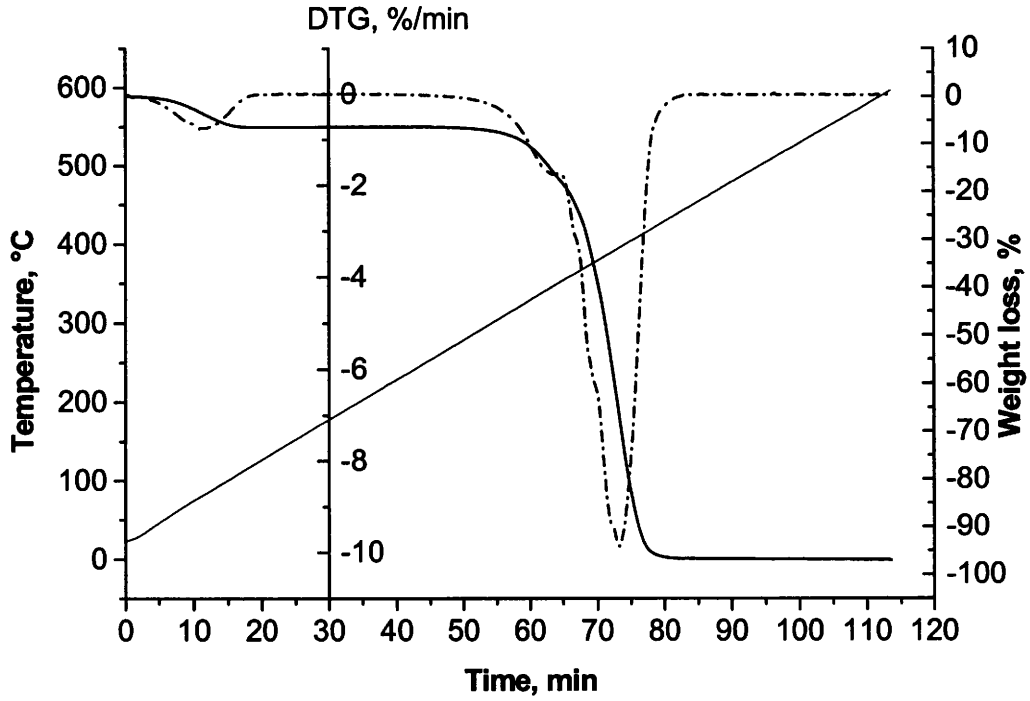

Fig. 39. TG/DTG profiles of PVP2.

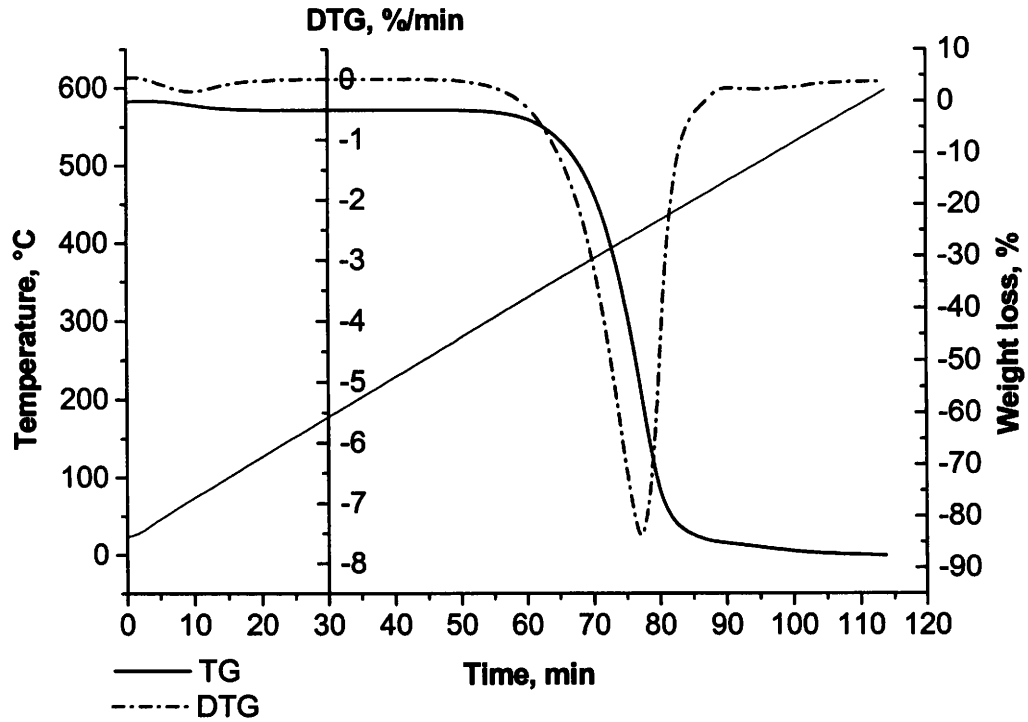

Fig. 40. TG/DTG profiles of PVP25.

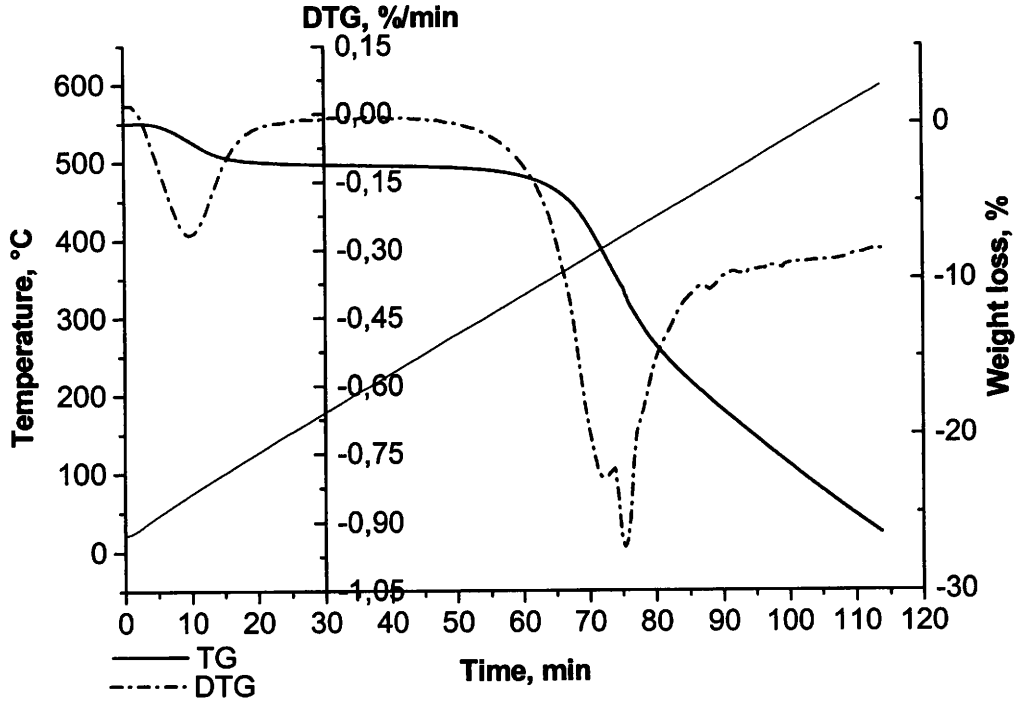

Fig. 41. TG/DTG profiles of PVP25ox

The thermograms of CTP-PVP2 and CTP-PVP25 blends (Figs. 42 and 43) seem to be, at first look, rather similar to those of the respective polymers. Apparently, the polymeric component has a predominant effect on the weight loss profile of the corresponding blend. The interactions between components induce, however, two relevant modifications to the thermal behavior of blend. First, this is an increase in the solid residue yield (by ~7 wt% for CTP-PVP2 and ~14 wt% for CTP-PVP25) compared to the value anticipated based on the behavior of single components. Other remarkable effect of blending consists in a decrease in the maximum weight loss temperature. For PVP25 the shift amounts to about 20°C compared to both the calculated value and the single polymer value. In the case of PVP2 the discrepancy between the temperatures of maximum weight loss of blend and single polymer is near 40°C. The explanation is that the presence of coal-tar pitch as a specific high boiling mixed solvent reduces the thermal stability of polymeric material thus lowering the depolymerization temperature. The thermogram of CTP-PVP25ox (Fig. 44) indicates a significant contribution of pitch to the weight loss profile in the low temperature region (250-350^{0}C). Moreover, the discrepancy between the experimental and calculated profiles appears in the same temperature range. Apparently, the polymer induces the delay and reduction of volatile

evolution from pitch. The effect can be due to dehydrogenative activity of oxygen functionalities present in PVP25ox which initiate the polymerization reactions of pitch constituent. A kind of analogy with the effects induced by air-blowing of pitch (Machnikowski et al. 2001, 2002b) is anticipated to occur. In the high temperature region, the experimental and calculated profiles are quite consistent, so suggesting that a condensed PVPox backbone is rather rigid and therefore less reactive toward pitch than molecules of PVP.

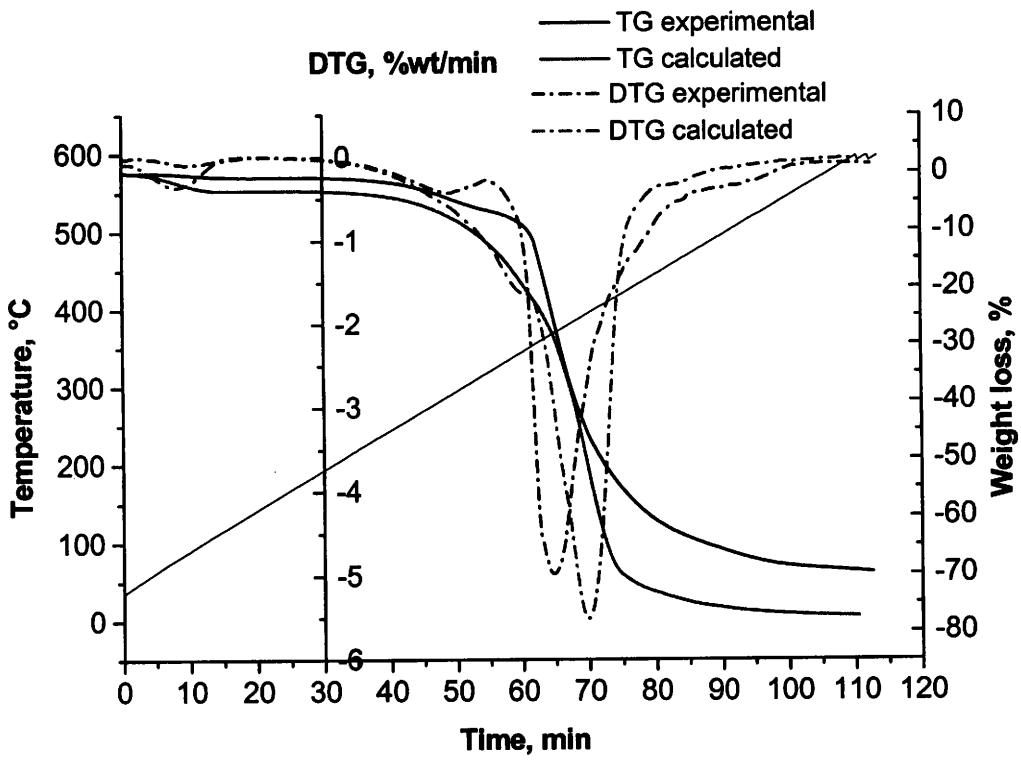

Fig. 42. TG/DTG profiles of CTP-PVP2 1:1 blend.

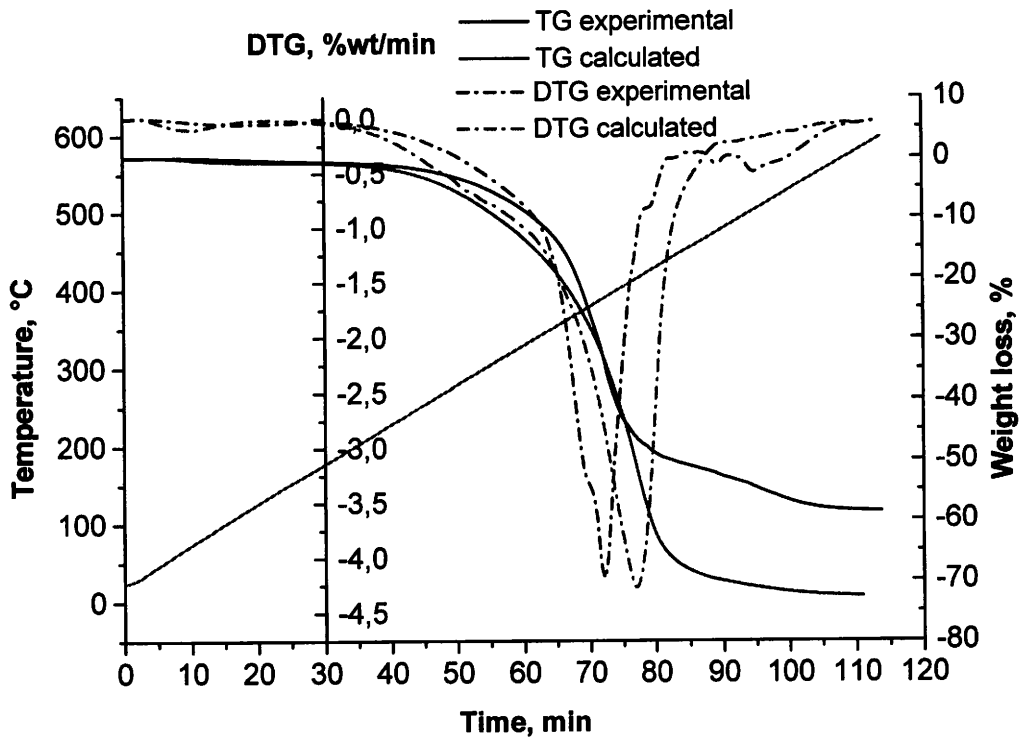

Fig. 43. TG/DTG profiles of CTP-PVP25 1:1 blend.

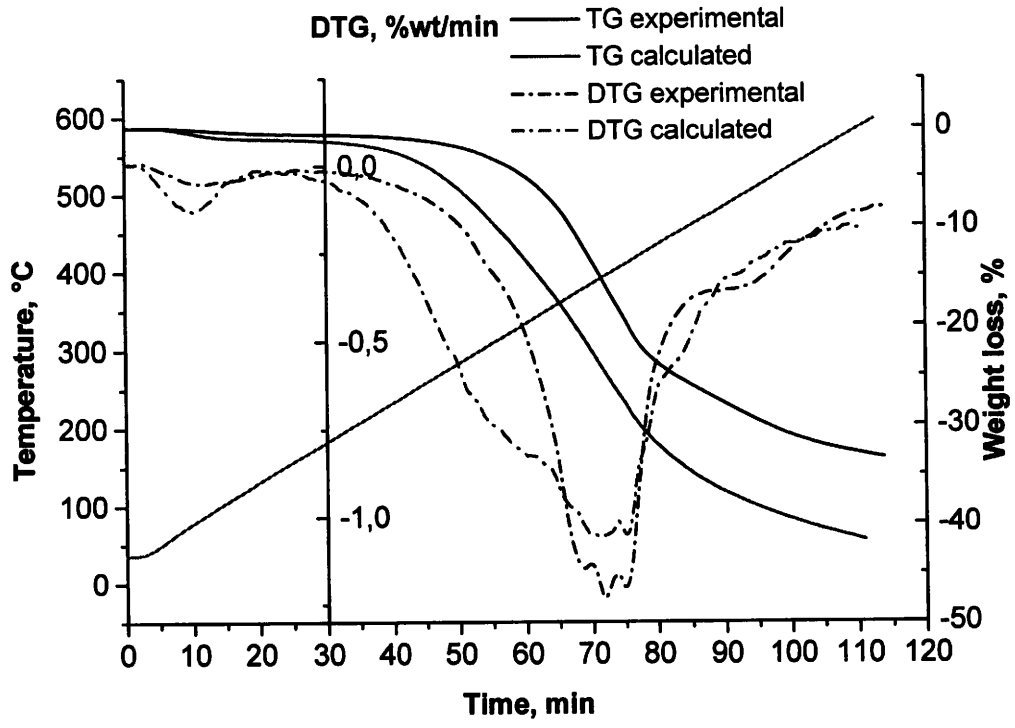

Fig. 44. TG/DTG profiles of CTP-PVP25ox 1:1 blend.

Table 11. Thermal decomposition characteristics of polyvinylpyridines and their blends with pitch

Sample	Major degradation step			Weight loss at
	Temp. range ^0C	T_{max}[1] ^0C	Weight loss %	600^0C %
PVP2	305-435	395	88.0	97.0
PVP25	308-475	410	83.0	87.5
PVP25ox	308-465	405	15.0	26.3
CTP-PVP2 1:1	320-460	370	56.0	70.0 (77.4)[2]
CTP-PVP25 1:1	230-440	390	48.5	58.7 (72.7)[2]
CTP-PVP25ox 1:1	250-470	390	25.5	33.3 (41.7)[2]

[1]Temperature of the maximum weight loss rate
[2] The anticipated weight loss

The FTIR analysis of gases evolved at 395^0C during PVP2 treatment (Fig. 45) confirms that 4-vinylpyridine monomer is the most abundant product at the temperature corresponding to the highest degradation rate. This spectrum shows a profile typical of 4-vinylpyridine with the specific absorptions at 1211, 988 and 822 cm^{-1} related to the bending of pyridine ring (Lebrun et al., 1998).

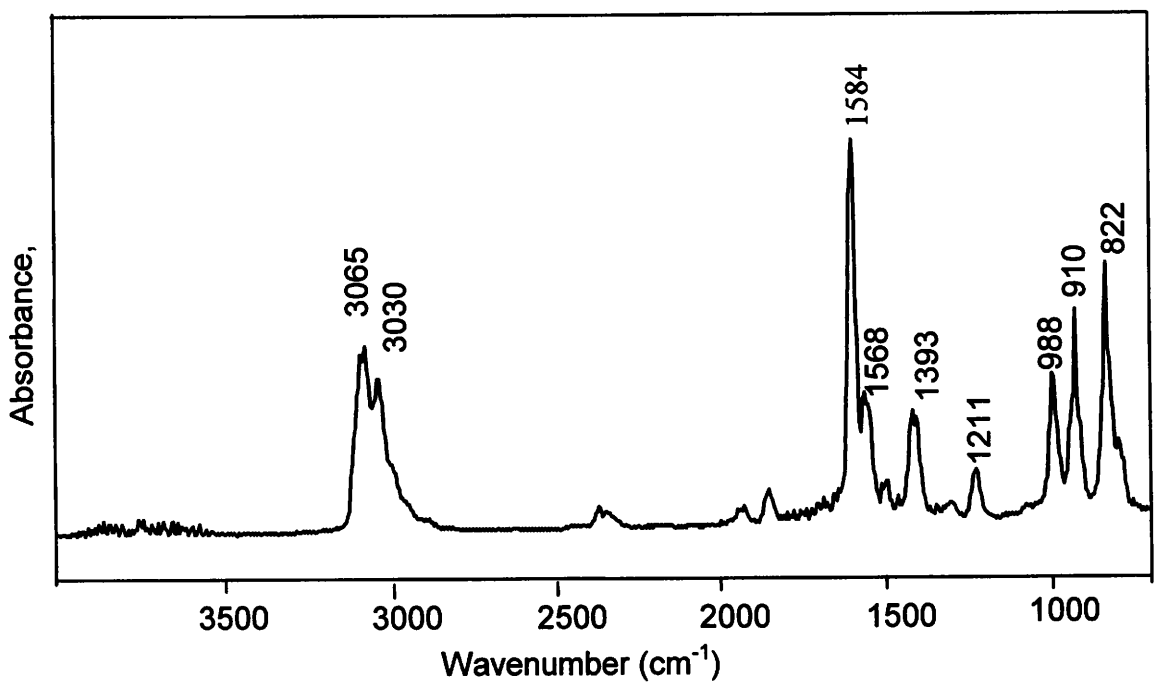

Fig 45. FTIR spectrum of gaseous products evolved from PVP2 at 395^0C.

Pyrolysis gas chromatography/mass spectrometry (Py-GC/MS) was additionaly used to provide more informations about the volatile degradation products of heat-treated PVP25 and PVP25ox. The pyrogram of PVP25 has a major peak at 2.59 min (Fig. 46). The mass spectroscopy indicates that this peak is mainly associated with the release of the 4-vinylpyridine monomer, as deduced from the presence of the most intense molecular ion at m/z 105 (Fig. 47). The ion at m/z 78 arises from the loss of m/z 27 from the molecular ion and is characteristic of the loss of HCN from the compound.

The pyrogram of PVP25ox (Fig. 48) has a major peak at 2.82 min. The mass spectrum of the compound giving rise to this peak is presented in Fig. 49. This compound has been identified with sizable uncertainty, based on the mass spectral library search, as 4-methyl-pyridne.

The peak present at 4.26 min on the PVP25ox pyrogram is associated with the presence of the heavier molecular compounds resulting from the fragmentation of partially condensed PVP25ox backbone. The corresponding most intense ion peak at m/z 119 has been attributed, based on the mass spectral library search, to 5-ethenyl-2-methyl-pyridine (Fig. 50).

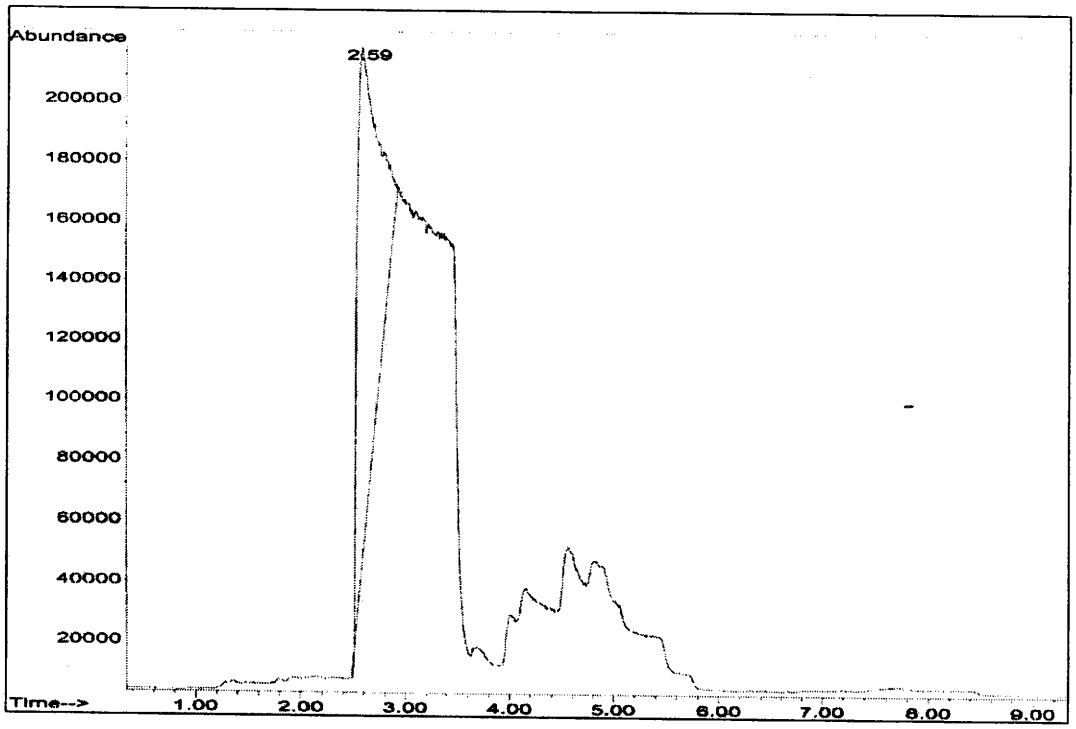

Fig. 46. Pyrogram of PVP25.

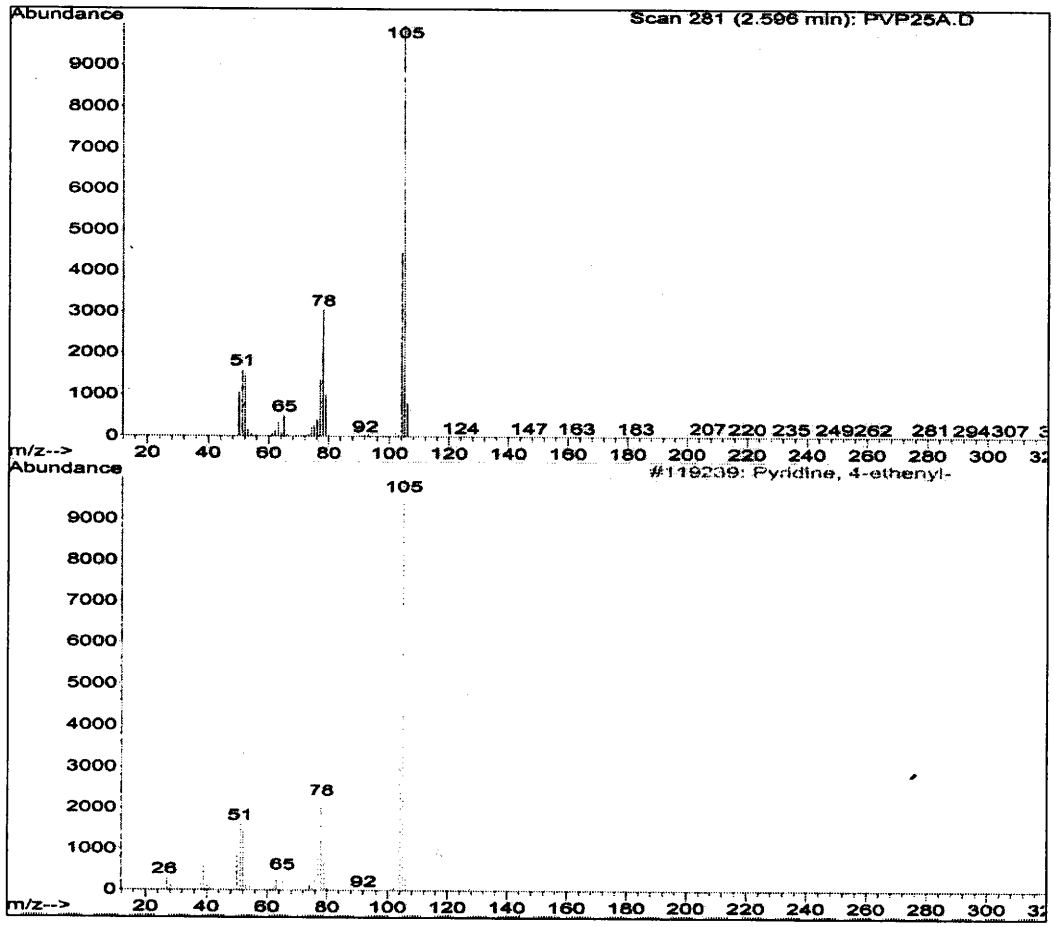

Fig. 47. Mass spectrum of the compound giving rise to peak at 2.59 min in pyrogram of PVP 25.

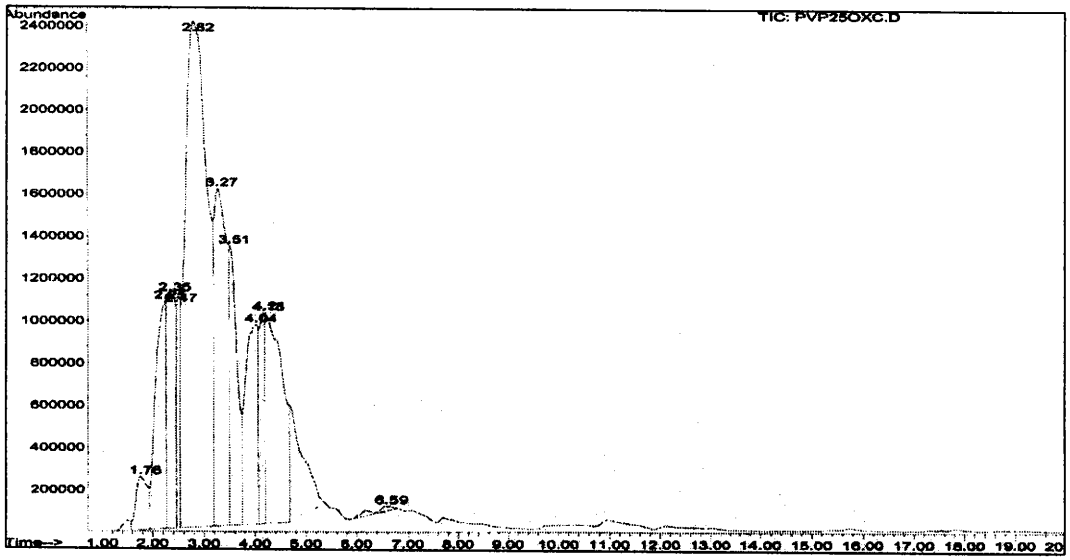

Fig. 48. Pyrogram of PVP25ox.

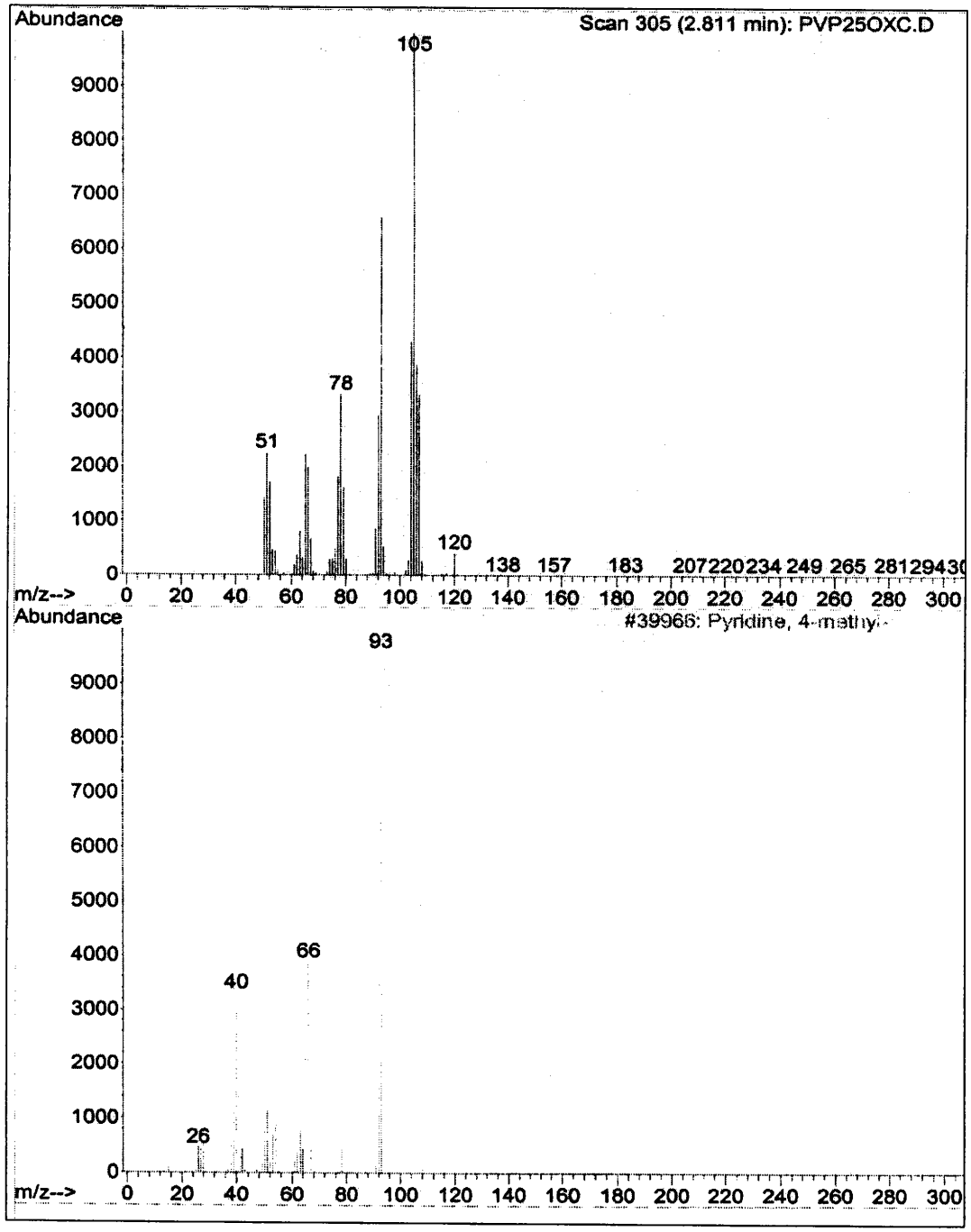

Fig. 49. Mass spectrum of the compound giving rise to peak at 2.81 min in PVP25ox pyrogram.

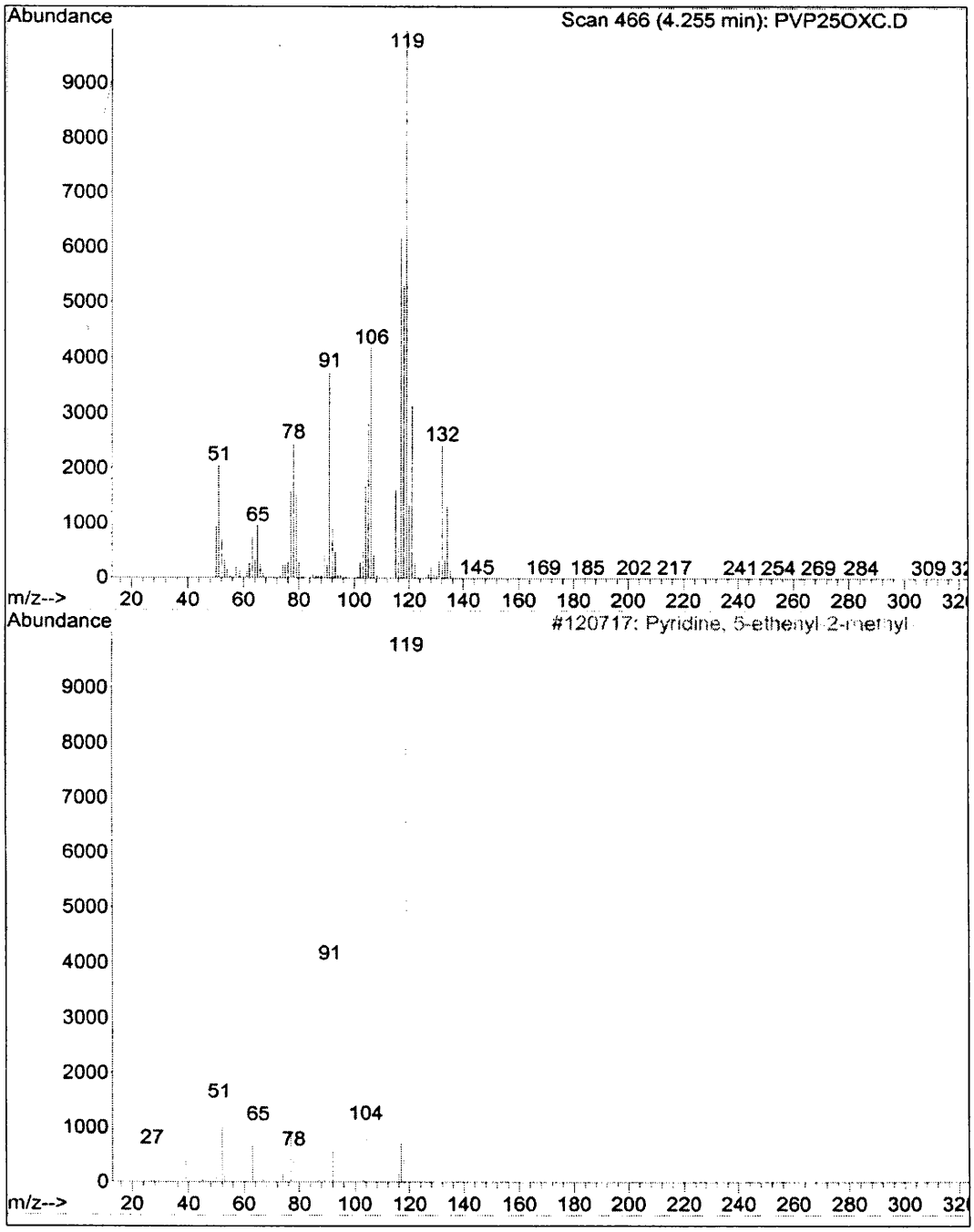

Fig. 50 Mass spectrum of the compound giving rise to peak at 4.25 min in PVP25ox pyrogram.

5.3.2. Structure and properties of co-pyrolysis products

5.3.2.1 Optical texture of semi-cokes from pitch-PVP25 and pitch-PVP25ox blends

Solid residues produced by the thermal treatment of PVP25 and PVP25ox at 520^0C show the totally isotropic optical texture.

PVP25 due to the predominating depolymerization into volatile oligomers on heat-treatment has a rather limited influence on the optical texture of carbons produced from blends with pitch. When the polymer content in a starting blend does not exceed 10 wt% the resultant semi-coke shows the optical texture of elongated flow domains and domains (Fig. 51), which is typical of the pristine pitch coke. A blend with 25 wt% of polymer (CTP-PVP25 3:1-S) gives still highly anisotropic semi-coke but of reduced proportion of elongated units (Fig. 52). The main components of the optical texture are domains (>60 μm) and small domains (30-60 μm) with some contribution of mosaics. Further increase in the PVP25 content in a blend to 50 wt% (CTP-PVP25 1:1-S) results in the reduction of anisotropic units size below 30 μm with coarse mosaics (10-30 μm) being a prevailing phase (Fig. 53).

The extent of the structural modification of carbons induced at comparable polymer proportion is definitely higher for PVPox than that observed for the unoxidized polymer. The elongated flow domain units disappear already at the content of 10 wt% of the polymer (Fig. 54). Coarse mosaics prevailing in the CTP-PVP25ox 3:1 semi-coke are presented in Fig. 55. The blend CTP-PVP25ox 1:1 gives completely isotropic product on carbonization.

Both PVP25 and PVP25ox give optically isotropic residue on carbonization, so one should assume a reduction of anisotropic development of blend coke due to polymer addition to pitch. The optical microscopy study does not supply the explanation of the stronger modifying effect of PVP25ox. First and foremost the reason can be a distinctly enhanced contribution of residue derived from PVP25ox than PVP25 to the blend coke, as expected based on coking values and thermal analysis data. We cannot however exclude that the more condensed and higher molecular weight backbones of the oxidized polymer behave partially as an inert in the co-pyrolysis system and hinder the mesophase development.

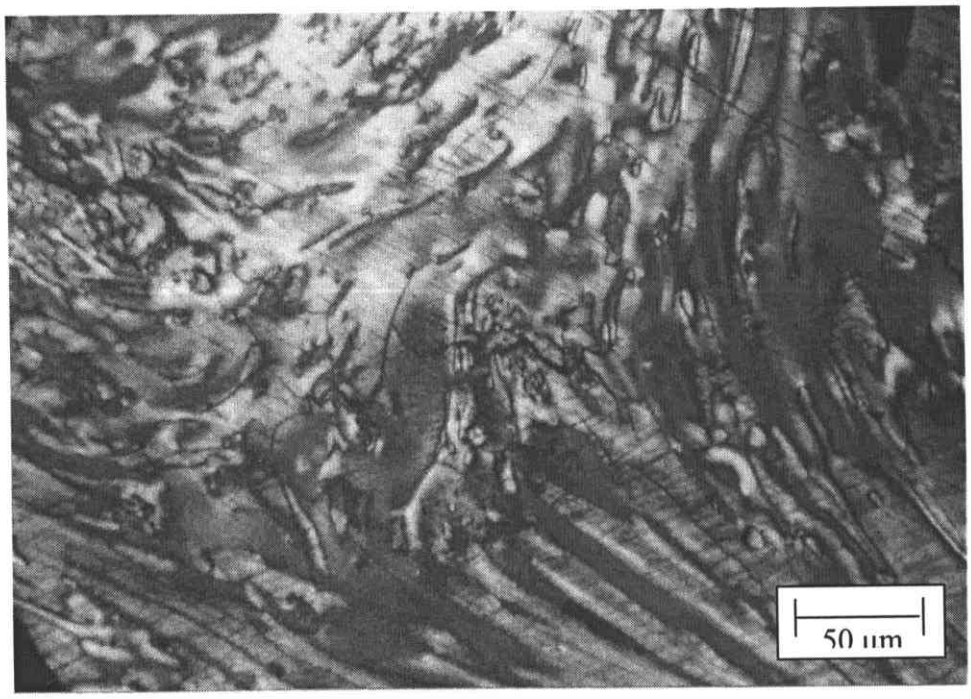

Fig. 51. Optical texture of semi-coke from blend with 10 wt% of PVP25.

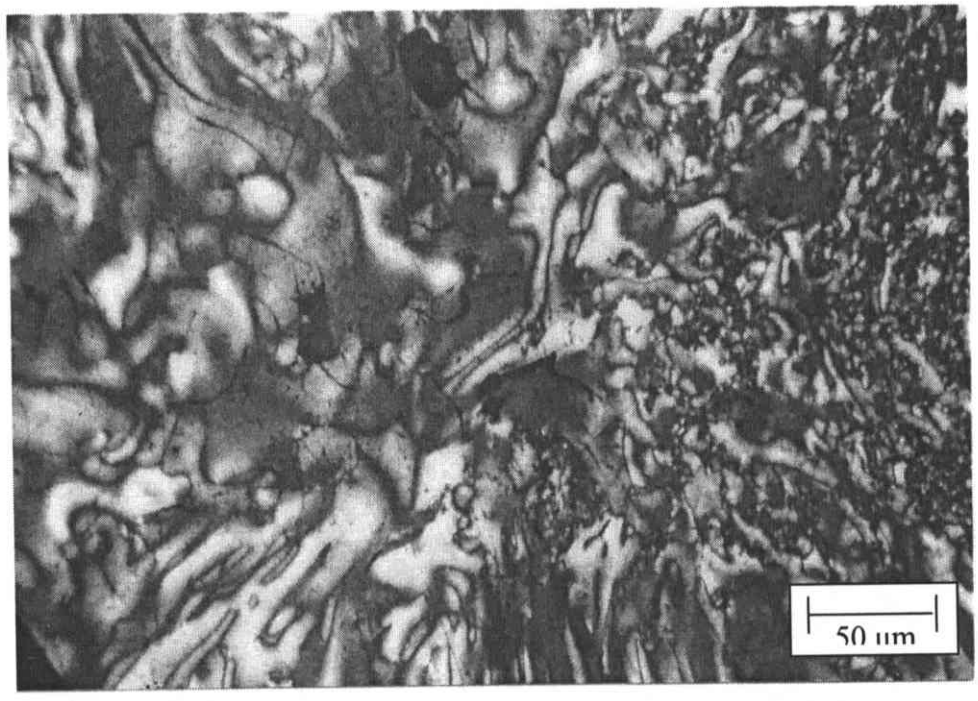

Fig. 52. Optical texture of semi-coke from blend with 25 wt% of PVP25.

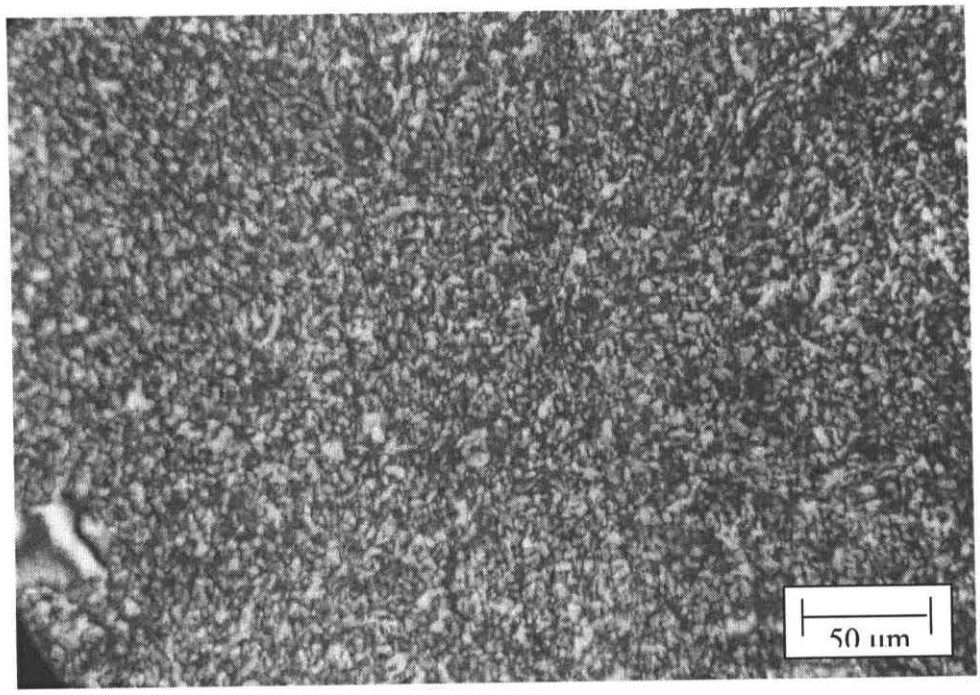

Fig. 53. Optical texture of semi-coke from blend with 50 wt% of PVP25.

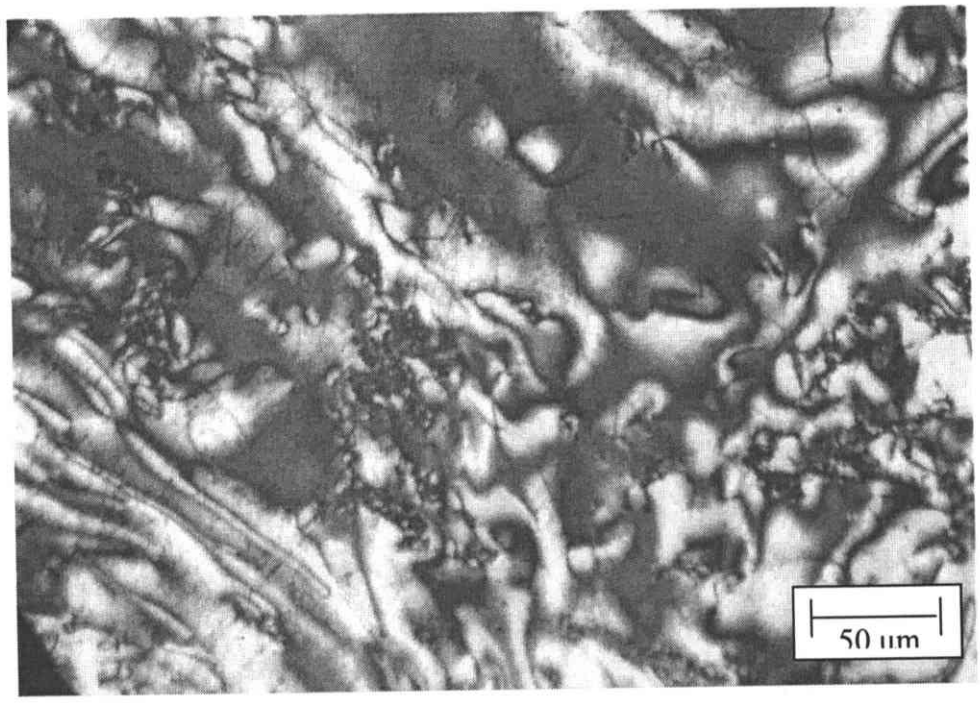

Fig. 54. Optical texture of semi-coke from blend with 10 wt% of PVP25ox.

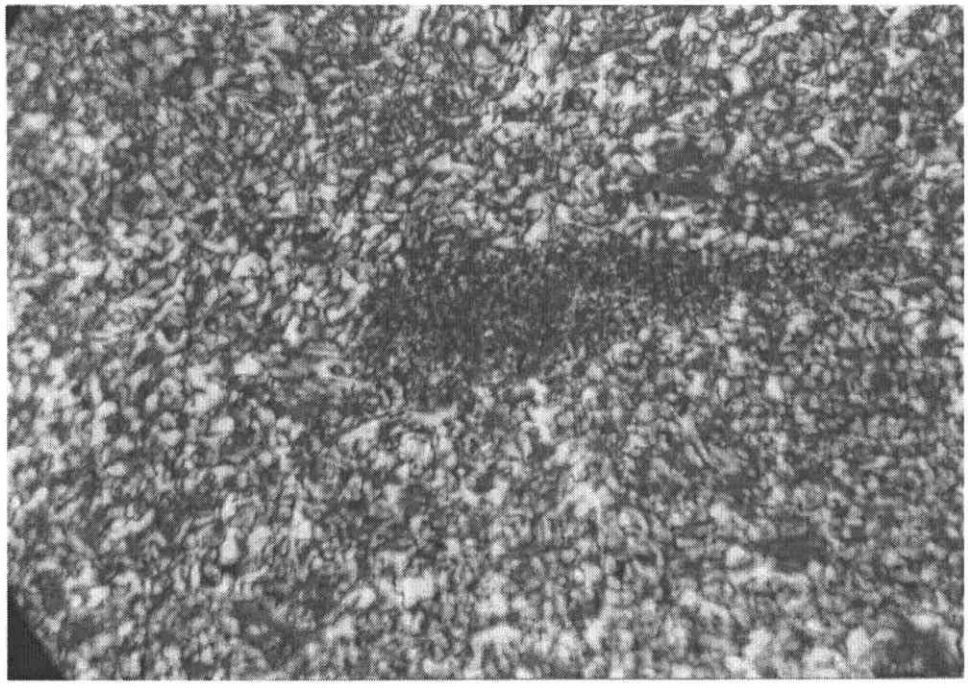

Fig. 55. Optical texture of semi-coke from blend with 25 wt% of PVP25ox.

5.3.2.2.Elemental composition of semi-cokes

Elemental composition of semi-cokes from PVP25, PVP25ox and blends with pitch is given in Table 12.

Heat treatment of PVP25 at 520^{0}C gives solid residue with nitrogen content of about 4.7 wt.%. The significant reduction of nitrogen proportion compared to the pristine PVP25 (~9 wt%) can be explained by the evolution of 4-vinylpyridine oligomers, accompanied by the loss of such low molecular nitrogen compounds as HCN and NH_3. The excessive oxygen content in PVP25 semi-coke, together with the elevated hydrogen level indicates the presence of water in the analyzed sample. The nitrogen content in the semi-cokes from CTP-PVP25 blends increases very moderately with the polymer proportion in the initial blend reaching 1.9 wt% at 1:1 components ratio. Such a behavior is not a surprise keeping in mind a big weight loss on PVP25 pyrolysis, therefore the limited contribution of polymer-derived material to the blend pyrolysis residue.

The elemental analysis of semi-cokes prepared from PVP25ox and CTP-PVP25ox blends gives a considerably higher proportion of nitrogen as compared to the corresponding semi-cokes derived from the unoxidized polymer. The strongest effect,

twofold increase in nitrogen content occurs for 3:1 and 1:1 blends. Apparently, the oxidative stabilization of PVP25 prior to blending results in the formation of more thermally stable backbone ensuring a better retention of nitrogen in the pyrolysis residue.

The preoxidation is an efficient method for the improvement of polyvinylpyridine properties for the synthesis of nitrogen containing carbonaceous materials.

Table 12. Elemental composition of semi-cokes derived from the blends of PVP25 and PVP25ox with pitch

Sample	Elemental composition, wt%					$(N/C)_{at.}$
	C	H	N	S	O[1]	
CTP-S	95.30	3.05	0.78	0.09	0.78	0.008
CTP-PVP25 9 :1-S	95.28	3.10	1.00	0.13	0.49	0.009
CTP-PVP25 3:1-S	95.36	3.10	1.13	0.13	0.28	0.010
CTP-PVP25 1:1-S	93.82	3.22	1.92	0.13	0.91	0.018
PVP25-S	85.98	3.94	4.69	0.00	6.39	0.047
CTP-PVP25ox 9:1-S	95.36	3.07	1.34	0.07	0.16	0.012
CTP-PVP25ox 3:1-S	93.31	3.24	2.25	0.09	1.11	0.020
CTP-PVP25ox 1:1-S	90.38	3.29	3.75	0.09	1.51	0.036
PVP25ox-S	83.69	3.46	6.91	0.00	5.40	0.071

[1]By difference

5.3.2.3. Chemical structure evolution on pyrolysis

Diffuse reflectance infrared Fourier Transform spectroscopy (DRIFT)

Diffuse reflectance spectra of PVP25 and PVP25ox as well as their blends with pitch (CTP-PVP25 1:1 and CTP-PVP25ox 1:1) are presented in Fig. 56. To compare the abundance of selected functional groups in studied materials, the linearization of the relationship between concentration and spectral response according the Kubelka-Munk function was applied (Koch et al., 1998).

PVP25 spectrum shows the absorption bands at 1596, 1556, 1490 and 1414 cm^{-1}, corresponding to ν(C=C) and ν(C=N) stretching in pyridinic rings (Bellamy, 1980). The peaks at 1216 and 1066 cm^{-1} are assigned to the in-plane C-H bend, while peaks at

996 and 820 are out-of-plane γ(C-H) deformation bands (Wu et al., 2003). The band at 820 cm^{-1} indicates the presence of two neighboring isolated hydrogen atoms in a PVP ring. The vinyl part of the PVP-DVB co-polymer gives rise to a 2930-2850 cm^{-1} band of ν(C-H) aliphatic stretch and C-H assymetric bend at 1448 cm^{-1}. In the region of stretching vibration of aromatic C-H group (3100-3000 cm^{-1}) appear the bands at 3065 and 3021cm^{-1} related to conjugated and non-conjugated aromatic modes, respectively.

Under conditions of blending both the pitch and PVP25 stay unreactive and the absorption profile of blend appears as the superimposition of the absorptions derived from both constituents. The pitch contribution includes the absorption band of aromatic C-H stretching vibration at 3050 cm^{-1} and the vibration of aromatic ring at 1600 cm^{-1} (Fig. 31). For the pitch this latter band displays a considerably lower intensity than the corresponding peak in PVP25. This is in agreement with the established view that C=C groups in the condensed aromatic rings absorb less strongly (Machnikowska et al., 2002). Apparently, the presence of sharp band at 880 cm^{-1} in the spectrum of CTP-PVP25 blend is attributable to isolated CH groups in more condensed aromatic structures of pitch than those of polymer. The pitch contribution is also poorly resolved pattern of vibration modes in the region 1290-1120 cm^{-1} assigned to several oxygen functionalities (Krztoń et al., 1995). Bands at 1556, 1414, 1216 and 996 cm^{-1} in the spectrum of CTP-PVP25 are related to PVP25 vibration modes.

The oxidation of PVP25 induces a remarkable transformation to the polymer backbone. The diminishing of bands at 2930-2850 cm^{-1} and 1446 cm^{-1} can be atributed to the oxygen induced dehydrogenation aliphatic (vinyl) part of the co-polymer. In consequence an extensive polymerisation and cross-linking of polymer can occur due to oxidation. The condensation of aromatic rings reflects in decrease in the intensity of bands at 1596, 1556, 1414, 1216, 1066 and 996 cm^{-1}. The formation of oxygen functionalities is confirmed by an increase in the intensity of the bands at 1320-1130 cm^{-1} attributed to the ν(C-O) and δ(O-H) vibration in phenols, aromatic ethers and esters. The relatively strong peak at 1680 cm^{-1} is brought about by the ν(C=O) stretch of conjugated ketonic compounds (Krztoń et al., 1995).

The lack of the band at 1680 cm^{-1} in the spectrum of the CTP-PVP25ox blend indicates that conjugated ketones formed on the oxidative stabilization of PVP25 are fully decomposed during the composition preparation at 250^{0}C. The intensity of the band at 1320-1130 cm^{-1}, does not change compared to PVP25ox spectrum, evidencing

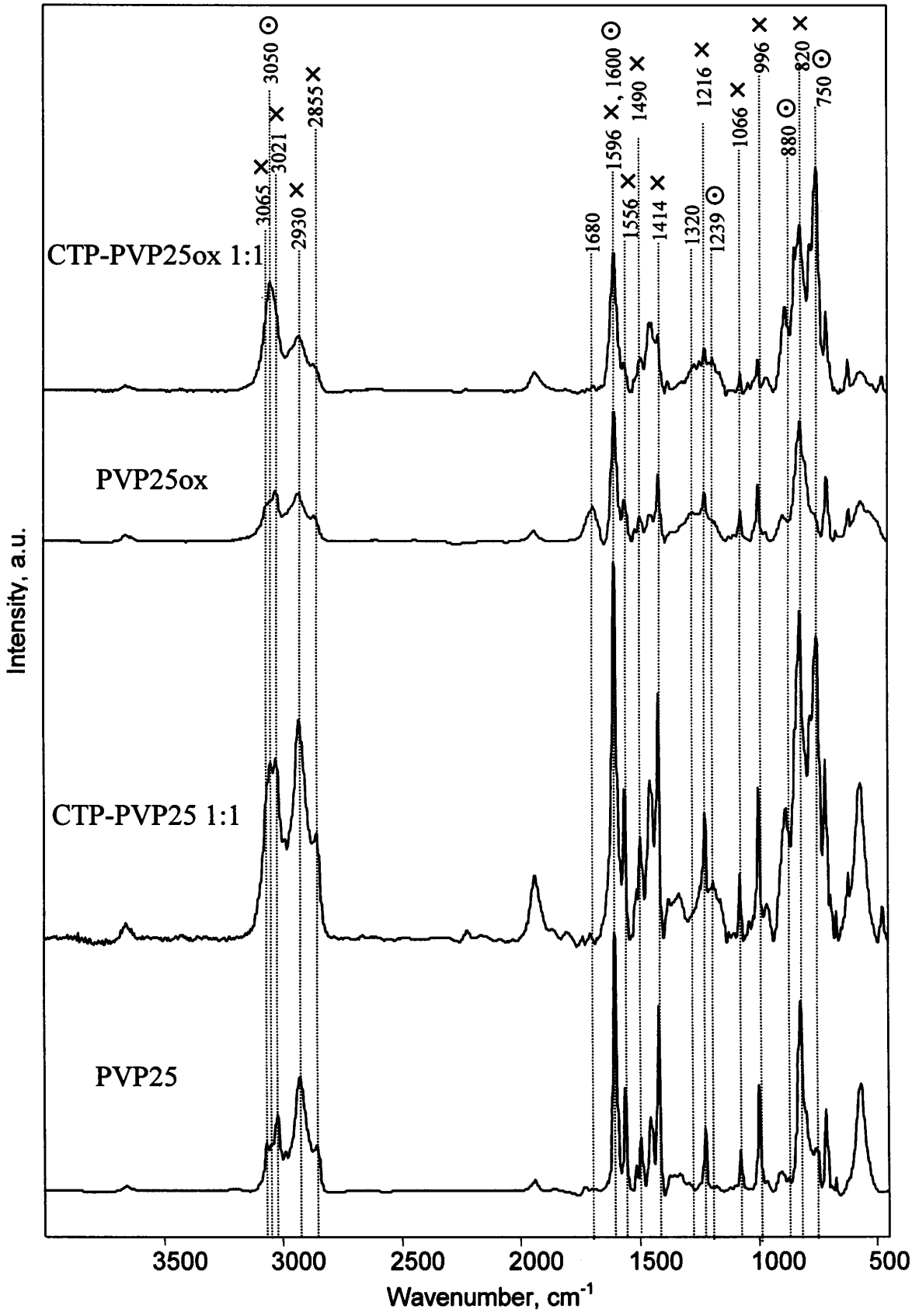

Fig. 56. DRIFT spectra of polyvinylpyridines and their blends with pitch: PVP25, CTP-PVP25 1:1, PVP25ox, CTP-PVP25ox 1:1

(× signal from PVP25, ⊙ signal from CTP).

that phenols, aromatic ethers and esters are rather thermally stable under conditions of blending.

DRIFT spectra of semi-cokes from PVP25, PVP25ox and their blends with pitch are presented in Fig. 57.

The spectrum of the PVP25 semi-coke reveals the following transformations of the polymer to occur on the heat treatment at 520^0C:

- An increase in the aromaticity reflected in the disappearance of aliphatic C-H bands at 2930-2850 cm^{-1} and 1448 cm^{-1}. The aromatization is also accompanied by an enhanced intensity of the band at 3050 cm^{-1} corresponding to conjugated aromatic systems.
- The condensation and/or substitution of the heteraromatic rings followed by an increase in the rigidity of the polymer backbone reflected in the disappearance of the bands at 1556, 1490 and 1414 cm^{-1} related to the skeletal vibration of pyridinic rings.

The condensation and/or substitution of aromatic rings can be also monitored by the evaluation of the intensity of bands within 900-700 cm^{-1} (Machnikowska et al., 2002). In this region, the bands with a maximum near 875, 820 and 760 cm^{-1} occur, corresponding to isolated CH groups, two neighboring CH groups and four neighboring CH groups on an aromatic ring, respectively. The remarkable increase in the intensity of the absorption at 875 cm^{-1} in PVP25-S spectrum accompanied by a relatively lower intensity of the peak at 820 cm^{-1} indicates a higher condensation degree of aromatic systems.

The spectra of semi-cokes from CTP-PVP25 1:1, PVP25ox and CTP-PVP25ox 1:1 show rather close similarity to that of PVP25-S. Characteristic differences appear, however, in the relative intensities of peaks located in the 900-700 cm^{-1} region, as an effect of specific extent of condensation and/or substitution of aromatic rings in a given material. The most intense peak at 820 cm^{-1} (two adjacent hydrogen atoms on a ring) in the spectra of semi-cokes from pure polymers can be related to a considerable extent of cross-linking. Strong intensity of 760 cm^{-1} band (four adjacent hydrogens) is characteristic of blend semi-cokes.

PVP25ox semi-coke is distinguishable by a relatively strong band in the region 1320-1130 cm^{-1}, which indicates the presence of numerous oxygen functionalities. The enhanced absorption in this range correlates with a higher oxygen content in the sample compared to other semi-cokes (Table 12).

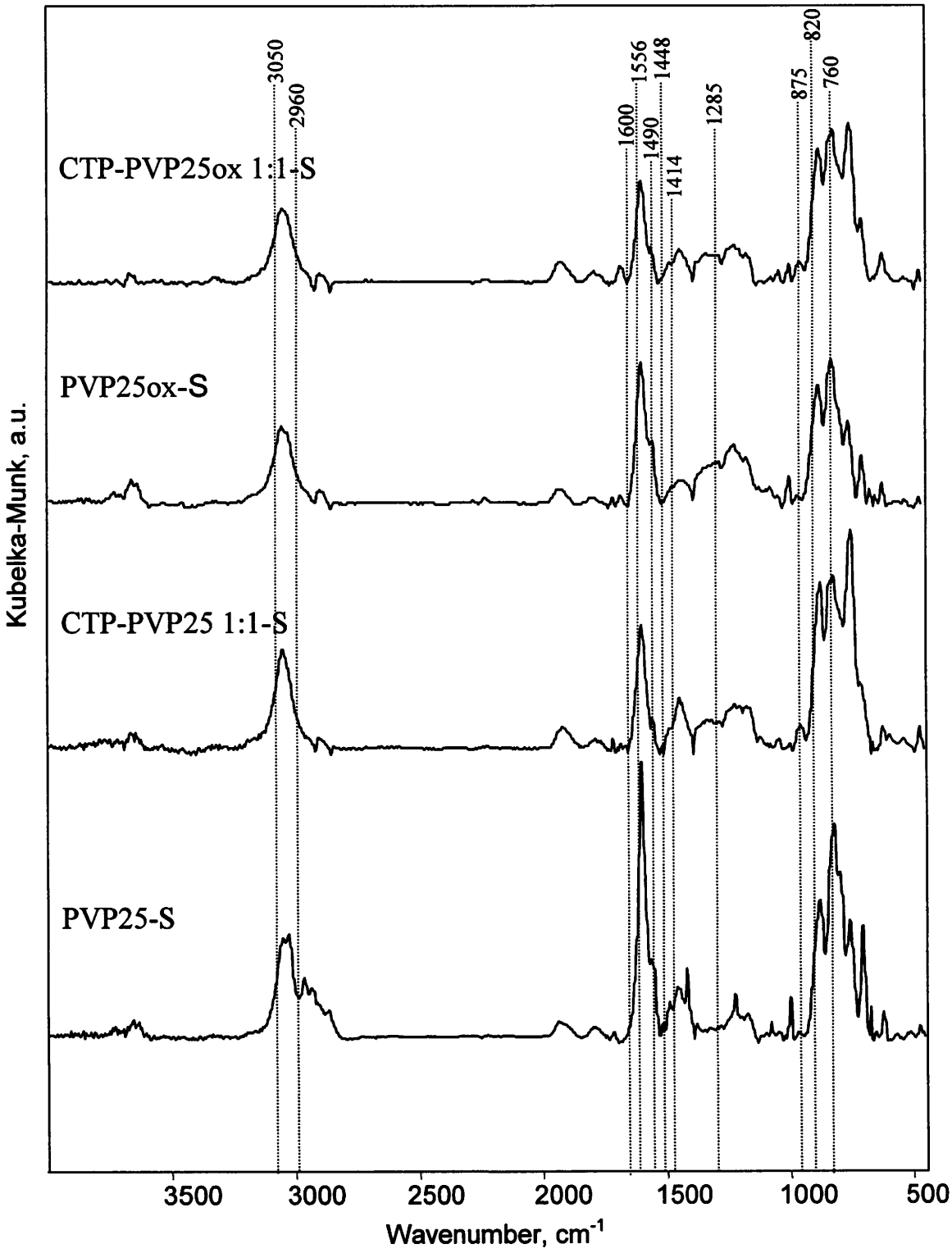

Fig. 57. DRIFT spectra of semi-cokes from polyvinylpyridines and their blends with pitch: PVP25-S, CTP-PVP25 1:1-S, PVP25ox-S, CTP-PVP25ox 1:1-S

X-ray photoelectron spectroscopy

XPS was used to monitor the evolution of nitrogen functionalities on thermal treatment of PVP25ox synthesized in the laboratory. Figs. 58-60 are N1s, C1s and O1s XPS spectra of PVP25ox and PVP25ox semi-coke.

The spectrum N1s of PVP25ox consists of one peak of pyridinic nitrogen centered at 398.7 eV (Fig. 58). There is no detectable amount of the oxidized pyridonic form.

The spectrum of PVP25ox heat-treated at 520^0C is fitted by three components. In addition to the predominant pyridinic form, the components centered at 400.6 eV and 396.2 eV have to be added to get a proper fit. The former peak (17.7 %) can be attributed to the pyridonic nitrogen created as an effect of substitution of pyridinic ring with oxygen functionalities during co-pyrolysis. The low binding energy constituent is quite abundant, amounts to about 33 % of the N1s peak area (Table 13), though its origin is unclear. The available literature does not supply a reasonable explanation for the presence of nitrogen form of this binding energy. A relevant observation is the lack of quaternary nitrogen in PVP25ox and its semi-coke.

C1s spectra of PVP25ox and its semi-coke presented in Fig. 59 have been fitted by three components of binding energies 282.6±0.4, 284.8±0.2 and 286±0.2 eV, corresponding to the carbidic carbon, graphitic carbon and carbon linked to nitrogen and/or to oxygen, respectively. It is interesting to note a significant contribution of carbidic carbon (about 8 and 28 % for PVP25ox and PVP25ox-S, respectively, Table 13). The peaks related to CN and/or C-OH bonds account for 8-10 % of the total C1s peak area. There is no component of binding energy about 288 eV which could be attributed to carbon doubly bound to oxygen.

The O1s XPS spectra show a well-defined peak at around 530.6 ±0.2 eV corresponding to oxygen in carbonyl groups (Fig. 60) (Biniak et al., 1997). In the case of PVP25ox it correlates with the carbonyl peak at 1680 cm^{-1} on DRIFT spectrum (Fig. 56). O1s spectrum of the PVP25ox-S reveals an additional contribution of the component present at 532.6±0.4 eV indicating presence of the hydroxyl and/or ether-like bonds.

Clearly, there is an inconsistency concerning the presence of oxygen functionalities when estimating the C1s and O1s spectra of PVPox and PVPox-S.

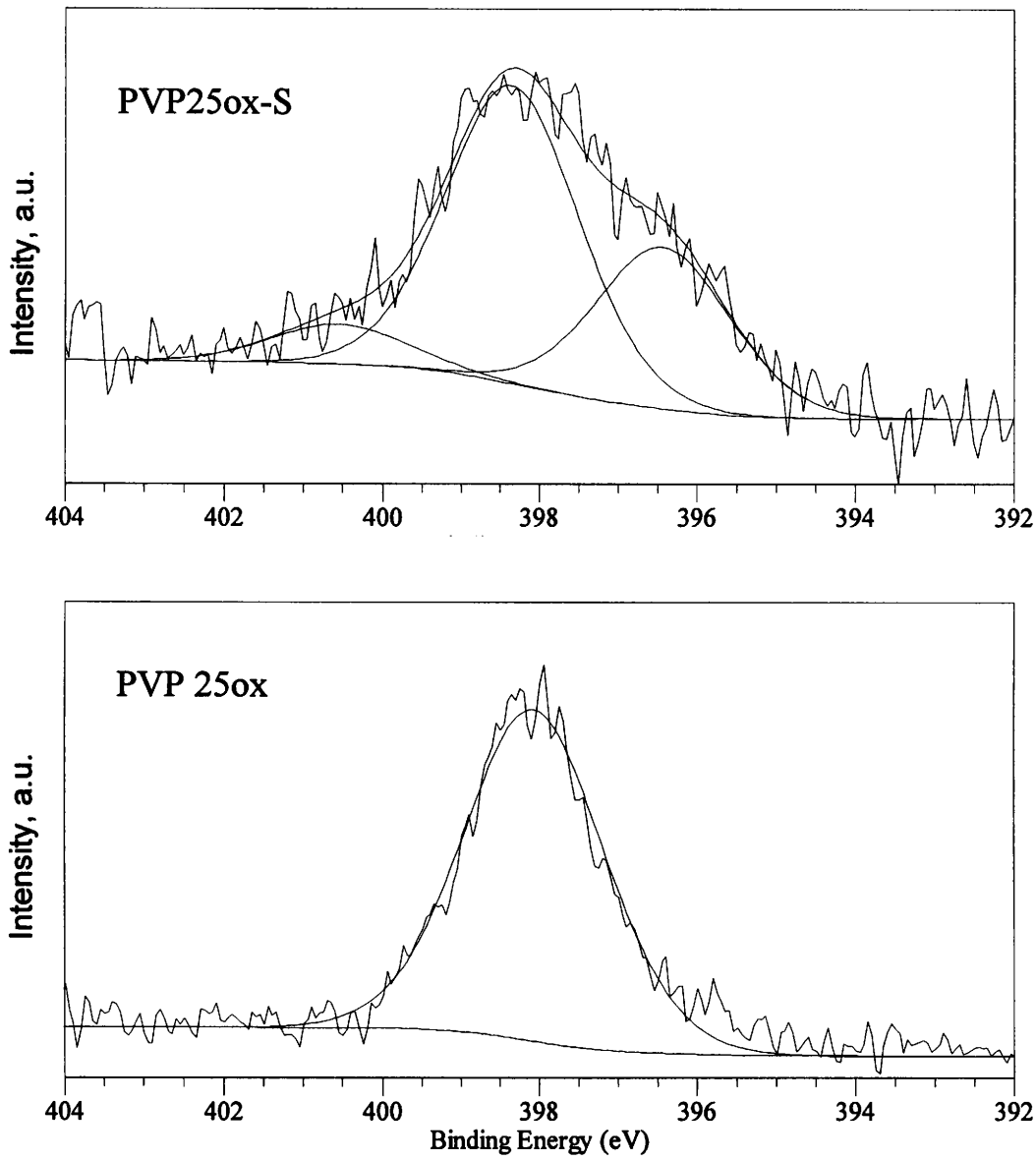

Fig. 58. N1s XPS spectra of PVP25ox and the derived semi-coke.

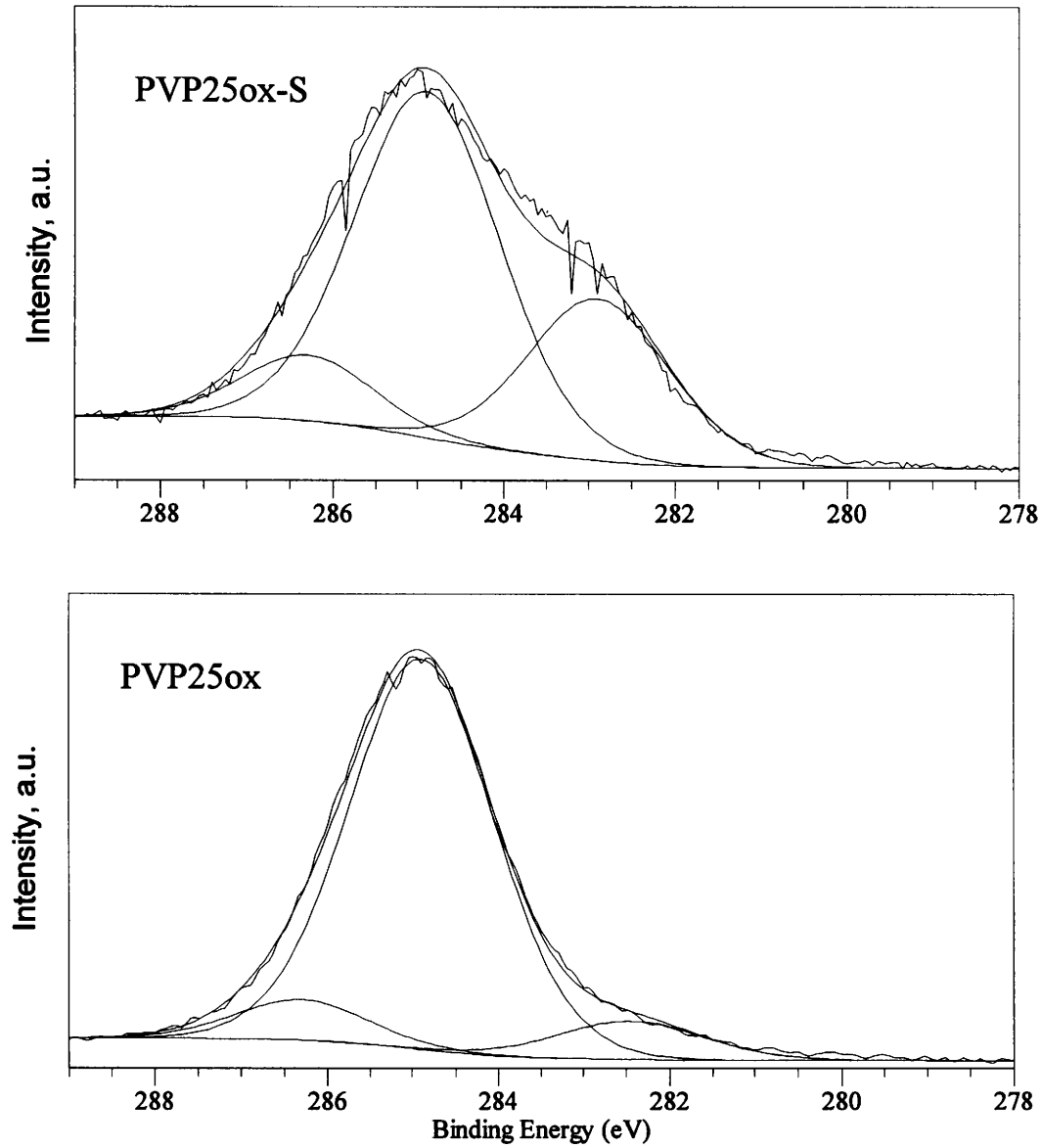

Fig. 59. C1s XPS spectra of PVP25ox and the derived semi-coke.

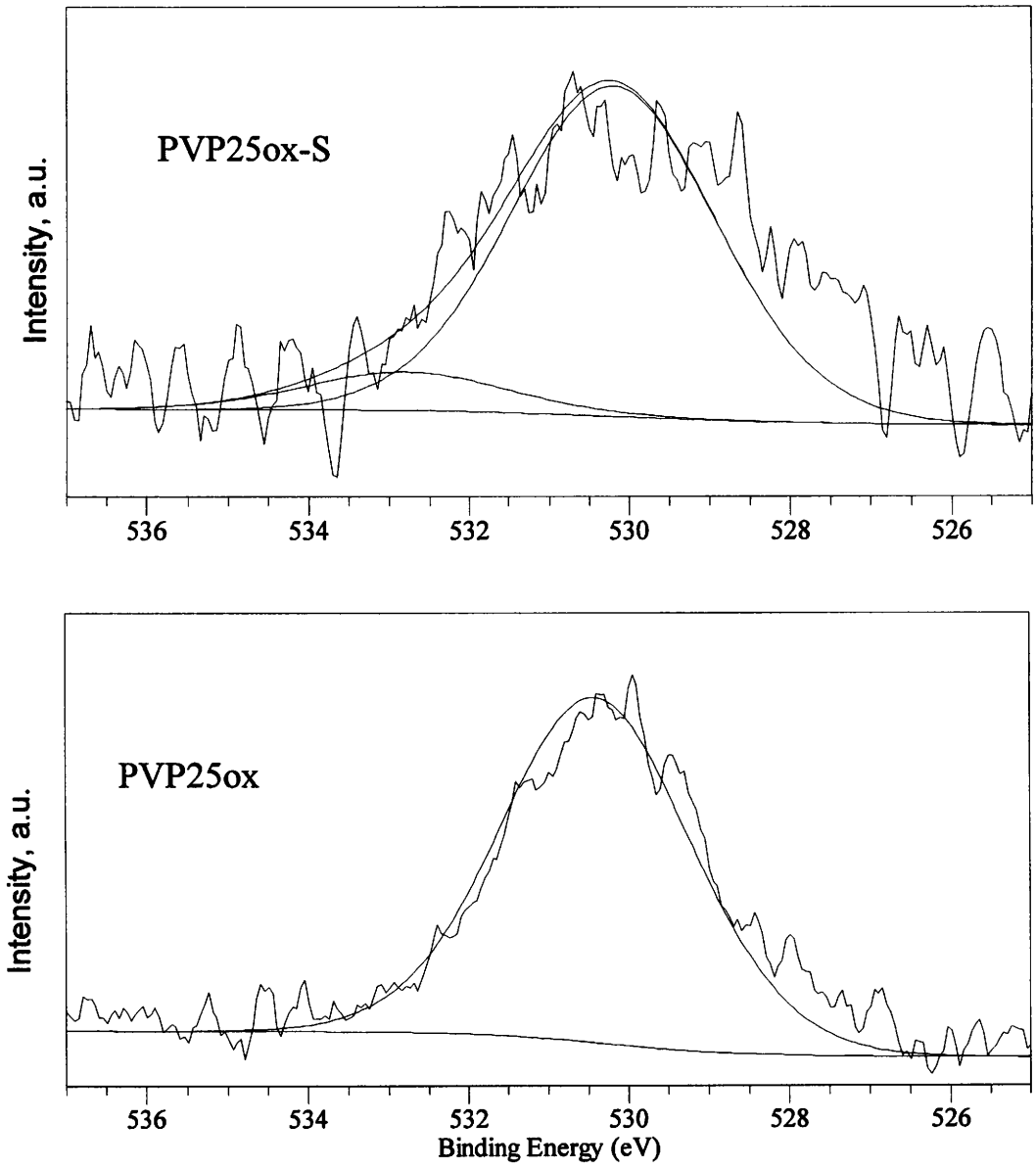

Fig. 60. O1s XPS spectra of PVP25ox and the derived semi-coke.

The surface composition analysis using XPS (Table 14) reveals rather homogeneous nitrogen distribution throughout the PVP25ox and PVP25ox-S samples. O/C atomic ratios suggest a lower oxygen level at the surface compared to the bulk of sample elemental analysis. We assume a possible desorption of the unstable oxygen groups from the surface during XPS analysis under vacuum.

Table 13. Distribution of carbon, nitrogen and oxygen forms in PVP25ox and the derived semi-coke

Peak	BE, eV	Possible assignment	**PVP25ox** %	**PVP25ox-S** %
C1s	282.6±0.4	carbidic	8.1	27.9
	284.8±0.2	C-H, C-C	84.1	61.6
	286.7±0.4	C-OH, C-N, C=N	7.8	10.5
N1s	396±0.3	(?)	0	32.6
	398.7±0.3	N-6	100.0	59.7
	400.3±0.3	N-5	0	7.7
O1s	530.6±0.2	C=O	100.0	90
	532.8±0.4	C-O-C, C-OH	0	10.0

Table 14. Elemental composition of PVP25ox and the derived semi-coke determined by XPS

Sample	Atomic concentration[1]			Atomic ratios			
	C	N	O	N/C		O/C	
				XPS	El.An.	XPS	El.An.
PVP25ox	87.3	8.1	4.5	0.093	0.083	0.052	0.074
PVP25ox-S	90.7	6.5	2.8	0.071	0.071	0.031	0.048

[1] C + N + O = 100%

5.4. Ammoxidation of pitch-derived carbonaceous materials

5.4.1. Preparation of starting carbonaceous materials for ammoxidation

The reaction with ammonia-air mixture (ammoxidation) was assessed as an alternative way of synthesis of nitrogen enriched coal-tar pitch based carbons. The idea is to prepare a carbonaceous material of the established pre-order as detected by the

anisotropic texture, using possibly mild conditions of thermal treatment to preserve the reactivity towards the reagents. Two types of materials were used in ammoxidation runs: pitch semi-coke (PS), and pitch derived mesophase (PM). The semi-coke was prepared under standard pyrolysis conditions used in the study (520^{0}C/2h). The sample of carbonaceous mesophase was produced by the heat-treatment of pitch at 430^{0}C for 8h with continuous stirring. The properties of the semi-coke and mesophase are given in Table 15.

Table 15. Properties of semi-coke and mesophase

Sample	Residue yield wt%	Ash content wt%	Volatile matter wt%	Anisotropic content vol%
PS	63.4	0.03	5.7	100.0
PM	79.6	n.d.	29.4	62.1

Pitch semi-coke is characterized by well developed flow type optical anisotropy (Fig. 61) The sample of mesophase is in fact a mesophase pitch containing about 62 vol% of anisotropic phase in the form of bulk mesophase (Fig. 62). The presence of residual isotropic pitch and a relatively high volatile content proves that the conversion of pitch into a carbonaceous solid is not completed yet.

To enhance the reactivity towards ammonia-air mixture, the PS and PM samples (ground below 0.3 mm) were oxidized with 30% nitric acid at 90^{0}C for 3 hours. Such a treatment appeared to be efficient in the ammoxidation of pitches and mesocarbon microbeads (Wachowska et al., 2000). Table 16 gives the elemental composition of the original samples PS and PM and the corresponding HNO_3 oxidation products PSox and PMox. The weight uptake during the oxidation of semi-coke and mesophase amounts to 12.4 and 10.8 wt%, respectively. The treatment is associated primarily with an increase in oxygen content to12 wt% in PSox and 9.1 wt% in PMox, however, the occurring nitration results in the enhanced nitrogen content to above 3 wt%.

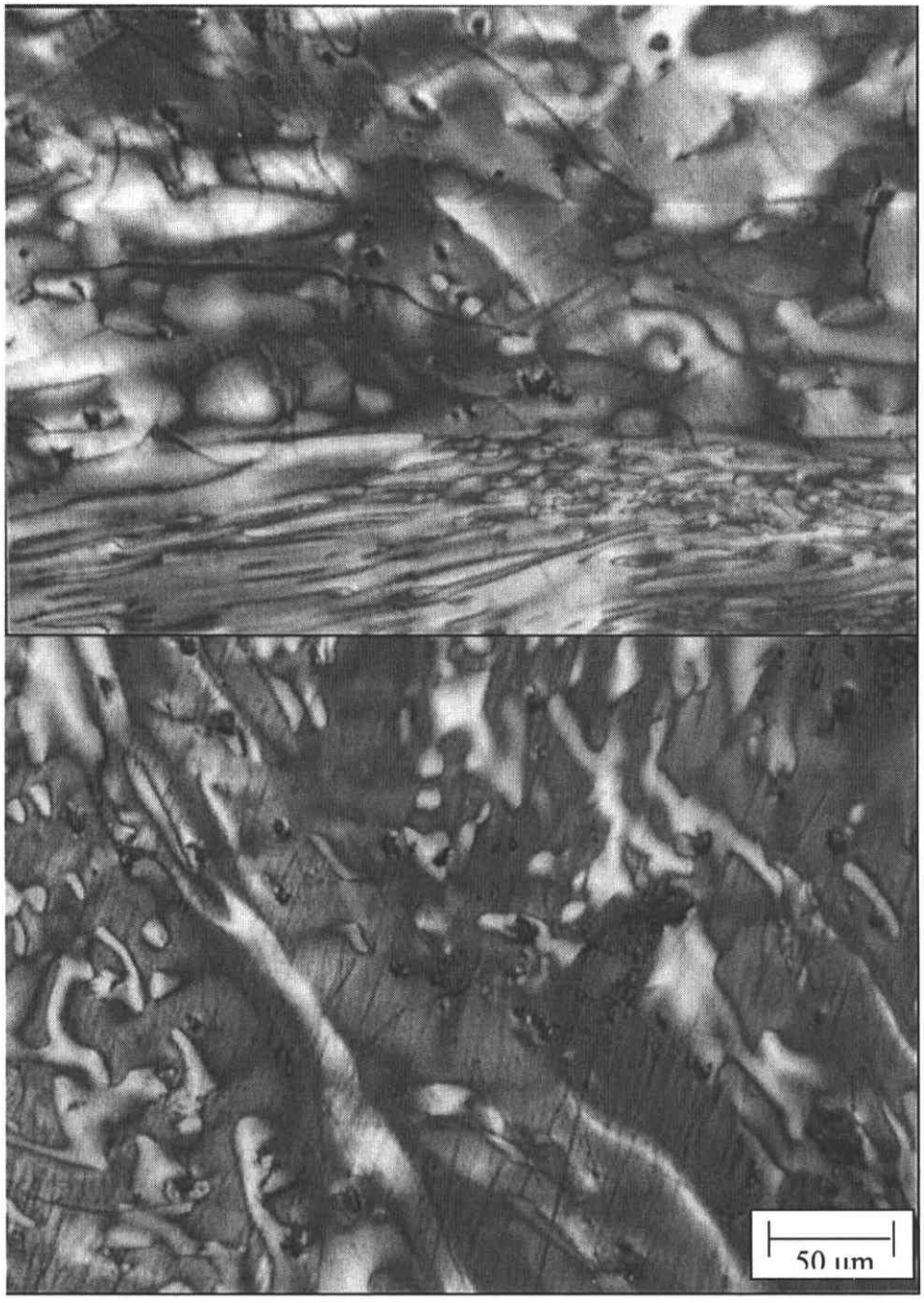

Fig. 61. Optical texture of semi-coke PS.

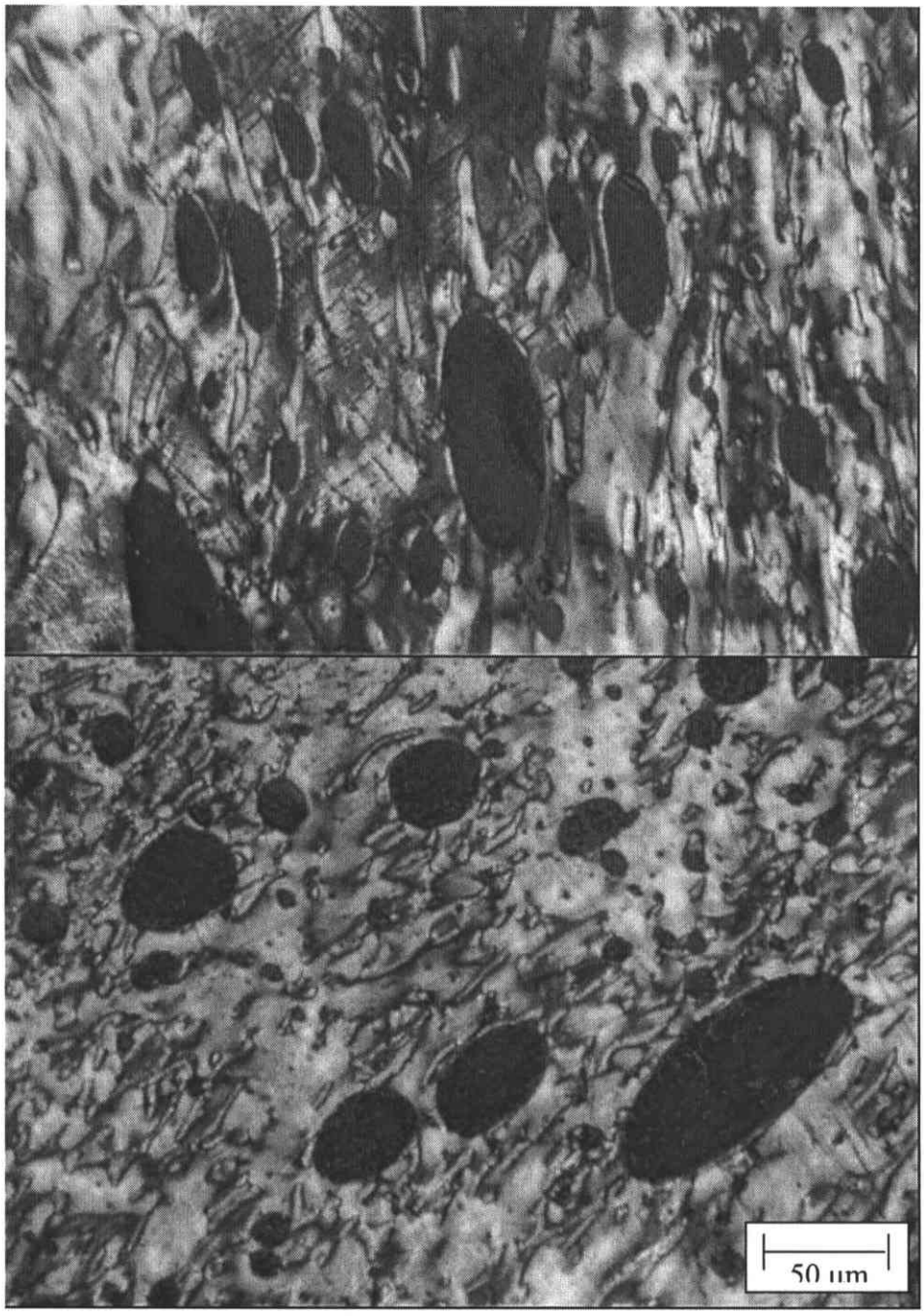

Fig. 62. Optical texture of mesophase PM.

Table 16. Elemental composition of the semi-coke and mesophase (parent and oxidized with HNO_3)

Sample	Elemental composition, wt%					$(H/C)_{at}$	(N/C_{at})	$(O/C)_{at}$
	C	H	N	S	O[1]			
PS	95.91	3.14	0.80	0.10	0.05	0.393	0.007	18.29
PSox	81.99	2.56	3.38	0.10	11.97	0.375	0.035	0.32
PM	95.19	3.76	0.85	0.21	0.05	0.474	0.008	19.43
PMox	84.40	3.26	3.23	0.06	9.05	0.464	0.033	0.41

[1]By difference

The careful evaluation of FTIR spectra of PSox and PMox (Fig. 63) indicates the creation of several functional groups as an effect of oxidation with HNO_3 of the original materials:

- lactones giving the absorptions attributed to ν(C=O) stretching at about 1715-1680 cm^{-1};
- quinones resulting in the weak band in the region 1660-1600 cm^{-1}
- nitro groups as suggest by the bands at 1525 cm^{-1} and 1340 cm^{-1} (Zawadzki, 1988); the band at 1525 cm^{-1} is also attributable to the amide groups, while the absorption at 1340 cm^{-1} may correspond to the C-N symmetric stretch of the lactams;
- carboxylic groups reflected in the weak band in the regions 3500-3100 cm^{-1} and 1275-1250 cm^{-1} in PSox only.

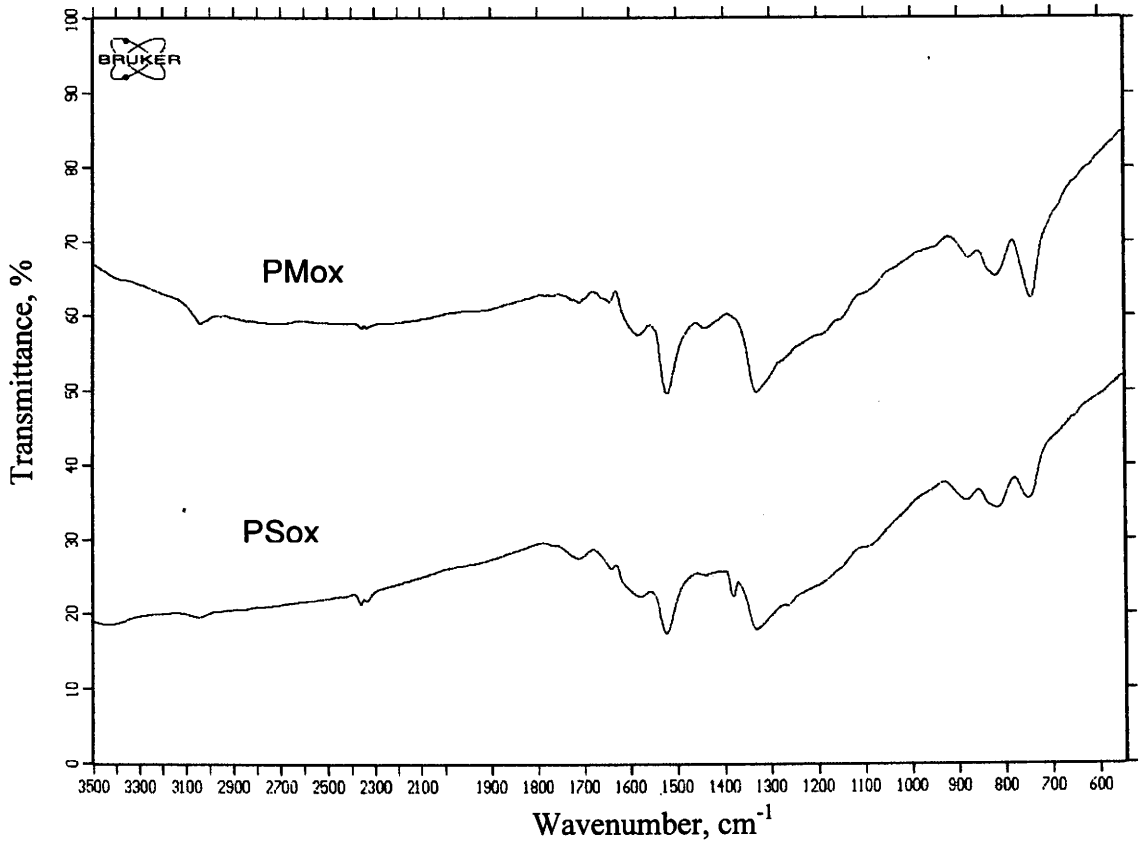

Fig. 63. FTIR spectra of PSox and PMox.

5.4.2. Synthesis of ammoxidized materials

The ammoxidation runs were performed at temperatures varying in the range of 250-400^{0}C while other reaction variables (time, flow rate and composition of gas) were fixed at constant values. The treatment of PS was associated with a limited weight uptake (up to 5 wt%), the ammoxidation of other materials (PSox, PM, PMox) led to the weight loss approaching 10 wt% in the case of reaction of PMox reacted under drastic conditions. The procedure used does not allow the precise determination of mass change during the ammoxidation. The thermoplasticity of mesophase resulted in self-sintering of the sample particles under ammoxidation conditions. This serious drawback was partially reduced by the oxidation with HNO_3 and the ammoxidation of PMox could be performed with a satisfactory result.

The progress of ammoxidation was controlled directly by the determination of elemental composition of products. The data for PS, PSox and PMox treated with ammonia-air mixture at various temperatures are given in Tables 17-19, respectively.

The variations in nitrogen and oxygen contents and N/O atomic ratio with ammoxidation temperature are presented in Figs 64-66.

Table 17. Elemental composition of the semi-coke treated at various ammoxidation temperatures

Sample	Elemental composition, wt%					$(H/C)_{at}$	$(N/C)_{at}$	$(N/O)_{at}$
	C	H	N	S	O[1]			
PS	95.91	3.14	0.80	0.10	0.05	0.393	0.007	18.29
PS 250	93.23	2.92	1.27	0.17	2.41	0.376	0.013	0.602
PS 275	91.63	2.82	1.69	0.12	3.74	0.369	0.016	0.516
PS 300	90.34	2.72	2.48	0.17	4.29	0.361	0.027	0.661
PS 325	86.81	2.76	3.96	0.40	6.43	0.382	0.039	0.704
PS 350	86.31	2.26	7.04	0.15	4.24	0.314	0.070	1.898
PS 400	86.44	2.38	7.81	0.04	3.33	0.330	0.077	2.680

[1]By difference

Table 18. Elemental composition of the preoxidized semi-coke treated at various ammoxidation temperatures

Sample	Elemental composition, wt%					$(H/C)_{at}$	$(N/C)_{at}$	$(N/O)_{at}$
	C	H	N	S	O[1]			
PSox	81.99	2.56	3.38	0.10	11.79	0.375	0.035	0.323
PSox 250	83.05	2.66	5.26	0.08	8.95	0.384	0.054	0.672
PSox 275	84.65	2.53	5.63	0.07	7.12	0.359	0.057	0.904
PSox 300	81.76	2.64	6.36	0.05	9.19	0.387	0.067	0.791
PSox 350	82.98	2.22	8.43	0.07	5.30	0.321	0.087	1.818

[1]By difference

Table 19. Elemental composition of the preoxidized mesophase treated at various ammoxidation temperatures

Sample	Elemental composition, wt%					$(H/C)_{at}$	$(N/C)_{at}$	$(N/O)_{at}$
	C	H	N	S	O[1]			
PMox	84.40	3.26	3.23	0.06	9.05	0.464	0.033	0.408
PMox 300	80.89	2.69	8.58	0.07	7.77	0.400	0.091	1.262
PMox 350	85.08	2.41	9.70	0.10	2.71	0.340	0.100	4.091

[1]By difference

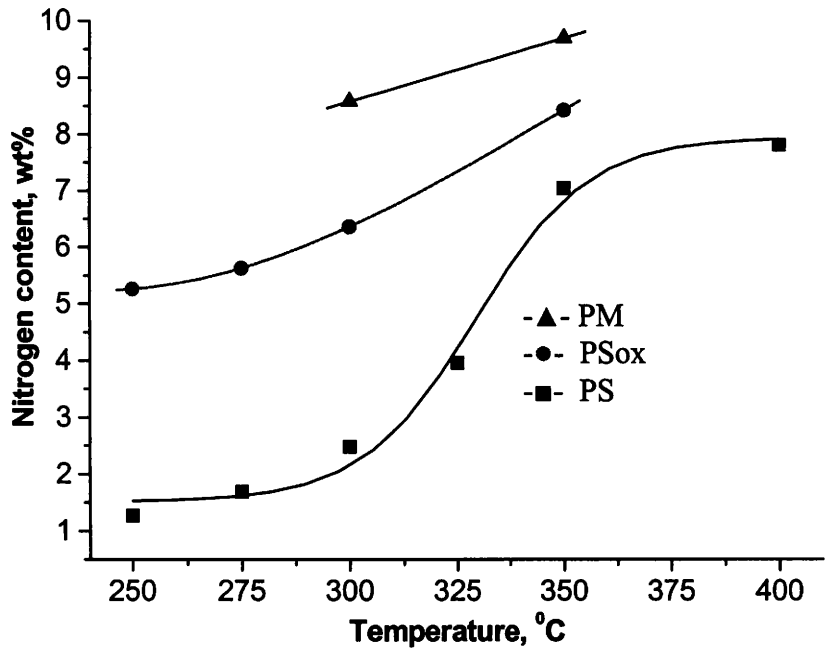

Fig. 64. Effect of the ammoxidation temperature on the nitrogen content.

A general trend in elemental composition is a continuous increase in the nitrogen content at the expense of carbon and hydrogen with the ammoxidation temperature. A maximum nitrogen content for a given material, i.e. 7.8 wt% for PS, 8.4 wt% for PSox and 9.7 wt% for PMox were reached at the highest reaction temperatures used.

Keeping in mind that the reaction is practically restricted to the available surface of particles and the elemental analysis data correspond to the bulk of sample, the results of ammoxidation can be regarded as very satisfactory.

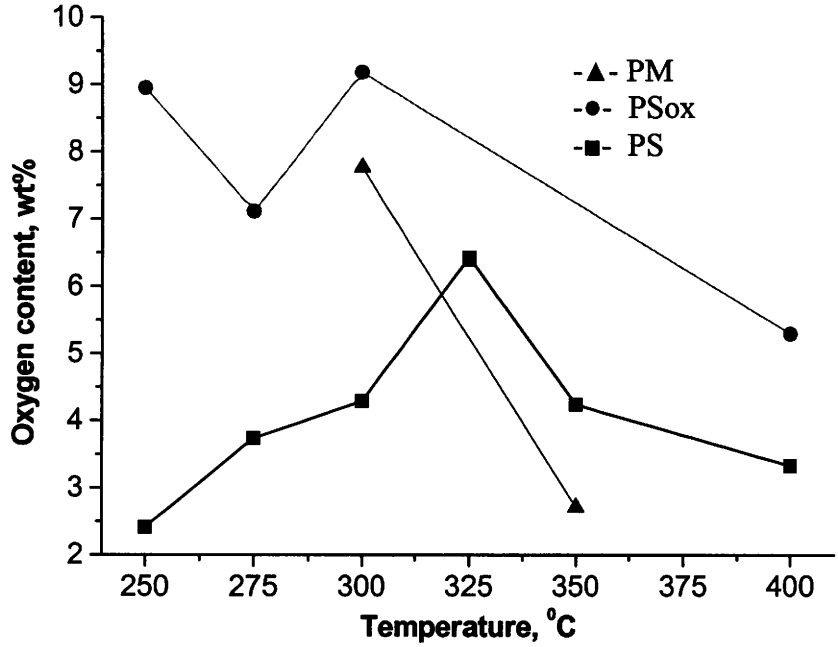

Fig. 65. Effect of the ammoxidation temperature on the oxygen content.

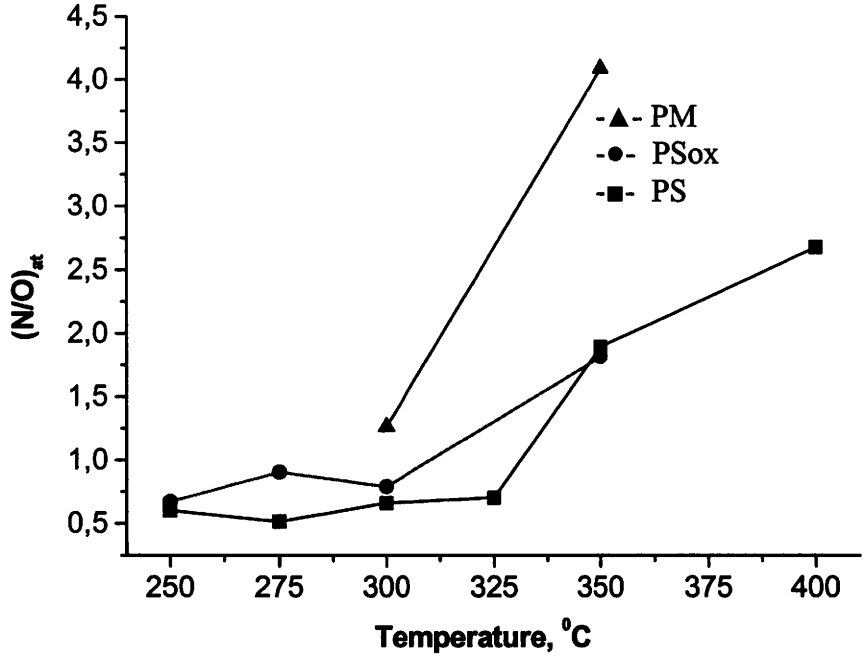

Fig. 66. Effect of the ammoxidation temperature on the $(N/O)_{at}$ ratio.

The preoxidation with HNO_3 facilitates the reaction leading to the incorporation of comparable amount of nitrogen at a temperature reduced by 50^0C (Fig. 64).

The oxygen content in the ammoxidized PS increases with reaction temperature up to 325^0C (6.4 wt%) but decreases with further temperature growth (Fig. 65). The behavior can be explained by the decomposition of less stable oxygen functionalities at elevated temperatures and the enhanced reaction with ammonia of the created acidic groups. In the case of PSox a decrease in oxygen content at mild ammoxidation conditions is due to the decomposition of least stable functionalities introduced by the HNO_3 treatment. At a higher temperature the behavior follows that in unoxidized material.

N/O atomic ratio increases in ammoxidized samples with the treatment temperature, the increase being faster above 300^0C (Fig. 66).

The results of the study suggest a somewhat bigger propensity of mesophase than semi-coke to nitrogen incorporation during ammoxidation at the same reaction conditions.

5.4.3. Evaluation of surface chemistry of ammoxidized materials

The nature of surface of the ammoxidized semi-coke and mesophase was studied using diffuse reflectance infrared Fourier transform spectroscopy (DRIFT) and X-ray photoelectron spectroscopy (XPS).

DRIFT study

Five ammoxidation products produced from PS, PSox and PMox at various reaction temperatures were selected for the DRIFT study. The spectral regions 2000-1000 cm^{-1} and 3500-2100 cm^{-1} were evaluated in details as most interesting in terms of oxygen and nitrogen groups.

In the 2000-1000 cm^{-1} spectral region six major absorption bands have been identified with the help of the minima of second derivative curves (Fig. 67).

- Shoulder at 1734 cm^{-1} related to the ν(C=O) stretching of lactones and/or carboxylic acids. The band intensity remains at the same level in all the samples.
- The peak at 1669 cm^{-1}, attributable to the presence of quinones. This band is most intense in PS 350 spectrum.
- The sharp peak at 1600 cm^{-1}, brought about by the aromatic rings stretching vibration as well as by C=O stretching vibration of carbonyl groups.

- The bands at 1524 cm^{-1} and 1335 cm^{-1}. These bands are assigned, respectively, to the asymmetric and symmetric stretching modes of nitro groups (Zawadzki, 1988). The band at 1525 cm^{-1} is also attributable to the amide groups, while the absorption at 1340 cm^{-1} may be also linked to the C-N symmetric stretch of the lactams. The highest intensity of these bands is observed the case of PSox 275 spectrum what suggests that the nitro and oxygen groups created upon treatment with nitric acid are readily decomposed or converted to other functionalities during thermal treatment at more severe conditions.
- The band at 1440 cm^{-1} assigned to methylene groups. The strongest absorption of this band occurs for PS 275.

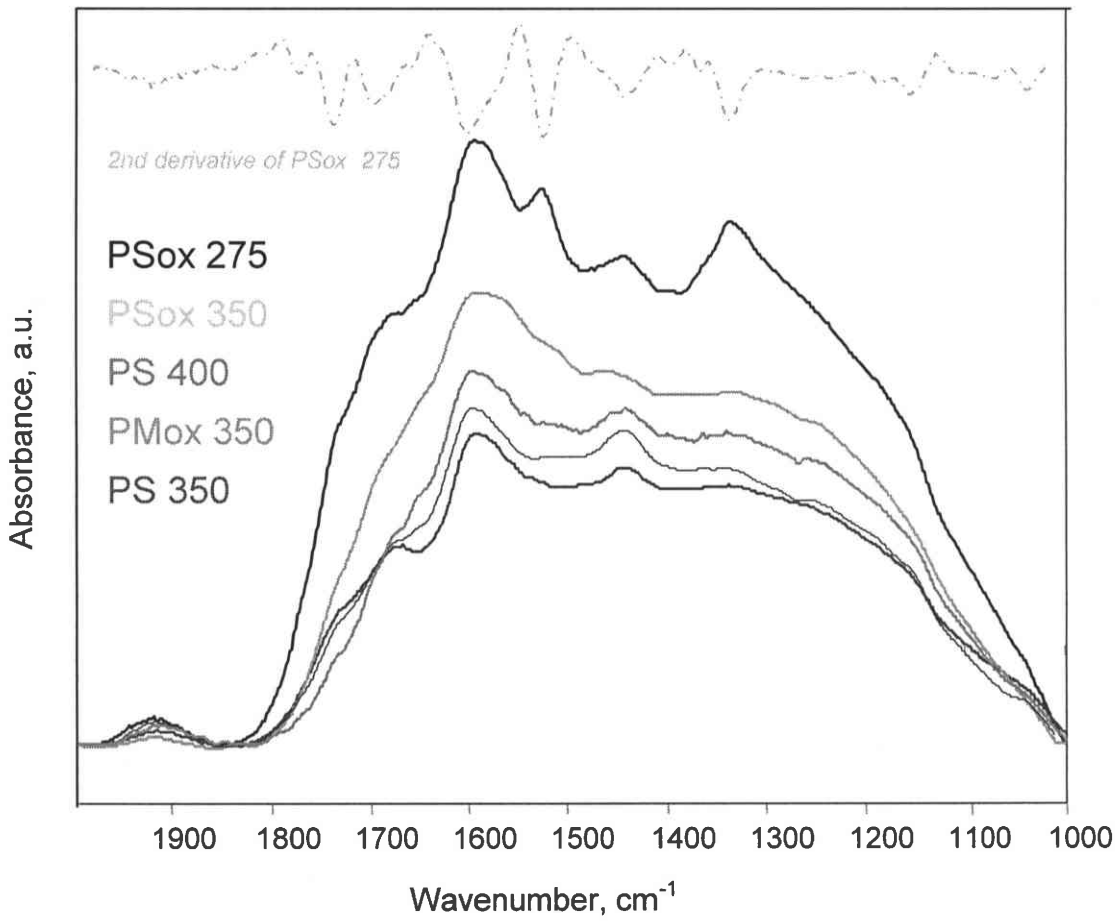

Fig. 67 DRIFT spectra in the 2000-1000 cm^{-1} region of the ammoxidized samples.

The 3500-2100 cm^{-1} region of DRIFT spectra of the ammoxidized samples after truncation and multipoint baseline correction are presented in Fig. 68. The peak observed at 2220-2215 cm^{-1} indicates the presence of nitrile groups. The peak intensity decreases in the order: PSox 350 > PSox 275 > PM 350 > PS 350 > PS 400, reflecting

the decomposition and / or conversion of nitrile groups occurring at higher temperatures. The peak at 3050 cm^{-1} corresponds to aromatic ν(C-H) modes.

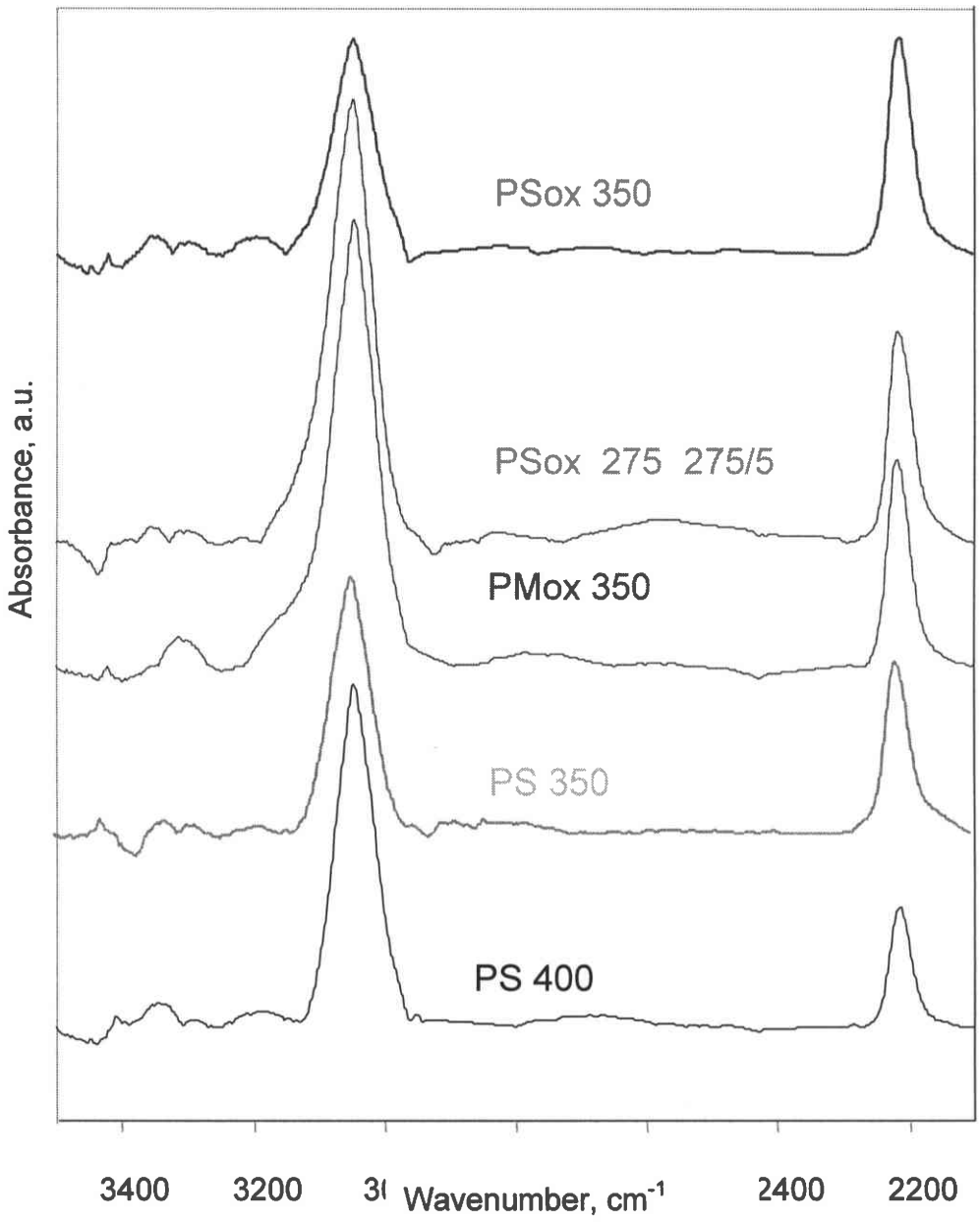

Fig. 68. DRIFT spectra in the 3500-2100 cm^{-1} region of the ammoxidized samples .

XPS study

Based on the amount of the introduced nitrogen the following ammoxidized samples were selected for further study:

PS 400 (PS-Am);

PSox 350 (PSox-Am);

PMox 350 (PMox-Am).

The N1s spectra of PS-Am , PSox-Am and PMox-Am were fitted by four to five components (Fig. 69).

The peak at about 399.7±0.2 eV can be ascribed to the convoluted mixture of non-cyclic compounds containing nitrogen groups like amides, alkylamides, nitriles and some cyclic functionalities like imides or lactams (Bekkum and Jansen, 1995). The concentration of this spectrum component is distinctly higher in the case of samples preoxidized with nitric acid than in PS-Am semi-coke (Table 20). The latter sample shows the enhanced contribution of the pyridinic nitrogen. The results of infrared and XPS spectroscopy indicate that the oxidation with nitric acid leads is accompanied by the creation of oxygen groups as well as the lactams and amides which are converted during the ammoxidation into thermally more stable groups like pyrroles and pyridines.

The peak at about 401.4 eV commonly attributed to the quaternary nitrogen occurring in condensed graphene rings is present in all the spectra, however distinctly enhanced level of this form is observed in PMox-Am sample (19%). Since the substitution of the graphene layer by nitrogen has been reported to occur at more severe conditions than applied in the ammoxidation (Pels et al., 1995), it seems to be more reasonable to ascribe this peak to other positively charged species like pyridinic-N associated with an adjacent or nearby located hydroxyl oxygen or carboxyl groups, protonated through formation of a H-bridge (Kelemen et al., 1994).

The peak centred at about 404.5 eV in the N1s spectrum of PMox-Am is assigned to the oxidized state of nitrogen atoms. The shift in the binding energy from the position of 402.6 eV corresponding to oxidized pyridinic-N, supports the presence of nitro groups.

The C1s peaks of all ammoxidation products have a similar shape (Fig. 70). The component at about 284.6± eV, ascribed to non-functionalized carbon, constitutes 76-80% of the peaks area. Peaks at about 286.4±0.2 eV and 287.8±0.2 eV can be ascribed to the non-deconvoluted mixture of the carbon linked to oxygen or nitrogen atoms. The former peak can be attributed to carbon linked with hydroxyl groups as well to carbon in amines or nitriles. The latter component corresponds to the carbonyl carbon in ketones, quinones or amides. The peaks at about 290 eV and 292 eV can be assigned to the presence of carboxyl/ester groups and to conjugated aromatic systems, respectively.

The O1s spectrum of PS-Am (Fig. 71) indicates the elevated contribution of groups containing oxygen double bonded to carbon. On the contrary, the surface of

ammoxidized samples produced from the oxidized precursors displays a higher proportion of ester and hydroxylic moieties.

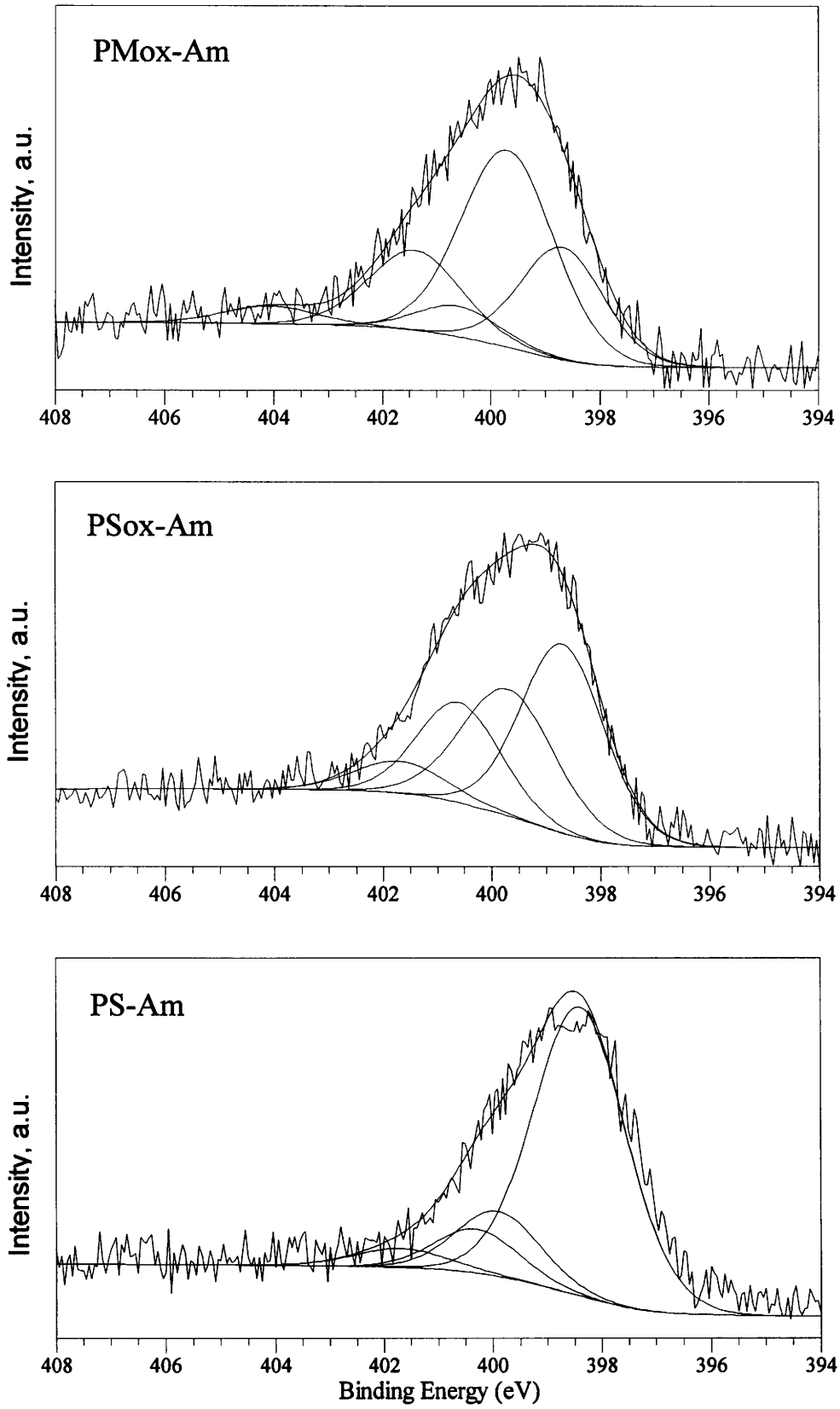

Fig. 69. N1s XPS spectra of ammoxidized samples: PS-Am, PSox-Am and PMox-Am.

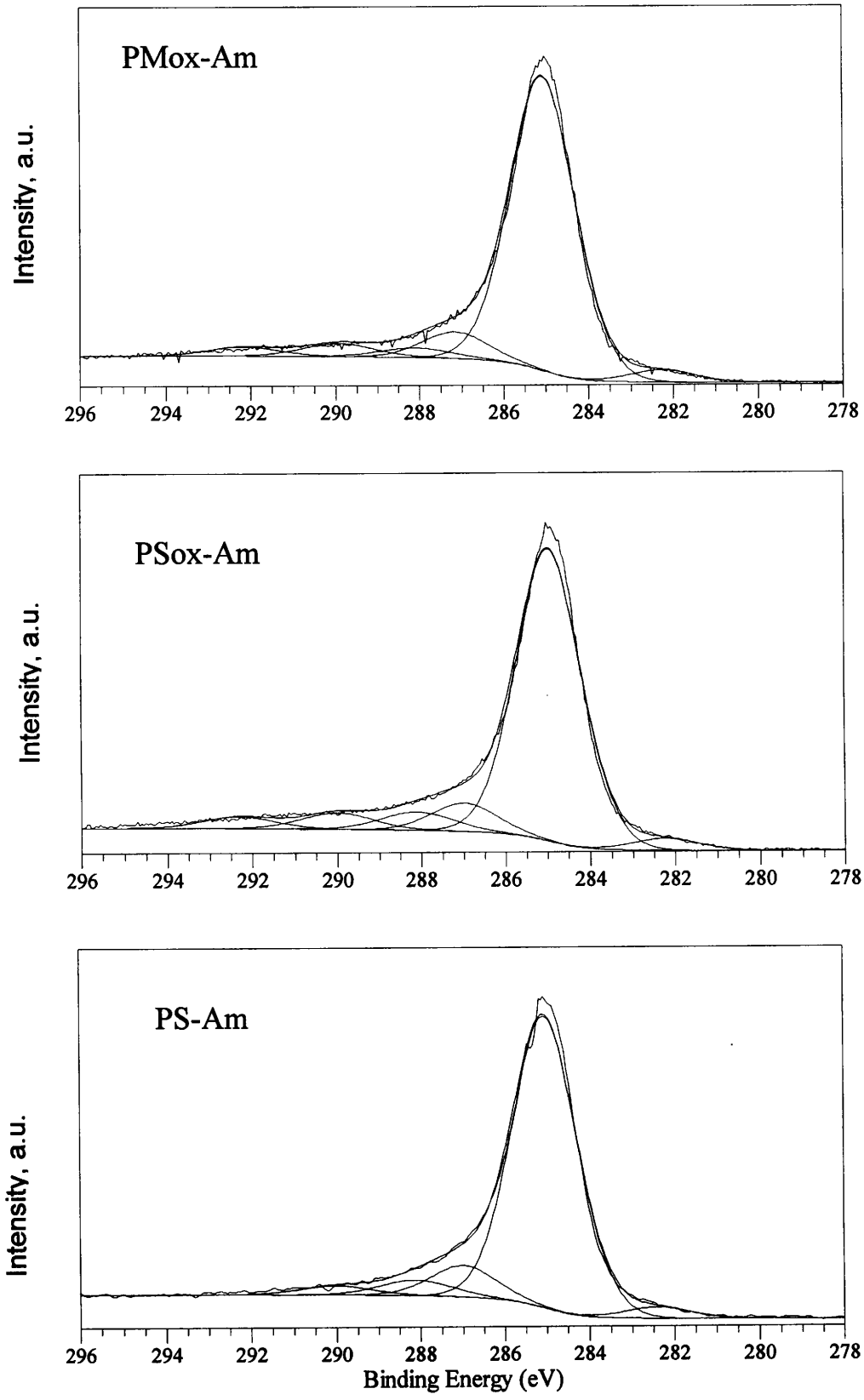

Fig 70. C1s XPS spectra of ammoxidized samples: PS-Am, PSox-Am and PMox-Am.

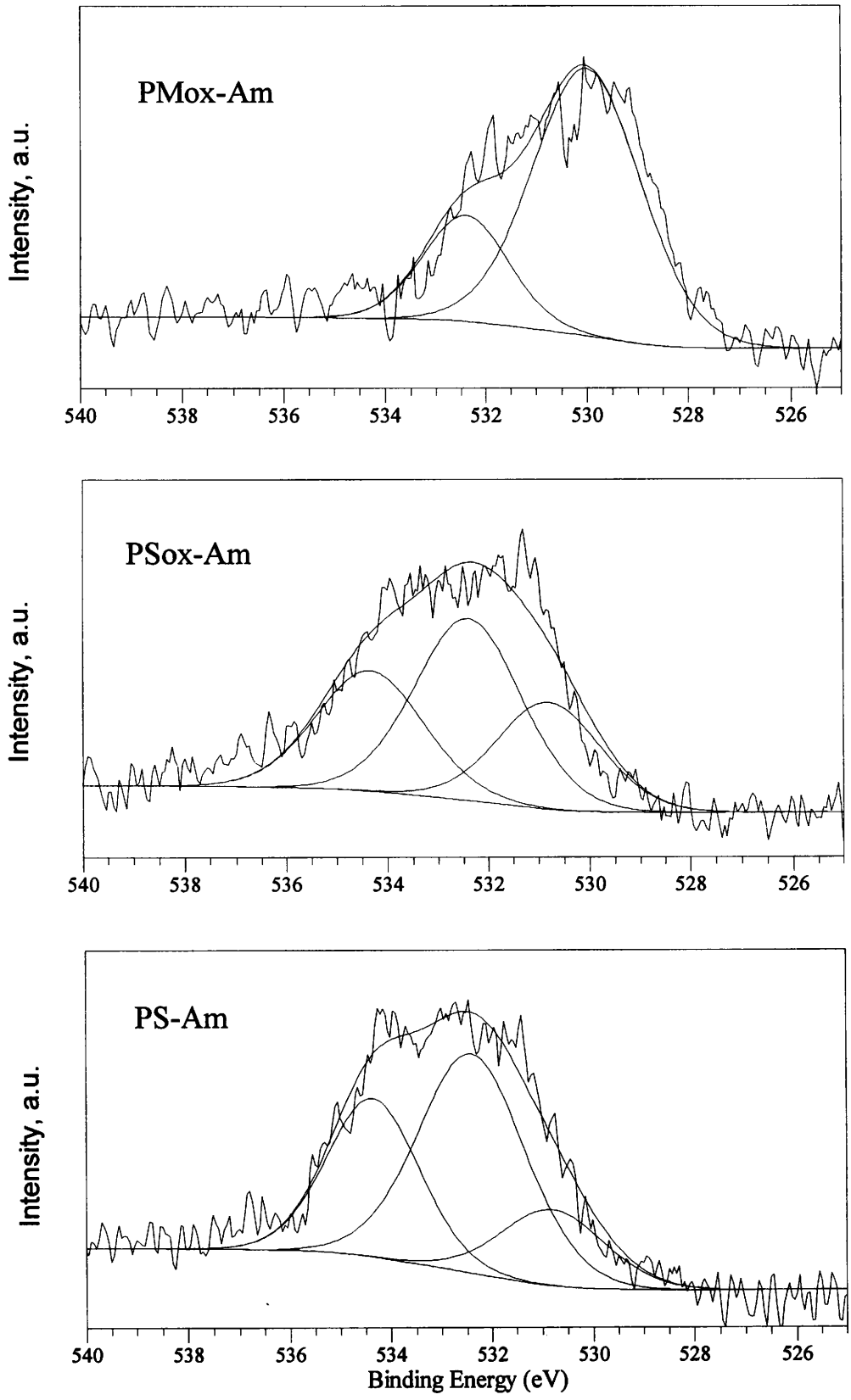

Fig 71. O1s XPS spectra of ammoxidized samples: PS-Am, PSox-Am and PMox-Am.

Table 20. Distribution of carbon, nitrogen and oxygen forms in the ammoxidized samples

Peak	BE eV	Possible assignment	**PS-Am** %	**PSox-Am** %	**PMox-Am** %
C1s	282.6±0.4	C carbidic	3.1	3.2	3.4
	284.8±0.2	C-H, C-C	80.7	76.1	80.7
	286.7±0.4	C-OH, C-N, C=N	8.6	7.4	7.2
	287.8±0.3	C=O	4.8	5.2	2.9
	289.7±0.4	COO	2.7	4.7	4.0
	291.6±0.5	plasmon / π- π* transitions	0.0	3.4	2.8
N1s	398.7±0.3	N-6	71.3	40.6	24.1
	399.7±0.2	N≡C- , -N-C=O	14.4	30.2	47.5
	400.3±0.3	N-5	9.7	21.6	6.9
	401.4±0.5	N-Q	4.6	7.6	18.7
	402-405	N-X	0.0	0.0	2.8
O1s	530.6±0.2	C=O	76.1	23.7	20.3
	532.8±0.4	C-O-C, C-OH	23.9	45.9	46.6
	535.2±0.4	H_2O, O_2 adsorbed	0.0	30.4	33.1

The surface elemental composition of the ammoxidized samples was studied by XPS. Results presented in Table 21 indicate that ammoxidation of oxidized with nitric acid samples leads to rather similar composition, both in the surface as well in the bulk of sample. Indeed, it seem that the oxidation enhances the depth of the nitrogen enrichment on the subsequent air-ammonia mixture treatment. Contrarily, the N/C and O/C atomic ratio determined by XPS for the PS-Am sample, are as much as twice higher, as the values from the elemental analysis. This proves that nitrogen uptake due to the ammoxidation of the samples which were not oxidized prior to the process is strongly limited to the surface layers.

Table 21. Elemental composition of ammoxidized samples determined by XPS

Sample	Atomic concentration[1]			Atomic ratios			
	C	N	O	N/C		O/C	
				XPS	El.An.	XPS	El.An.
PS-Am	84.2	10.8	5.0	0.127	0.077	0.060	0.029
PSox-Am	88.6	7.0	4.4	0.079	0.087	0.049	0.048
PMox-Am	88.8	7.2	4.0	0.080	0.100	0.046	0.024

[1] C + N + O = 100%

5.5. The behavior of nitrogen enriched semi-cokes on thermal treatment in inert and oxidative atmosphere

This chapter is concerned with the evaluation of the behavior of nitrogen enriched semi-cokes prepared by co-pyrolysis and ammoxidation on the subsequent carbonization and activation treatment at 800-900^{0}C. The study is focused on the qualitative and quantitative characterization of volatile release (TG-FTIR) and the understanding the nature of carbons produced in the inert and oxidative conditions (elemental analysis, XPS). The studied semi-cokes prepared from the respective single components and pitch-polymer blends by heat-treatment at 520^{0}C for 2h are: CTP-S, CTP-PAN 9:1, CTP-PAN 3:1-S, CTP-PAN 1:1-S, PAN-S, CTP-PVP25ox 3:1-S, CTP-PVP25ox 1:1-S and PVP25ox-S

5.5.1. Structural evolution of nitrogen enriched carbonaceous materials produced by co-pyrolysis

The carbonaceous materials used in this part of the study are semi-cokes PAN-S, CTP-PAN 1:1-S, PVP25ox-S and CTP-PVP25ox 1:1-S.

5.5.1.1. Weight loss behavior

The thermograms of semi-cokes of PAN-S, CTP-PAN 1:1-S, PVP25ox-S, and CTP-PVP25ox 1:1-S heat-treated in the inert atmosphere up to 900^{0}C are presented in

Figs 72-75. Some characteristics of the thermal behavior of the semi-cokes are given in Table 22.

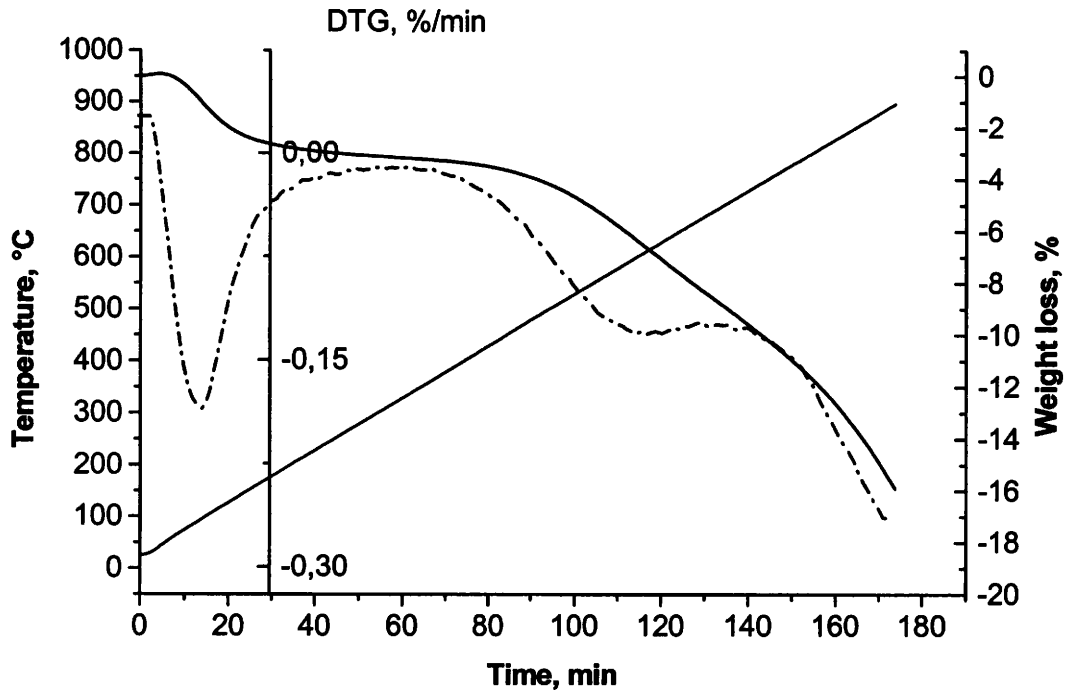

Fig. 72. TG/DTG profiles of PAN semi-coke.

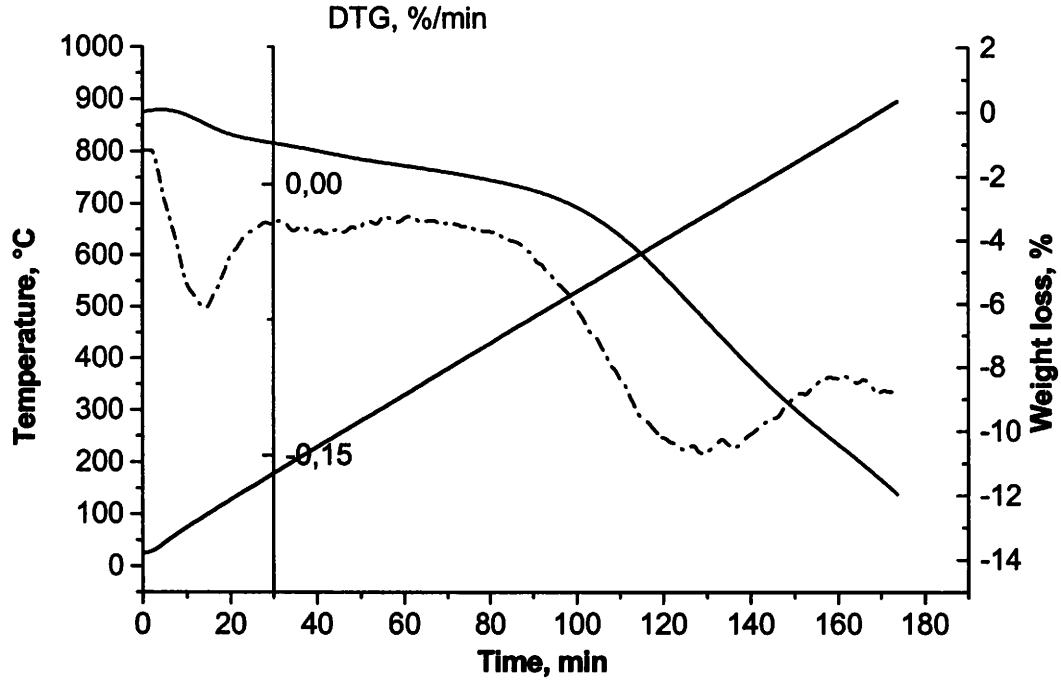

Fig. 73. TG/DTG profiles of CTP-PAN 1:1 semi-coke.

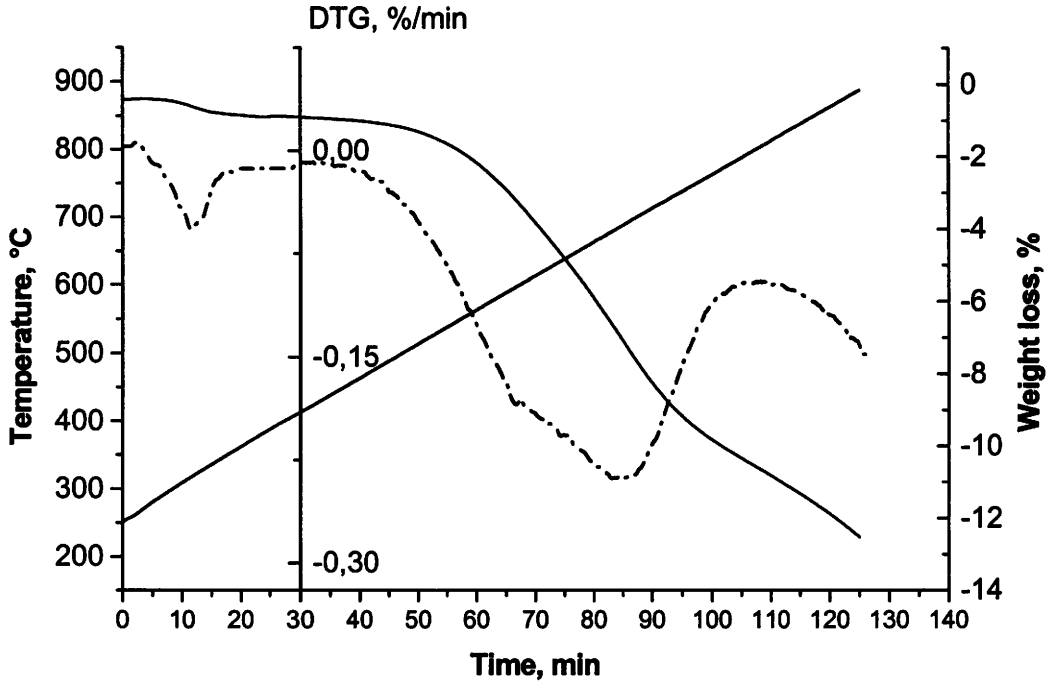

Fig. 74. TG/DTG profiles of PVP25ox semi-coke.

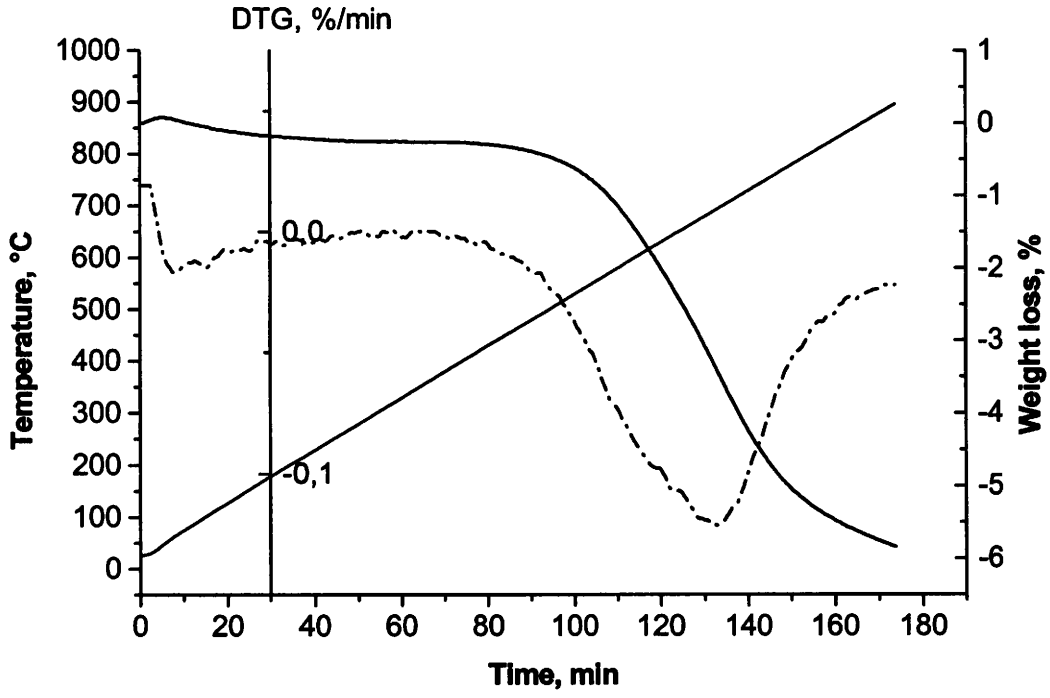

Fig. 75. TG/DTG profiles of CTP-PVP25ox 1:1 semi-coke.

Table 22. Thermal decomposition characteristics of the semi-cokes prepared from the polymers and the pitch-polymer blends

Sample	Temperature range[1] ^0C	T_{max}[2] ^0C	Weight loss at 900^0C wt%
PAN–S	420-680	625	15.9
CTP-PAN 1:1-S	440-820	670	11.9
PVP25ox-S	480-790	680	12.5
CTP-PVP25ox 1:1-S	470-900	700	5.8

[1]Temperature range of the major degradation step
[2] Temperature of the maximum weight loss rate

The DTG curves of all the samples indicate two or three ranges of the weight loss. A sharp peak with the maximum at about 100^0C corresponds to desorption of water. This peak is most discernible in the case of PAN-S of the highest nitrogen content and the weakest in CTP-PVP25ox-S where the nitrogen content is relatively low. This suggests that nitrogen atoms constitute strong active sites for the water sorption on the surface of materials.

The second region of enhanced weight loss covers a broad and characteristic of a given material temperature range from about 420^0C to $700\text{-}800^0C$. A maximum weight loss rate is centered at 625^0C for PAN-S and between $670\text{-}700^0C$ for other semi-cokes. This corresponds to the region of secondary devolatization reactions ($670\text{-}720^0C$) in the conventional carbonaceous materials, which is associated with the release of hydrogen and methane, and to a lower extent of carbon oxide. The difference in the maximum weight loss temperatures between PAN-S and PVP25ox-S suggests a higher thermal stability of the latter semi-coke. This is also confirmed by the lower weight loss on the heat treatment up to 900^0C of the PVP25ox semi-coke as compared with PAN-S (12.5% and 15.9%, respectively). The maxima of the DTG peaks of semi-cokes from polymers are shifted to a lower temperature as compared with the corresponding semi-cokes obtained from the co-pyrolysis. Characteristic of the former semi-cokes is an additional high temperature region of the enhanced weight loss which starts above 750^0C.

The FTIR analysis of gases evolved during the semi-cokes treatment (Figs.76-78) reveals that the main volatile by-products detectable using this technique are HCN, NH_3, CO_2, CO and low molecular aliphatic hydrocarbons. The intensity of signal

attributed to particular species as and the temperature of maximum evolution rate varies for different materials (Tables 23, 24). In the case of PAN-S and CTP-PAN 1:1-S the maximum intensity of the ammonia evolution (640 and 700^{0}C) precedes distinctly the maximum of hydrogen cyanide evolution. In contrast, for the semi-coke from CTP-PVP25ox blend the maximum of HCN evolution is centered at the temperature by about 50^{0}C lower than that of NH_3. Moreover, the signal of NH_3 is much more intense than the signal of HCN. The intensity ratio of the NH_3 and HCN signals are the same for PAN and CTP-PAN 1:1 semi-cokes what suggests a similar pathway of the decomposition of nitrogen functionalities in both studied samples. This is in agreement with XPS analysis indicating very similar contributions of particular nitrogen species in these semi-cokes.

Rather surprising is a large amount of carbon dioxide which is detected in the analyzed gases over the whole temperature range. The evolution commences at about 50^{0}C and increases with the temperature up to a maximum at 350^{0}C for PAN-S and above 550^{0}C for the other samples. The low temperature evolution can be ascribed to the desorption from strong basic sites associated with nitrogen. Apparently, up to about 400^{0}C, the CO_2 signal is the most intense for the PAN-S displaying a high concentration of nitrogen. Above 200^{0}C a relevant contribution to the CO_2 absorption is expected due to the decomposition of oxygen functionalities, initially of carboxylic groups and later also lactones and anhydrides (Otake and Jenkins, 1993; Rodriguez-Reinoso, 1997), which could be formed upon the exposure of the materials on air.

We cannot however exclude the generation of some amount of CO_2 due to the getting of air traces into carrier gas stream.

Carbon oxide occurs in the evolved gas at a reasonable proportion as an effect of decomposition of CO-forming oxygen functionalities, including carbonyl, quinone, ether and phenol groups (Rodriguez-Reinoso, 1997).

The absorbances profiles of the particular gases evolved from CTP-PVP25ox semi-coke show that some quantities of low molecular weight aliphatic compounds are formed in the temperature range of 500-700^{0}C. This phenomenon can be explained by the scission of aliphatic hydrocarbons from the non-condensed vinyl part of polymer. None low molecular weight aliphatics, including methane, were detected on the thermal treatment of PAN derived semi-cokes.

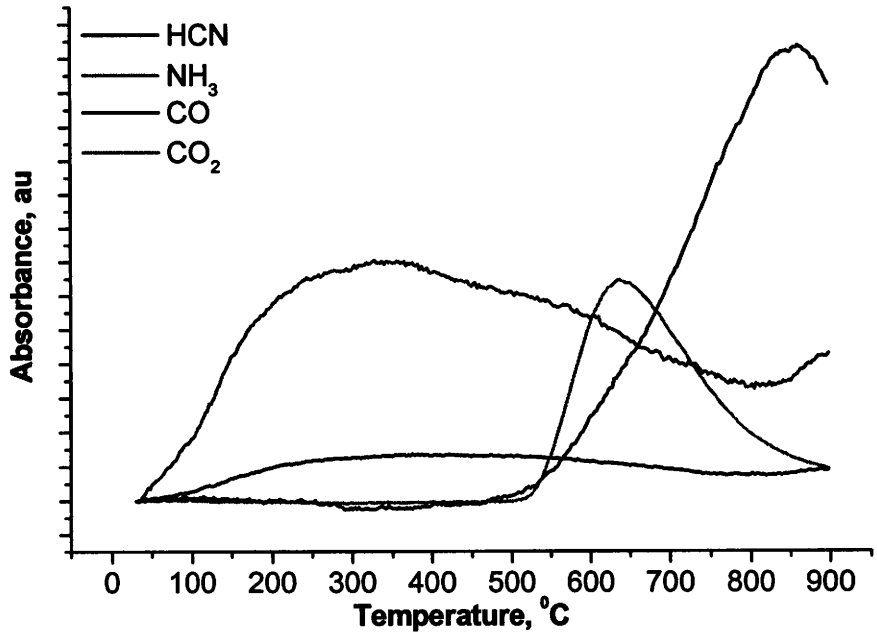

Fig. 76. Evolution of gases on thermal treatment of PAN semi-coke.

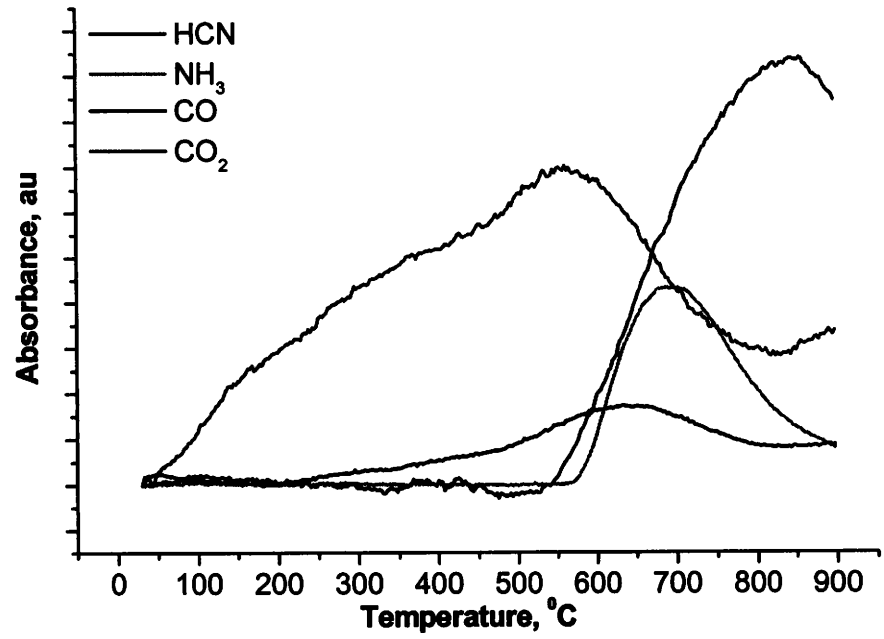

Fig. 77. Evolution of gases on thermal treatment of CTP-PAN 1:1 semi-coke.

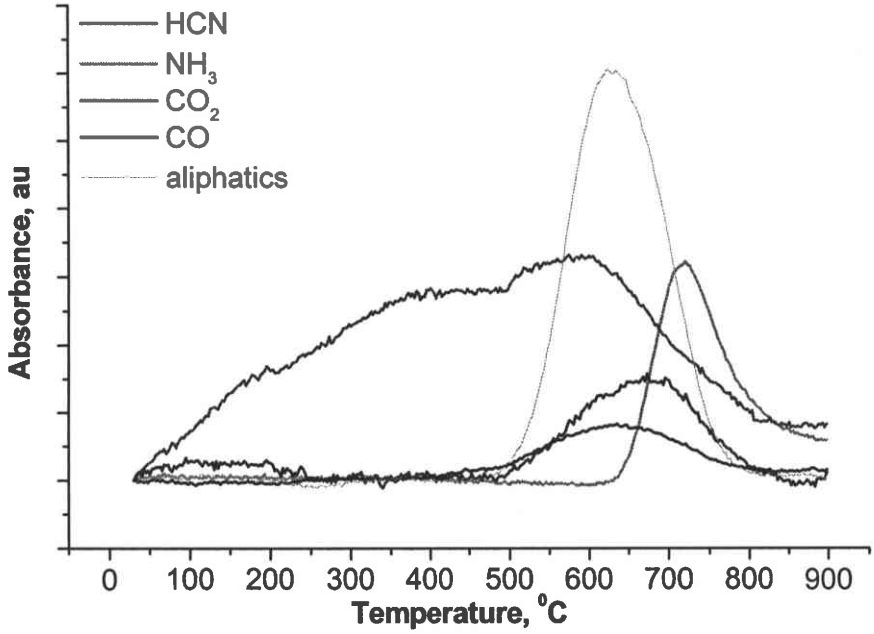

Fig. 78. Evolution of gases on thermal treatment of PVP25ox semi-coke.

Table 23. Temperature of the maximum evolution of gaseous products on thermal treatment of the semi-cokes prepared from the polymers and the pitch-polymer blends

Sample	Temperature of the maximum evolution rate, ^{0}C				
	CO_2	CO	HCN	NH_3	aliphatics
PAN-S	348	300-600	860	640	not detected
CTP-PAN 1 :1-S	560	630	840	700	not detected
CTP- PVP25ox 1:1-S	590	630	670	720	620

Table 24. Relative signal intensities of the evolved gases determined based on the peak areas

Sample	Relative peak area[1]				
	S_{CO2}	S_{CO}	S_{HCN}	S_{NH3}	$S_{aliphatics}$
PAN-S	0.46	0.09	0.14	0.31	not detected
CTP-PAN 1:1-S	0.49	0.09	0.11	0.31	not detected
CTP- PVP25ox 1:1-S	0.63	0.07	0.16	0.11	0.03

[1] $S_{CO2}+ S_{CO}+ S_{NH3}+ S_{aliphatics}=1$

Carbonization and activation of carbonaceous materials produced by co-pyrolysis of pitch with polymers

The semi-cokes obtained by the pyrolysis of the polymers and pitch-polymer blends at 520^{0}C were steam-activated at 800^{0}C, up to a burn-off of ca. 50%. In the parallel runs the samples were carbonized at 800^{0}C in nitrogen atmosphere. A typical weight loss curve of the activation runs performed in the study is presented in Fig. 79.

The heating of a semi-coke at 5 K/min up to 520^{0}C (6000s) in a nitrogen stream implies a little mass change. The next more inclined part of the curve corresponds to the heating under nitrogen to the final temperature of 800^{0}C with the related release of gaseous products. The beginning of gasification with steam (activation) at 9600s is marked by a much faster weight loss. The slope of curve in this region and corresponding time required to reach the 50 wt% burn-off is a measure of the reactivity of a given sample and varies widely from one activated sample to another. The treatment of the semi-cokes in the inert atmosphere for the time established for an activation of a given material (carbonization), allows to evaluate the "pure" thermal stability during treatment.

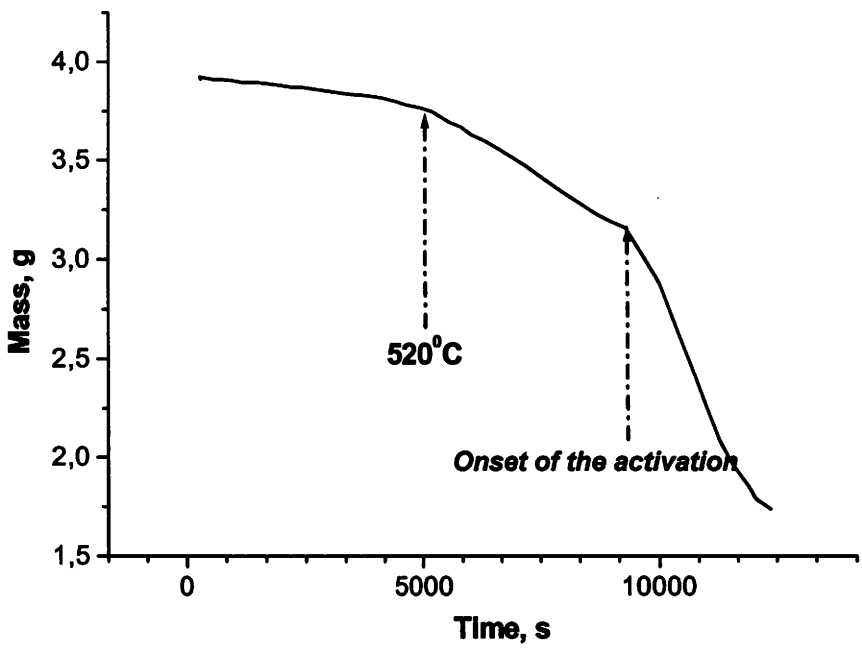

Fig. 79. The weight loss profile on PAN semi-coke activation.

The characteristics of the carbonization and activation process are given in Table 25. The activation time needed to reach the intended burn-off decreases for both the series of pitch-polymer blends in the order:
CTP-S > CTP-PAN 9:1-S > CTP-PAN 3:1-S > CTP-PAN 1:1-S > PAN-S and CTP-S > CTP-PVP25ox 3:1-S > CTP-PVP25ox 1:1-S > PVP25ox-S (Table 25). According to these data, the samples containing a significant proportion of the introduced nitrogen are more reactive toward steam. Apparently, the shortest activation time was noted for PAN. The data presented in Table 25 indicate that the trend in the thermal stability of the samples, measured as a weight loss on carbonization at 800^0C is the same as for the gasification rate. The least stable is PAN-S (29.4% weight loss), while the most persistent are the CTP and CTP-PAN 9:1 semi-cokes (8.7% weight loss).

In general the activation times of semi-cokes prepared from PVP25ox and its blends with the pitch are longer than those of corresponding PAN derived semi-cokes. Similarly the semi-cokes of the former series show a higher thermal stability.

If exclude the catalytic effects, the gasification rate or reactivity towards steam of any carbonaceous material depends primarily on its structural ordering and associated microporosity. Increasing the proportion of PAN or PVPox in the blend with pitch leads to a gradual degradation of the structural ordering as reflected by the depression of anisotropic development. One can assume that in the nano-scale the polymer derived material represents a poorer ordering which is more readily gasified. In this sense the abundance of nitrogen as associated with the disordered material coincides with the enhanced gasification rate. It is also possible that nitrogen atoms constitute the sites more readily oxidized by steam. Fig. 80 presents a relationship between activation time and the nitrogen content in the studied materials. The observed trend indicates that the activation time is inversely proportional to the nitrogen content in the semi-cokes.

It should be noticed that the obtained burn-off levels differ in few cases from the intended value of 50 wt%. The significant discrepancy occurs for CTP-PAN 3:1-S (45.2 wt%) and for PVP25ox-S (57.9 wt%).

Table 25. Characteristics of the carbonization and activation process for the semi-cokes from the co-pyrolysis of pitch with N-polymers

Sample	Weight loss on carbonization wt%	Time of activation h	Burn-off wt%
CTP-S	8.7	4.20	51.5
CTP-PAN 9:1-S	8.7	3.00	50.0
CTP-PAN 3:1-S	14.1	2.25	45.2
CTP-PAN 1:1-S	20.6	1.25	50.0
PAN-S	29.4	0.75	50.0
CTP-PVP25ox 3:1-S	12.0	3.58	47.7
CTP-PVP25ox 1:1-S	14.7	2.83	50.0
PVP25ox-S	19.6	2.25	57.9

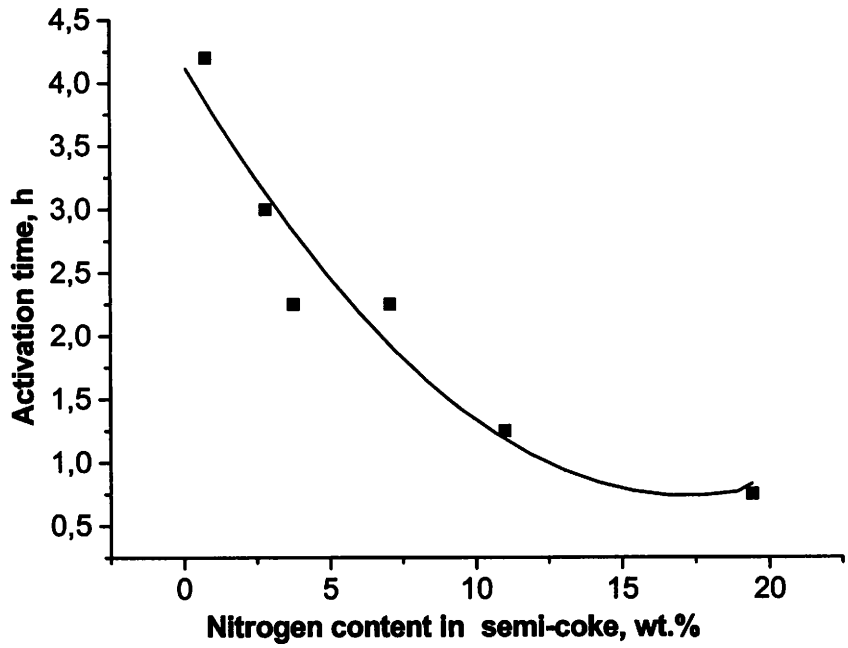

Fig. 80. Influence of the nitrogen content in the semi-cokes on the activation time.

5.5.1.2. Microtexture characteristics of the carbonization and activation products derived from pitch-PAN blends

The carbonization and activation products (800^0C) obtained from blends of the pitch with polyacrylonitrile (CTP-PAN 3:1-C, CTP-PAN 3:1-A, CTP-PAN 1:1-C and CTTP-PAN 1:1-A, respectively) were characterized in terms of the microtexture ordering using transmission electron microscopy (TEM).

The CTP-PAN 3:1-C and CTP-PAN 3:1-A when viewed by transmission electron microscopy reveal the presence of the domains of a size 600-800 nm as a predominant unit (Figs. 81-82). In the case of the activated carbon the boundaries of the domains are coarser then in the carbonized sample, what can be attributed to the porosity development due the to the steam activation.

The 002 DF image of the CTP-PAN 1:1-C coke (Fig.83) shows the presence of the smaller domains (400-700 nm) corresponding to the deteriorated texture observed by the optical microscopy. The increase of the PAN proportion is manifested in the presence of the small spherulites (approximately 200 nm). These spherical units are not observed in the texture of the activated sample, displaying pattern of the small, coarsed misoriented domains (Fig. 84).

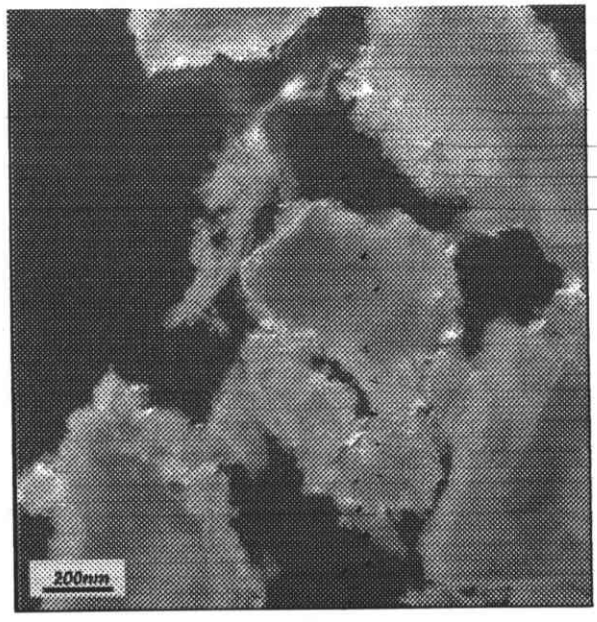

Fig. 81. 002 dark field TEM image of the CTP-PAN 3:1-C coke.

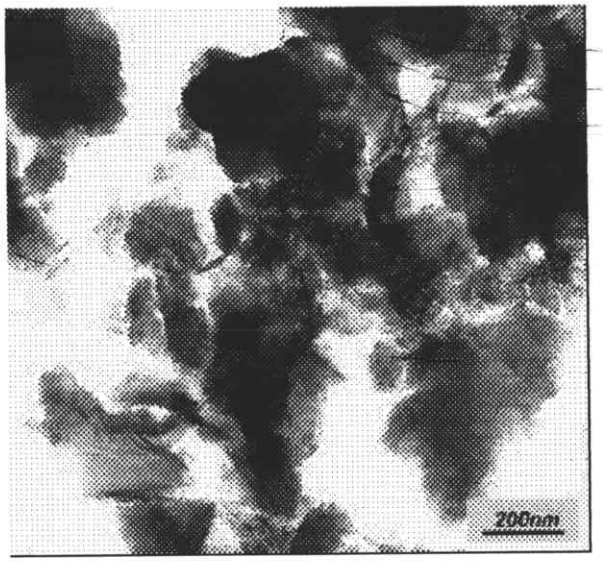

Fig. 82. Bright field TEM image of the CTP-PAN 3:1-A carbon.

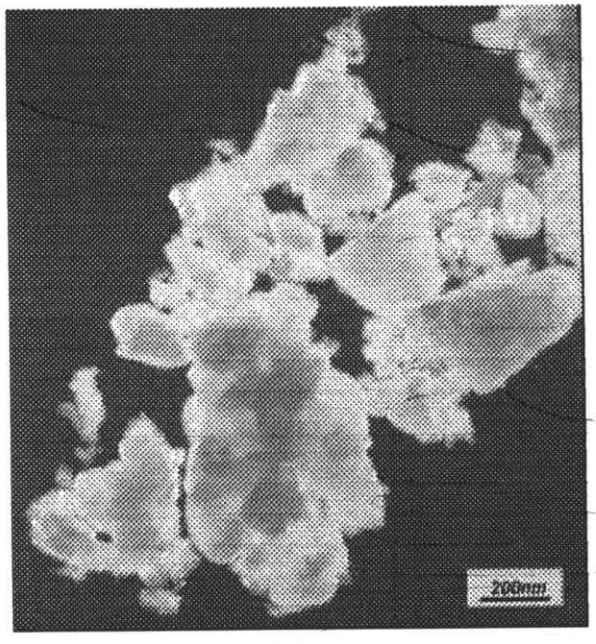

Fig. 83. 002 dark field TEM image of the CTP-PAN 1:1-C coke.

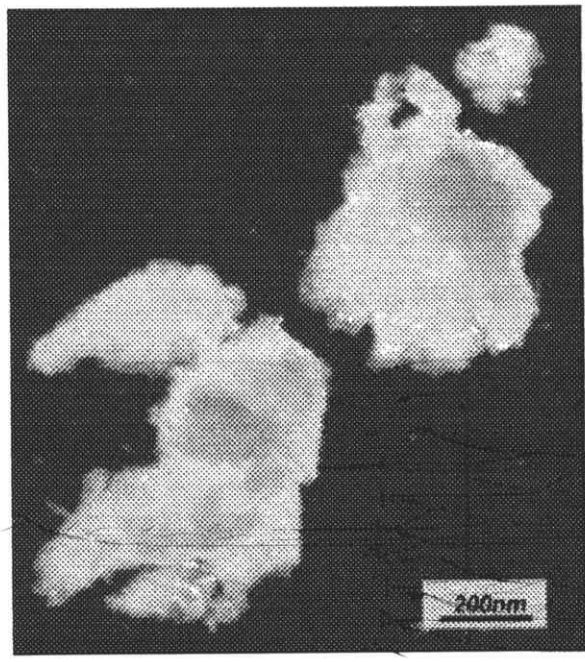

Fig. 84. 002 dark field TEM image of the CTP-PAN 1:1-A carbon.

5.5.1.3. Elemental composition of the carbonization and activation products produced from pitch-polymer blends

The elemental analyses of the carbonization and activation products from pitch-PAN blends are given in Table 26. Despite a considerable release of nitrogen on heat-treatment of blend semi-cokes to 800^{0}C, the carbonization products can be regarded as very rich in nitrogen carbons. It is interesting to note that the blend cokes contain more nitrogen than it would be attained by a simple mixing at respective weight ratio of single component cokes. A beneficial effect of blending on the nitrogen content in resultant carbons is more distinct for blends of moderate proportion of PAN in pitch.

The loss of the nitrogen on the activation is about twice higher. This intense removal of nitrogen on the activation can be attributed to the preferential burn-off of the amorphous phase containing most of the heteroatom.

The enhanced oxygen level in the carbonization products can be attributed to the sorption of H_2O and CO_2 on the nitrogen polar sites existing in the material and/or to the formation of pyridine N-oxides and pyridones due to the post-pyrolysis oxidation. The reactions like these were reported to occur during storing the nitrogen-containing chars in air (Pels et al., 1995, Schmiers et al., 1999). In general, the activated materials

contain more oxygen than the carbonized samples. An explanation can be the formation of C-O and C=O bonds in the oxidizing atmosphere (László et al., 2001).

Table 26. Elemental composition of carbonization and activation products from pitch-PAN blends

Sample	Elemental composition, wt%					$(N/C)_{at}$
	C	H	N	S	O[1]	
CTP-C	97.01	0.80	0.83	0.14	1.22	0.007
CTP-A	92.99	0.97	0.80	0.25	5.08	0.007
CTP-PAN 9:1-C	93.43	0.72	4.24 (2.24)[2]	0.09	1.52	0.039
CTP-PAN 9:1-A	92.90	1.57	1.56	0.22	3.75	0.014
CTP-PAN 3:1-C	87.20	0.91	6.28 (4.24)[2]	0.25	5.36	0.062
CTP-PAN 3:1-A	88.23	1.37	3.11	0.14	7.15	0.030
CTP-PAN 1:1-C	86.30	0.70	8.89 (7.66)[2]	0.23	3.88	0.088
CTP-PAN 1:1-A	87.95	0.98	4.40	0.13	6.54	0.043
PAN-C	80.86	0.86	14.48	0.05	3.75	0.153
PAN-A	85.10	0.98	7.58	0.05	6.29	0.076

[1]By difference
[2]Calculated based on the additivity rule

The elemental analyses of the carbonization and activation products of pitch-PVP25ox blends are given in Table 27. Blending of pitch with PVP25ox leads to the carbons of moderate nitrogen content. A relevant part of nitrogen present in semi-cokes is lost on the heat-treatment to 800^{0}C. Data presented in Table 27 show that the nitrogen content in the blend cokes is comparable to that anticipated based on the additivity rule from the single components. The activation of PVP25ox blends results in the loss of approximately 70 wt% of nitrogen present at the semi-coke stage. As a result the nitrogen content in activated carbons from pitch-PVP25ox blends is below 2 wt%.

Table 27. Elemental composition of carbonization and activation products from pitch-PVP25ox blends

Sample	Elemental composition, wt%					$(N/C)_{at}$
	C	H	N	S	O[1]	
CTP-C	97.01	0.80	0.83	0.14	1.22	0.007
CTP-A	92.99	0.97	0.80	0.25	5.08	0.007
CTP-PVP25ox 3:1-C	94.95	0.68	1.78 (2.00)[2]	0.16	2.43	0.016
CTP-PVP25ox 3:1-A	92.50	1.18	1.15	0.165	5.00	0.011
CTP-PVP25ox 1:1-C	92.42	0.58	3.02 (3.09)[2]	0.17	3.80	0.028
CTP-PVP25ox 1:1-A	92.35	0.69	1.74	0.17	5.05	0.016
PVP25ox-C	88.48	0.94	5.34	0.11	5.13	0.052
PVP25ox-C	89.31	1.35	2.19	0.04	7.11	0.021

[1]By difference
[2]Calculated based on the additivity rule

5.5.1.4. Evolution of nitrogen and oxygen functionalities on the carbonization and activation of PAN and PVP25ox derived semi-cokes

X-ray photoelectron spectroscopy

The evolution of nitrogen and oxygen functional groups on the thermal treatment of PAN and PVP25ox semi-cokes in an inert and oxidative atmosphere was monitored by XPS. The C1s, N1s and O1s spectra of the PAN derived products of carbonization at 800^{0}C and activation with steam are presented in Figs 85-87, respectively. The corresponding spectra of PVP25ox derived materials are given in Figs. 88-90. Distribution of carbon, nitrogen and oxygen forms in the resultant PAN and PVP25ox cokes is given in Table 28.

The deconvolution of the C1s spectra of PAN-C and PAN-A yields several peaks which are assigned to the graphitic carbon present in C-C and C-H bonds (peak at 284.8±0.2 eV) and to the carbon atoms occurring in the nitrogen and oxygen moieties (peaks at 286.4 ±0.2 eV, 287.8±0.3 eV and 289.7 ±0.2 eV). Contribution of carbon atoms occurring in the conjugated aromatic systems is reflected in the presence of the peak at 291.6 ±0.2 eV. The treatment of PAN semi-coke at 800^{0}C modifies markedly the distribution of carbon species. The concentration of the graphitic carbon,

constituting about 82% in the PAN semi-coke C1s peak decreases to about 70% in the PAN-C and PAN-A, in favor of carbon linked to the oxygen and/or nitrogen atoms (Table 27).

Neither origin of the material (PAN, PVP25ox or blends) nor a type of treatment applied (carbonization or activation) has a noticeable effect on the distribution of carbon forms in the analyzed materials.

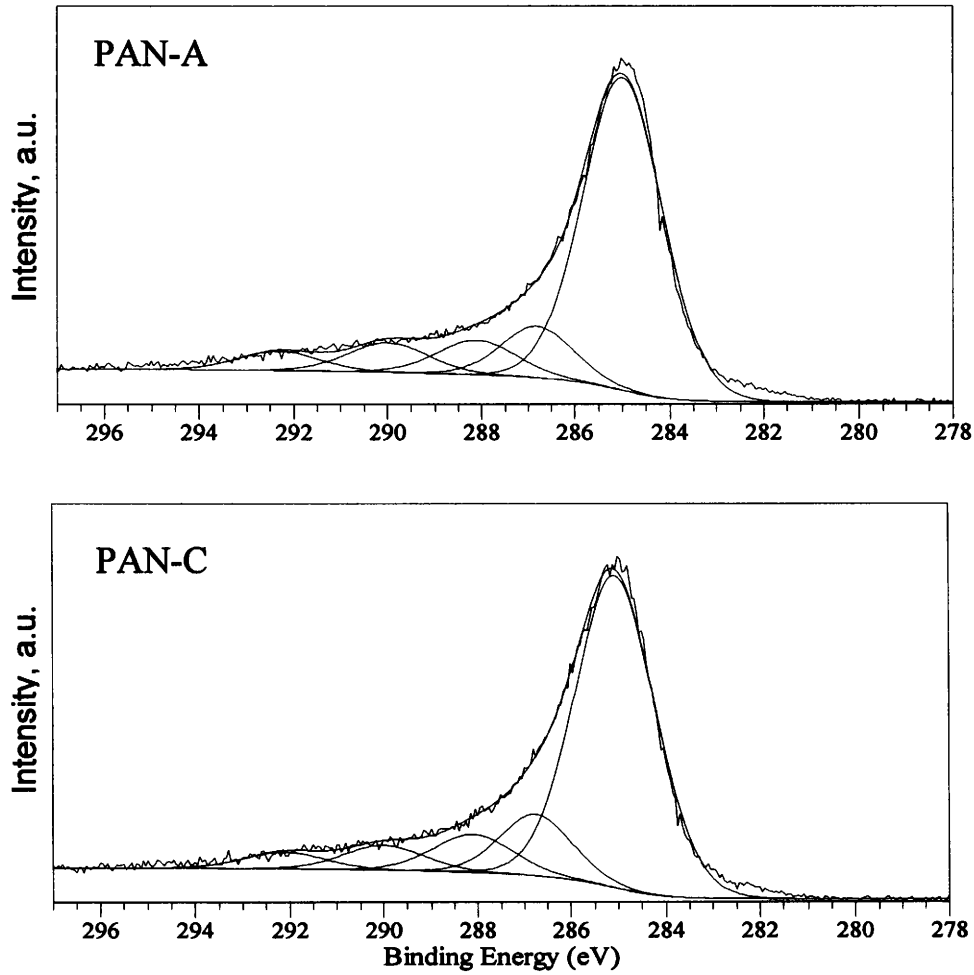

Fig. 85. C1s XPS spectra of carbonization (PAN-C) and activation (PAN-A) products derived from PAN.

The deconvolution of N1s peak in PAN-C and PAN-A spectrum gives four components (Fig. 86) – pyridinic N (N-6), pyrrolic/pyridonic N (N-5), quaternary N (N-Q) and nitrogen oxide (N-X).

The N1s peak shape of PAN semi-coke undergoes a considerable change during carbonization at 800^{0}C. Broadening of N1s regions is associated with the creation of new functionalities comprising quaternary nitrogen and oxidized forms of nitrogen. The contribution of N-6 and N-5 constituting of 64 and 36% of nitrogen in the starting semi-coke falls to about 45 and 21%, respectively. The quaternary nitrogen appears at the expense of N-5 and N-6 form as a result of the extension of pyrrolic rings and condensation of the pyridinic cycles, respectively. Presence of the peak assigned to the oxidized forms of nitrogen can indicate the oxidation of the cokes upon exposure to air.

The evolution of nitrogen functionalities in the carbonized PAN conforms the scheme of the transformation of nitrogen functionalities on severe heat-treatment of N-polymeric precursors proposed by Pels et al. (1995).

Main effect of the oxidative atmosphere during the treatment is the decrease of the N-6 form in favor of the N-5 and N-X (Table 28). This suggests that pyridinic-N is oxidized to N-oxides and pyridones. The concentration of the N-Q is very similar in PAN-C and PAN-A and amounts to about 25%.

The enhanced content of N-5 and N-X in the activated material seems to result from the generation of these functionalities as a transitional stage in the gasification of carbonaceous material. The distribution of nitrogen functionalities in PAN-A resembles that reported by László et al. (2001) for the PAN based activated char (Table 28).

Three different peaks were identified in the O1s spectra of PAN-C and PAN-A (Fig. 87). The peak at 530.4±0.4 eV corresponds to C=O moieties in ketones, lactones and carbonyls, peak at 532.7±0.9 eV to carbonyl oxygen atoms in esters, amides, carboxylic anhydrides and oxygen atoms in hydroxyls and ethers, and peak at 535.2±0.4 eV to the chemisorbed oxygen and/or water (Biniak et al., 1997; László et al., 2001). The distribution of oxygen functionalities in PAN-C and PAN-A is very similar, revealing that ethers and hydroxyl groups constitute main part of the oxygen population (Table 28).

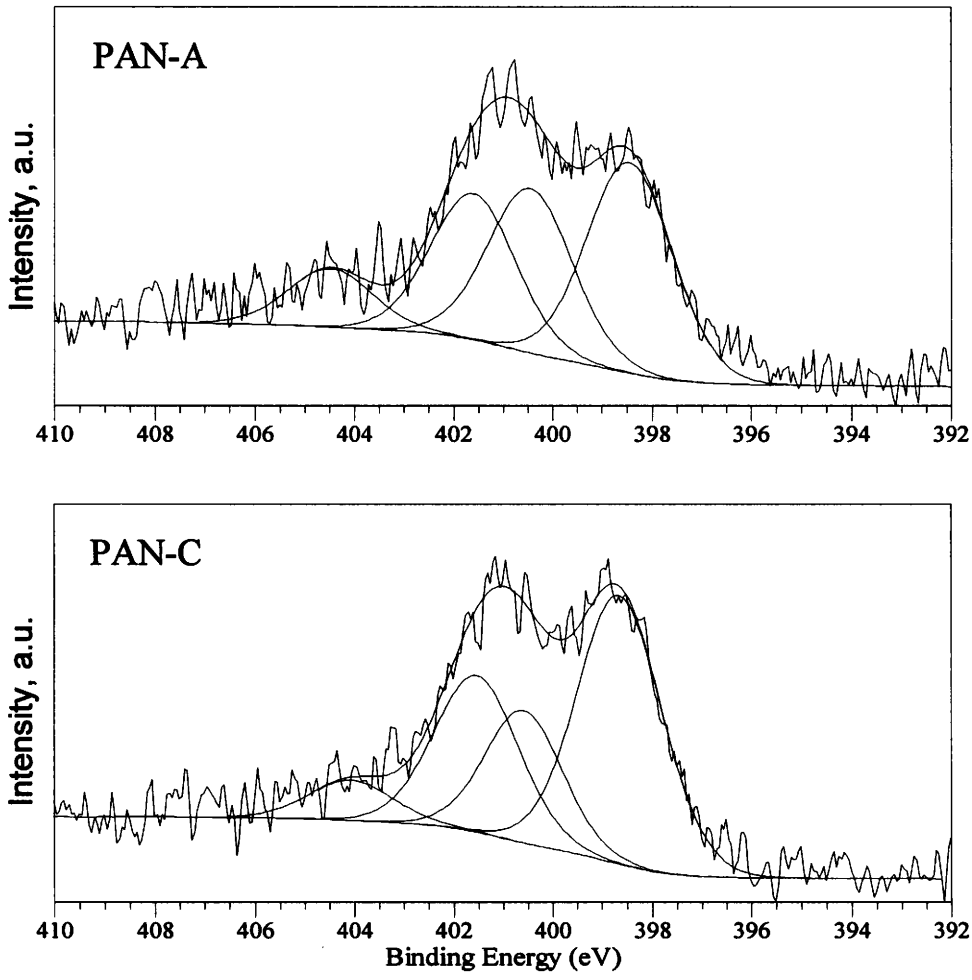

Fig. 86. N1s XPS spectra of carbonization (PAN-C) and activation (PAN-A) products derived from PAN.

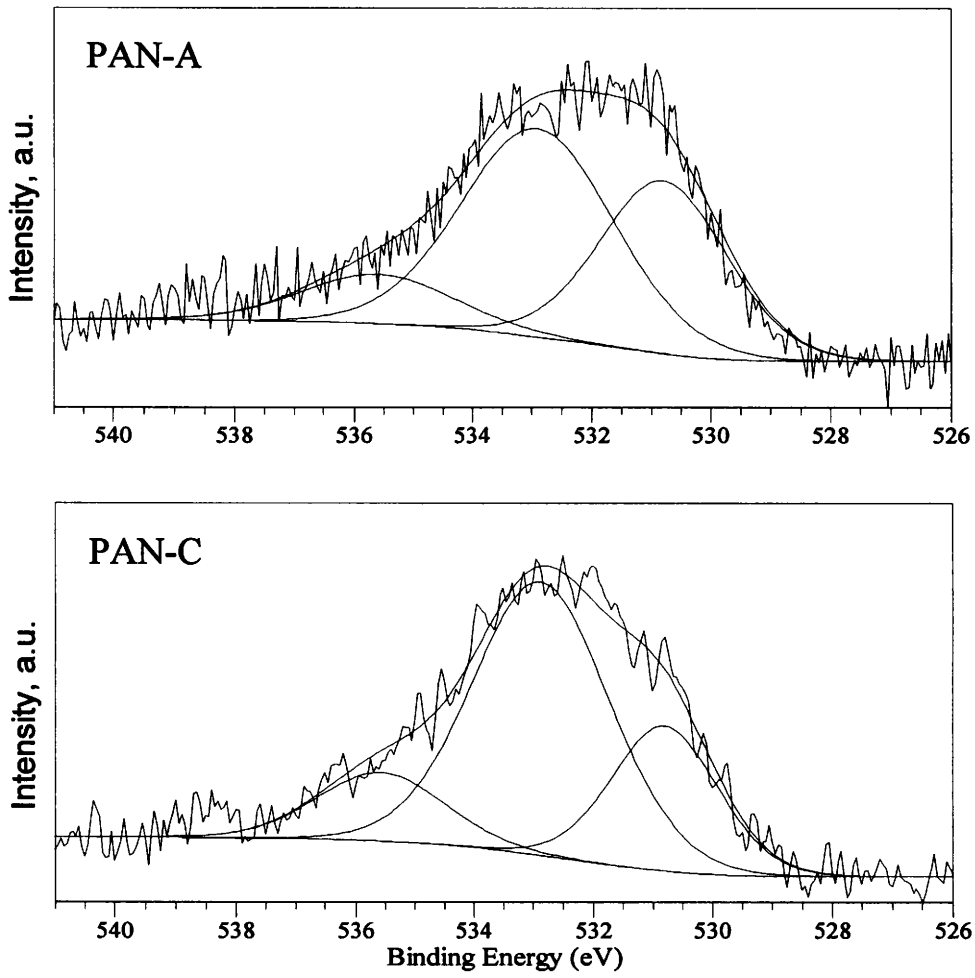

Fig. 87. O1s XPS spectra of carbonization (PAN-C) and activation (PAN-A) products derived from PAN.

C1s, N1s and O1s regions of the XPS survey spectra of carbonization and activation product of PVP25ox are presented in Figs 88-90. Very similar distribution of different forms of the elements in PVP25ox-C and PVP25ox-A proves that treatment in oxidative and inert atmosphere modify in similar way the surface chemistry of the PVP25ox semi-coke. The high temperature treatment results in the partial conversion of N-6 and N-5 functionalities of semi-coke into N-Q form which accounts for 26-29% of the total nitrogen present in 800^{0}C samples. The pyridinic and pyrrolic/pyridonic groups are identified at this stage in similar concentrations in both samples. The quality of the N1s spectrum of the PVP25ox-A is considerably worse than in the case of other polymer-derived cokes due to a lower level of nitrogen.

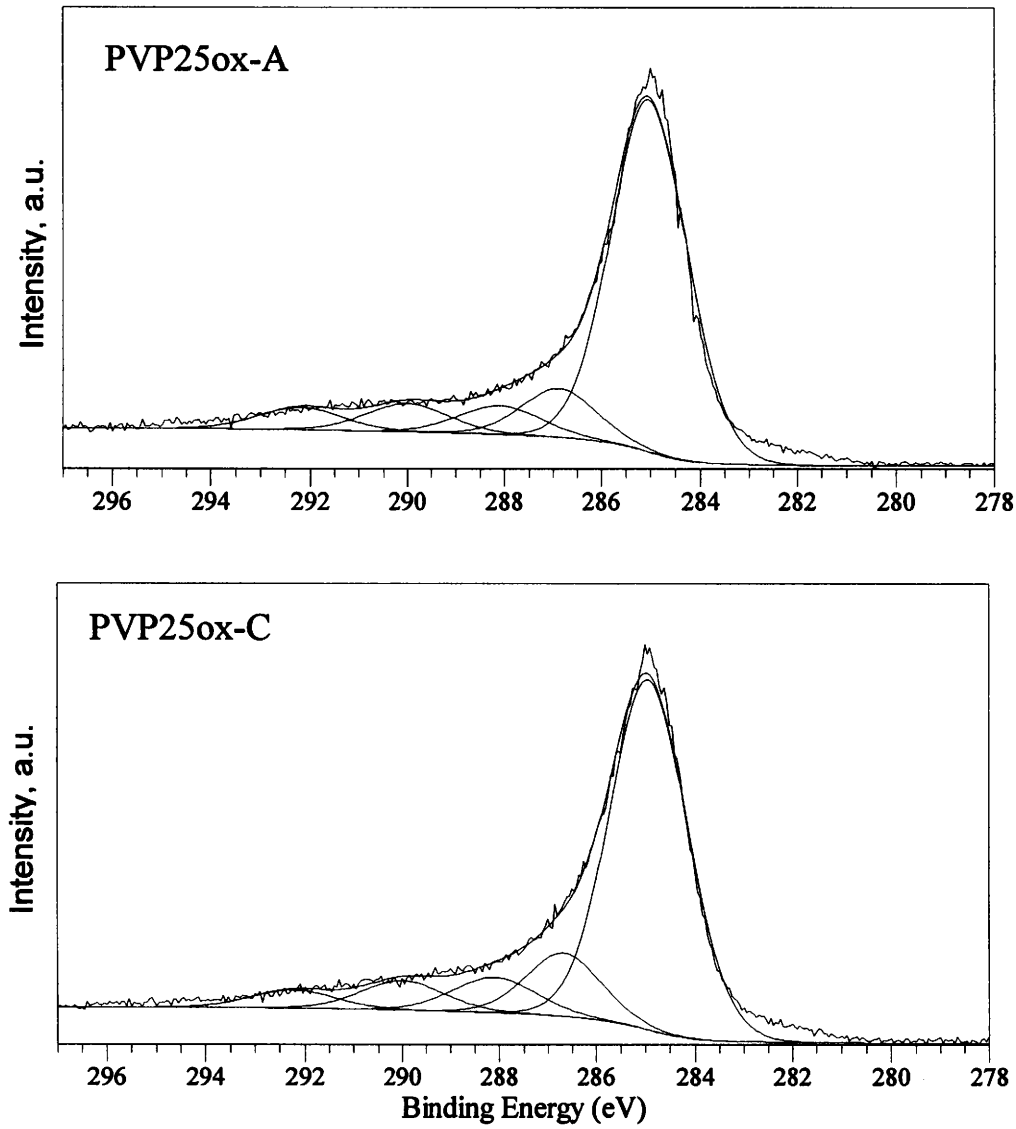

Fig. 88. C1s XPS spectra of carbonization (PVP25ox-C) and activation (PVP25ox-A) products derived from PVP25ox.

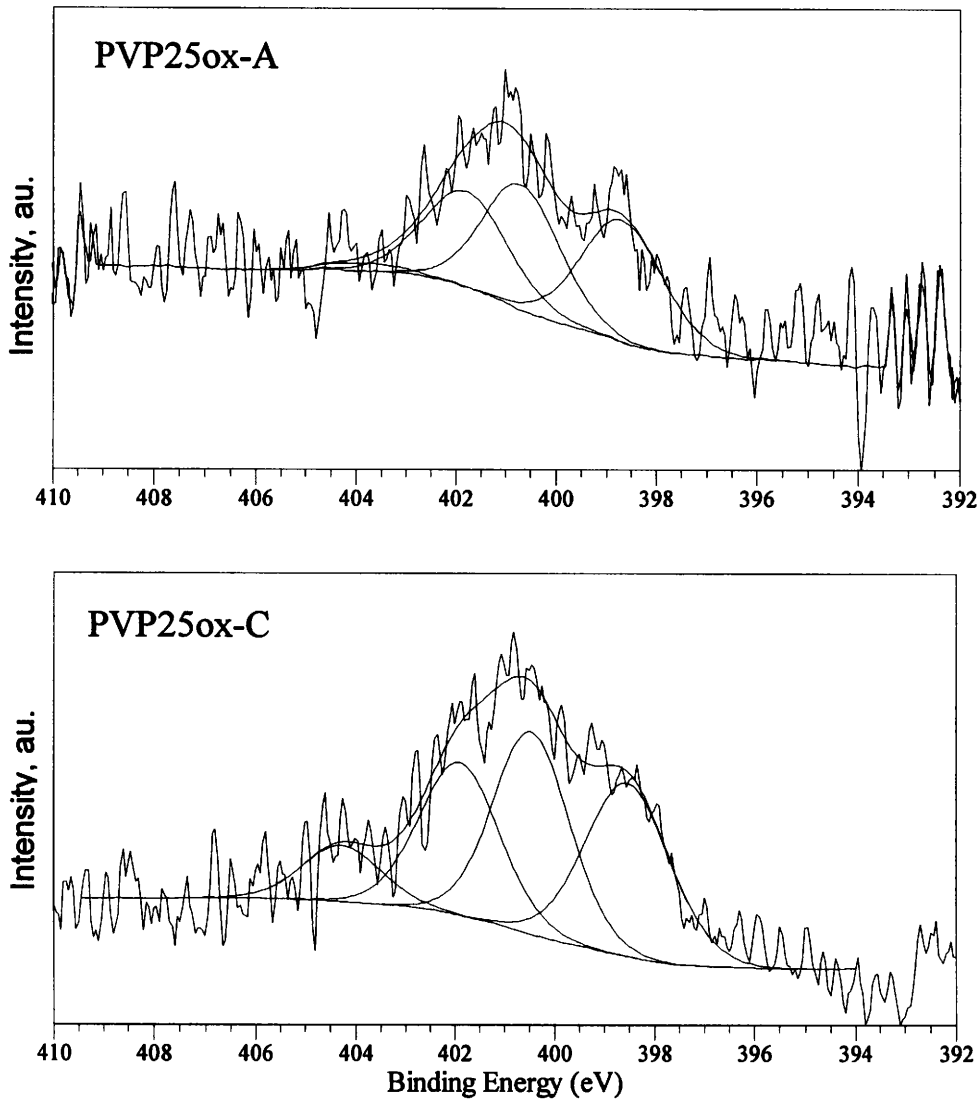

Fig. 89. N1s XPS spectra of carbonization (PVP25ox-C) and activation (PVP25ox-A) products derived from PVP25ox.

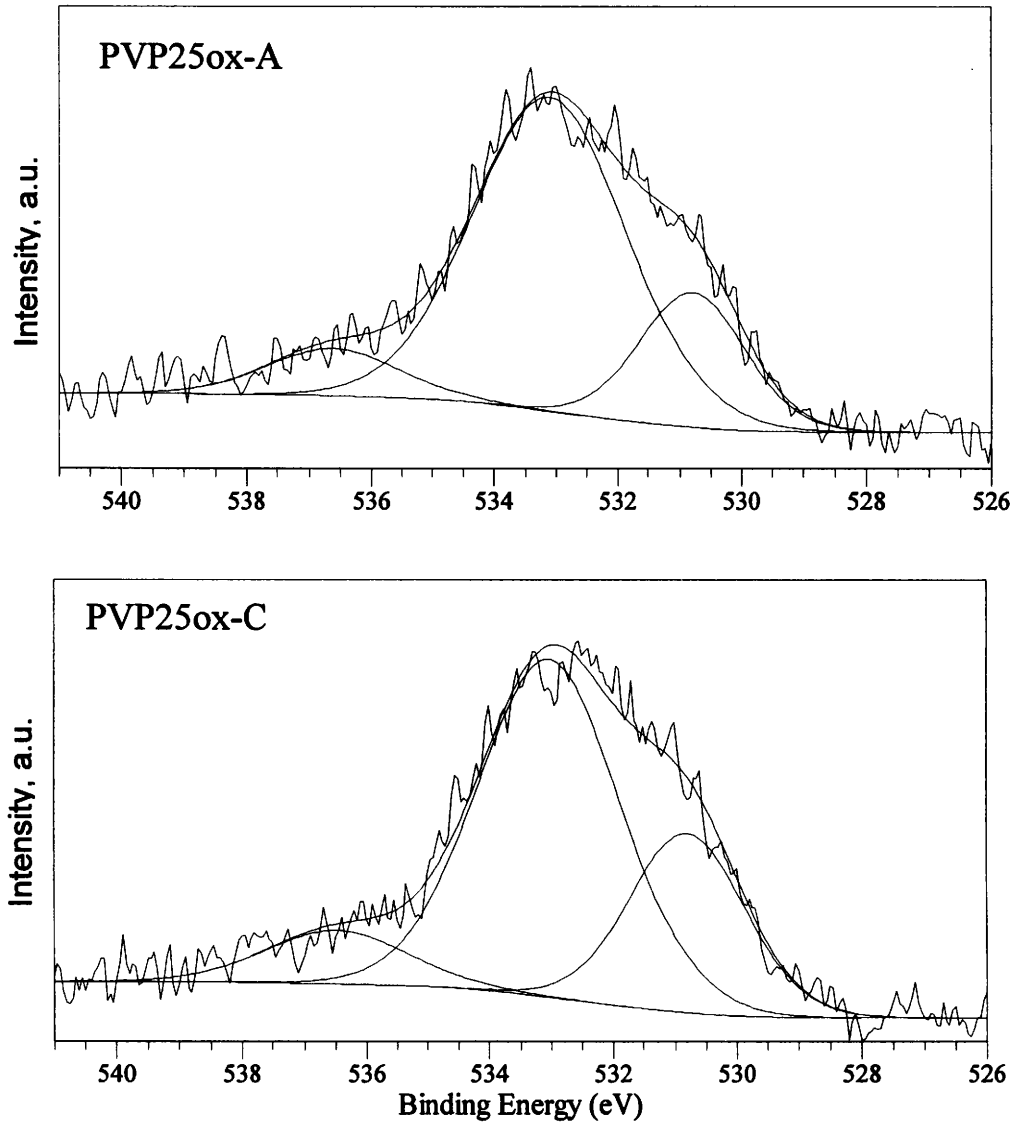

Fig. 90. O1s XPS spectra of carbonization (PVP25ox-C) and activation (PVP25ox-A) products derived from PVP25ox.

The surface composition of the carbonization and activation products of PAN and PVP25ox derived semi-cokes is presented in Table 29. In the case of nitrogen the data from XPS and elemental analysis are fairly consistent, so indicating rather homogeneous distribution of the element in the samples. There is no evidence of preferential gasification of nitrogen sites during activation.

Contrarily, except for PVP25ox-A, surface analysis gives considerably higher concentration of oxygen, thus supporting the view of enhanced sensitivity of nitrogen containing carbons to oxygen binding.

Table 28. Distribution of carbon, nitrogen and oxygen forms in carbonization and activation products derived from PAN and PVP25ox

Peak	BE	Possible	PAN -C	PAN -A	PVP25ox-C	PVP25ox-A
	eV	assignment	%	%	%	%
C1s	284.8±0.2	C-H, C-C	69.9	70.3	69.8	72.1
	286.7±0.4	C-OH, C-N, C=N	12.4	10.6	12.3	10.0
	287.8±0.3	C=O	8.5	7.9	7.6	6.5
	289.7±0.4	COO	5.5	6.7	6.4	6.4
	291.6±0.5	plasmon / π- π^* transitions	3.7	4.4	3.9	5.0
N1s	398.7±0.3	N-6	45.6	34.7	31.4	35.0
	400.3±0.3	N-5	20.9	28.3	32.9	34.0
	401.4±0.5	N-Q	26.7	25.2	26.4	28.9
	402-405	N-X	6.8	10.0	9.3	2.1
O1s	530.6±0.2	C=O	25.0	35.8	27.0	20.7
	532.8±0.4	C-O-C, C-OH	60.9	52.0	63.0	70.2
	535.2±0.4	H_2O, O_2 adsorbed	14.1	12.2	10.0	9.1

Table 29. Elemental composition of the carbonization and activation products of PAN and PVP25ox determined by XPS

Sample	Atomic concentration[1]			Atomic ratios			
	C	N	O	N/C		O/C	
				XPS	El.An.	XPS	El.An.
PAN-C	82.3	10.5	7.2	0.127	0.153	0.088	0.035
PAN-A	85.5	7.3	7.2	0.084	0.076	0.085	0.055
PVP25ox-C	87.2	4.2	8.6	0.047	0.052	0.099	0.043
PVP25ox-A	92.6	1.6	5.8	0.017	0.021	0.063	0.060

[1] C + N + O = 100%

5.5.2. Structural evolution of nitrogen enriched carbonaceous materials produced by ammoxidation of pitch-derived materials

5.5.2.1. Weight loss behavior

Figs. 91-93 present TG/DTG curves obtained during the heat-treatment of ammoxidation products derived from semi-coke (PS-Am), oxidized semi-coke (PSox-Am) and oxidized mesophase (PMox-Am), respectively.

The TG/DTG curves are fairly similar for the materials. A sharp peak observed on the DTG curves near 100°C can be attributed to 1-2% weight loss due to desorption of water. The major weight loss resulting from the thermal degradation of ammoxidized materials occurs in all cases over a wide temperature interval. Specific of a given sample are temperatures of initial and maximum weight loss and the final weight loss (Table 30). No plateau in TG curve is attained even at the maximum temperature of the experiments (900°C). As expected, the PMox-Am is distinguished by the lowest thermal stability as indicated by the beginning of weight loss already at 250°C. The preoxidation seems to result in a reduced temperature of the maximum weight loss rate (630°C) and the enhanced total weight loss (near 15 wt%) compared to the unoxidized semi-coke (725°C and 10.6 wt%, respectively). These results suggest that less stable functionalities are generated by the ammoxidation of preoxidized samples.

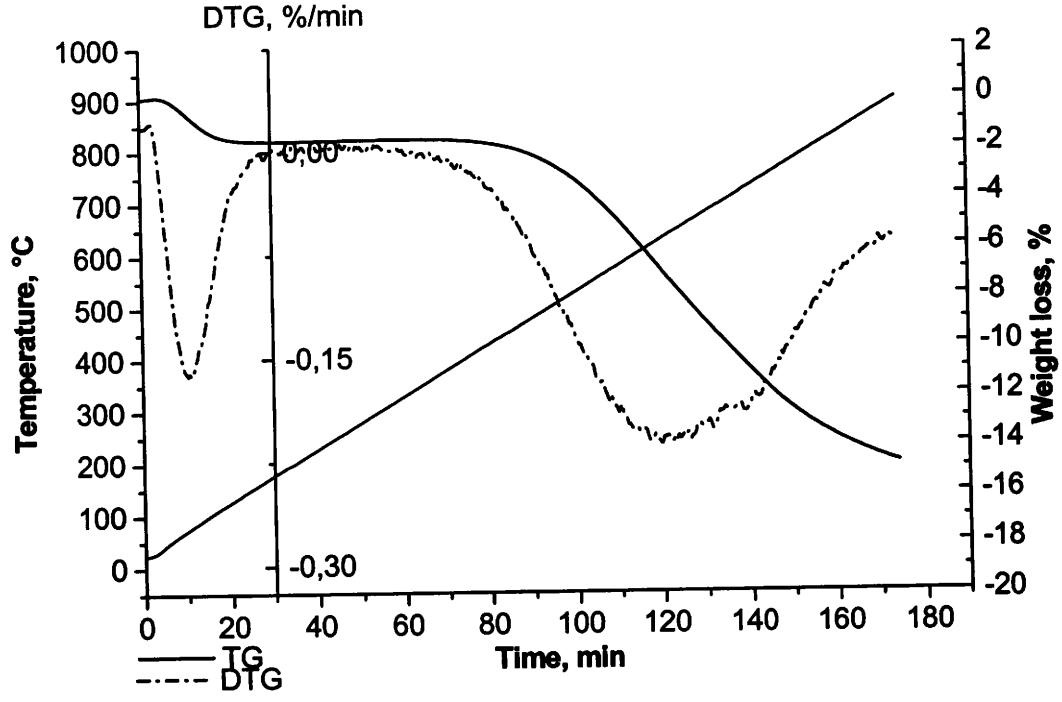

Fig. 91. TG/DTG profiles of PS-Am.

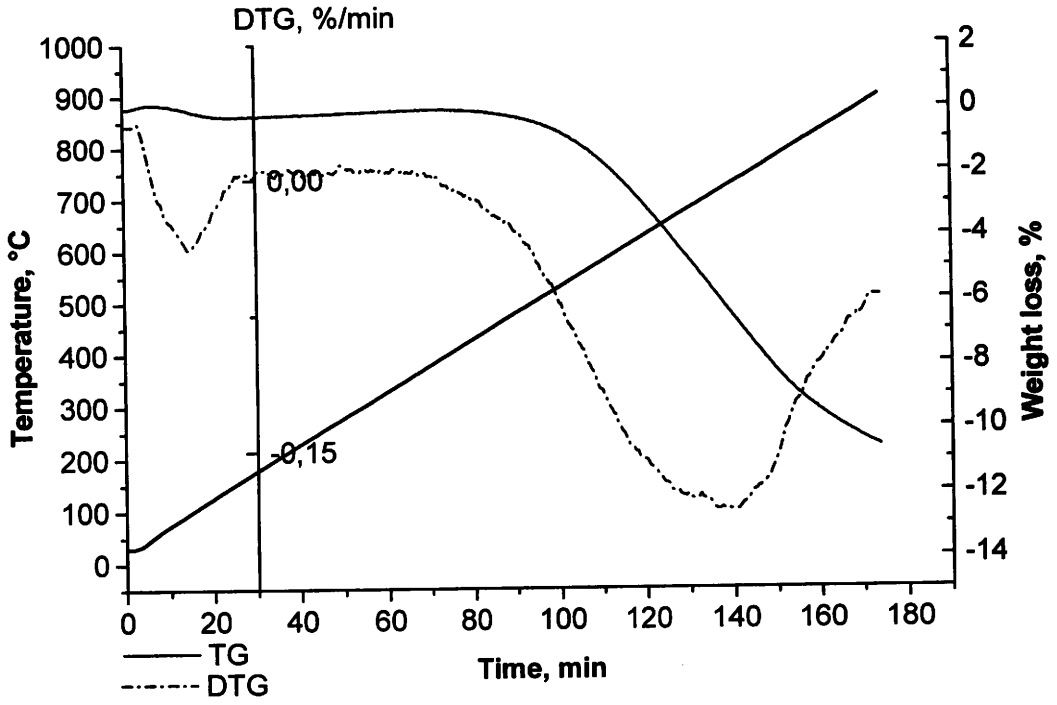

Fig. 92. TG/DTG profiles of PSox-Am.

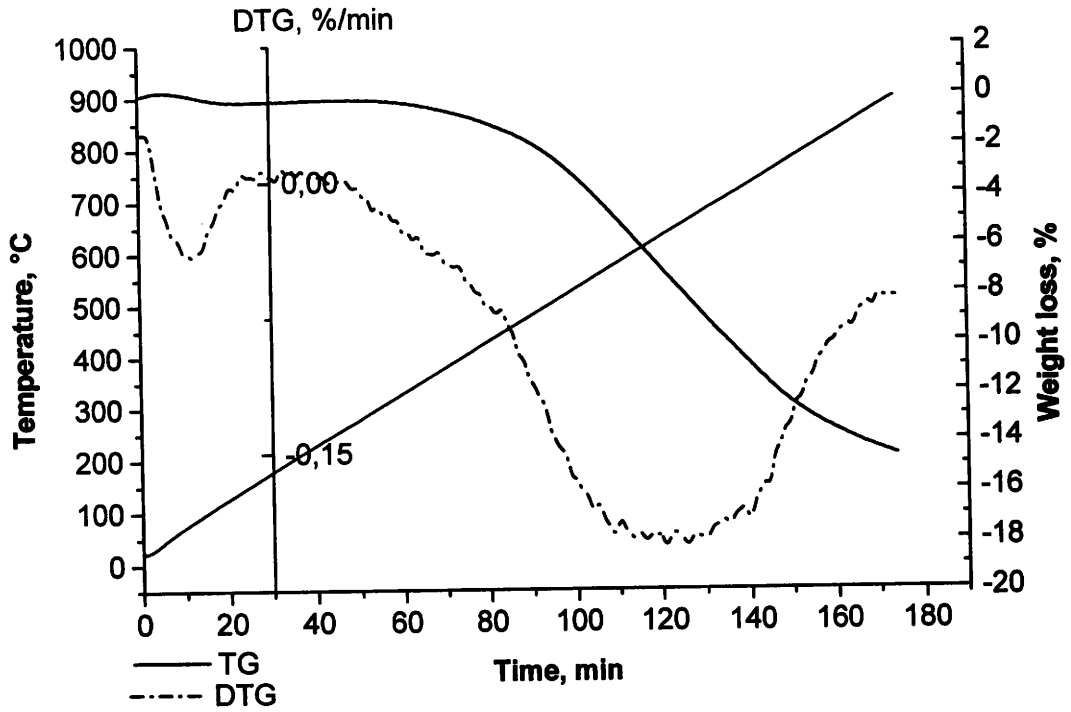

Fig. 93. TG/DTG profiles of PMox-Am.

Table 30. Thermal decomposition characteristics of the ammoxidized samples

Sample	Onset of the thermal degradation ^0C	T_{max}[1] ^0C	Weight loss at 900^0C wt%
PS-Am	390	725	10.6
PSox-Am	325	625	14.8
PMox-Am	250	630	14.6

[1]Temperature of the maximum volatile evolution rate

The gaseous species evolved during the heat-treatment of the ammoxidized samples were identified with the TGA-FTIR technique. Evolution patterns of the gases evolving in the temperature range 30-900^0C are presented in Figs 94-96. The evolution of HCN, NH_3 and CO commences above 400^0C. Hydrogen cyanide is the major degradation product accounting for the weight loss at relatively high temperatures with a maximum centered above 700^0C. The shape and intensity of the HCN peak is very similar in the analyzed samples. The peak evolution of NH_3, the other nitrogen-bearing gas precedes that of HCN by about 100^0C (Table 31). PS-Am produces less ammonia than the ammoxidation products of preoxidized materials (Table 32).

CO is a minor gaseous by-product accompanying the heat treatment of the ammoxidized samples.

As in the case of pitch-polymer blends (Chapter 5.5.1) the release of CO_2 on the heat-treatment of ammoxidized materials starts at low temperature (50^0C) and occurs over the very wide temperature range. It seems that all factors discussed previously should be considered here as contributing to the big absorption.

Characteristic of PS-Am is that the release of the analyzed gases is shifted to a higher by about 30-50^0C temperature compared to PSox-Am and PMox-Am. This clearly proves that the pretreatment with HNO_3 reduces the thermal stability of surface groups introduced by ammoxidation.

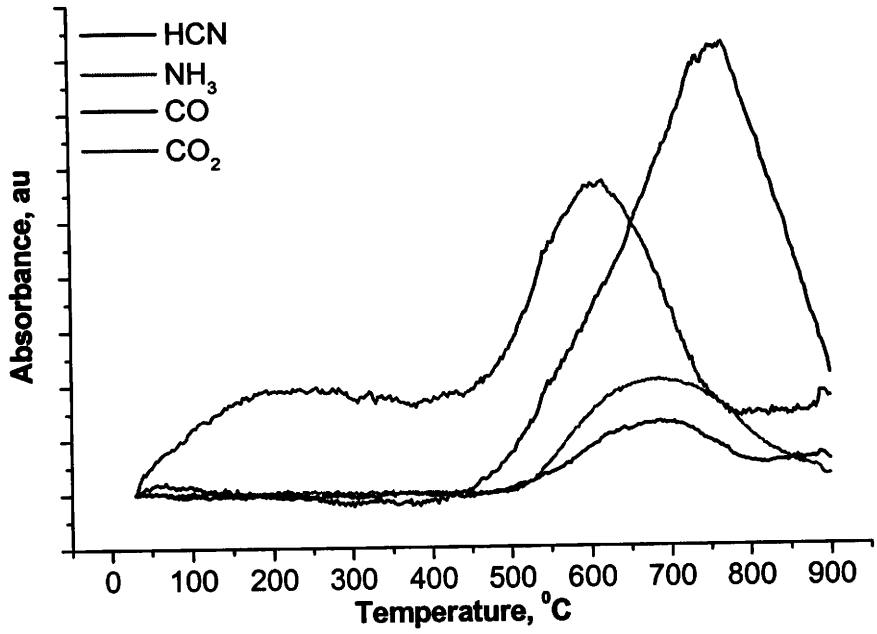

Fig. 94. Evolution of gases on heat-treatment of ammoxidized semi-coke PS-Am.

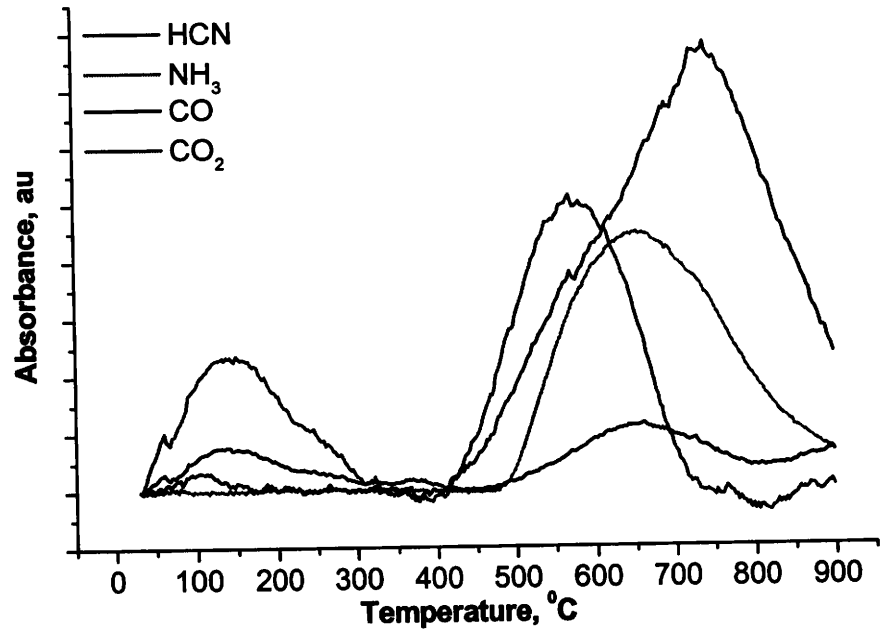

Fig. 95. Evolution of gases on heat-treatment of ammoxidized semi-coke PSox-Am.

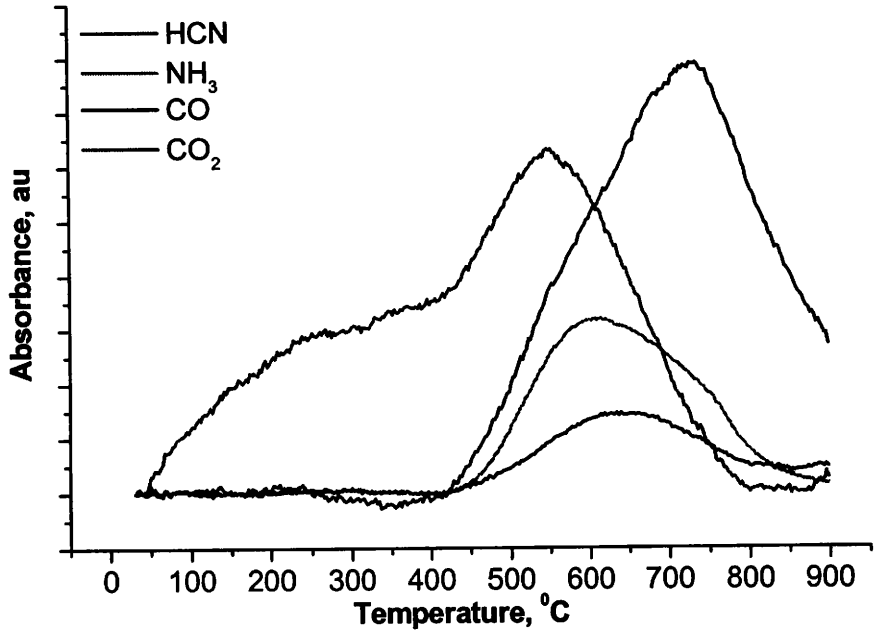

Fig. 96. Evolution of gases on heat-treatment of ammoxidized mesophase PMox-Am.

Table 31. Temperature of the maximum evolution rate of gaseous products on the thermal treatment of the ammoxidized samples

Sample	Temperature of the maximum evolution, ^{0}C			
	CO_2	CO	HCN	NH_3
PS-Am	615	690	770	685
PSox-Am	140 , 570	135 , 650	740	650
PMox-Am	547	638	735	615

Table 32. Relative signal intensities of the evolved gases determined based on the peak areas

Sample	Relative peak area[1]			
	S_{CO2}	S_{CO}	S_{HCN}	S_{NH3}
PS-Am	0.43	0.07	0.40	0.10
PSox-Am	0.31	0.09	0.39	0.21
PMox-Am	0.41	0.07	0.39	0.13

[1] $S_{CO2}+ S_{CO}+ S_{NH3}+ S_{aliphatics}=1$

Carbonization and activation of the carbonaceous materials produced by ammoxidation of pitch-derived products

The procedure applied in the carbonization runs of ammoxidation products is that described in the previous chapter (5.5.1). Data presented in Table 33 show that the burn-off level attained in the experiments varies from 40 wt% for PSox-Am to near 50 wt% for PS-Am. The evaluation of the reactivity towards steam from the activation time is in this situation doubtful.

The highest weight loss on the carbonization was measured for the ammoxidized mesophase, what is no a surprise when keeping in mind a lower temperature of heat-treatment (430^{0}C) during the sample preparation.

Table 33. Characteristics of the carbonization and activation process of the ammoxidized samples

Sample	Weight loss on carbonization 800°C wt%	Time of activation h	Burn-off on activation wt%
PS-Am	12.8	5.2	49.0
PSox-Am	10.6	1.2	40.0
PMox-Am	15.0	2.7	45.0

Elemental composition of the carbonization and activation products of the ammoxidized precursors

Results of the elemental analyses for the carbonization and activation products are given in Table 34.

Strong water sorption properties of the analyzed materials generate a serious problem in a proper determination of elemental composition. All the samples were dried to a constant weight before the analysis, however, some amount of water could be adsorbed during operations preceding the measurement. The determinations most affected by the presence of moisture are hydrogen content (overestimated) and carbon content (underestimated) and the oxygen content as calculated by difference. The measured value of nitrogen content is regarded as correct within the normal analysis error limit.

According to our knowledge the hydrogen content above 1 wt% is excessive for the conventional carbonaceous material heat-treated at 800^{0}C. On the other hand the strong hydrophilic sites in association with large surface area can generate an enhanced hydrogen content as specific of a given material.

Both the ammoxidized precursors which are oxidized with the nitric acid display similar stability of nitrogen functionalities on the carbonization treatment (loss of about 40 wt% of nitrogen), whilst less stable is the semi-coke PS-Am, loosing about 50% of the initial nitrogen. The thermal treatment in the oxidative conditions is accompanied by a considerably higher loss of nitrogen as compared to the treatment in an inert atmosphere. The drastic reduction of nitrogen content during the activation can be explained by the location of nitrogen groups mostly at the outer surface of particles, which is most exposed to the gasification. It is also possible that nitrogen atoms constitute active sites being preferentially gasified with steam.

The ammoxidized materials loose on the thermal treatment noticeably bigger proportion of nitrogen than N-semicokes derived from the polymer-pitch blends. This different behavior can be explained by a lower thermal stability of the non-cyclic nitrogen functionalities, which comprise a significant part of the introduced nitrogen.

Table 34. Elemental composition of the carbonization and activation products of ammoxidized materials

Sample	Elemental composition, wt%					$(N/C)_{at}$
	C	H	N	S	O[1]	
PS-C	95.12	0.74	4.05	0.20	0.11	0.036
PS-A	94.43	0.77	1.26	0.14	3.40	0.011
PSox-C	90.15	1.59	5.00	0.16	3.10	0.048
PSox-A	93.77	0.83	2.58	0.11	2.71	0.024
PMox-C	88.22	1.48	5.71	0.25	4.34	0.056
PMox-A	93.27	0.69	1.68	0.20	4.16	0.015

[1]By difference

X-ray photoelectron spectroscopy

Surface elemental composition for the carbonization and activation products of the ammoxidized precursors is presented in Table 35. The data are consistent with

elemental analysis results in terms of strongly reduced nitrogen content in the activated materials compared to those heat-treated in an inert atmosphere. The nitrogen content decreases with the extent of burn-off. There are no meaningful differences in the surface oxygen proportion between carbonized and activated materials. Comparable N/C atomic ratios determined by XPS and elemental analysis suggest rather uniform distribution of the element in the bulk of particles of materials derived from preoxidized precursors.

Contrarily, a large discrepancy between the values observed for the PS-Am derived materials indicates that nitrogen is concentrated mostly in the outer surface layers. A similar effect of oxidation with nitric acid was already noticed for the ammoxidation products (Chapter 5.4.4).

Table 35. Elemental composition of the carbonization and activation products from ammoxidized precursors determined by XPS

Sample	Atomic concentration[1]			Atomic ratios			
	C	N	O	N/C		O/C	
				XPS	El.An.	XPS	El.An.
PS-C	90.1	5.8	4.1	0.064	0.036	0.046	0.009
PS-A	93.2	2.2	4.6	0.029	0.011	0.050	0.027
PSox-C	90.8	4.4	4.7	0.048	0.048	0.052	0.026
PSox-A	92.9	2.7	4.4	0.029	0.024	0.047	0.021
PMox-C	90.5	4.9	4.5	0.054	0.056	0.050	0.039
PMox-A	93.8	2.3	3.9	0.024	0.015	0.041	0.033

The C1s, N1s and O1s XPS spectra of the carbonization products of the ammoxidized materials are presented in Figs 97-99, respectively. The distribution of the different functional groups in the carbonized samples is shown in Table 36.

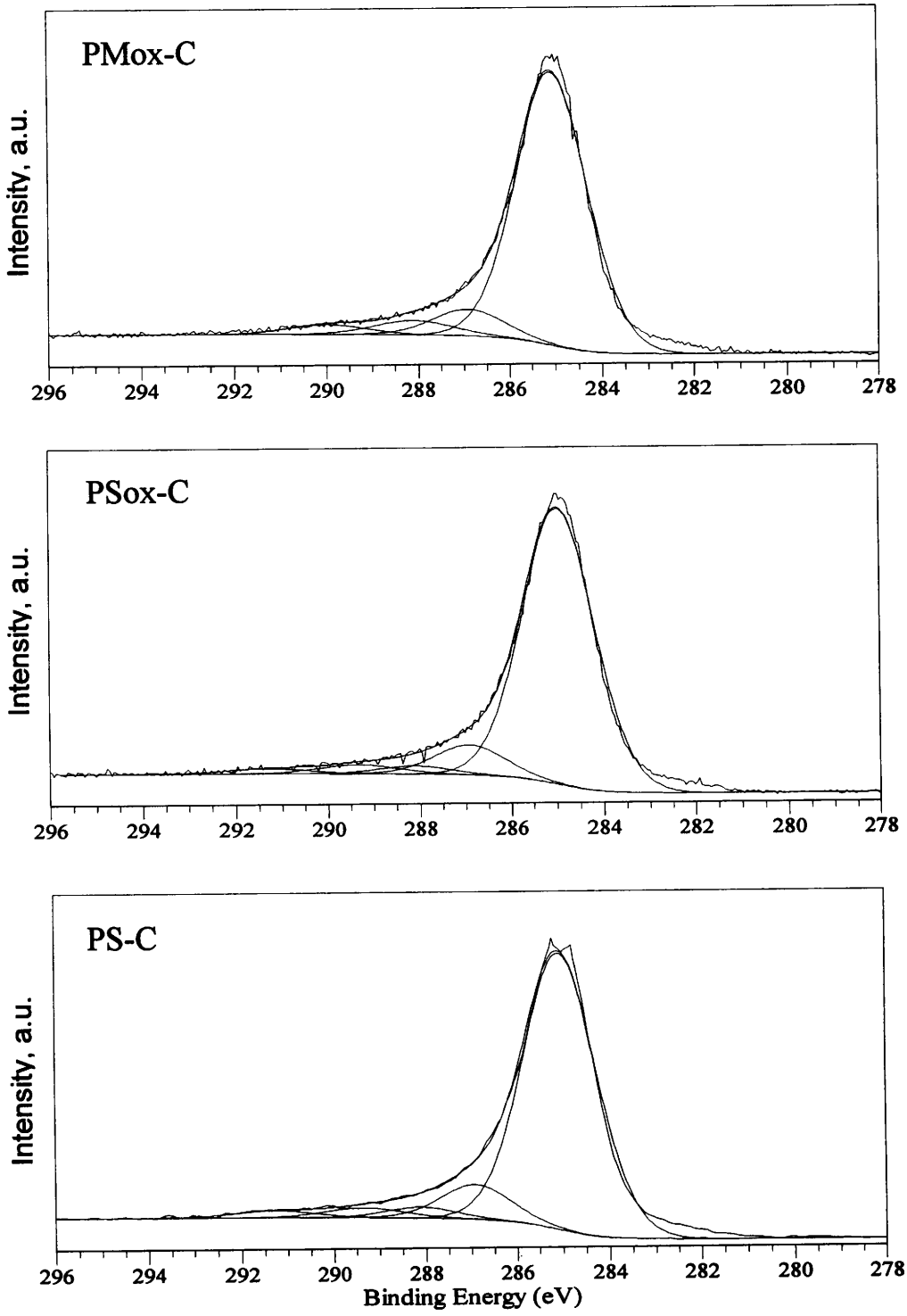

Fig. 97. C1s XPS spectra of the carbonization (800^{0}C) products derived from ammoxidized materials.

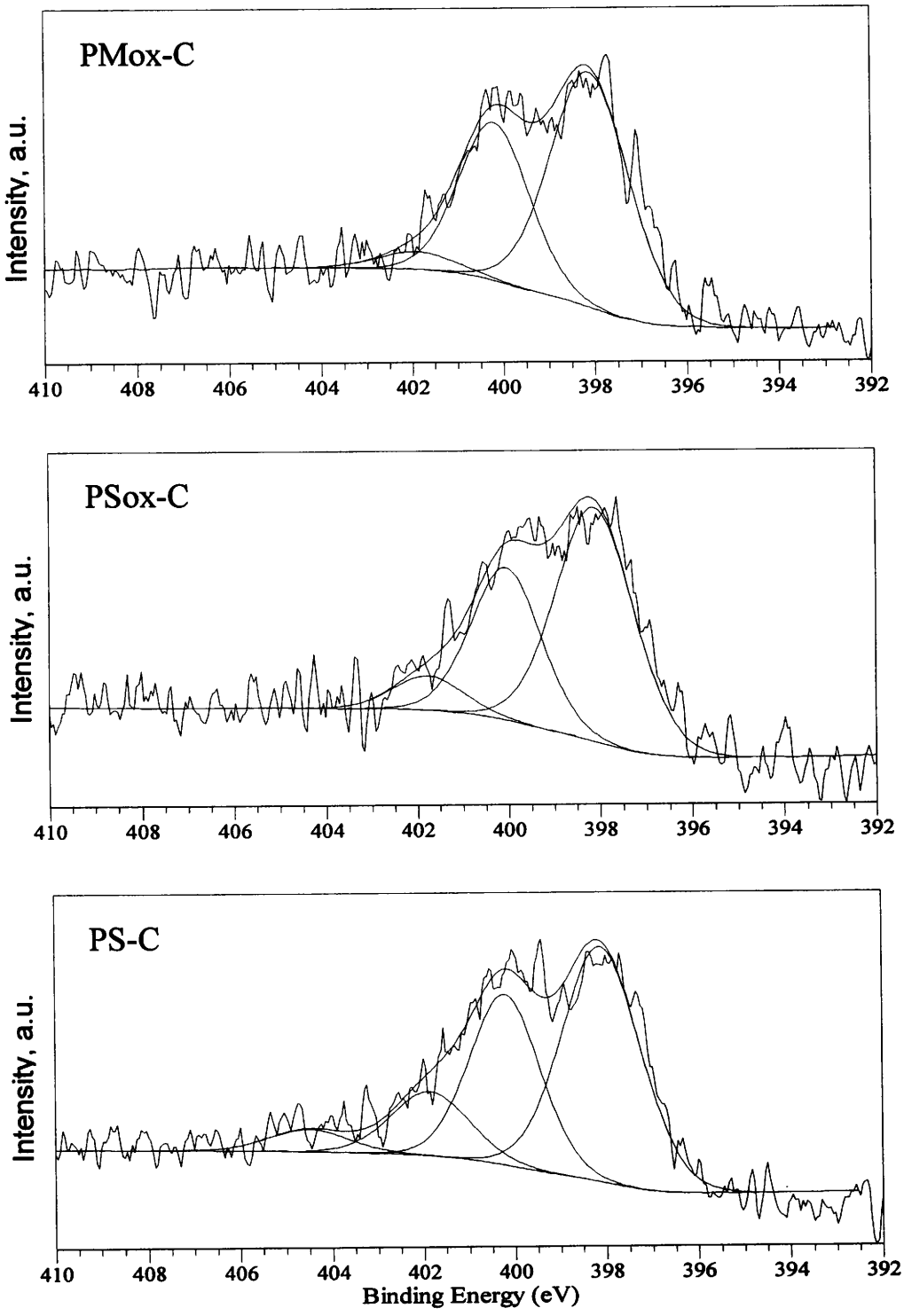

Fig. 98. N1s XPS spectra of the carbonization (800^{0}C) products derived from ammoxidized materials.

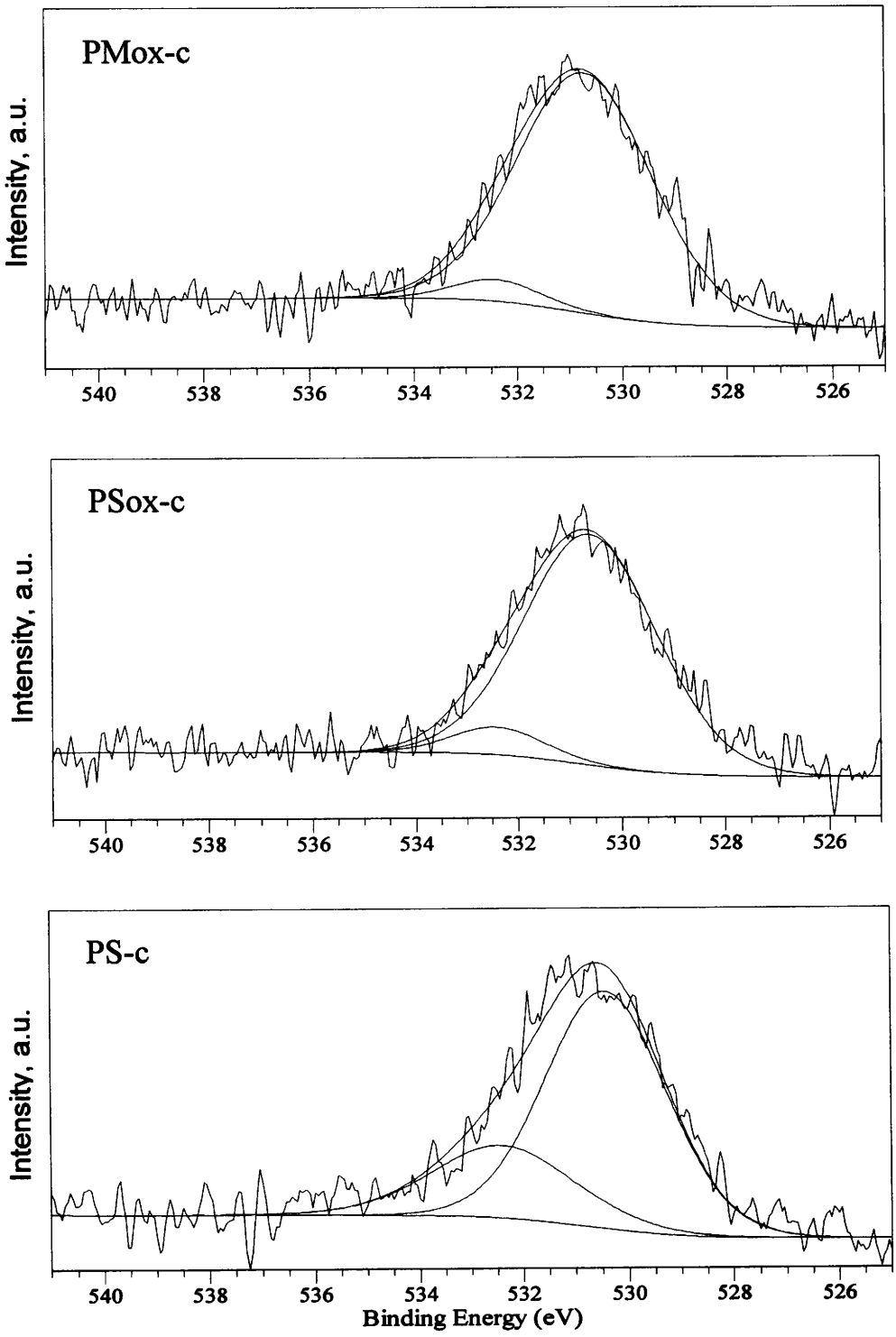

Fig. 99. O1s XPS spectra of the carbonization (800^{0}C) products derived from ammoxidized materials.

Table 36. Distribution of carbon, nitrogen and oxygen forms in carbonization products derived from ammoxidized materials

Peak	BE	Possible assignment	PS-C	PSox-C	PMox-C
	eV		%	%	%
C1s	284.8±0.2	C-H, C-C	81.5	83.9	83.9
	286.7±0.4	C-OH, C-N, C=N	9.9	9.0	8.0
	287.8±0.3	C=O	3.1	2.4	4.8
	289.7±0.4	COO	3.2	3.0	3.3
	291.6±0.5	plasmon / π- π* transitions	2.3	1.8	0
N1s	398.7±0.3	N-6	49.5	58.2	59.6
	400.3±0.3	N-5	32.4	34.2	36.0
	401.4±0.5	N-Q	13.4	7.6	4.4
	402-405	N-X	4.7	0	0
O1s	530.6±0.2	C=O	73.2	92.3	94.4
	532.8±0.4	C-O-C, C-OH	26.8	7.7	5.6

There is no meaningful difference in the C1s spectra of the carbonized materials. The graphitic component constitutes above 80% of the total surface carbon with a somewhat higher contribution of the oxidized carbon in PS-C.

The common effect of the treatment is a slight increase in the concentration of the graphitic component as compared to the precursors.

The deconvolution of the N1s band (Fig. 98) indicates that the component present in the spectra of the ammoxidized precursors at about 399.7±0.2 eV, disappears completely during the treatment. It means the decomposition and/or conversion of amides, imides, nitriles or lactams to the thermally more stable pyridinic, pyridonic/pyrrolic and quaternary nitrogen. The pyridinic groups are the most common form of nitrogen in the materials and constitute 50-60% of the total nitrogen. The lower proportion of the pyridinic nitrogen in favor of the quaternary form (13% compared to 4-7% in other materials) is specific of PS-C. Pyrrolic/pyridonic nitrogen occurs at similar level 32-36% in all the studied materials.

The deconvolution of the O1s spectra (Fig. 99) reveals that most of the oxygen is bound in the form of the C=O groups in different chemical surroundings (ketone, quinone, carboxylic moieties).

The relative distribution of carbon and nitrogen functional groups in the carbonization products derived from different ammoxidized materials is presented in Fig. 100. Despite noticeably difference in the chemical composition of the ammoxidized precursors, the cokes from the carbonization at 800^0C present similar surface chemistry. It is in agreement with the results of Pels et al. (1995) showing that the XPS N1s spectra of the chars prepared at severe pyrolysis conditions are very similar and the distribution of the nitrogen functionalities in the parent materials are not relevant for the final distribution of the char bound nitrogen.

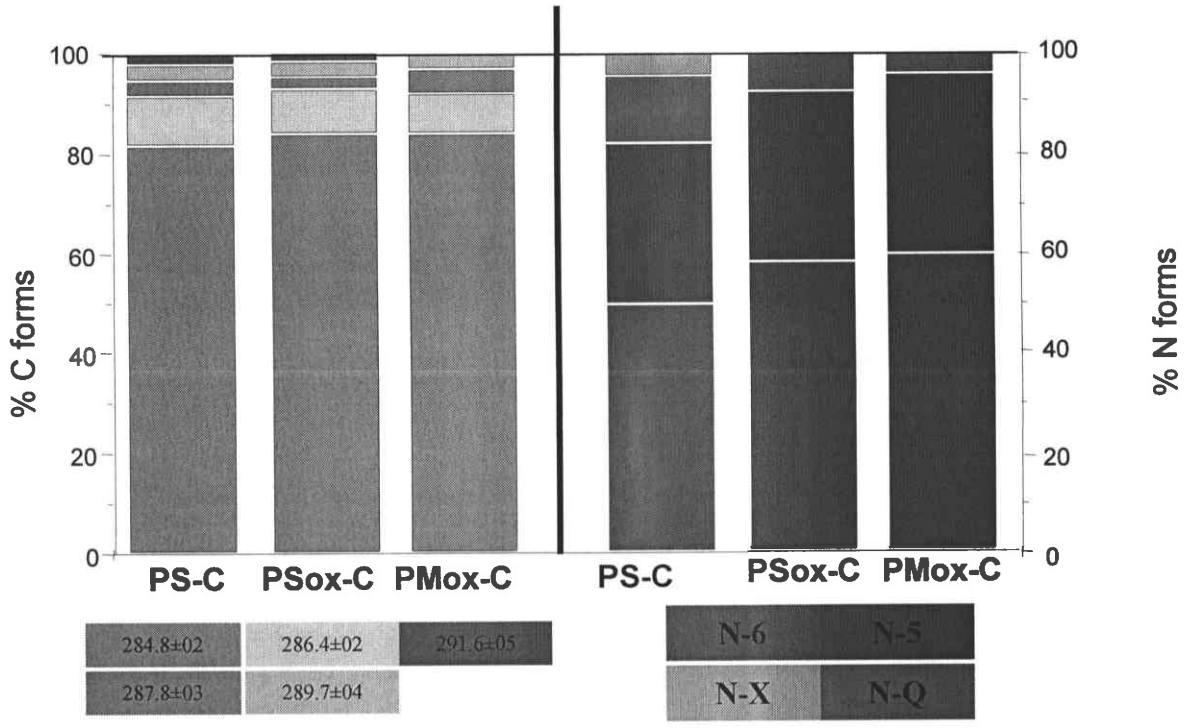

Fig. 100. Distribution of the carbon and nitrogen functionalities in the carbonization (800^0C) products derived from ammoxidized materials.

The C1s, N1s and O1s spectra of the activated carbons derived from the ammoxidized materials are presented in Figs 101-103. The relative distribution of carbon, nitrogen and oxygen functionalities is given in Table 37.

The oxidative treatment results in the diminution of the proportion of the graphitic carbon by 4-7% compared to the corresponding materials prepared under inert conditions. Instead, the activation gives rise to the formation of C-O functionalities what reflects in the somewhat enhanced intensity of the peaks at about 288 eV and 290 eV representing the carbon in carbonyl and carboxylic groups, respectively.

As can be concluded based on the shape of the N1s peaks (Fig. 102), the activation induces a significant change in the distribution of nitrogen functionalities of the ammoxidized samples. As in the case of the carbonization, the thermally unstable groups which are created on the ammoxidation, are fully decomposed or converted into more resistant forms.

Compared to the carbonization products, the corresponding activated carbons are characterized by lower by 20-28% pyridinic nitrogen concentration in favor of pyrrolic/pyridonic, N-oxide and quaternary forms. Apparently, the removal of nitrogen during the gasification with steam, as evidenced by elemental analysis, occurs via intermediate stage of the oxidized nitrogen form creation. The quaternary nitrogen constitutes from 18% (PSox-A) to 25-26% (PS-A, PMox-A).

The enhanced level of the N-Q form can be ascribed to the combined effect of the condensation of the graphene layers on thermal treatment, the conversion of N-5 form due to the decarboxylation of the pyridonic groups and ring extension of the pyrrolic form and the preferential gasification of nitrogen occurring at the edges of layers.

The fitting of the O1s spectra (Fig. 103) reveals that oxygen occurs mostly in the form of C=O groups. Characteristic of activated carbons compared to the carbonization produtcs is an enhanced proportion of oxygen singly bonded to the carbon atom (C-O-C, C-OH).

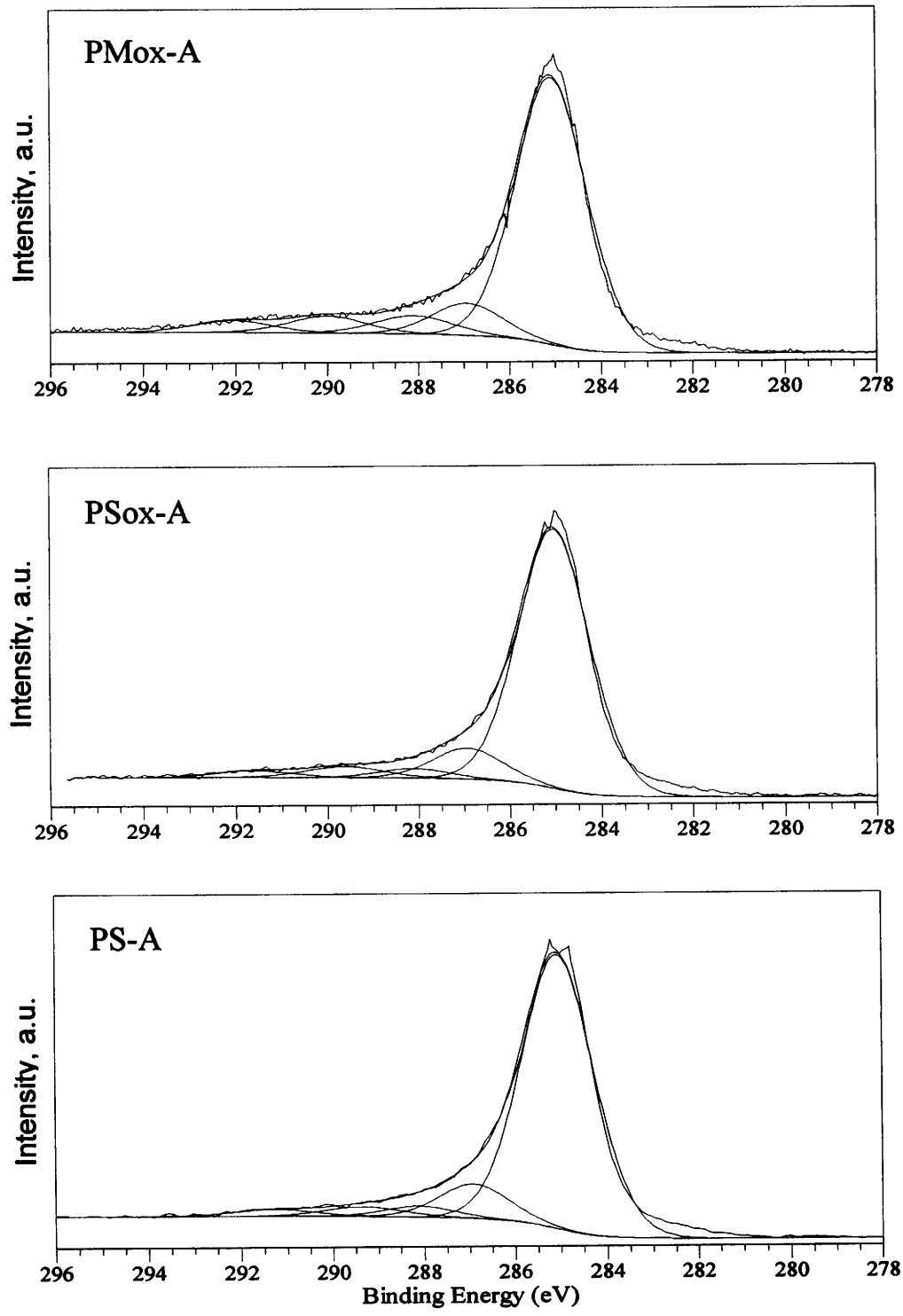

Fig. 101. C1s XPS spectra of the activated carbons derived from ammoxidized materials.

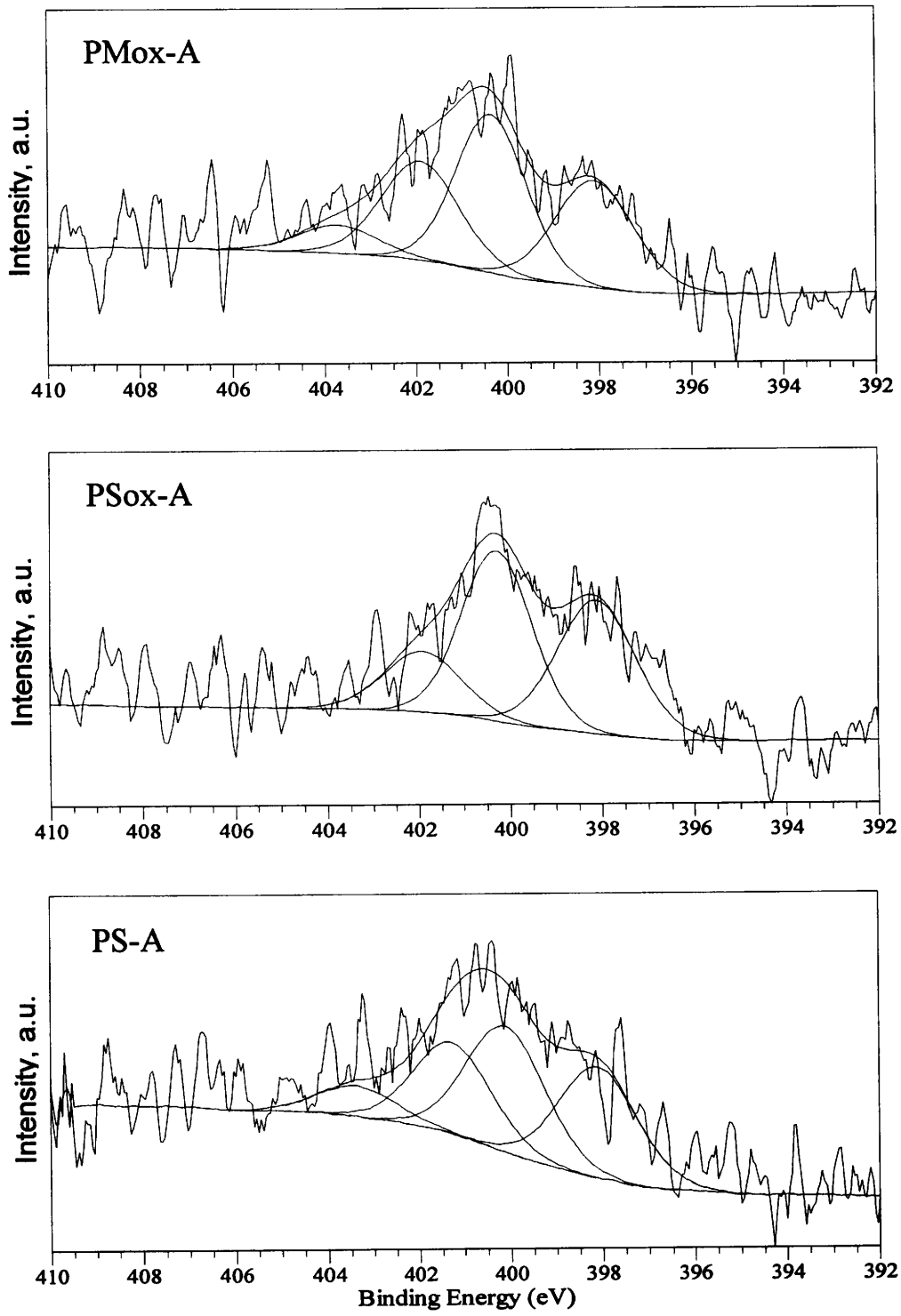

Fig 102. N1s XPS spectra of the activated carbons derived from ammoxidized materials.

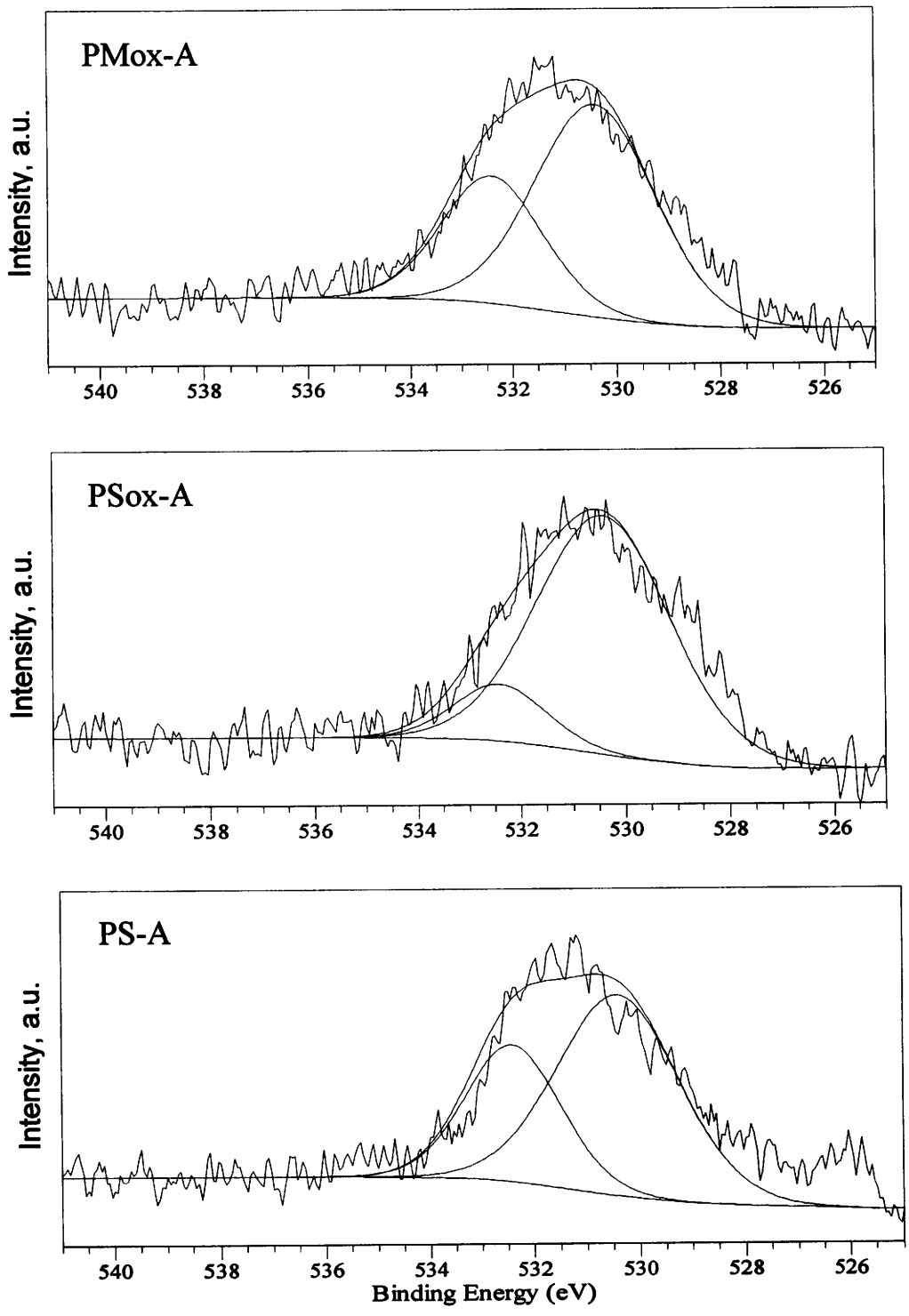

Fig. 103. O1s XPS spectra of the activated carbons derived from ammoxidized materials.

Table 37. Distribution of carbon, nitrogen and oxygen forms in activation products derived from ammoxidized samples

Peak	BE eV	Possible assignment	PS-A (%)	PSox-A (%)	PMox-A (%)
C1s	284.8±0.2	C-H, C-C	77.7	81.4	76.1
	286.7±0.4	C-OH, C-N, C=N	8.4	9.6	9.1
	287.8±0.3	C=O	5.5	3.0	5.7
	289.7±0.4	COO	4.8	3.8	5.3
	291.6±0.5	plasmon / π- π^* transitions	3.5	2.2	3.8
N1s	398.7±0.3	N-6	30.1	38.4	28.4
	400.3±0.3	N-5	35.1	44.1	37.9
	401.4±0.5	N-Q	25.4	17.5	26.3
	402-405	N-X	8.5	0	7.4
O1s	530.6±0.2	C=O	66.1	85.8	66.1
		C-O-C, C-OH	33.9	14.2	33.9

The distribution of carbon and nitrogen functional groups in the activated carbons derived from the ammoxidized materials is presented in Fig. 103. While the activated carbons PS-A and PMox-A show quite similar distribution of the occurring forms of carbon and nitrogen, the PSox-A is clearly distinguishable by an enhanced content of pyridinic and pyrrolic/pyridonic nitrogen at the expense of quaternary and N-oxide forms. It seems that the difference should be related rather to a lower extent of burn-off during the treatment with steam (40 wt% vs. 45 and 49 wt%) than any specific behavior of nitrogen forms created on ammoxidation of the preoxidized semi-coke.

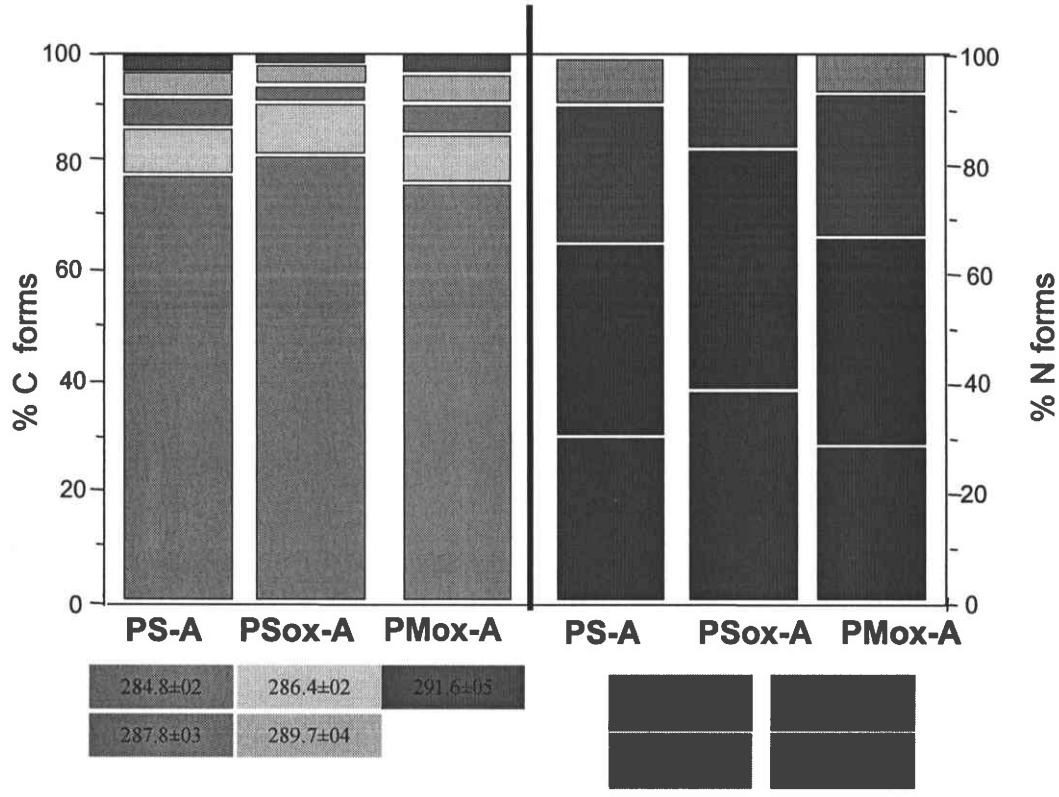

Fig. 104. Distribution of carbon and nitrogen functionalities in the activated carbons derived from ammoxidized materials.

5.6. Determination of surface properties of N-doped carbons

5.6.1. Porosity development in activation products

The nitrogen adsorption-desorption isotherms of activated carbons prepared from pitch-PAN blends are presented in Fig. 105. The porosity characteristics of the carbons are given in Table 38.

The variation of pore volume and BET surface area with PAN content in the parent blend is presented in Figs. 106 and 107, respectively. The produced activated carbons are characterized by a moderate extent of the porosity development at the 50 wt% burn-off level. The porosity, expressed by the total pore volume (V_T) and the BET surface area (S_{BET}) increases with the PAN proportion in the parent blend and reaches a maximum 0.346 cm^3/g and 832 m^2/g, respectively, for the activated carbon from 1:1 blend, next slightly decreases. All the produced activated carbons are microporous in character with the micropore contribution growing with polymer proportion in blend.

A noticeable adsorption /desorption hysteresis observable for CTP-PAN 9:1-A and CTP-PAN 3:1-A (Fig. 105) corresponds with a larger contribution of mesopores to the porous system in these activated carbons.

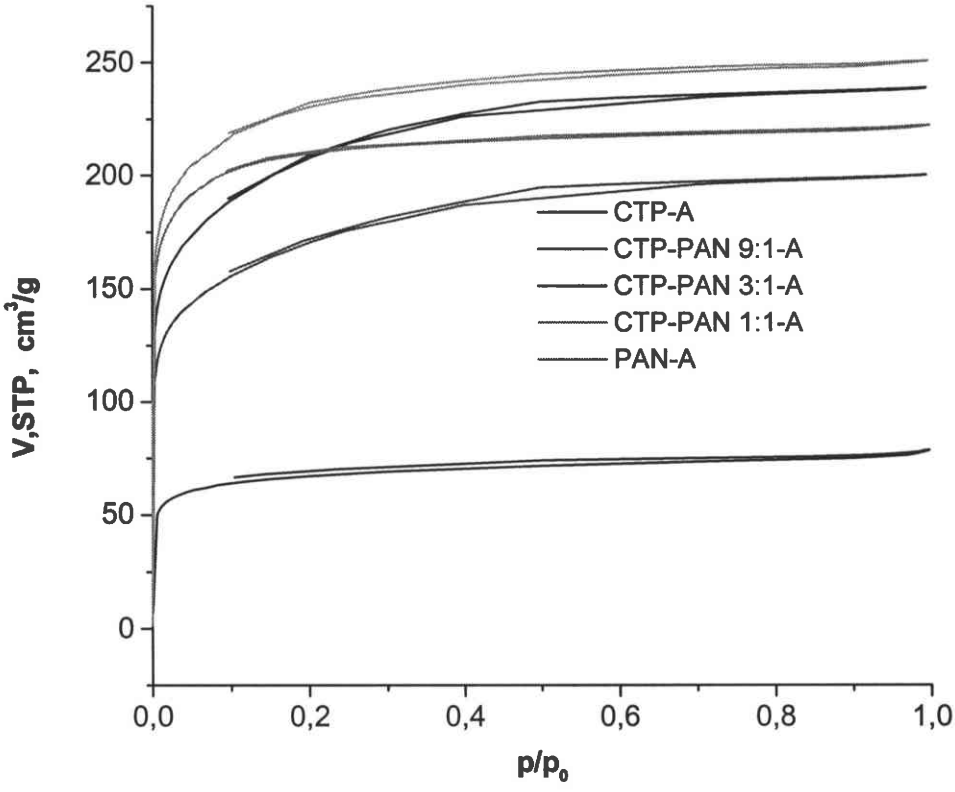

Fig. 105. Nitrogen adsorption isotherms of activated carbons derived from pitch-PAN blends.

Table 38. Porosity parameters of activated carbons prepared from pitch-PAN blends

Sample	Sorption of N_2 at 77K						
	Total pore volume V_T cm^3/g	Micropore volume V_{micro} cm^3/g	Micropore ratio %	Mesopore volume distribution cm^3/g			BET surface area S_{BET} m^2/g
				2-3 nm	3-5 nm	5-50 nm	
CTP-A	0.112	0.097	86.6	0.005	0.004	0.006	256.4
CTP-PAN 9:1-A	0.285	0.235	82.5	0.027	0.016	0.007	619.6
CTP-PAN 3:1-A	0.339	0.284	84.1	0.033	0.012	0.010	747.2
CTP-PAN 1:1-A	0.346	0.308	89.0	0.018	0.008	0.012	832.1
PAN-A	0.316	0.295	93.4	0.009	0.005	0.007	807.5

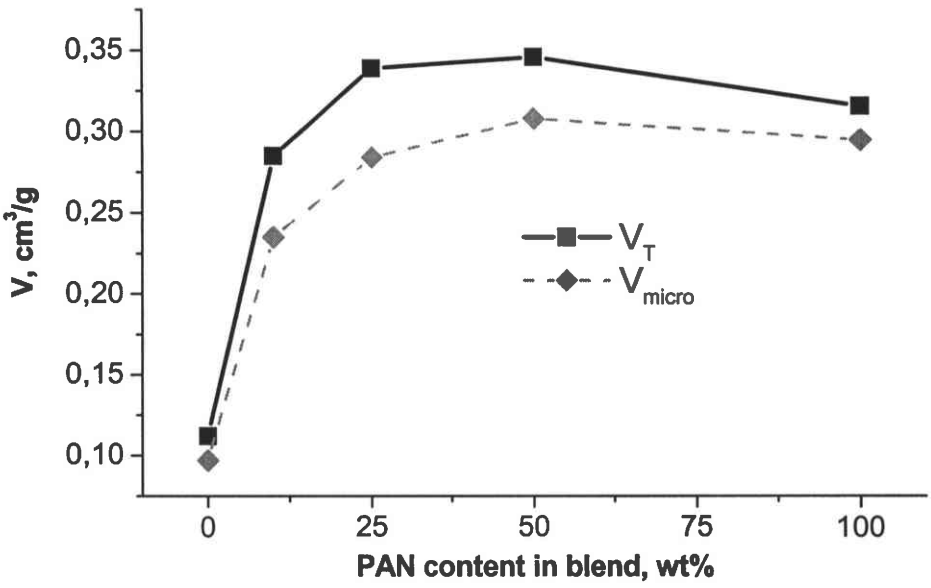

Fig. 106. Effect of the PAN addition to coal-tar pitch on the pore volume of the resultant activated carbons.

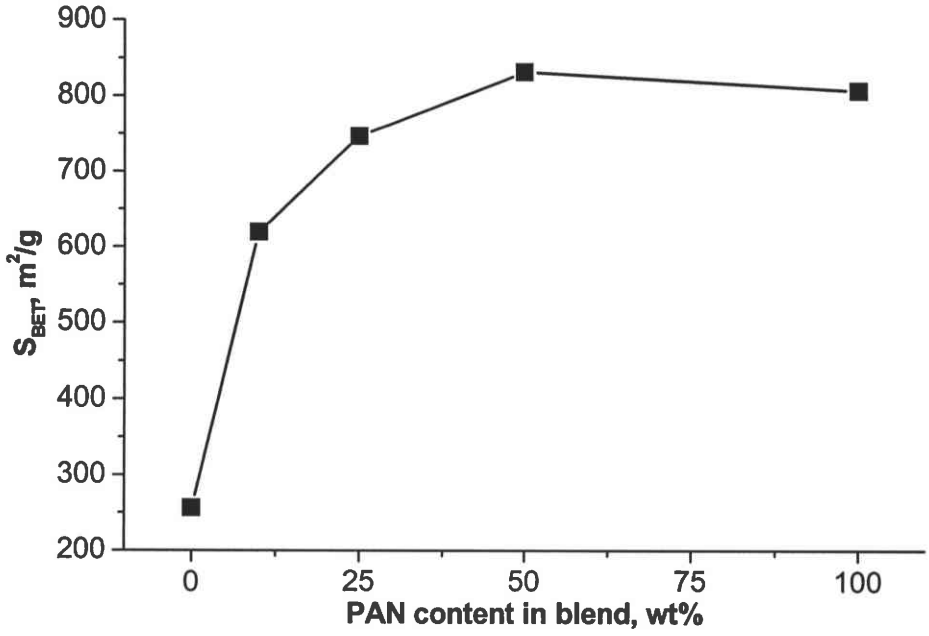

Fig. 107. Effect of the PAN addition to coal-tar pitch on the BET surface area of the resultant activated carbons.

The nitrogen adsorption/desorption isotherms of activated carbons prepared from pitch-PVP25ox blends are presented in Fig. 108.

The porosity characteristics of the activated carbons prepared from pitch-PVP25ox blends are presented in Table 39. The variation of pore volume and BET surface area with PVPox content in the parent blend is presented in Figs. 109 and 110, respectively.

The total pore volume, micropore volume and the surface area of the studied activated carbons increase linearly with the polymer content in blend. The activated carbon prepared from the pure PVP25ox reveals most developed porosity amongst all the materials studied (V_T = 0.567 m^3/g, S_{BET} = 1417 m^2/g). S_{BET} of the CTP-PVP25ox 1:1 activated carbon is slightly higher than the value determined for the corresponding pitch-PAN blend carbon. CTP-PVP25ox blends give essentially microporous carbons, with the contribution of mesopores ranging from 7% for PVP25ox -A to approximately 13% for other samples.

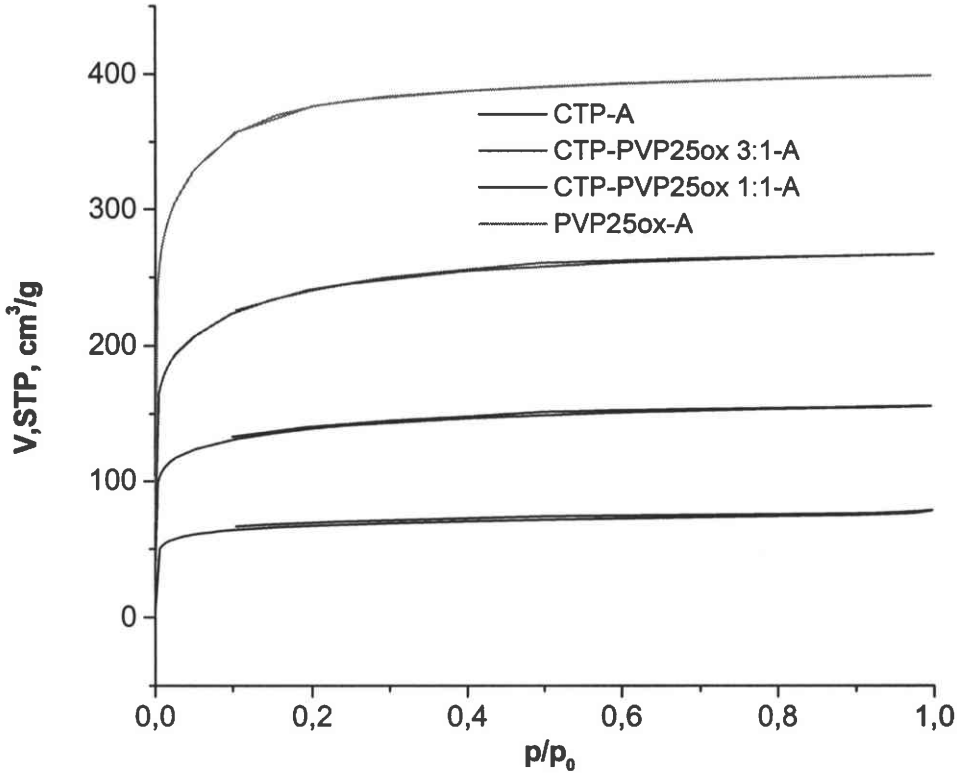

Fig. 108. Nitrogen adsorption isotherms of activated carbons derived from pitch-PVP25ox blends.

Table 39. Porosity parameters of activated carbons prepared from pitch-PVP25ox blends

Sample	Sorption of N_2 at 77K						
	Total pore volume V_T cm^3/g	Micropore volume V_{micro} cm^3/g	Micropore ratio %	Mesopore volume distribution cm^3/g			BET surface area S_{BET} m^2/g
				2-3 nm	3-5 nm	5-50 nm	
CTP-PVP25ox 3:1-A	0.222	0.195	87.8	0.013	0.009	0.005	518.5
CTP-PVP25ox 1:1-A	0.380	0.332	87.4	0.027	0.013	0.008	889.0
PVP25ox-A	0.567	0.525	92.6	0.027	0.010	0.005	1417.0

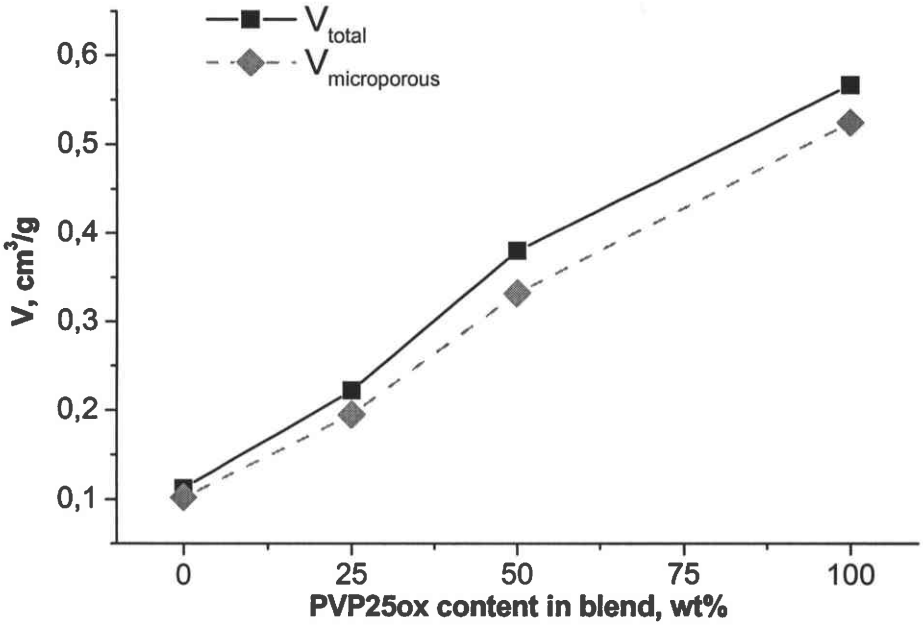

Fig. 109. Effect of the PVP25ox addition to coal-tar pitch on the pore volume of the resultant activated carbons.

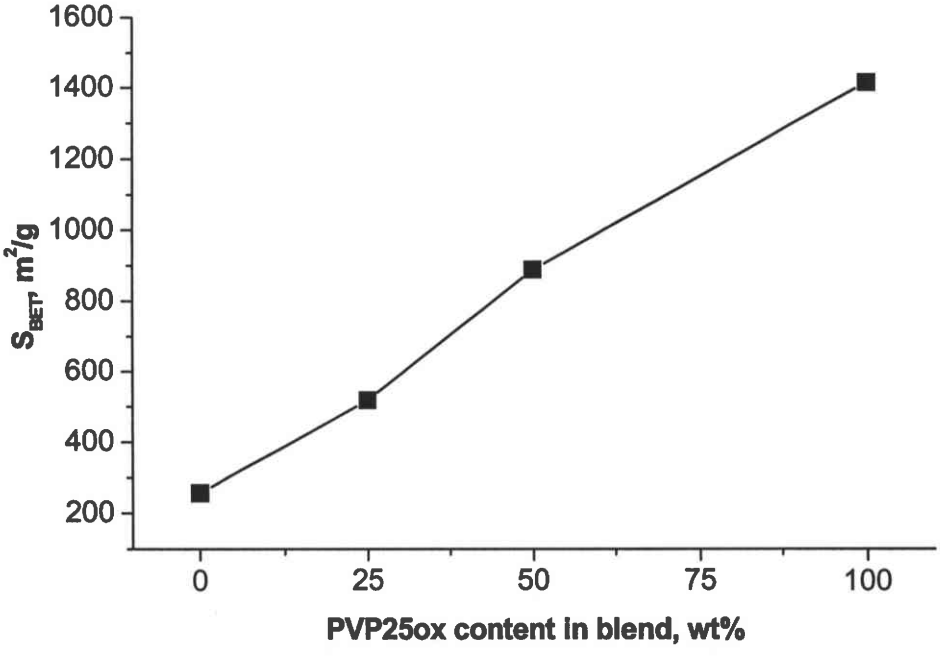

Fig. 110. Effect of the PVP25ox addition to coal-tar pitch on the BET surface area of the resultant activated carbons.

The nitrogen adsorption/desorption isotherms of activated carbons derived from the ammoxidized materials are presented in Fig. 111. The data characterizing the porosity of the carbons (Table 40) indicate a limited development of pores. The V_T and S_{BET} of both semi-coke derived products (PS-A and PSox-A) are close to the values measured for the activation product from the parent pitch semi-coke.

The activation of ammoxidized mesophase leads to near twice bigger both the total pore volume and surface area.

A series of ammoxidized carbons which is activated here represents a developed optical anisotropy, i.e. relatively high degree of structural ordering. The results show that in the case of ammoxidation of pitch semi-coke, the following gasification with steam occurs principally on the outer surface of particles. Preoxidation with nitric acid seems to open partially the access to the inner part of mesophase particles. A result is a larger extent of porosity development in the PMox-A. PSox-A is characterized by similar to PS-A the pore volume and surface area but at a considerably lower burn-off (40 and 49 wt.%, respectively). The ammoxidation of preoxidized mesophase seems to offer a possibility of preparing the activated carbon with moderately developed porosity while maintaining the ordering characteristic of optically anisotropic material.

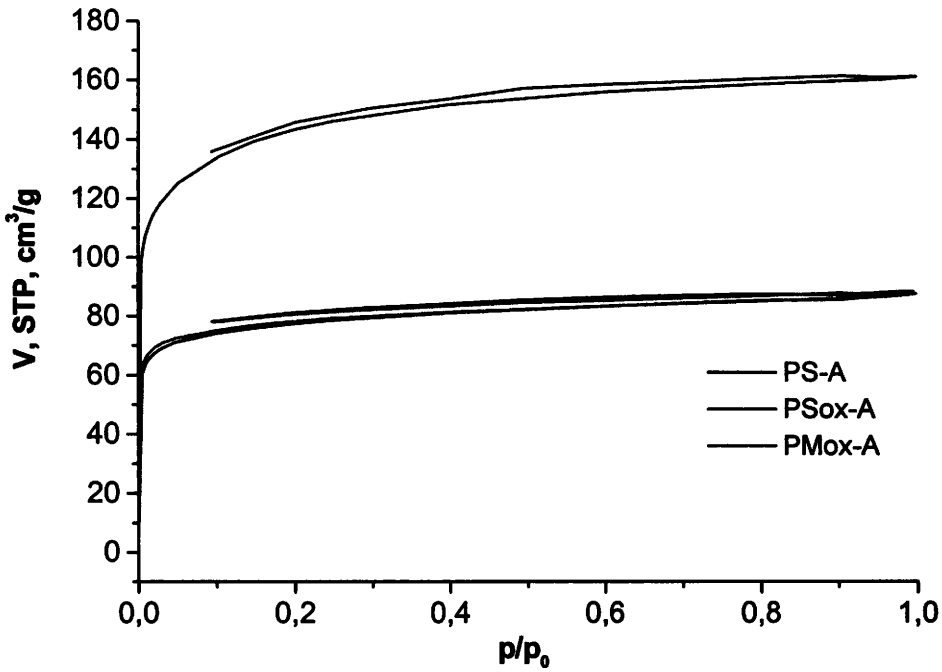

Fig. 111. Nitrogen adsorption isotherms of activated carbons derived from ammoxidized samples.

Table 40. Pore volume and surface area of the activated cokes derived from the ammoxidized precursors determined by gas adsorption

Sample	Sorption of N_2 at 77K						
	Total pore volume V_T cm^3/g	Micropore volume V_{micro} cm^3/g	Micropore ratio %	Mesopore volume distribution cm^3/g			BET surface area S_{BET} m^2/g
				2-3 nm	3-5 nm	5-50 nm	
PS-A	0.126	0.113	89.7	0.005	0.004	0.003	299.4
PSox-A	0.125	0.113	90.4	0.005	0.003	0.004	304.8
PMox-A	0.230	0.203	0.015	0.015	0.009	0.004	530.9

5.6.2. Polarity of nitrogen doped carbons

All the prepared materials show an unusual propensity to adsorb water when exposed to air. The water sorption ability could be therefore a rough indication of the polarity of the surface. To measure the values, the samples were dried at 105-110°C for 1 hour and next kept in an open air until constant weight to establish an equilibrium state at a given humidity of the environment. The relative weight uptake during the conditioning is regarded as the water sorption ability of a given material.

Table 41 contains the data on water sorption measured for three series of samples of the study, i.e. semi-cokes (520°C), carbonization products (800°C) and activated carbons. For the co-pyrolysis derived materials, there is a significant increase in the sorption ability with the polymer content in parent blend i.e. with nitrogen content in the analyzed material. It is interesting to note about twice higher sorption in the case of material heat-treated at 800°C compared to the corresponding semi-coke. The increase occurs despite considerably reduced nitrogen content during the treatment. This can mean a strong effect of nitrogen surrounding in the carbonaceous matter on the water sorption activity.

In the case of activated carbons the situation is more complex due to the possible contribution of porosity development, in addition to nitrogen content, to the water sorption. Fig. 112 demonstrates an evident lack of the correlation between BET surface area and moisture content in the produced activated carbons. Contrarily, there is a

satisfactory correlation, keeping in mind an approximative character of the evaluation, between nitrogen content and propensity to the water sorption (Fig. 113). This relationship is practically linear in the case of activated carbons derived from CTP-PAN blends. Again, in most cases the activated carbons show enhanced sorption ability compared to carbonized materials despite the drastically reduced nitrogen content. More advanced examinations are necessary to clarify this complex relationship.

The materials derived from the ammoxidation show a moderate capability of water sorption but any reasonable correlation cannot be drawn from the experimental results.

We assume that nitrogen functionalities present on the activated carbon surface constitute the basic sites, both in terms of Lewis as well as Brönsted definition, accounting for the strongly polar properties of the materials.

Table 41. Water sorption of nitrogen enriched carbons at various stages of treatment

Parent materials	Semi-coke (520^0C) (wt%)	Carbonized coke (800^0C) (wt%)	Activated carbon (wt%)
CTP	0.10	0.00	1.20
CTP-PAN 9:1	0.55	1.09	4.07
CTP-PAN 3:1	1.58	2.84	4.23
CTP-PAN 1:1	3.21	6.07	6.01
PAN	4.70	7.68	9.68
CTP-PVP25ox 3:1	0.46	0.59	3.02
CTP-PVP25ox 1:1	1.34	2.54	3.32
PVP25ox	2.43	8.36	2.25
PS-Am	3.39	0.90	3.45
PSox-Am	2.68	1.20	5.20
PMox-Am	1.81	2.86	2.60

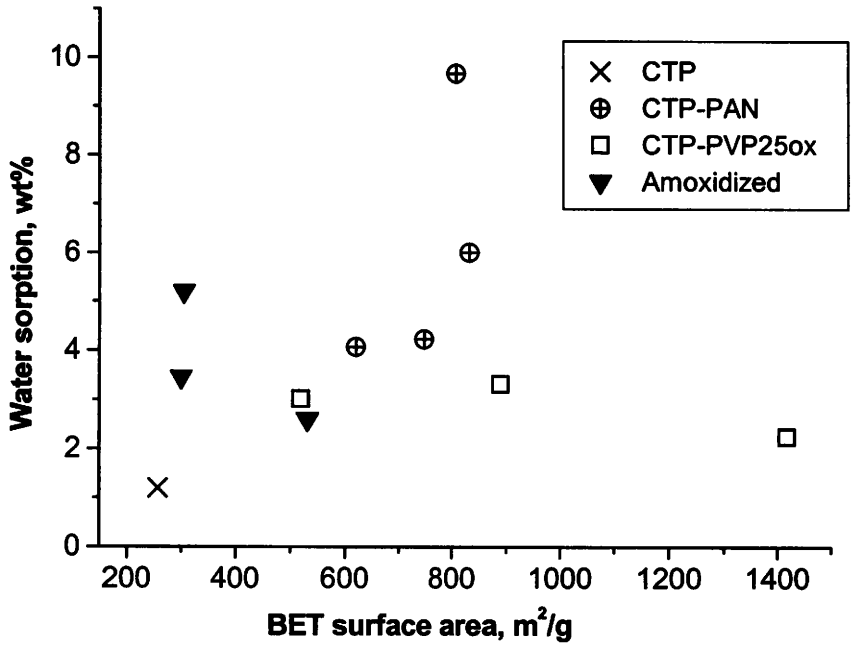

Fig. 112. Water sorption of the nitrogen enriched activated carbons vs. BET surface area.

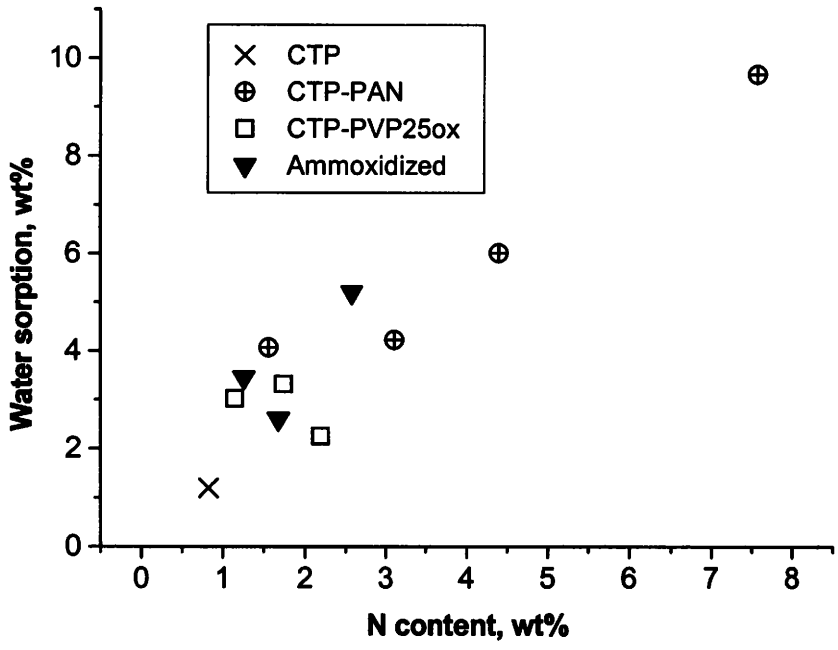

Fig. 113. Water sorption of the nitrogen enriched activated carbon vs. nitrogen content.

5.7. Evaluation of nitrogen doped carbons as a potential anode material in lithium-ion cell

Introducing of heteroatoms, mostly boron and nitrogen as a substituent for carbon in the graphene layer is considered as one of the possible ways of improvement of performance of carbon material used as an anode in lithium-ion cell. The foreign atoms modify the electron donor/acceptor properties of the graphene layers, and are consequently expected to affect the interactions during insertion and deinsertion of lithium.

In this part of the thesis the evaluation of lithium insertion/deinsertion behavior in relation to the nitrogen content and structural ordering was performed for a series of carbons prepared by heat-treatment at 1050^0C (calcination) of semi-cokes from pitch-PAN blends.

The materials used here include calcined carbons derived from single components (CTP-K and PAN-K) and their blends in various weight ratios (CTP-PAN 9:1-K; CTP-PAN 3:1-K, CTP-PAN 1:1-K).

5.7.1. Composition of calcined carbons from pitch-polyacrylonitrile blends

The proximate and elemental analyses of the calcination products are given in Table 42. A noticeable weight uptake due to water adsorption of the PAN and CTP-PAN 1:1 cokes, when exposed to air, proves a strong surface polarity. The calcined materials show considerably reduced nitrogen content compared to the corresponding semi-cokes (Table 5) and carbonized at 800^0C carbons (Table 26). The higher nitrogen content in the parent material, the bigger extent of its release on calcination treatment. Nitrogen and nitrogen containing compounds seem to have a relevant contribution to the enhanced weight loss on the preparation of PAN-K and CTP-PAN 1:1-K. Nevertheless the series of the calcined materials display a noticeable concentration of residual nitrogen.

Table 42. Elemental composition of calcined carbons from CTP-PAN blends

Sample	Weight loss on calcination wt%	Moisture wt%	Elemental composition wt%, daf basis				
			C	H	N	S	$(N/C)_{at}$
CTP-K	4.4	0.0	98.52	0.33	0.39	0.06	0.003
CTP-PAN 9:1-K	5.8	0.1	97.04	0.30	2.53 (1.0)[1]	0.06	0.022
CTP-PAN 3:1-K	7.3	0.9	96.27	0.19	3.81 (2.0)[1]	0.10	0.034
CTP-PAN 1:1-K	17.4	3.8	92.46	0.30	4.79 (3.5)[1]	0.08	0.044
PAN-K	19.8	4.9	91.00	0.41	6.69	0.11	0.063

[1]Calculated according to the additivity rule

X-ray photoelectron spectroscopy

The surface composition obtained by XPS analysis for the CTP-PAN 9:1-K, CTP-PAN 1:1-K and PAN-K is presented in Table 43. The N/C atomic ratio is similar in the bulk and at the surface of the cokes prepared from the polyacrylonitrile and CTP-PAN 1:1 blend, indicating rather uniform distribution of nitrogen in these samples. The signal-to-noise ratio in the nitrogen XPS region of CTP-PAN 9:1-K is to low to measure the concentration of the element. The enhanced oxygen content in the N-carbons is an effect of post-treatment surface oxidation on contact with air which is promoted by the presence of active nitrogen sites.

Table 43. Elemental composition of cokes (1050^0C) derived from pitch-PAN blends determined by XPS

Sample	Atomic concentration[1]			Atomic ratios		
	C	N	O	N/C		O/C
				XPS	El.An.	XPS
CTP –PAN 9:1-K	93.8	n.d.	6.2	0.000	0.022	0.066
CTP-PAN 1:1-K	87.0	5.5	7.5	0.063	0.044	0.086
PAN-K	85.5	6.4	8.1	0.075	0.063	0.095

[1] C + N + O = 100%

N1s, C 1s and O 1s XPS spectrum of calcined carbons derived from PAN and CTP-PAN blends are presented in Figs. 114-116, respectively. The relative distribution of carbon, nitrogen and oxygen functionalities in these materials is given in Table 44.

N1s spectra (Fig. 114) are fitted by four components which are assigned to pyridinic, pyrrolic/pyridonic, quaternary and oxidized nitrogen functionalities.

The pyridinic nitrogen is the most common (about 50%) form in PAN and CTP-PAN 1:1 cokes. It is interesting to note a significantly higher contribution of the quaternary nitrogen in the PAN coke compared to CTP:PAN 1:1 coke (30 and 14%, respectively) at the expense of pyrrolic/pyridinic form and, to lower extent, of pyridinic one. This is in contrast with very similar N1s XPS profile of semi-cokes from the same parent materials (pyridinic to pyrrolic/pyridonic nitrogen ratio 64:36 (Chapter 5.2.2.3). This suggests that transformation pathway of nitrogen functionalities is different in the case of both calcined products. Despite the relatively high treatment temperature, the calcined PAN coke contains a limited proportion of quaternary nitrogen, and the pyridinic and pyrrolic/pyridonic forms constitute about 60% of the total nitrogen. N-oxides seem to appear as an effect of the post-treatment oxidation of the pyridinic nitrogen.

C1s spectra (Fig. 115) of all the samples comprise four components. Peak at 285±0.1 eV corresponds to carbon atoms forming CC bonds. A similar for all the carbons contribution of the next peak centered at 287.1 ±0.1 eV (14.5%) is rather surprising. One could expect a lower intensity of the peak for CTP-PAN 9:1-K due to reduced nitrogen content.

Three different peaks are disinguishable in the O1s spectra of the carbons (Fig 116). The distributions of the oxygen structures in the carbons prepared from PAN and CTP-PAN 1:1 blend are very similar each other revealing that main part of the oxygen (~65%) occurs as C=O functionalities (Table 44). The intensity of the peak attributed to chemisorbed water increases with the nitrogen content in the N-carbons. The most abundant forms of oxygen in the CTP-PAN 9:1-K are hydroxyl groups and ethers (about 60%). O1s peaks of PAN-K and CTP-PAN 1:1-K are relatively broad what suggests that they may represent a variety of oxygen moieties with only slightly different binding energies.

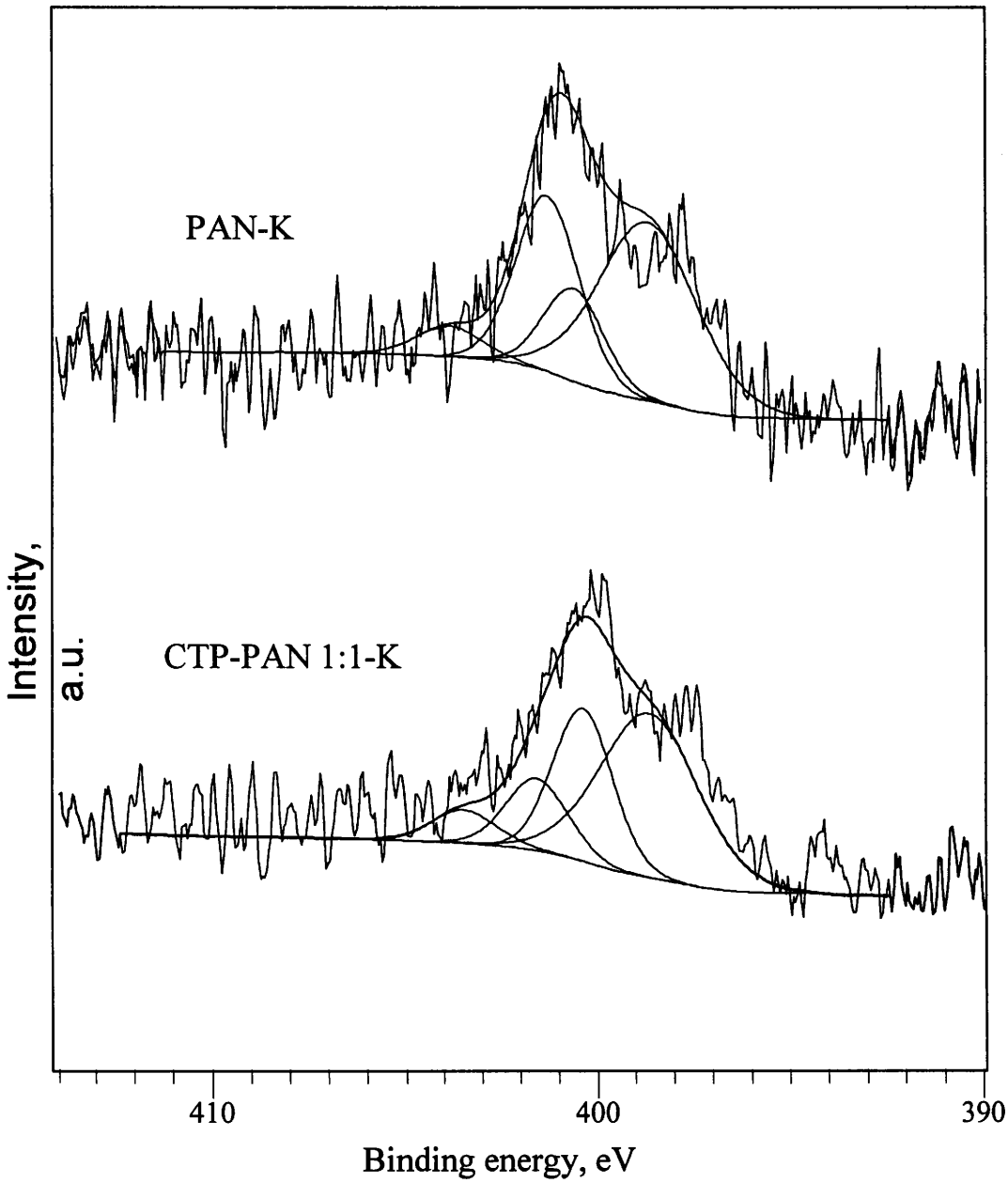

Fig. 114. N1s spectra of calcination (1050^{0}C) products derived from PAN and CTP-PAN 1:1 blend.

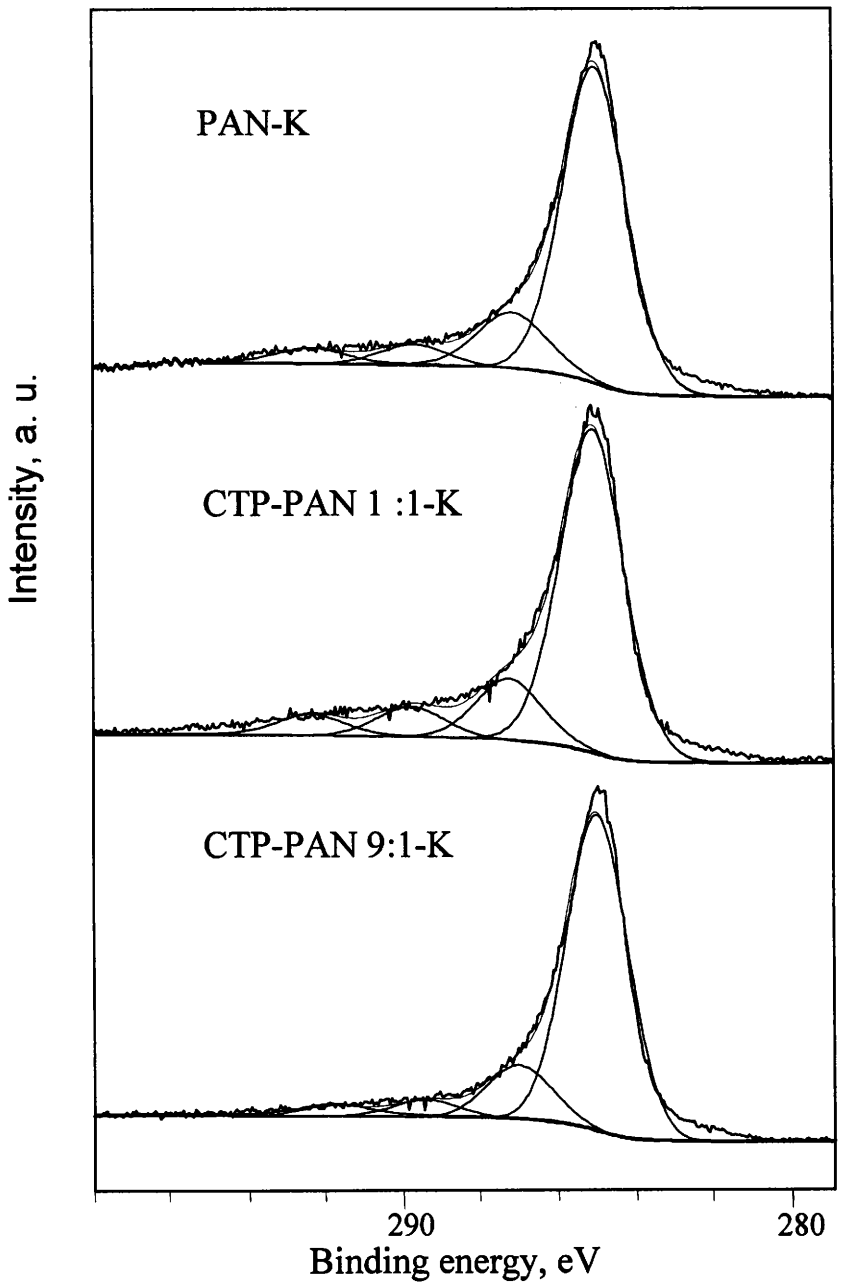

Fig. 115. C1s spectra of calcination (1050^{0}C) products derived from PAN and CTP-PAN blends.

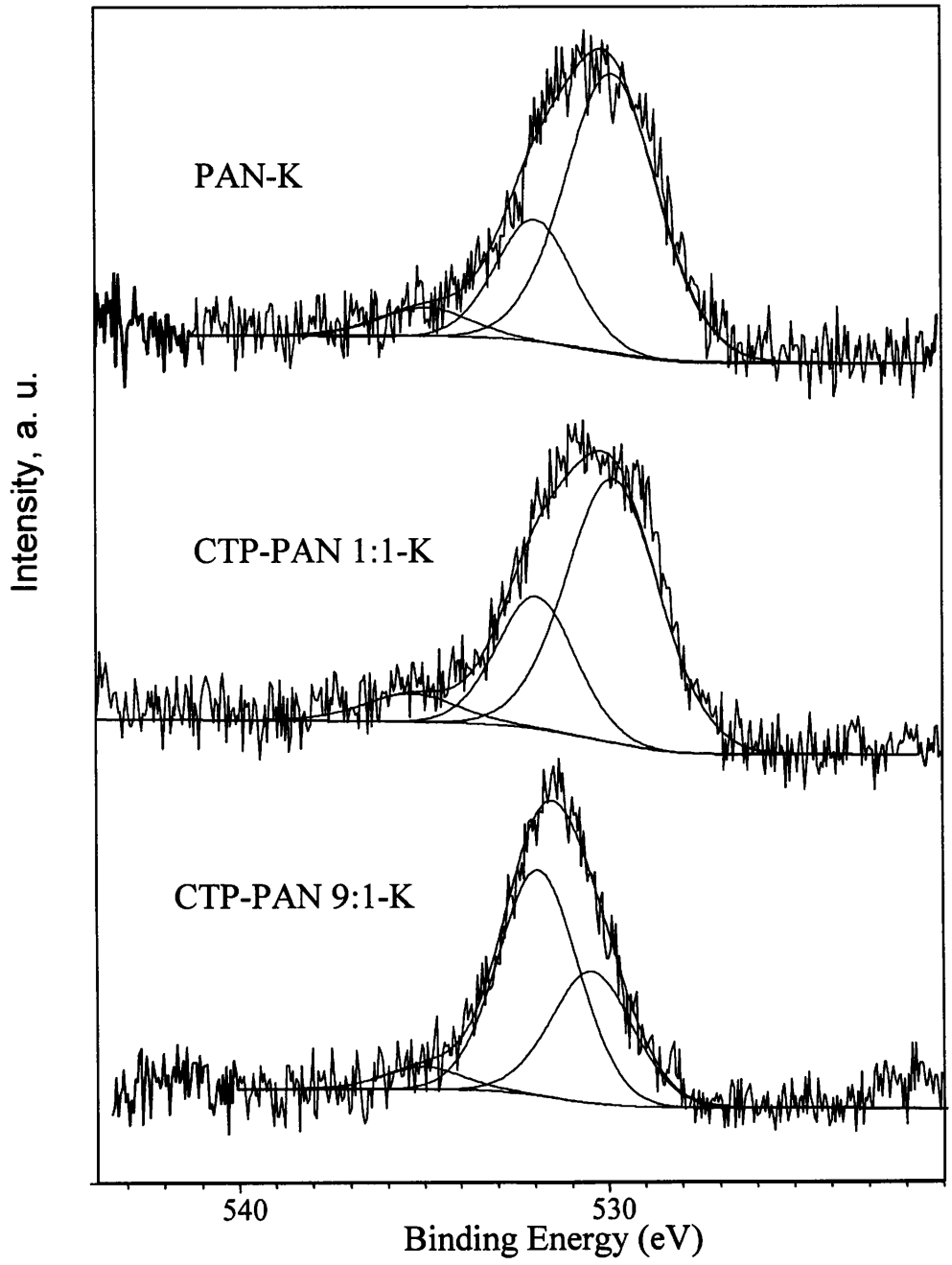

Fig. 116. O1s spectra of calcination (1050^{0}C) products derived from PAN and CTP-PAN blends.

Table 44. Distribution of the carbon, nitrogen and oxygen form in the carbons (1050^{0}C) derived from CTP-PAN blends.

Peak	BE eV	Possible assignment	**CTP-PAN 9:1-K** (%)	**CTP-PAN 1:1-K** (%)	**PAN-K** (%)
C1s	284.8±0.2	C-C	77.9	72.7	75.8
	286.7±0.4	C-OH, C-N, C=N	14.5	14.6	14.8
	287.8±0.3	C=O	4.8	7.7	5.6
	291.6±0.5	plasmon / π- π* transitions	2.9	4.9	3.9
N1s	398.7±0.3	N-6	n.d	52.5	46.3
	400.3±0.3	N-5	n.d	25.0	15.2
	401.4±0.5	N-Q	n.d	14.0	30.1
	402-405	N-X	n.d.	8.5	8.4
O1s	530.6±0.2	C=O	35.4	65.6	67.8
	532.8±0.4	C-O-C, C-OH	58.9	27.5	24.9
	535±0.2	H_2O, O_2 adsorbed	5.7	6.9	7.3

5.7.2. Multiscale structural and textural characteristics of the CTP-PAN derived cokes

The effect of the PAN addition on the multiscale organization of the resultant calcined carbons (1050^{0}C) was examined using X-ray Diffraction (XRD), optical microscopy, transmission electron microscopy (TEM) and sorption of N_2 and CO_2.

Structural ordering

The structural parameters determined for the calcined carbons from CTP-PAN blends from the XRD analysis are reported in Table 45. The addition of PAN to the pitch results in a distinct reduction of the stacking arrangement in the produced carbons as detected by the increase of interlayer distance d_{002} and the decrease of the apparent crystallite height L_c. The number of graphene sheets in an average stack of the coke

decreases from about 5.8 in the CTP-K to 4.2 in the PAN-K. In contrast, the size of the graphene sheets, L_a, is similar for all the samples and amounts to about 3 nm. The parameter R, which is empirically correlated to the inverse of the fraction of single graphene sheets (Liu et al., 1996) diminishes from 8.6 for the pitch carbon to 3.5 for the PAN carbon. The former value is in good agreement with that reported earlier for the coal-tar pitch coke (Zheng et al. 1996). Using the estimation given by Liu and coworkers (1996), the ratio R = 3.5 determined for the PAN carbon corresponds to a single-layer fraction equal to about 0.2, while the fraction is almost negligible for the pitch coke.

Table 45. XRD parameters and optical texture of the nitrogen doped carbons (1050°C) from the CTP-PAN blends

Sample	d_{002} nm	L_c (002) nm	L_a (100) nm	R	Dominant optical texture
CTP-K	0.3490	1.68	3.00	8.6	Flow domains
CTP-PAN 9:1-K	0.3501	1.55	3.00	6.3	Fine to coarse mosaics
CTP-PAN 3 :1-K	0.3547	1.48	3.20	5.1	Very fine mosaics
CTP/PAN 1 :1-K	0.3546	1.22	3.06	4.2	Isotropic
PAN-K	0.3570	1.15	2.97	3.5	Isotropic

Optical texture

The structural results from XRD correlate well with a gradual degradation of the optical texture of the pitch carbon when PAN is added. At the micrometer scale, the decrease of optically anisotropic domains is much more obvious than the slight evolution observed at the nanometer scale. Fig. 117 shows flow domains for the CTP-K (10 μm), coarse and medium mosaics (3-5 μm) for the CTP-PAN 9:1-K and fine mosaics (ca. 1 μm) for the CTP-PAN 3:1-K. Carbonization of PAN and CTP-PAN 1:1 gives in both cases an isotropic non-graphitisable product (domain size << 1 μm).

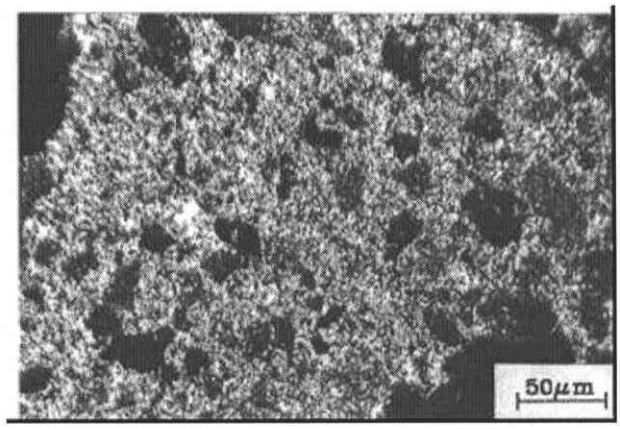

CTP-PAN 3:1-K

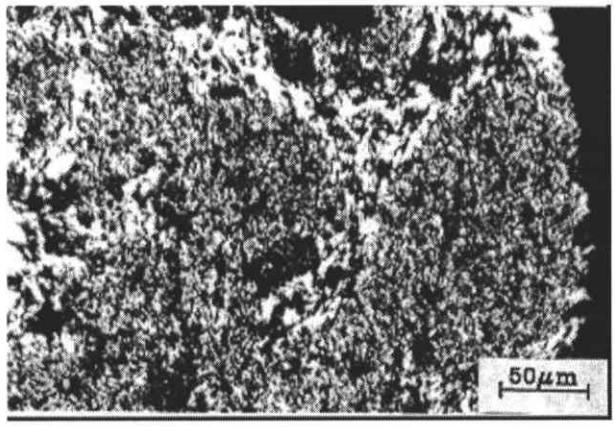

CTP-PAN 9:1-K

CTP-K

Fig. 117. Optical texture of carbons (1050^{0}C) from pitch-PAN blends: CTP-K, CTP-PAN 9:1-K and CTP-PAN 3:1-K

Microtexture

The CTP and CTP-PAN 9:1 carbons when viewed by transmission electron microscopy using the 002 LF mode reveal practically the same type of microtexture with nanometric basic structural units (BSUs) oriented in parallel to form domains extended over thousands nanometers (Fig. 118). Some contribution of smaller domains of about 100 nm in size distinguishes the CTP-PAN 9:1-K from the CTP-K, which confirms the observations by optical microscopy on these two carbons. The 002 DF image of the PAN coke (Fig. 119) shows a quite uniform microtexture of misoriented small domains (about 5 nm) responsible for the optically isotropic texture. The 002 LF image (Fig. 120) reveals that the misoriented domains of parallel BSU form mesopore walls of typical size 5-10 nm. The CTP-PAN 1:1-K represents quite a similar type of microtexture, however, some larger domains (100 nm) corresponding to the very fine mosaics observed by optical microscopy can be detected using the 002 DF mode (Fig. 121).

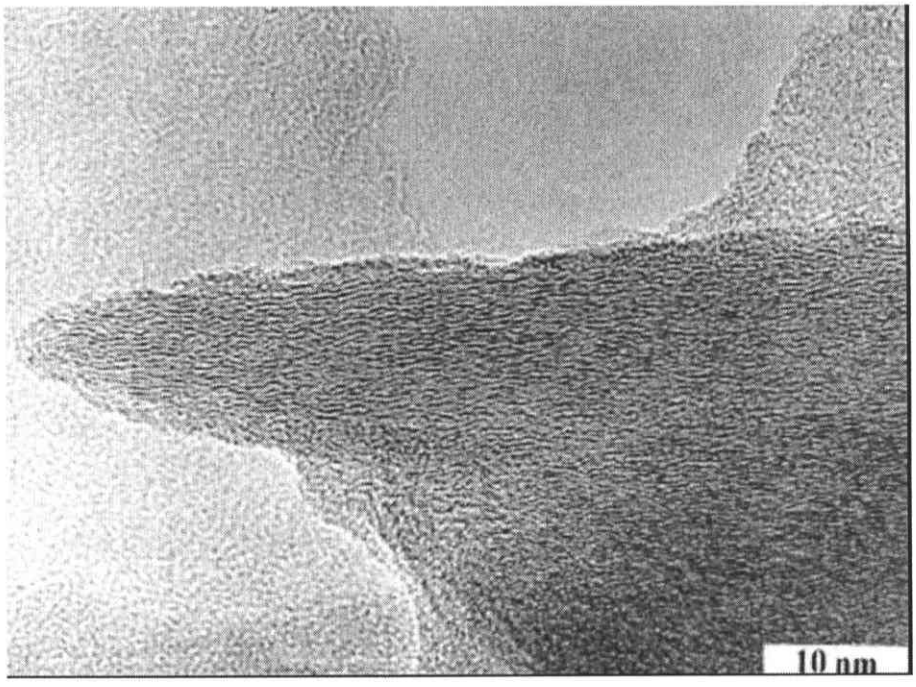

Fig. 118. 002 lattice fringes TEM image of the CTP-PAN 9:1-K.

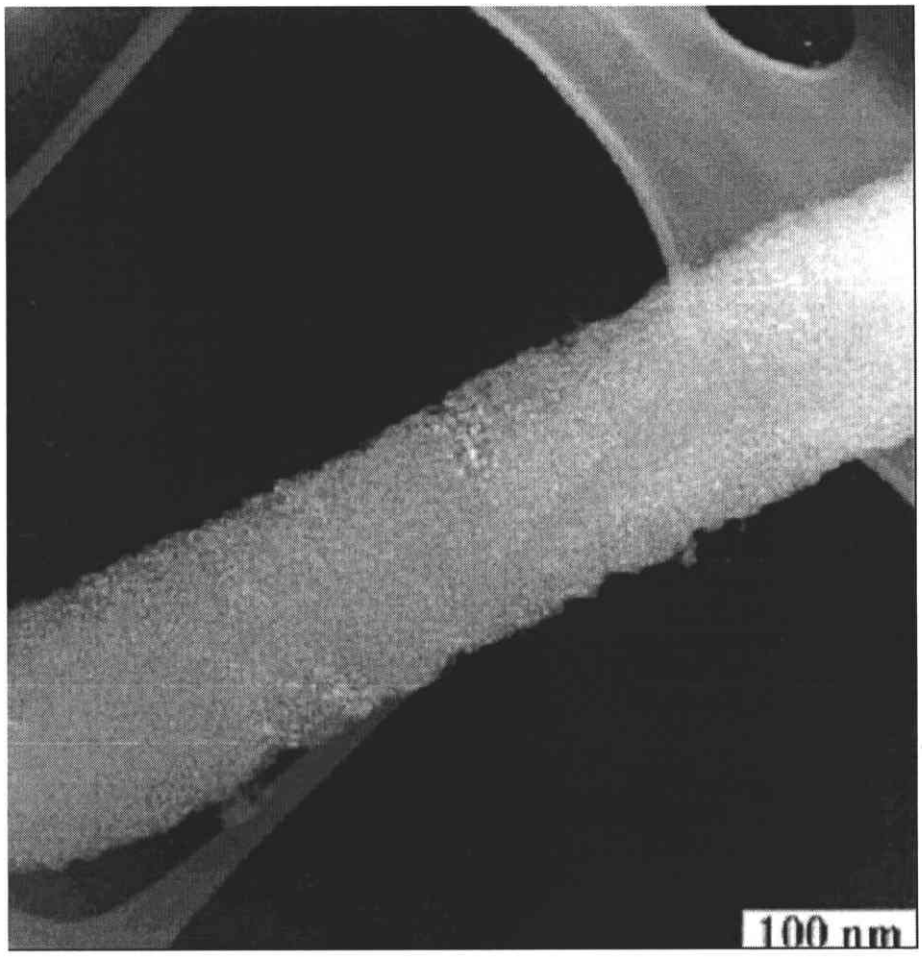

Fig. 119. 002 dark field TEM image of the PAN-K.

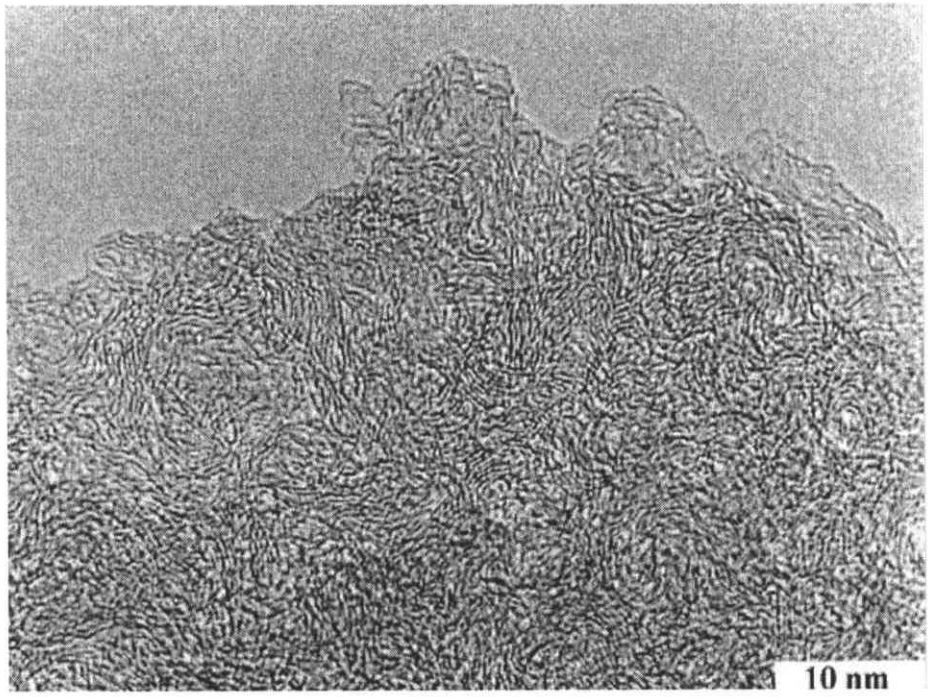

Fig. 120. 002 lattice fringes TEM image of the PAN-K

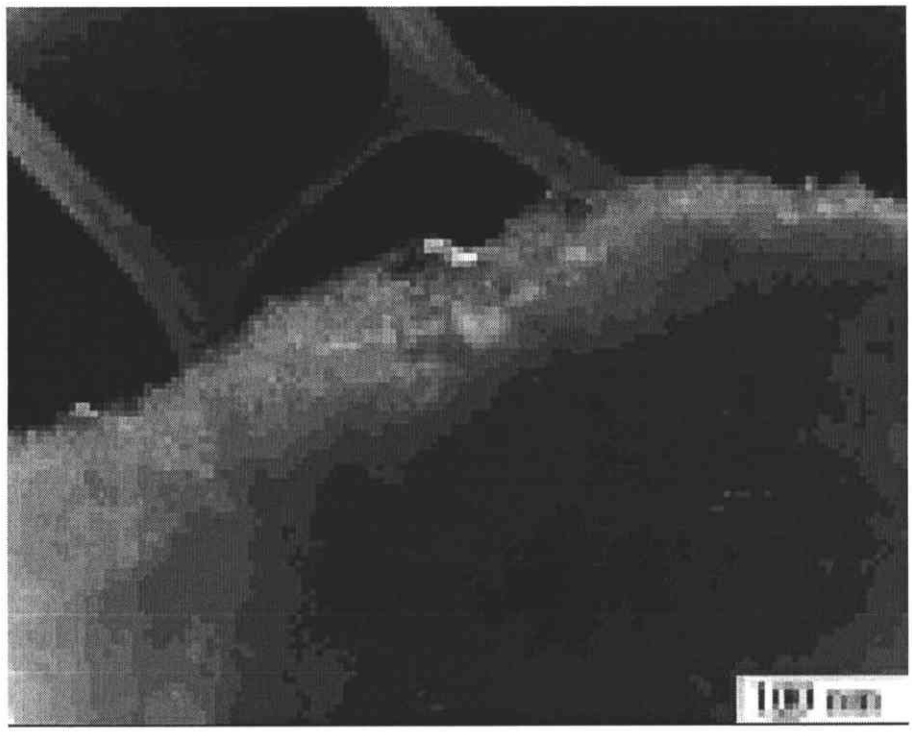

Fig. 121. 002 dark field TEM image of the CTP-PAN 1:1-K.

Porosity

The data reported in Table 46 from the nitrogen and carbon dioxide adsorption isotherms show a moderate increase in the carbons porosity, including ultramicropores accessible for CO_2 only, with the PAN proportion in the blends. PAN gives a completely microporous carbon with ultramicropores constituting about half of the total porosity. The largest pore volume, and in particular mesopore volume is observed for the CTP-PAN 1:1 carbon (1050^0C). The corresponding S_{BET} and S_{DR} values are of about 33 m^2/g and 85 m^2/g, respectively.

All the above data demonstrate a progressive structural and microtextural deterioration of the carbons produced from the blends with an increasing proportion of PAN, i.e. with an increasing amount of incorporated nitrogen. The blend containing 10 % of PAN gives a soft carbon with 2.5 wt% of nitrogen, however of lower degree of structural ordering compared to the pitch coke. In contrast, the PAN and CTP-PAN 1:1 derived carbons, which contain 6.7 and 4.8 wt% of nitrogen, respectively, are typical hard carbons of isotropic appearance, with a large extent of misorientation of the structural units and a noticeable porosity. Finally, the pyrolysis of the blend with 25 %

of PAN (CTP-PAN 3:1) produces a carbon of intermediate structural and microtextural properties and a moderate nitrogen content (3.8 wt%).

Table 46. Pore volume and surface area of the carbons (1050^0) derived from pitch-PAN blends

Sample	Sorption of N_2 at 77 K (micropores >0.5nm and mesopores)			Sorption of CO_2 at 25°C (ultramicroporosity < 0.5 nm)	
	Total pore volume V_T cm^3/g	Mesopore volume V_{meso} cm^3/g	BET surface area S_{BET} m^2/g	Pore volume V_{CO2} cm^3/g	DR surface area S_{DR} m^2/g
CTP-K	0.001	n.d.	1.3	n.d	n.d.
CTP-PAN 9:1-K	0.005	0.002	7.3	0.006	16.6
CTP-PAN 3 :1-K	0.008	0.002	12.8	0.013	33.5
CTP-PAN 1 :1-K	0.023	0.008	33.1	0.033	85.4
PAN-K	0.012	0.000	29.0	0.023	59.6

5.7.3. Electrochemical properties of the CTP-PAN derived cokes

The lithium insertion into the nitrogen enriched carbons was evaluated from the charge/discharge characteristics of two electrode lithium/carbon cells. The values of irreversible capacity were easily estimated from the comparison of the first and second discharge cycles whereas the reversible lithium insertion degree was estimated from the charge passed during the second deinsertion process. It is noteworthy that quite different electrochemical behaviours are observed depending on the proportion of PAN in the precursor blend. The charge/discharge galvanostatic profile of the pitch carbon treated at 1050°C is presented in Fig. 122. The hysteresis between charge and discharge is remarkably very small. The irreversible capacity reaches a low value, X = 0.2 (X = 1 corresponds to 372 mAh/g), which is typical for soft carbons formed at about 1000°C. This carbon is characterized by a low specific surface area (1.3 m^2/g) and a low content of hydrogen or other heteroatoms, which are considered as active sites for the electrolyte decomposition. Very similar electrochemical characteristics are shown by the CTP-PAN 9:1 carbon. This means that for this soft carbon of structural characteristics very close to the CTP carbon, the enhancement of the nitrogen content to 2.5 wt% does not affect the reversible and irreversible capacity.

Contrarily, for the materials with the highest nitrogen content (6.7 and 4.8 wt%), obtained by pyrolysis of the pure PAN and of the blend with 50 % of PAN, respectively, an increase of irreversible capacity up to X_{irr} = 0.5-0.6 is observed. This occurs without any significant change in the reversible capacity, X_{rev} = 0.8-0.9. Applying a short circuit between the electrodes, in order to estimate the maximal capacity, does not allow any enhancement of the observed value. An example of galvanostatic curve is shown for the CTP-PAN 1:1 carbon in the Fig. 123. The electrochemical characteristic is comparable to the saccharose coke (Gautier et al., 1998) and clearly different from the soft carbons, due to the marked hysteresis and the more important irreversible capacity. Additionally, while the reduction process starts at about 0.8 V vs Li for the CTP-PAN 1:1 nitrogen enriched carbon, it already begins at higher potential (ca. 1.1 V vs Li) for the CTP carbon. The electrochemical behaviour of the CTP-PAN 3:1 carbon of intermediate structural ordering and nitrogen content is rather close to that of PAN and CTP-PAN 1:1 hard carbons (X_{irr} = 0.45, X_{rev} = 0.9).

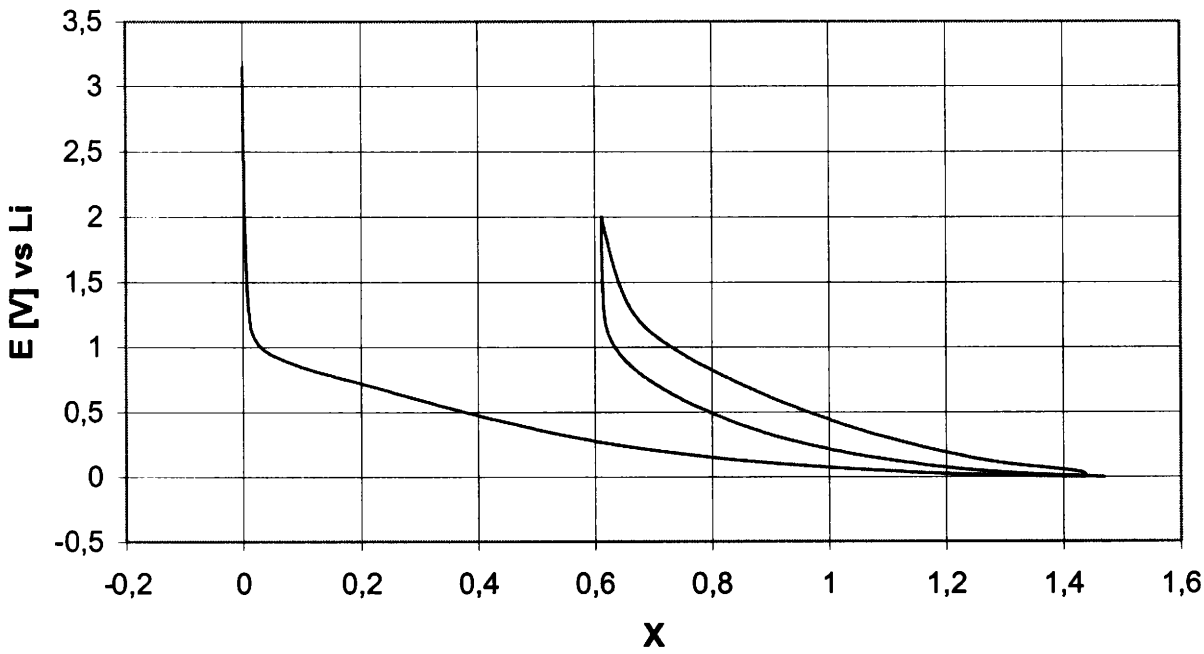

Fig. 122. Galvanostatic charge/discharge characteristics for lithium insertion into the CTP carbon (1050°C) at 20 mA/g.

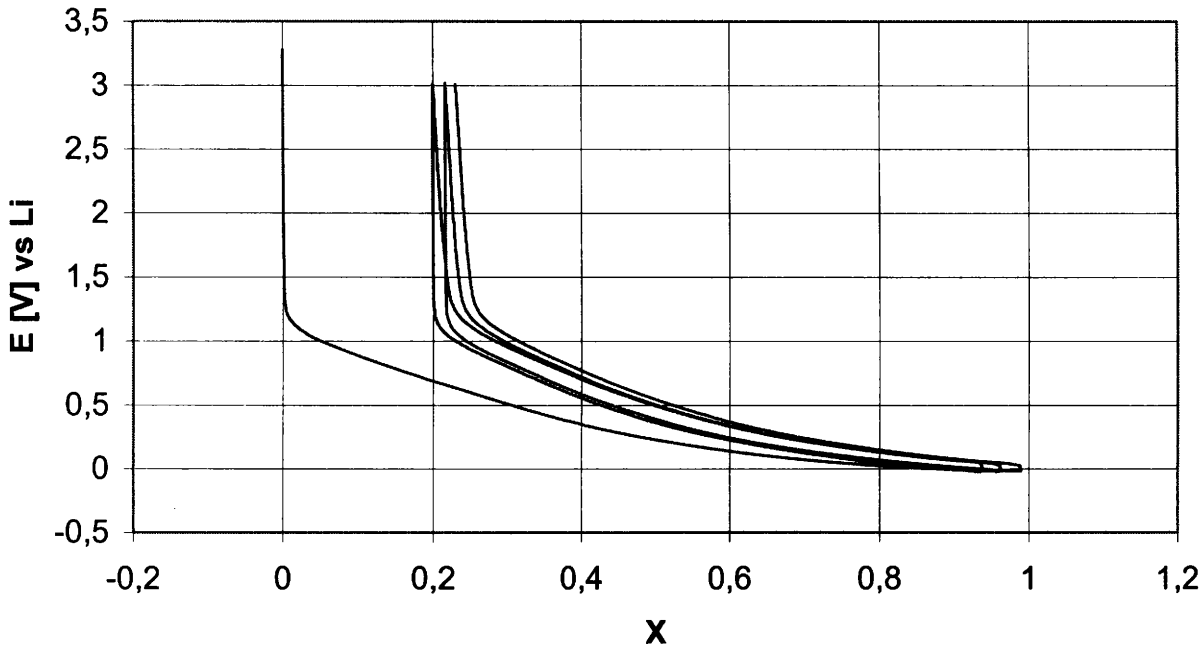

Fig. 123. Galvanostatic charge/discharge characteristics for lithium insertion into the CTP-PAN 1:1 carbon (1050°C) at 20 mA/g.

The values of irreversible X_{irr} and reversible X_{rev} capacity for the different materials are summarized in the Table 47. It is noteworthy that for all carbons the value of X_{rev} is comparable, independently of the $(N/C)_{at}$ ratio. This means for materials of comparable structure and microtexture, such as the PAN and CTP-PAN 1:1 ccarbons, that the change of electron donor/acceptor character which is induced by the presence of nitrogen in the polyaromatic layers has a negligible influence on the reversible insertion of lithium. Hence, the decrease of reversible capacity mentionned by Yung et al. (1997) for carbons obtained from polyacrylonitrile at different heat treatment temperatures would be rather due to different microtextures or amounts of hydrogen to which, according to the proposition of some authors, the lithium atoms bind preferentially (Zheng and Dahn, 1999).

The hard carbons derived from the heat-treatment of phenolic resin at 1000°C are characterised by a noticeable reversible capacity, X_{rev} = 1.45, with a long low voltage plateau and a limited hysteresis. They contain a significantly higher fraction of single layer graphene sheets than the cokes studied in this work (0.4 - 0.5 (Liu et al.,

1996) compared to the maximum value of 0.2 for the PAN carbon). Therefore, the absence of small nanopores where the lithium could be reversibly stored is the reason for the low values of X_{rev} observed in our samples. Although the open microporosity of carbons from phenolic resin is quite developed (BET specific surface area = 240 m^2/g), their irreversible capacity is only X_{irr} = 0.54 (Zheng and Dahn, 1999). The irreversible capacity of the PAN and CTP-PAN 1:1 carbons, reaches a comparable value, despite a relatively low value for the BET specific surface area (ca. 30 m^2/g). Since the extent of disorder of these materials is apparently smaller, the high value of irreversible capacity seems to be related with the high nitrogen content. Moreover, the major nitrogen form is pyridinic for both PAN and CTP-PAN 1:1 carbons (Table 44) and they have a strong affinity for moisture (Table 42). Hence, during the first reduction, the solvated lithium cations are trapped by the lone pairs of electrons of the pyridinic groups on the carbon surface where they are decomposed. The slightly higher irreversible capacity observed for the PMR-PAN 1:1 coke, compared to the PAN coke, correlates well with the presence of mesopores which favour the access of the voluminous solvated lithium cations to the active sites.

Table 47. The values of irreversible (X_{irr}) and reversible (X_{rev}) capacities of the carbons from the different blends

Blend	X_{irr}[1]	X_{rev}[1]
CTP	0.2	0.8
CTP-PAN 9:1	0.25	0.75
CTP-PAN 3 :1	0.45	0.9
CTP-PAN 1 :1	0.6	0.9
CTP	0.5	0.8

[1]X =1 corresponds to 372 mAh/g, i.e. to the insertion of 1 lithium for 6 carbon atoms

VI. Summarizing Discussion

The general objective of the thesis is to explore the possibilities of synthesis of coal-tar pitch based carbons enriched with nitrogen and to understand the structure and properties of the resultant materials. The ways used for introducing nitrogen into the carbonaceous material network comprise the pyrolysis of selected nitrogen containing polymers in the pitch matrix and the ammoxidation of pitch derived materials. These synthesis methods enable the preparation of carbonaceous materials with differentiated the content and distribution of nitrogen functionalities and structural ordering.

Co-pyrolysis of coal-tar pitch with N-polymers

Four polymeric additives (polyacrylonitrile, polyvinylpyridine and their oxidized derivatives) were used in the thesis as nitrogen carriers in the co-pyrolysis with the coal-tar pitch. The polymers differ each other in terms of nitrogen content, mechanism of thermal degradation including the stability and solid residue yield as well as the reactivity toward pitch constituents on the co-treatment.

The reactions of polymer or pitch-polymer blend conversion of fundamental importance for the characteristics of the resultant carbonaceous solids occur in the low temperature stage of heat-treatment i.e. below 500-600°C.

The mechanism of polyacrylonitrile (PAN) pyrolysis involves primarily the rearrangement of the linear polymer chain into the condensed heteroaromatic structure. The conversion is associated with the evolution of oligomeric products and low molecular weight nitrogen bearing gases as HCN and NH_3, however gives the solid residue with a considerable, comparable to coal-tar pitch yield (about 45 wt%).

Polyvinylpyridine (PVP) displays nearly complete depolymerization, typical of the vinyl polymer backbone, at heat treatment at 500°C. In the case of PVP cross-linked with 25 wt% of divinylbenzene (PVP25) used in this study the pyrolysis residue amounts to about 10 wt% only.

The oxidation of the polymers in air at 300°C results in an enormous increase in the pyrolysis residue yield, by about 35 and 60 wt% for PAN and PVP25, respectively. FTIR analysis clearly demonstrates the oxygen induced dehydrogenation of vinyl part of PVP co-polymer which results in the extensive cross-linking and enhanced stability.

When added to coal-tar pitch, a polymer modifies its thermal behavior in a specific way which depends on the interactions occurring between blend components. The nature and extent of the interactions are evaluated in the study from the weight loss behavior on the blend pyrolysis and the nitrogen content and optical texture in the resultant residue.

Generally observed phenomenon is an increase in the pyrolysis residue yield of a pitch-polymer blend compared to the anticipated yield according to the additivity rule. In the case of 1:1 blends the discrepancy, as determined by TG, amounts to 12-14 wt% for PAN and PVP25 and about 8 wt% for the oxidized forms of the polymers. Another interesting feature of pitch-PAN co-pyrolysis is an enhancement of nitrogen content in the residue compared to the calculated values.

The coal-tar pitch gives on the pyrolysis an anisotropic material of flow type optical texture. Solid residues produced from all the polymers used show the totally isotropic texture characteristic of disordered non-graphitizing carbons. The co-pyrolysis results in the degradation of anisotropic development to the extent, which is dependent not only on the component proportions but also on the nature of polymer added.

The addition of PAN to pitch leads to the formation of co-pyrolysis products with rather homogeneous optical texture but strongly restricts the development of anisotropy. With increasing proportion of PAN in the blend there occurs a gradual replacement of flow type texture by mosaics followed by the reduction of mosaic size until a typical hard carbon of isotropic appearance is produced from the CTP-PAN 1:1 blend.

The experimental findings lead to the following mechanism of co-pyrolysis of pitch with PAN. Radicals generated during thermal degradation of PAN abstract hydrogen from pitch molecules what results in the decrease of the light oligomers evolution. The coal-tar pitch seems to be therefore a stabilizer of radicals, preventing extensive degradation of PAN. On the other hand, the abstraction of hydrogen generates radicals within pitch matrix so promoting condensation and cross-linking reactions of pitch constituents. A consequence is an extensive deterioration of the optical texture of carbonization residue, which suggests rather strong dehydrogenation activity of the created polymer fragments. FTIR and XPS analyses reveal a similar evolution of nitrogen functionalities on heat treatment of PAN and CTP-PAN blend. It seems, therefore, that the direct chemical interactions between PAN fragments and pitch molecules, which could produce a new type of recombined macromolecules via the

radical or condensation mechanisms are rather limited. Therefore the principle of the interactions can be defined as indirect chemical modifications of both pitch and PAN involving hydrogen transfer reactions.

The pyrolysis of CTP-PANox blend leads to the heterogeneous product with the residue derived from non-melting polymer being readily distinguishable by the isotropic appearance. The heterogeneous optical texture proves that the extent of interactions of components on the co-treatment is limited. Some increase in the residue yield from blend compared to the anticipated value can appear due to the dehydrogenative activity of oxygen groups resulting in the polymerization and cross-linking of pitch molecules.

The inertness of the oxidized PAN towards pitch on co-pyrolysis causes that this form of polymer is not suitable as a component of blend used for the preparation of nitrogen containing carbons.

The tendency to depolymerization of polyvinylpyridine on heat-treatment justifies a little effect of the polymer on the chemical composition and optical texture of pyrolysis residue from the blend. A noticeable increase in nitrogen content (1.9 wt%) and deterioration of anisotropy is observed with 50 wt% of the polymer in the blend only. Discrepancies of experimental TG/DTG profiles of blend compared to those anticipated (shift to a lower temperature of maximum weight loss rate and an increase in the residue yield) seem to be induced by the reduction of thermal stability of polymer by coal-tar pitch acting as a solvent. Some fragments resultant from depolymerization can contribute to the residue yield by reaction with pitch constituents via dehydrogenation mechanism.

The oxidized form of PVP25 is much more active additive in terms of nitrogen introducing and deterioration of the optical texture of resultant blend semi-coke. The major reason is a greater mass contribution to the blend semi-coke. The pyrolysis of CTP-PVP25ox 1:1 blend gives a completely isotropic material containing 3.75 wt% of nitrogen. Moreover, the TG/DTG analysis shows the delay and reduction of volatile evolution from pitch due to dehydrogenative activity of oxygen functionalities present in PVP25ox which initiate the polymerization reactions of pitch constituent.

PAN is very efficient nitrogen bearer in the co-pyrolysis due to both high nitrogen content in the parent polymer (about 25 wt%) and relatively high residue yield as resulting from the scheme of rearrangement on thermal treatment. The superior carbonization behavior is transferred to the blends ensuring satisfactory nitrogen content in the blend residue at a relatively low proportion of polymer in the parent blend.

PVP25ox is another nitrogen containing polymer which is of interest for the co-pyrolysis with pitch. Due to lower heteroatom proportion in the parent polymer (7.7 wt%) it is a less efficient nitrogen carrier than PAN, however, the location of nitrogen in the 6-membered pyridinic ring could be meaningful with respect to the element evolution on thermal treatment.

Introducing of nitrogen into the carbon network during the co-pyrolysis of pitch with the N-polymers is associated with the reduction of anisotropic development during the co-pyrolysis. The effect is partially a polymer type dependent. Somewhat surprisingly the co-pyrolysis with PAN enables receiving richer in nitrogen semi-cokes while preserving anisotropic appearance. An example is the mosaic texture of CTP-PAN 3:1 semi-coke with 7.1 wt% of nitrogen as compared to totally isotropic CTP-PVP25ox 1:1 semi-coke containing 3.75 wt% N only. This suggests that the deterioration of optical texture of blend residue is not intrinsically related to the introducing of nitrogen atoms but rather to the contribution of polymer derived disordered matter. The another relevant factor, which should be considered is the structural aspect of polymer degradation as generating fragments of differentiated ability to be accommodated within the mesophase system during co-pyrolysis. In the case of oxidized PVP the extensively cross-linked vinyl derived part of the co-polymer is believed to be thermally stable and behave as inert in the carbonizing system.

Semi-cokes (520°C) from single polymers and blends contain nitrogen as a part of ring systems. Mostly this is pyridinic-N (about 60 %) with a minor contribution of pyrrolic/pyridonic form. A relevant observation is the lack of quaternary nitrogen at this stage of treatment.

Ammoxidation of pitch derived semi-coke and mesophase

The reaction with ammonia-air mixture was used for the synthesis of nitrogen enriched carbons having established a pre-order during the preceding thermal treatment as detected by the anisotropic texture. As distinct from the co-pyrolysis, the ammoxidation is expected to result in introducig nitrogen groups only at the surface of particles which is available for the reacting mixture.

Under appropriate reaction conditions (ammonia-air 1:3 ratio, sufficiently high ammoxidation temperature, 350-400°C) the process appears to be a quite efficient way of nitrogen incorporation into pitch semi-coke and pitch mesophase. For three different materials used in the study i.e. pitch semi-coke (PS) and oxidized in nitric acid both

pitch semi-coke (PSox) and pitch mesophase (PMox), the ammoxidation enhances the nitrogen content in the bulk of sample to 8-10 wt%. Keeping in mind that the reaction occurs mostly at the surface of particles the results of the treatment can be regarded as very satisfactory.

The preoxidation with nitric acid plays a beneficial role in terms of the ammoxidation kinetics, lowering the activation barrier what enables to introduce the same or higher amount of nitrogen under milder reaction conditions. Moreover, the pretreament induces some changes in the nitrogen distribution and functionalities. In the case of pretreated materials PSox-Am and PMox-Am, the similar N/C atomic ratio from the elemental analysis and XPS suggests rather homogenous nitrogen distribution in the bulk of sample particles. Similar comparison for PS-Am indicates a preferential location of nitrogen at the surface of particles. As a result, the non-oxidized semi-coke of the lowest total nitrogen content is distinctive by the highest concentration of surface nitrogen. The enhanced nitrogen content determined by elemental analysis can be due to ammonia weakly bound to the acidic in character surface. This part of nitrogen is released during sample preparation for XPS analysis.

The ammoxidation creates the significant proportion of aliphatic nitrogen groups comprising amides, imides and nitriles. These thermally unstable functionalities constitute about 15% of the introduced nitrogen in PS-Am but considerably more (30 and 48%) in preoxidized samples. Interestingly, the N1s XPS spectra of all the ammoxidized samples reveal the presence of peak at about 401.4 eV which is the most intense in the case of the PMox-Am. The peak centered at this position is commonly attributed to the positively charged quaternary nitrogen occurring in condensed graphene rings. Since here this form was created under rather mild conditions, it seems resonable to attribute the peak to positively charged species like pyridinic-N associated with an adjacent or nearby located hydroxyl oxygen or carboxyl groups, protonated through formation of a H-bridge, (Kelemen et al., 1994).

Behavior of nitrogen containing semi-cokes on the heat-treatment in inert and oxidative atmosphere

The nitrogen containing semi-cokes, prepared by co-pyrolysis and ammoxidation were further treated under condition simulating the manufacturing of structural and porous carbons. This part of the study is focused on the evaluation of the

stability of incorporated nitrogen and transformation its form during heat-treatment in the inert atmosphere and activation with steam at 800°C.

Characteristic of all the nitrogen containing semi-cokes is an enhanced weight loss on the subsequent heat-treatment compared to the pitch semi-coke. The extent of the loss can be related to the polymer proportion in a parent blend or rather to the nitrogen content in the resultant semi-coke. On heat-treatment to 800-900°C the weight loss amounts to about 4.5 wt% for CTP, ~ 10 wt% for CTP-PAN 1:1 and PVP25ox and 15 wt% for PAN semi-cokes. In the case of ammoxidation products the measured weight loss of 10-15 wt% covers also unstable oxygen groups. Nitrogen bearing light compounds as ammonia and hydrogen cyanide and possibly molecular nitrogen are meaningful components of volatiles evolved during the treatment.

Fig. 124 presents the variation of nitrogen content in the CTP-PAN blend derived materials on the heat-treatment and activation used in the study. In terms of nitrogen release the behavior of blends is similar to that of pure polymer. The relative proportion of nitrogen which is excessive, therefore unstable at a given stage of heating increases with the polymer ratio in the blend. For the heat-treatment at 800°C it reaches about 25 % in pure PAN. This means that the pitch matrix hinders to a certain extent the nitrogen evolution, the effect being most pronounced for CTP-PAN 9:1 ratio.

The carbon-nitrogen structures loose their stability above 800°C as indicated by the drop of nitrogen content in the calcined materials. Nevertheless, the comparison of nitrogen content in calcined PAN carbons (6.7 wt%) and 1:1 and 3:1 blend carbons (4.8 and 3.8 wt%, respectively) proves that on the drastic treatment the blending with pitch is quite effective in nitrogen retaining in the carbon network. Likely, the system should be considered as a solid solution with a specific for a given temperature "solubility" of nitrogen in carbon network.

Co-pyrolysis of oxidized PVP with pitch leads to carbonaceous materials of lower nitrogen content compared to the corresponding PAN blends. The stability of the created nitrogen structures seems to be lower than those present in PAN blend semi-coke of comparable nitrogen content. PVP25ox semi-coke looses on carbonization at 800°C about 30 % of the original nitrogen (Fig. 125). Moreover, the linear increase in the nitrogen content with PVP25ox proportion in the blend indicates the lack of interactions between pitch and polymer, which would result in the retention of nitrogen in the carbonization products.

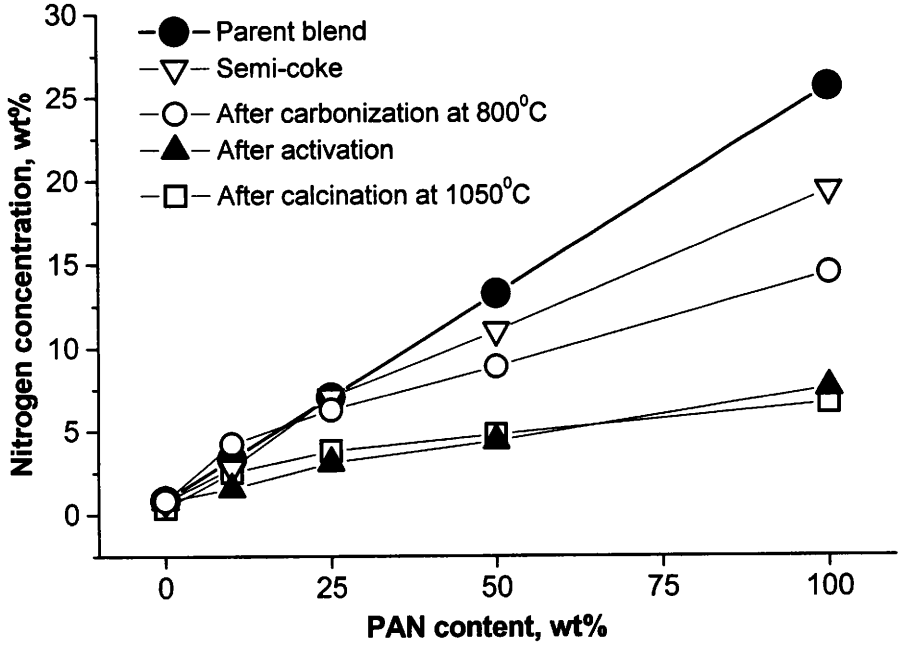

Fig. 124. Variation of the nitrogen content on consecutive stages of the thermal treatment of the CTP-PAN blends.

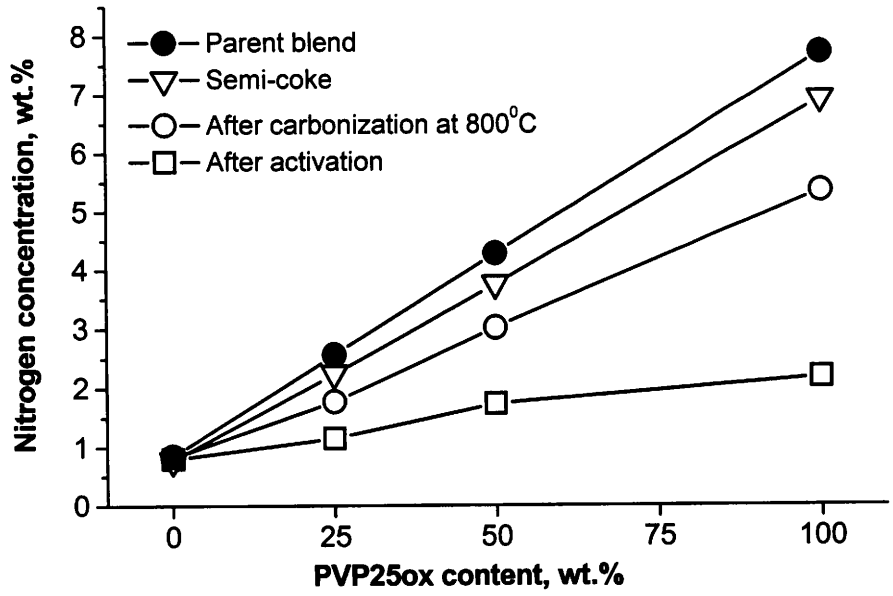

Fig. 125. Variation of the nitrogen content on consecutive stages of the thermal treatment of the CTP-PVP25ox blends.

The nitrogen functionalities formed by the ammoxidation display significantly lower thermal stability than those created by the co-pyrolysis (Fig. 126). 40-50 % of nitrogen introduced by ammoxidation is lost during the carbonization at 800°C stage. The preoxidation with nitric acid seems to lead to more resistant nitrogen forms, despite a higher proportion of unstable aliphatic functionalities present in the ammoxidized material. Such a behavior can be related to more homogenous nitrogen distribution in the bulk of particles in the case of preoxidized samples as deduced from the comparison of elemental analysis and XPS data. This means also that the unstable groups can be, at least in part, transformed into stable ring systems on heat-treatment.

The activation with steam of semi-cokes from the co-pyrolysis to about 50 wt% burn-off results in about twice higher reduction in nitrogen content compared to the respective treatment in inert atmosphere. The preferential removal of nitrogen seems to be due to its association with the disordered polymer derived material, which is more readily gasified. It is also possible that nitrogen atoms constitute the sites more readily oxidized by steam. For a set of nitrogen containing semi-cokes prepared in the study there is a good inverse correlation between the activation time required to reach 50 wt% burn-off and the nitrogen content in the initial material (semi-coke).

The activation of ammoxidation products leads to a greater reduction of nitrogen content, especially in the case of unoxidized semi-coke PS. This result is in agreement with the earlier observation concerning the ammoxidation reaction, which is specifically restricted to the surface of particles in this case.

While analyzing any correlation for the activated carbons one has to realize that the burn-off level reached individually for a given material induces a relevant effect to the nitrogen content and nitrogen form contribution. Unfortunately, in some cases the real burn-off differs noticeably from the anticipated 50 %.

The conversion of nitrogen forms present in the co-pyrolysis and ammoxidation products during heat-treatment and activation is presented in Figs 127-131. The distribution of nitrogen forms from the XPS spectra deconvolutions is related here to the content of nitrogen obtained by elemental analysis. This assumes a homogeneous distribution of nitrogen functionalities in the bulk of material, which is not a real case for some of the samples. Therefore the evaluation can be regarded as a very approximate only.

The distribution of nitrogen forms in the carbonization and activation products is strongly influenced by the way of nitrogen incorporation (co-pyrolysis or

ammoxidation) and the atmosphere during the treatment (inert gas or steam). The pyridinic form is the most common in the carbonized materials, constituting from 35% up to 60% of the residual nitrogen. Characteristic of all ammoxidation derived materials is a low proportion of quaternary nitrogen as an effect of substitution occurring at the edge of aromatic lamellae or graphene layers. The activated carbons contain a considerable proportion of pyridonic nitrogen, thus indicating that this form is an intermediate stadium in nitrogen removal on steam gasification. The quaternary nitrogen constitutes a comparable part (20-30%) of the residual nitrogen in nearly all the activated materials. The presence of N-oxides in many products of carbonization and activation should be attributed rather to the post-treatment reactivity of the nitrogen sites on the surface. The burn-off level seems to influence not only residual nitrogen content but also the distribution of various forms.

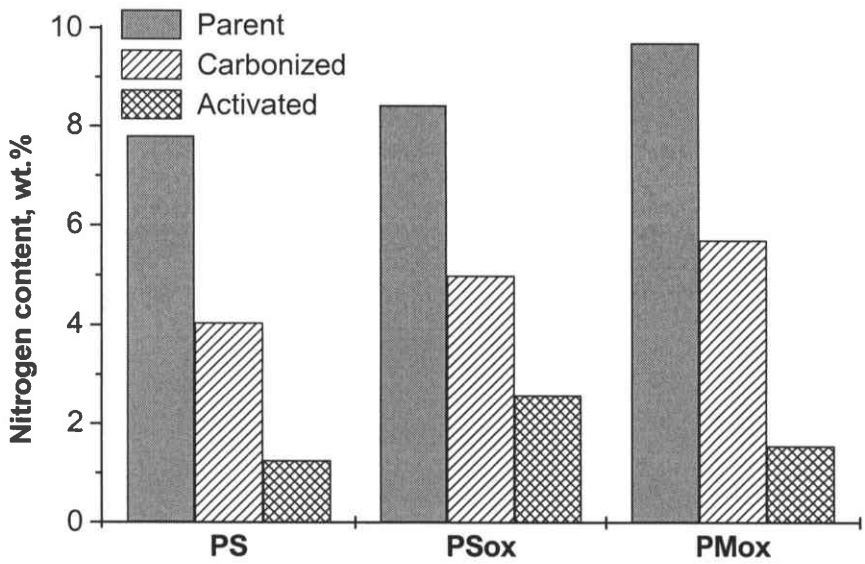

Fig. 126. Variation of the nitrogen content on consecutive stages of the thermal treatment of the ammoxidized samples.

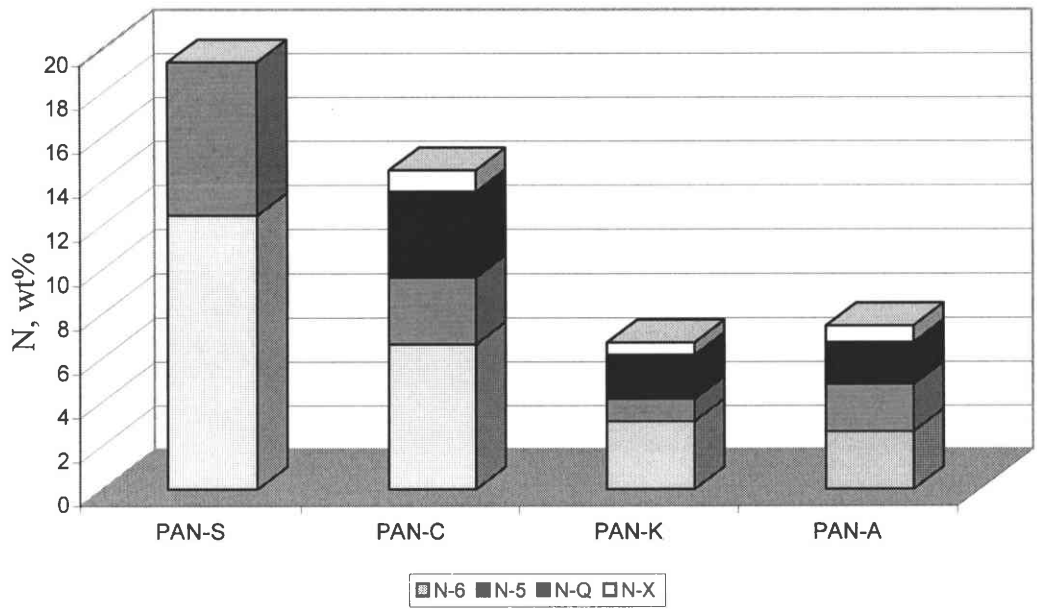

Fig. 127. Evolution of nitrogen functionalities on the consecutive stages of the thermal treatment of PAN.

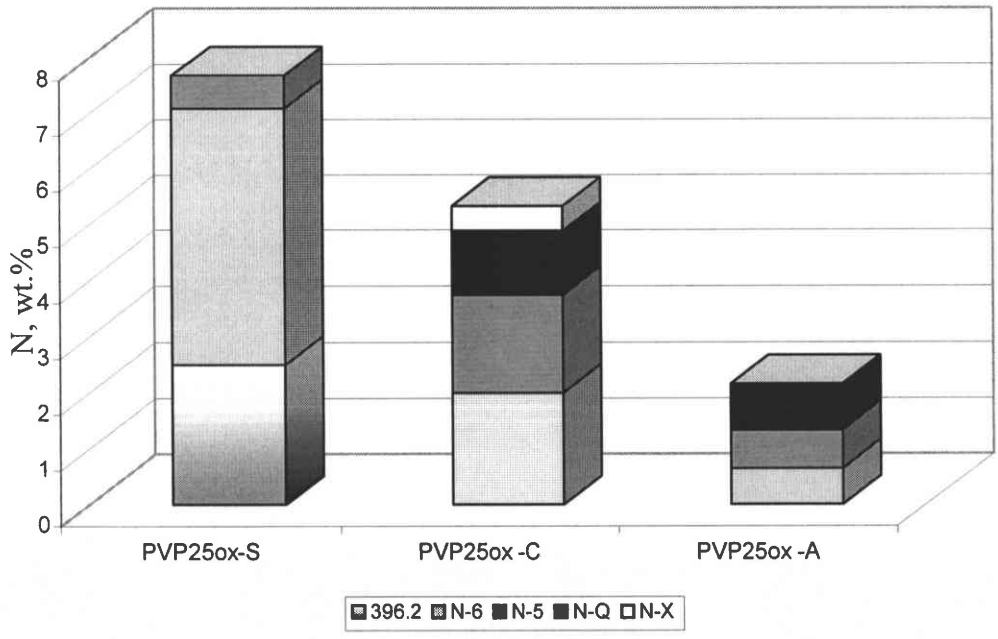

Fig. 128. Evolution of nitrogen functionalities on the consecutive stages of the thermal treatment of PVP25ox.

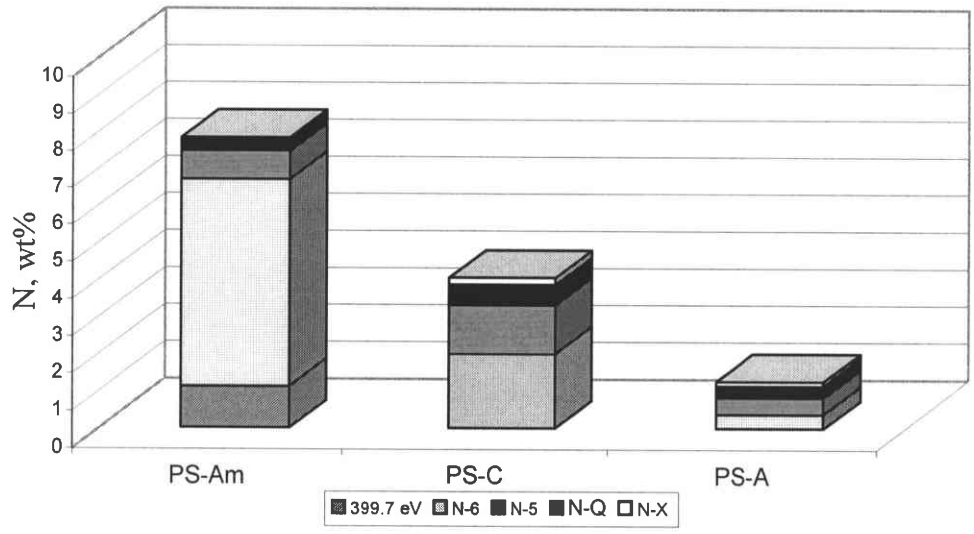

Fig. 129. Evolution of nitrogen functionalities on the consecutive stages of the thermal treatment of PS-Am.

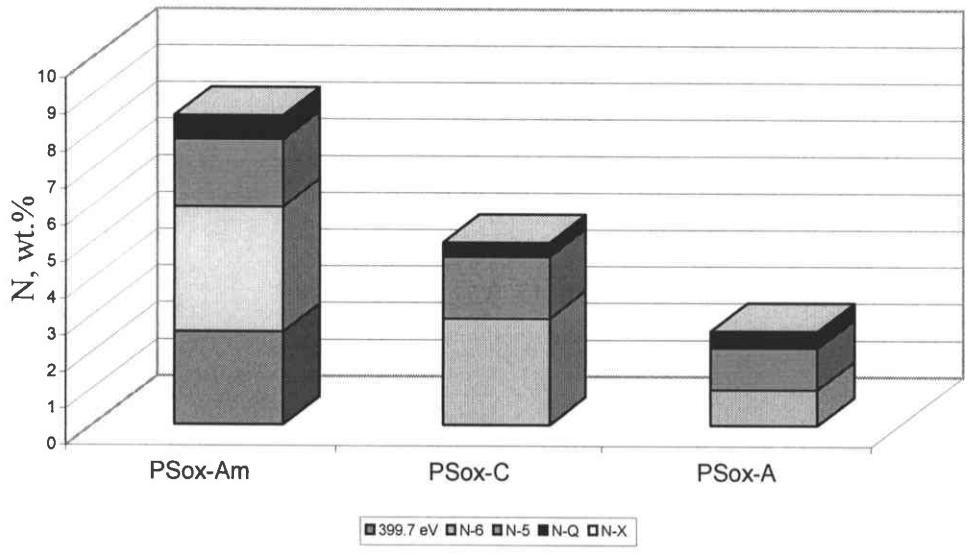

Fig. 130. Evolution of nitrogen functionalities on the consecutive stages of the thermal treatment of PSox-Am.

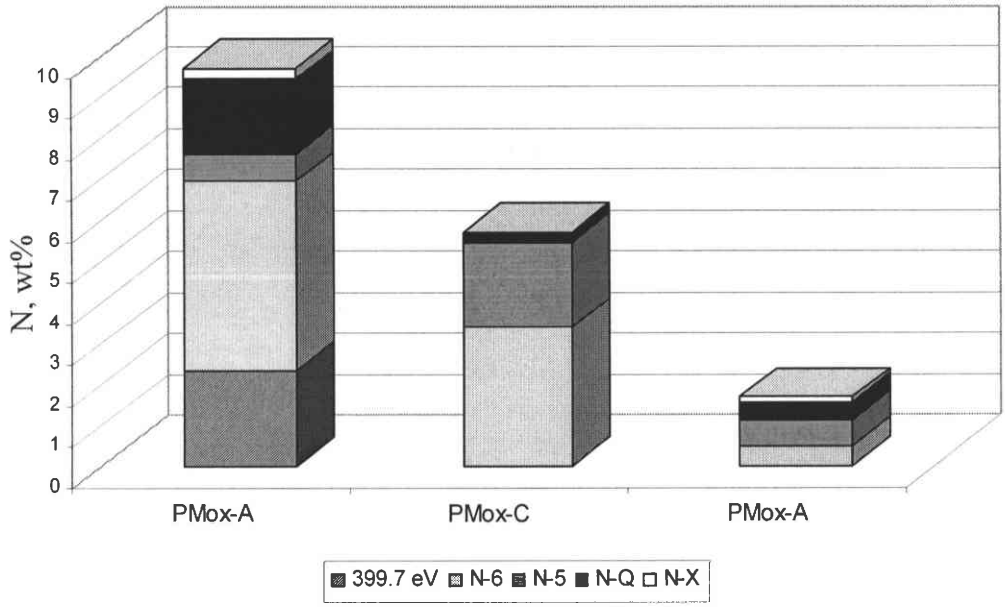

Fig. 131. Evolution of nitrogen functionalities on the consecutive stages of the thermal treatment of PMox-Am.

In the past several investigations were made to correlate the formation of the NH_3 and HCN on heat-treatment with the composition of char. These efforts were mainly inspired by the fact that these gases are the intermediate products of conversion of nitrogen present in coals into the nitrogen oxides during fluidized-bed combustion. It is believed that NH_3 is transformed to NO_x, while HCN is oxidized to N_2O. Kambara et al. (1995) reported that the quaternary nitrogen tend to be released as ammonia, while the rupture of pyridinic and part of pyrrolic rings leads to hydrogen cyanide.

Fig. 132 presents the ratios of the areas of peaks corresponding to the evolution of HCN and NH_3 during thermogravimetry to 900^0C of nitrogen containing semi-cokes. The random dispersion of the experimental points for the ammoxidized semi-cokes indicates the lack of correlation suggested by Kambara between the evolution of NH_3 and the content of quaternary nitrogen. Hence the results of the present study support the view of Stańczyk (1997) and Wójtowicz et al. (1995) that there is no close dependence between the char-bound nitrogen functionalities and NH_3-HCN concentrations in the evolved gases. Possibly the other factors, such as the porosity have an influence on the composition of gas phase.

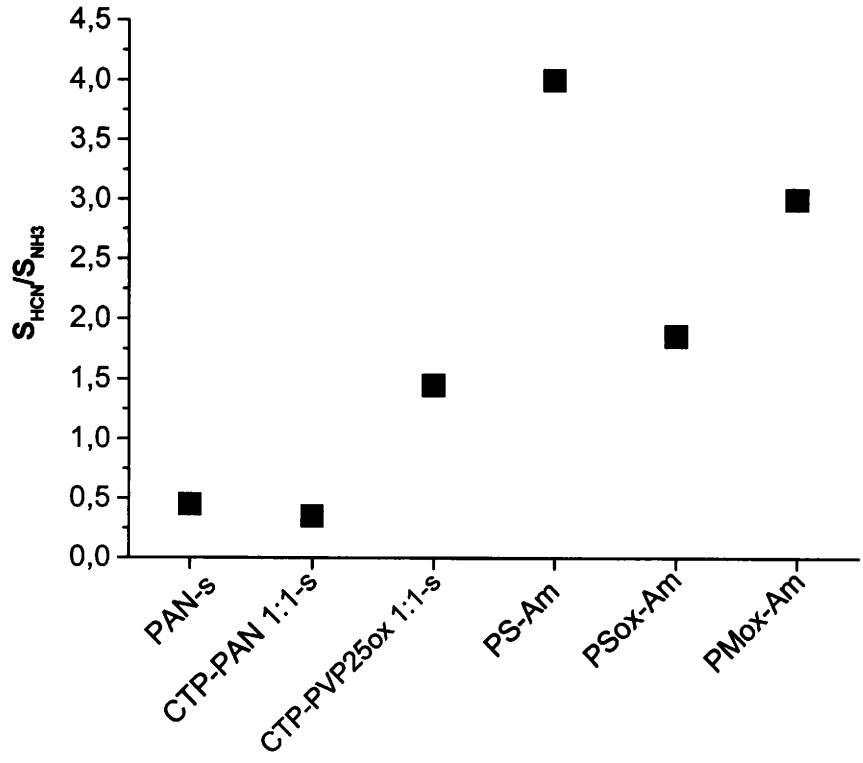

Fig. 132. The ratio of the HCN/NH_3 peaks evolution area determined for the heat-treated nitrogen containing precursors.

Porosity characteristics of nitrogen containing activated carbons from co-pyrolysis and ammoxidation

Adsorption is among the most attractive fields of possible application of nitrogen enriched carbons. The preliminary characterization of the activated carbons from pitch-polymer blends and ammoxidation products as adsorbents includes the determination of porosity development and polarity of surface.

The activated carbons prepared from PAN-containing precursors by steam activation up to 50 wt% burn-off show a moderate extent of porosity development. A maximum total pore volume V_T and BET surface area S_{BET} (0.346 cm^3/g and 832 m^2/g, respectively) is measured for the activated carbon from CTP-PAN 1:1 blend. Pure polymer gives slightly less porous activation product. Apparently, the tendency of the polymer to form on pyrolysis large condensed systems of aromatic rings is not favorable in terms of porosity development. Blending with an aromatic precursor as pitch

unexpectedly improves the ability, resulting in addition in the increase of mesopore ratio. Most developed porosity amongst all the activated carbons studied (V_T = 0.567 m^3/g, S_{BET} = 1417 m^2/g) is characteristic of PVP25ox. In that case the micropores can be readily generated in the cross-linked polyvinyl derived part of polymer carbon. Quite good activation performance is shown also by the CTP-PVP25ox 1:1 blend. Generally, only blends of considerable polymer content which give disordered carbons of anisotropic appearance are promising precursors of activated carbons with a relatively well developed porosity. Activated carbons produced from pitch-polymer blends are microporous in character.

It should be noticed an interesting activation behavior of the ammoxidized mesophase when preoxidized with nitric acid. The activation gives porous carbon with moderately developed porosity (V_T = 0.23 m^3/g, S_{BET} = 531 m^2/g) while maintaining the ordering characteristic of optically anisotropic material.

All nitrogen containing carbonaceous materials show a strong polarity of the surface as indicated by the unusual propensity to water sorption. For the series of activated carbons the ability increases almost proportionally to nitrogen content, therefore the presence of nitrogen atoms at the surface is mostly responsible for the enhanced polarity.

The preliminary evaluation suggests that the co-pyrolysis of pitch with the N-polymers and the ammoxidation of mesophase can be a source of activated carbons of specific surface properties with possible application in the field of SO_2 adsorption and NOx adsorption and reduction. According to Muñiz and coworkers (1998) adsorption capacity towards NOx is mainly influenced by the density of the basic surface groups instead of the porosity properties of the carbonaceous material. In this sense both CTP-PAN 1:1 and CTP-PAN 3:1 display sufficient density of active sites to meet these requirements. More detailed study which is required to explore these possibilities, it is behind the scope of the thesis.

Evaluation of nitrogen doped carbons as a potential anode material in lithium-ion cell

There is still a controversy about the role of nitrogen substituted for carbon atoms in the lattice of low temperature carbons in the lithium insertion / deinsertion behavior. In an attempt to clarify the doubts a series of calcined carbons with varying

nitrogen content and different characteristics in terms of structural ordering and porosity is prepared by the heat-treatment at 1050^0C of semi-cokes from pitch-PAN blends.

The lithium insertion /deinsertion tests show that all the nitrogen enriched carbons have a relatively low value of reversible capacity, in the range of X = 0.8 – 0.9 (X = 1 corresponds to 372 mAh/g, i.e. to the insertion of 1 lithium for 6 carbon atoms). This means that the presence of nitrogen in the network, which is associated with a change in the character of carbon material from the typical "soft" into disordered "hard", does not enhance the lithium storage ability. Moreover, the micropores and ultramicropores, which are generated on the pyrolysis of PAN and PAN-pitch blends seem to be not available for lithium storage. On the other hand the irreversible capacity increases with the nitrogen content to X = about 0.5, especially that nitrogen occurs mostly in the pyridinic form. It is believed that the lone pair of electrons contribute to the trapping of solvated lithium cations on these groups which act as active sites for the electrolyte decomposition during the first reduction, leading to the enhanced irreversible capacity. The inferior behavior can be also attributed to the presence of oxidized forms of nitrogen (pyridonic-N and N-oxides) in the materials.

The results lead to the conclusion that one cannot expect any improvement of the lithium storage capacity of nanostructured carbons by the substitution of nitrogen in the graphene layers. The most suitable carbon materials should be rather free of heteroatoms such as nitrogen, oxygen, which are generally active sites for the decomposition of electrolyte. Rather than modifying the electron donor properties, the presence of well-sized nanopores could be an issue for the enhancement of reversible capacity.

VII. Conclusions

Co-pyrolysis of coal-tar pitch with polyacrylonitrile and preoxidized polyvinylpyridine cross-linked with 25 wt% of divinylbenzene can be used as a convenient way for the preparation of carbonaceous materials of enhanced nitrogen content and homogeneous, at optical microscopy level, texture. Increasing the polymer proportion in the blend reduces the structural ordering in resultant materials until a typical hard carbon is produced in the case of 1:1 blends.

PAN is particularly efficient nitrogen carrier during the co-pyrolysis. The superior carbonization behavior of the polymer is transferred to blends ensuring synthesis of carbons with elevated nitrogen content using blends of relatively poor polymer proportion, while preserving a certain extent of anisotropic development. The synergistic effects occurring during co-pyrolysis contribute to the enhanced both the carbonaceous residue yield and nitrogen content.

At semi-coke stage (520°C) the co-pyrolysis derived carbons contain nitrogen in ring systems, mostly as pyridinic-N with a lower contribution of pyrrolic/pyridonic-N. There is no quaternary nitrogen at this stage of treatment.

Heat-treatment of nitrogen containing semi-cokes up to 800°C is accompanied by the loss of excess nitrogen (20-30 %) in the form of ammonia and hydrogen cyanide. The interactions occurring at the co-pyrolysis stage result in the noticeable retaining nitrogen in the carbon network during the drastic treatment of pitch-PAN blends. The blends containing 25 and 50 wt% of polymer give calcined at 1050°C carbons containing 4-5 wt% of nitrogen, respectively.

Ammoxidation of pitch derived semi-coke and mesophase under appropriate conditions (ammonia-air ratio 1:3, 350-400°C) generates an abundance of nitrogen functionalities on the surface of particles, corresponding to 8-10 wt% of nitrogen in a bulk of sample. The nitrogen incorporation is facilitated by the oxidizing pretreatment with nitric acid. A large part (40-50 %) of the nitrogen groups is thermally unstable and readily desorbs or decomposes on heat-treatment.

The gasification with steam up to 50 wt% burn-off results in twice higher reduction of nitrogen content in resultant activated carbons compared to the treatment in inert atmosphere due to the preferential reaction with polymer derived phase which is more disordered and nitrogen richer. The blends containing above 25 wt% of PAN give activated carbons of porosity development which is comparable to that of PAN carbon

with somewhat enhanced mesopore contribution. Despite rather moderate pore volume and surface area ($V_T \sim 0.35$ cm^3/g, $S_{BET} \sim 800$ m^2/g), the activated carbons seem to be an attractive material for application in SO_2 and NO_x removal due to a high density of nitrogen polar sites on the surface. PVP25ox derived activated carbon is characterized by the most porous texture ($V_T \sim 0.57$ cm^3/g, $S_{BET} \sim 1400$ m^2/g) among the prepared materials, however the development is associated with a reduced nitrogen content and surface polarity. The nitrogen enriched activated carbons with a moderate development of porosity ($S_{BET} = 530$ m^2/g) can be produced from materials with established preorder by using ammoxidation of mesophase which is preoxidized with nitric acid.

The evaluation of lithium insertion / deinsertion behavior of pitch-PAN blend derived carbons shows that the presence of nitrogen in the network does not enhance the lithium storage ability. All the nitrogen enriched carbons have a relatively low value of reversible capacity (X = 0.8 – 0.9), moreover the irreversible capacity increases to X = about 0.5 with the nitrogen content. The inferior behavior can be attributed to the presence of nitrogen mostly as pyridinic with a contribution of oxidized (pyridonic-N and N-oxides) forms and to the lack of micro- and ultramicropores available for lithium.

References

Abotsi G.M.K., Scaroni A.W., 1990, *Reactions of carbons with ammonia: effects on the surface charge and molybdenum adsorption,* Carbon 28, 79-84

Ahmed S.N., Baldwin R., Derbyshire F., McEnaney B., Stencel J., 1993, *Catalytic reduction of nitric oxide over activated carbons*, Fuel 72, 287-292

Andrzejak A., Wachowska H., 1970, *Badanie procesu utleniania węgli brunatnych mieszanką powietrzno-amoniakalną,* Prace Kom.Mat.-Przyr.PTPN 12, Poznań, 110-115

Azhari S.J., Diab M.A., 1998, *Thermal degradation and stability of poly(4-vinylpyridine) homopolymer and copolymers of 4-vinylpyridine with methyl acrylate*, Polym. Degrad. Stab. 60, 253-256

Bacon R., 1973, *Carbon fibers from rayon precursors*, In: Chemistry and Physics of Carbon (P. Walker, P.A. Thrower eds.), Marcel Dekker, Inc., New York, v.9, pp.2-102

Bagreev A., Strelko V., Lahaye J., 1996, *Porous structure and surface chemistry of nitrogen containing carbons from polymers*, Ext. Abstr. The European Conference "Carbon 96", Newcastle upon Tyne, UK, pp.14-15

Bahl O.P., Shen Z., Lavin G.J., Ross R.A., 1998, *Manufacture of carbon fibers,* In: Carbon fibers, Third edition, Revised and Expanded (J.P Donnet, T.K. Wang, S. Rebouillat, J.C.M. Peng eds), Marcel Dekker, New York, pp.1-83

Baranauskaus V., Durrant S.V., Tosin M.C., Peterlevitz A.C., Li B.B., Castro S.G., 1999, *Nitrogenated diamond produced by introducing ammonia into the gas feed in hot filament CVD*, Thin Solid Films 355-356, 161-167

Bellamy L.J., 1975, *The Infra-red Spectra of Complex Molecules*, Chapman, London, v.1

Bimer J., Sałbut P.D., Berłożecki S., Boudou J.-P., 1998, *Modified active carbons from precursors enriched with nitrogen functions: sulfur removal capabilities*, Fuel 77, 519-525.

Biniak S., Szymański G., Siedlewski J., Świątkowski A., 1997, *The characterization of activated carbons with oxygen and nitrogen surface groups*, Carbon 35, 1799-1810

Boehm H.P., 1994, *Some aspects of the surface chemistry of carbon blacks and other carbons*, Carbon 32, 759-769

Boutique J.P., Verbist J.J., Fripiat J.G., Delhalle J., Pfister-Guillouzo G., Ashwell G.J., 1984, J. Am. Chem. Soc. 106, 7374.

Brooks J.D., Taylor G.H., 1965, *The formation of graphitizing carbons from the liquid phase*, Carbon 3, 185-193

Brooks J.D., Taylor G.H., *The formation of some graphitizing carbons*, 1968, In: Chemistry and Physics of Carbon, (P.L. Walker, Jr., ed.), Marcel Dekker, Inc., New York, v.4, pp.243-286

Brzozowska T., Zieliński J., Machnikowski J., 1998, *Effect of polymeric additives to coal tar pitch on carbonization behaviour and optical texture of resultant cokes*, J. Anal. Appl. Pyrolysis 48, 45-58

Buckley A.N., 1994, *Nitrogen functionality in coals determined by X-ray photoelectron spectroscopy*, Fuel Process. Technol. 38, 165-179

Burg P., Fydrych P., Cagniant D., Nanse G., Bimer J., Jankowska A., 2002, *The characterization of nitrogen-enriched activated carbons by IR, XPS and LSER methods*, Carbon 40, 1521-1531

Byrne J.F., Marsh H., 1995, *Introductory overview*, In :Porosity in carbons (J.W. Patrick ed.), Edward Auckland – a member of the Hodder Headline Group, pp.1-48

Cagniant D., Gruber R., Boudou J.P., Bilem C., Bimer J., Salbut P.D., 1998, *Structural characterization of nitrogen-enriched coals*, Energy Fuels 12, 672-681

Carasco-Marín F., Utrera-Hidalgo E., Rivera Utrilla J., Morena- Castilla, 1992, *Adsorption of SO_2 in flowing air onto activated carbons from olive stones*, Fuel 71, 575-578

Celina M., Ottesen D.K., Gillen K.T., Clough R.L., 1997, *FTIR emmision spectroscopy applied to polymer degradation,* Polym. Degrad. Stab. 58, 15-31

Coleman M.M., Sivy G.T., Painter P.C., Snyder R.W., Gordan B., 1983, Carbon 21, 255-261

Collin G., Bujnowska B., Polaczek J, 1997, *Co-coking of coal with pitches and waste plastics*, Fuel Process. Technol. 50, 179-184

Contescu A., Vass M., Contescu C., Putyera K., Schwarz J.A., 1998, *Acid buffering capacity of basic carbons revealed by their continuous pK distribution*, Carbon 36, 247

Culler S.R., 1993, *Diffuse reflectance infrared spectroscopy : sampling techniques for qualitative/ quantitative analysis of solids,* In: Practical sampling techniques for infrared analysis (P.B. Coleman ed.), CRC Press, 94-105

Dalton S., Heatley F., Budd P.M., 1999, *Thermal stabilization of polyacrylonitrile fibres*, Polymer 40, 5531-5543

DeBarr J.A., Lizzio J.A., 1995, *New insights on the mechanism of SO_2 removal by carbon,* 22nd Biennial Conference on Carbon, San Diego, 562

Dias M.L., Bruno M.I., de Santa Maria L.C., 1997, *4-vinylpyridine polymerization with soluble catalysts,* Eur. Polym. J. 33, 1559-1562

Edstrom T., Lewis I.C., 1969, Carbon 7, 85-91

Figueiredo J.L., Pereira M.F.R., Freitas M.M.A., Órfão J.J.M., 1999, *Modification of the surface chemistry of activated carbons*, Carbon 37, 1379-1389

Fitzer E., Mueller K., Schaeffer W., 1971, *The chemistry of pyrolytic conversion of organic compounds to carbon,* In: Chemistry and Physics of Carbon, (P.L. Walker, Jr., ed.), Marcel Dekker, Inc. New York, v.7, pp. 237-383

Fitzer E., Mueller D.J., 1975, *The influence of oxygen on the chemical reactions during stabilization of PAN as carbon fiber precursor*, Carbon 13, 63-69

Fitzer E., Frohs W., Heine M., 1986, *Optimization of stabilization and carbonization treatment of PAN fibers and structural characterization of the resultant carbon fibers*, Carbon 24, 387-395

Franklin R.E., 1951a, *Structure of graphitic carbons,* Acta Cryst. 4, 253

Franklin R.E., 1951b, *Crystallite growth in graphitizing and non-graphitizing carbons,* Proc. Roy.Soc. A209, 196

Frąckowiak E., Béguin F., 2001, *Carbon materials for the electrochemical storage energy in capacitors*, Carbon 39, 937-950

Gautier S., Frąckowiak E., Machnikowski J., Rouzaud J.N., Béguin F., 1998, *Mechanism of lithium insertion in different kind of carbons,* Mol. Cryst. Liq. Cryst. 310, 359-364

Granda M., Bermejo J., Moinelo S.R., Menendez R., 1990, *Application of extrography for characterization of coal tar and petroleum pitches,* Fuel 69, 702-705

Greinke R.A., 1986, *Kinetics of petroleum pitch polymerization by gel permeation chromatography*, Carbon 24, 677-686

Greinke R.A., 1994, *Early stages of petroleum pitch carbonization- kinetics and mechanism,* In: Chemistry and Physics of Carbon (P.A. Thrower ed.), Marcel Dekker Inc., New York, v.24, pp.1-43

Groszek A.J., 1987, *Graphitic and polar surface sites in carbonaceous solids*, Carbon 25, 717

Gupta A., Harrison I.R., 1997, *New aspects in the oxidative stabilization of PAN-based carbon fibers : II*, Carbon 35, 809-818

Iyama S., Yokono T., Sanada Y., 1986, *Development of anisotropic texture in co-carbonization of low rank coal with pitch-evaluation from hydrogen donor and acceptor abilities of coal and pitch,* Carbon 24, 423-428

Inagaki M., Tachikawa H., Nakahashi T., Konno H., Hishiyama Y., 1998, *The chemical bonding state of nitrogen in kapton-derived carbon film and its effect on the graphitization process,* Carbon 36, 1021-1025

Jankowska H., Świątkowski A., Ościk J., Kusak R., 1983, *Adsorption from benzene-ethanol binary solutions on activated carbons with different contents of oxygen surface components*, Carbon 21, 117-120

Jansen R.J.J., Bekkum H.V., 1994, *Amination and ammoxidation of activated carbons*, Carbon 32, 1507-1515

Jansen R.J.J., Bekkum H.V., 1995, *XPS of nitrogen-containing functional groups on activated carbon*, Carbon 33, 1021-1027

Jurewicz K., Babeł K., Ziólkowski A., Wachowska H., Kozłowski M., 2002, *Ammoxidation of brown coals for supercapacitors*, Fuel Process. Technol. 77-78, 191-198

Jüntgen H., Richter E., Kuhl H., 1988, *Catalytic activity of carbon catalysts for the reaction of NO_x with NH_3*, Fuel 67, 775-780

Kambara S., Takarada T., Toyoshima M., Kato K., 1995, *Relation between functional forms of coal nitrogen and NOx emissions from pulverized coal combustion*, Fuel 74, 1247-1253

Kapteijn, Moulijn, Matzner S., Boehm H.-P., 1999, *The development of nitrogen functionality in model chars durin gasification in CO_2 and O_2*, Carbon 37, 1143-1150

Kartel N.T., Puziy A.M., 1996, *Peculiarity in carbonization of copolymers to obtain synthetic carbons*, In: Ext.Abstr. The European Conference "Carbon 96", Newcastle upon Tyne,UK, pp. 525-528

Kelemen S.R., Gorbaty M.L., Kwiatek P.J., 1994, *Quantification of nitrogen forms in argonne premium coals*, Energy & Fuels 8, 896

Kelemen S.R., Gorbaty M.L., Kwiatek P.J., Fleischer, 1998, *Nitrogen transformations in coal during pyrolysis*, Energy & Fuels 12, 159-173

Koch A., Krztoń A., Finqueneisel G., Heintz O., Weber J.V., 1998, *A study of carbonaceous char oxidation in air by semi-quantitative FTIR spectroscopy,* Fuel 77, 563-569

Koh M., Nakajima T., 2002, *Adsorption of aromatic compounds on C_xN – coated activated carbon,* Carbon 38, 1947-1954

Konno H., Nakahashi T., Inagaki M., Sogabe T., 1999, *Nitrogen incorporation into boron-doped graphite and formation of BN bonding,* Carbon 37, 471-475

Kouvetakis J., Kaner R.B., Sattler M.L., Bartlett N., 1986, *A novel graphite-like material of composition BC_3 and nitrogen-carbon graphites,* J. Chem. Soc. Chem. Commun. 24, 1758-1759

Krztoń A., Cagniant D., Gruber R., Pająk J., Fortin F., Rouzaud J.N., 1995, *Application of Fourier self-deconvolution to the FT-i.r. characterization of coals and their N-methyl 2-pyrrolidinone extraction products,* Fuel 74, 217-225

Lahaye J., Nanse G., Bagreev A., Strelko V., 1999a, *Porous structure and surface chemistry of nitrogen containing carbons from polymers,* Carbon 37, 585-590

Lahaye J., Nanse G., Fioux P., Bagreev A., Broshnik A., Strelko V., 1999b, *Chemical transformation during the carbonization in air and the pyrolysis under argon of vinylpyridine-divinylbenzene copolymer by X-ray photoelectron spectroscopy,* Appl. Surf. Sci.147, 153-174

Laskorin B.N., 1983, *Ion exchange materials for hydrometallurgy, waste water cleaning and water treatment,* Moscow, VNIIKhT

László K., Bóta, Nagy L.G., 2000, *Comparative adsorption study on carbons from polymer precursors,* Carbon 38, 1965-1976

László K., Tombácz E., Josepovitz K., 2001, *Effect of activation on the surface chemistry of carbons from polymer precursors,* Carbon 39, 1217-1228

Lebrun C., Deniau G., Viel P., Lécayon G., 1998, *Electrosynthesis of poly(4-vinylpyridine) films on metallic surfaces under anodic and cathodic polarizations: structure and properties of the organic coatings,* Surf. Coat. Technol. 100-101, 474-479

Leon Y Leon C.A., Radovic L.R., 1994, *Interfacial Chemistry and Electrochemistry of carbon surfaces* , Chemistry and Physics of Carbon, (P.A Thrower, ed.), Marcel Dekker, Inc. New York, v.24, 213-310

Lewis I.C., 1980 *Thermal polymerization of aromatic hydrocarbons,* Carbon 18, 191-196

Lewis I.C., 1982, *Chemistry Of Carbonization,* Carbon 20, 519-529

Li L., Quinlivan P.A., Knappe D.R.U., 2002, *Effects of activated carbon surface chemistry and pore structure on the adsorption of organic contaminants from aqueous solution*, Carbon 40, 2085-2100

Li C.-Z., Buckley A.N., Nelson P.F., 1998, *Effects of temperature and molecular mass on the nitrogen functionality of tars produced under high heating rate conditions*, Fuel 77, 157-164

Li X.G., 1999, *High-resolution thermogravimetry of poly(4-vinylpyridine-co-divinylbenzene)*, React. Funct. Polym. 42, 53-58

Liu Y., 1996, *Mechanism of lithium insertion in hard carbons prepared by pyrolysis of epoxy resins,* Carbon 34, 193-200

Machnikowski J., Gerus-Piasecka I., Kubica K., Machnikowska H., 2001, *High softening point pitches produced by air-blowing of QI-free coal-tar derived precursors,* Polish Journal of Chemical Technology 3, 11-16

Machnikowski J., Machnikowska H., Brzozowska T., Zieliński J., 2002a *Mesophase development in coal-tar pitch modified with various polymers*, J. Anal. Appl. Pyrolysis 65, 147-160

Machnikowski J., Kaczmarska H., Gerus-Piasecka I., Díez M.A., Alvarez R., García R., 2002b, *Structural modification of coal-tar pitch fractions during mild oxidation-relevance to carbonization behavior,* Carbon 40, 1937-1947

Machnikowska H., Krztoń A., Machnikowski J., 2002c, *The characterization of coal macerals by diffuse reflectance infrared spectroscopy*, Fuel 81, 245-252

Marsanich K., Barontini F., Cozzani V, Petarca L., 2002, *Advanced pulse calibration technique for the quantitative analysis of TG-FTIR data,* Thermochim. Acta 390, 153-168

Mangun C.M., Benak K.R., Economy J., Foster K.L., 2001, *Surface chemistry, pore size and adsorption properties of activated carbon fibers and precursors treated with ammonia*, Carbon 39, 1809-1820

Marchand A., 1971, Chemistry and Physics of Carbon, (P.L. Walker, Jr., ed.), Marcel Dekker, Inc. New York, v.7, 155-193

Marsh H., Menendez R.,1989, *Mechanism of formation of isotropic and anisotropic carbons,* Introduction to Carbon Science, Butterworths, London, 37-73

Martin S.C., Liggat J.J., Snape C.E., 2001, *In situ NMR investigation into thermal degradation and stabilization of PAN*, Polym. Degrad. Stab. 74, 407-412

Martínez-Alonso A., Bermejo J., Granda M., Tascón J.M.D., 1992a, *Suitability of thermogravimetry and differential thermal analysis techniques for characterization of pitches,* Fuel 71, 611-617

Martínez-Alonso A., Bermejo J., Tascón J.M.D., 1992, *Thermoanalytical studies of pitch pyrolysis. Comparison with polycyclic aromatic hydrocarbons,* J. Therm. Anal. 38, 811-820

Matzner S., Boehm H.P., 1998, *Influence of nitrogen doping on the adsorption and reduction of nitric oxide by activated carbons*, Carbon 36, 1697-1709

Mikhalovsky S.V., Glushakov V.G., Noscov A.M., Kozynchenko A.P., Volkov V.B., 1996, *Heteroatoms in active carbons: methods of introduction and effect of their adsorptive and catalytic properties*, Ext. Abstr. The European Conference "Carbon 96", Newcastle UK, 30-31

Mochida I., Shimizu K., Korai Y., Otsuka H., Fujiyama S., 1988, *Structure and carbonization properties of pitches produced catalytically from aromatic hydrocarbons with HF/BF_3*, Carbon 26, 843-852

Mochida I., An K.H., Korai Y., 1995a, *Preparation of nitrogen containing pitches from quinoline and isoquinoline by aid of $AlCl_3$*, Carbon 33, 1069-1077

Mochida I., An K.H., Korai Y., 1995b, *Catalytic condensation of isoquinoline into pitch in higher yield in the presence of nitro solvents*, Carbon 33, 1079-1084

Mochida I., An K.H., Sakanishi K., Korai Y., 1996, *Preparation of nitrogen-rich pitches from diazanaphtalenes using $AlCl_3$*, Carbon 34, 601-608

Mochida I., Shimizu K., Korai Y., Otsuka H., Fujiyama S., 1988, Carbon 26, 843-852

Mochida I., Ku C.H, Yoon S.H., Korai Y., 1999, *Anodic performances of anisotropic carbon derived from isotropic quinoline pitch*, Carbon 37, 323-327

Muñiz J., Herrero J.E., Fuertes A.B., 1998, *Treatments to enhance the SO_2 capture by activated carbon fibres*, Appl. Catal. B 18, 171-179

Muñiz J., Marbán G., Fuertes A.B., 1999, *Low temperature selective reduction of NO over polyarylamide-based carbon fibres,* Appl. Catal. B 23, 25-35

Nakahashi T., Konno H., Inagaki M., 1998, *Chemical state of nitrogen atoms in carbon films prepared from nitrogen-containing polymer films*, Solid State Ionics 113-115, 73-77

Nakajima T., Koh M., 1997, *Synthesis of high crystalline carbon-nitrogen layered compounds by CVD using nickel and cobalt catalysts*, Carbon 35, 203-208

Neely J.W., 1981, *Characterization of polymer carbons derived from porous sulfonated polystyrene*, Carbon 19, 27- ,

Otake Y., Jenkins R.G., 1993, *Characterization of oxygen-containing surface complexes created on a microporous carbon by air and nitric acid treatment*, Carbon 33, 109-121

Pels J.R., Kapteijn F., Moulijn J.A., Zhu Q., Thomas K.M., 1995, *Evolution of nitrogen functionalities in carbonaceous materials during pyrolysis,* Carbon 33, 1641-1653

Pielichowski J., Puszyński, 1978, *Preparatyka związków wielkocząsteczkowych,* Wydawnictwa Politechniki Krakowskiej, Kraków

J. Pielichowski, A. Puszyński, *Chemia polimerów*, 1998, Wydawnictwa AGH, Kraków

de la Puente G., Pis J.J. Menéndez J.A., Grange P., 1997, *Thermal stability of oxygenated functions in activated carbons,* J. Anal. Appl. Pyrolysis 43, 125-138

Ratner B., Castner D., 1997, *Electron spectroscopy for chemical analysis,* In: Surface Analysis- The Principal Techniques (J.C. Vickerman ed.), John Willey & Sons Ltd, New York, v.1, pp.542-554

Raymundo-Piñero E., Cazorla-Amoros D., Linares-Solano A., Find J., Wild U., Schlögl R., 2002, *Structural characterization of N-containing activated carbon fibers prepared from a low softening point petroleum pitch and melamine resin*, Carbon 40, 597-608

Rodríguez-Reinoso F., 1997, *Activated carbon: structure, characterization, preparation and applications,* In: Introduction to Carbon Technologies (H. Marsh ., E.A. Heintz, F. Rodríguez-Reinoso eds.), Universidad de Alicante, Secreteriado de Publicaciones, pp. 35-101

Rouzaud JN , 1 989, *C ontribution o f t ransmission e lectron m icroscopy t o t he s tudy o f coal carbonization processes*, In: Coal Characterization for Conversion Processes (V. Prins, K.A. Nater, H.A.G. Chermin, J.A. Moulijn eds.), Elsevier, 55

Schmiers H., Friebel J., Streubel P., Hesse R., Köpsel R., 1999, *Change of chemical bonding of nitrogen of polymeric N-heterocyclic compounds during pyrolysis*, Carbon 37, 1965-1978

Seah M.P., 1990, *Practical Surface Analysis* (D.Briggs and M.P. Seah, eds.), John Wiley & Sons Ltd, New York, v.1, pp. 542-554

Singer L.S., Lewis I.C., 1984, *Electron-nuclear double resonance (ENDOR) of pitches,* Carbon 22, 487-492

Sotowa C., Watanabe Y., Yatsunami S., Korai Y., Mochida I., 1999, *Catalytic dechlorination of 1,2-dichloroethane into vinyl chloride over polyacrylonitrile-based active carbon fiber*, Appl. Catal. A 180, 317-323

Stańczyk K., Dziembaj R., Piwowarska Z., Witkowski S., 1995, *Transformation of nitrogen structures in carbonization of model compounds determined by XPS*, Carbon 33, 1383-1392

Stöhr B., Boehm Hp., Schlögl R., 1991, *Enhancement of the catalytic activity of activated carbons in oxidation reactions by thermal treatment with ammonia or hydrogen cyanide and observation of superoxide species as a possible intermediate*, Carbon 29, 707-720

Suh D.J., Park T.-J., Ihm S.-K., 1993, *Effect of surface oxygen groups of carbon supports on activated carbons with different contents of oxygen surface complexes*, Carbon 31, 427-435, 1993

Surianarayanan M., Vijayaraghavan R., Raghavan K.V., 1992, *Spectroscopic investigations of polyacrylonitrile thermal degradation*, J. Polymer. Sci. 36, 2503-2512

Uchiyama T., Kawauchi A., DuVal D.L., 1998, *Quick identification of polymeric dye transfer inhibitors in laundry detergents by pyrolysis-gas chromatography/mass spectrometry*, J. Anal. Appl. Pyrolysis 45, 111-119

Van Krevelen D.W., 1974, *Properties of Polymers*, Elsevier

Wachowska H., Machnikowski J., Fiedorow R., Kozlowski M., 2000, *A study on obtaining pitch enriched with nitrogen*, In: Ext. Abstr. 1st World Conference on Carbon Eurocarbon 2000, Berlin, 541-542

Wójtowicz M.A., Pels J.R., Moulijn J.A., 1995, *The fate of nitrogen functionalities in coal during pyrolysis and combustion*, Fuel 74, 507-516

Wu Y., Fang S., Jiang Y., 1999, *Effects of nitrogen on the carbon anode of a lithium secondary battery*, Solid State Ionics 120, 117-123

Wu K.H., Wang Y.R., Hwu W.H., 2003, *FTIR and TGA studies of poly(4-vinylpyridine-co-divinylbenzene)-Cu(II) complex*, Polym. Degrad. Stab 79, 195-200

Xie F., Phillips J., Silva I.F., Palma M.C., Menéndez J.A., 2000, *Microcalorimetric study of acid sites on ammonia- and acid-pretreated activated carbons*, Carbon 38, 691-700

Xue T.J., Mckinney M.A., Wilkie C.A., 1997, *The thermal degradation of polyacrylonitrile*, Polym. Degrad. Stab. 58, 193-202

Yokono T., Miyazawa K., Sanada Y., Marsh H., 1979, *Relations between free valence and thermal reactivity of polynuclear aromatic hydrocarbons*, Fuel 58, 692-694,

Yung Y., Suh M.C., Lee H., Kim M., Lee S.-I., Shim S.C., Kwak J., *Electrochemical insertion of lithium into polyacrylonitrile-based disordered carbons,* 1997, J. Electrochem. Soc. 144, 4279-4284

Zander M., Collin G., 1993, *A review of significance of polycyclic aromatic chemistry for pitch science*, Fuel 72, 1281-1285

Zawadzki J., 1987a, *Infrared studies of SO_2 on carbons – I. Interaction of SO_2 with carbon films* , Carbon 25, 431-436

Zawadzki J., 1987b, *Infrared studies on SO_2 on carbons – II. The SO_2 species adsorbed on carbon films*, Carbon 25, 495-502

Zawadzki J., 1988, *IR Spectroscopy in Carbon Surface Chemistry* In: Chemistry and Physics of Carbon (P.A. Thrower ed.), Marcel Dekker Inc. New York v.24, pp. 148-380

Zhang G.F., Geng D.S., Yang Z.J, 1999, *High nitrogen amounts incorporated diamon films deposited by the addition of nitrogen in a hot-filament CVD system*, Surf. Coat. Technol. 122, 268-272

Zheng T, Xing W, Dahn JR, 1996, *Carbons prepared from coals for anodes of lithium - ion cells,* Carbon 34, 1501-1507

Zhu Q., Thomas K.M., Russell A.E., 1996 *Determination of the nitrogen functionality in carbons using XANES spectroscopy*, In: Ext. Abstr. The European Conference "Carbon 96", Newcastle UK, 14-15

Zhou X.,Goh S.H., Lee S.Y., Tan K.L., 1998, *XPS and FT i.r studies of interactions in poly(carboxylic acid) / poly(vinylpyridine) complexes*, Polymer 39, 3631-3640